

**CARTILAGE ENGINEERING: DESIGNING AN IMPROVED SYSTEM
FOR EFFECTING REPAIR OF ARTICULAR CARTILAGE DEFECTS**

by

Chelsea Shields Bahney

A DISSERTATION

Presented to the Department of Cell & Developmental Biology
and the Oregon Health & Science University
School of Medicine
in partial fulfillment of
the requirements for the degree of
Doctor of Philosophy

August 2010

School of Medicine
Oregon Health & Science University

CERTIFICATE OF APPROVAL

This is to certify that the PhD dissertation of
Chelsea Shields Bahney
has been approved

Brian Johnstone (Mentor/Advisor)

Bill Horton (Thesis Committee Chair)

Hans Peter Bächinger

Jamie FitzJ eaaie

Owen McCarty

Jami ittneii

J ai ei Ftnz eitzea

TABLE OF CONTENTS

LIST OF FIGURES	iv
LIST OF ABBREVIATIONS	vi
ACKNOWLEDGMENTS	viii
ABSTRACT	x
CHAPTER 1: INTRODUCTION & BACKGROUND	1
1.1 TISSUE ENGINEERING FOR REPAIR OF ARTICULAR CARTILAGE DEFECTS	1
1.2.1 Endochondral Ossification	4
1.2.2 Joint Specification at the Interzone	5
1.2.3 Cavitation	9
1.2.4 Metalloproteinases in Development.....	12
1.3 STRUCTURE & FUNCTION OF ARTICULAR CARTILAGE.....	14
1.3.1 Types of Cartilage	14
1.3.2 Anisotropic Assembly and Biomechanical Properties of Articular Cartilage.....	15
1.4 CELL CHOICES IN CARTILAGE ENGINEERING	19
1.4.1 Articular Chondrocytes	19
1.4.2 Mesenchymal Stem Cells	20
1.4.3 Embryonic Stem Cells & Induced Pluripotent Stem Cells	23
1.5 SCAFFOLD DESIGN	24
1.5.1 Hydrogels	24
1.5.2 Photopolymerization	25
1.5.3 Bioresponsive Hydrogels	27
1.5.4 Bioactive Hydrogels	31
1.6 OSTEOARTHRITIS: THE CLINICAL SIGNIFICANCE OF CARTILAGE ENGINEERING	35
1.7 THESIS AIMS & OUTLINE OF WORK.....	37
CHAPTER 2: MATERIALS & METHODS	39
2.1 PREPARATION OF HYDROGEL SCAFFOLDS.....	39
2.1.1 Semi-Interpenetrating Networks	39
2.1.2 Peptide Synthesis.....	39
2.1.3 Bioresponsive Hydrogels	40
2.1.4 Degradation Testing	42
2.1.5 Bioactive Scaffolds	42
2.2 CELL CULTURE.....	43
2.2.1 Isolation and Expansion of Human Mesenchymal Stem Cells	43
2.2.2 Isolation and Culture of Human Articular Chondrocytes	43
2.2.3 Photoencapsulation using Ultraviolet (UV) Light	44
2.2.4 Photoencapsulation using Visible Light.....	44

2.2.5 <i>In vitro</i> Hydrogel Culture	45i
2.3 LIVE-DEAD STAINING	45i
2.4 BIOCHEMICAL ANALYSIS	46i
2.5 GENE EXPRESSION ASSAYS.....	47i
2.6 HISTOLOGY AND IMMUNOHISTOCHEMISTRY	47i
2.6.1 Toluidine Blue Staining for Hydrogels	48i
2.6.2 Collagen I Immunohistochemistry	48i
2.6.3 Collagen II and X Immunohistochemistry	49i
2.6.3 MMP-7 Immunohistochemistry	49i
2.6.4 Fluorescence <i>In Situ</i> Hybridization (FISH).....	50i
2.7 ZYMOGRAPHY	51i
2.8 MECHANICAL TESTING	51i
2.9 SWELLING RATIO CALCULATIONS (Q).....	53i
CHAPTER 3: VISIBLE LIGHT PHOTOPOLYMERIZATION.....	54i
3.1 ABSTRACT	55i
3.2 INTRODUCTION.....	55i
3.3 RESULTS	59i
3.4 DISCUSSION	62i
3.5 CONCLUSION	70i
CHAPTER 4: BIORESPONSIVE SCAFFOLD	71i
4.1 ABSTRACT	72i
4.2 INTRODUCTION.....	73i
4.3 RESULTS	75i
4.3.1 Identification of MMP-7 as Candidate Enzyme for Bioresponsive Hydrogels	75i
4.3.2 Design and Degradation Kinetics of Bioresponsive Hydrogels.....	77i
4.3.3 <i>In Vitro</i> Chondrogenesis of hMSCs in MMP-7 Bioresponsive Hydrogels.....	79i
4.4 DISCUSSION	83i
4.5 CONCLUSIONS	87i
CHAPTER 5: BIOACTIVE SCAFFOLDS.....	88i
5.1 ABSTRACT	89i
5.2 INTRODUCTION.....	90i
5.3 RESULTS	92i
5.3.1 Hydrogels Undergo Chondrogenesis in the Absence of Dexamethasone.....	92i
5.3.2 TGF- β 1 Withdrawal During Hydrogel Culture Affects Collagen Biosynthesis.....	94i
5.3.2 Tethered TGF- β 1 is Insufficient for Maintaining Chondrogenesis.....	97i
5.4 DISCUSSION	99i

5.5 CONCLUSIONS & FUTURE DIRECTIONS.....	102i
CHAPTER 6: COCULTURE	104i
6.1 ABSTRACT	105i
6.2 INTRODUCTION.....	105i
6.3 RESULTS	108i
6.3.1 Comparing chondrogenesis of human MSCs to ACs in hydrogel scaffolds.....	108i
6.3.2 Coculture of hMSCs and hACs.....	111i
6.3.3 Transwell culture of hMSCs and hACs.....	112i
6.3.4 hMSCs influence hACs in coculture	113i
6.4 DISCUSSION	119i
CHAPTER 7: CONCLUSIONS & FUTURE DIRECTIONS	125i
7.1 BIORESPONSIVE HYDROGELS.....	125i
7.1.1 Optimize Scaffold Degradation.....	126i
7.1.2 Explore Scaffold Utility using other Chondrogenic Cell Types	132i
7.2 BIOACTIVE SCAFFOLDS.....	138i
7.3 COCULTURE.....	143i
7.3.1 Identifying Soluble Mediators of Coculture Effect.....	144i
7.3.2 Optimizing the <i>In Vitro</i> Coculture System.....	147i
7.3.3 Chondrogenesis and Hypertrophy of Cocultured Hydrogels <i>In Vivo</i>	148i
APPENDIX A: MECHANICAL STIMULATION DURNING CHONDROGENESIS	150i
A.1 ABSTRACT	151i
A.2 INTRODUCTION.....	151i
A.3 RESULTS	154i
A.3.1 Bioreactor Design and Validation	154i
A.3.2 Mechanical Stimulation of Hydrogels with Encapsulated MSCs	154i
A.3.1 MATE Verification & Validation Testing	159i
A.3.3 Detecting Scaffold Degradation with MATE.....	161i
A.4 DISCUSSION	161i
REFERENCES.....	164i

LIST OF FIGURES

CHAPTER 1: INTRODUCTION & BACKGROUND

- FIGURE 1.1 SCHEMATIC REPRESENTATION OF CARTILAGE ENGINEERING
FIGURE 1.2 ENDOCHONDRAL OSSIFICATION
FIGURE 1.3 REGULATION OF TRANSIENT CHONDROCYTE PHENOTYPE DURING EMBRYONIC BONE DEVELOPMENT
FIGURE 1.4 CAVITATION DURING SYNOVIAL JOINT MORPHOGENESIS
FIGURE 1.5 ARTICULAR CARTILAGE FORM AND FUNCTION
FIGURE 1.6 CELL-MEDIATED, BIORESPONSIVE DEGRADABLE HYDROGEL FOR TISSUE ENGINEERED CARTILAGE
FIGURE 1.7 BIOACTIVE SCAFFOLDS

CHAPTER 2: MATERIALS & METHODS

- FIGURE 2.1 SCHEMATIC DIAGRAM OF PEPTIDE-CONTAINING PEGDA
TABLE 2.1 TAQMAN PRIMERS

CHAPTER 3: VISIBLE LIGHT PHOTOINITIATION OF MESENCHYMAL STEM CELL-LADEN BIORESPONSIVE HYDROGELS

- FIGURE 3.1 SPECTROPHOTOMETRIC ABSORBANCE OF PHOTOINITIATORS AND MACROMER FORMULATIONS
FIGURE 3.2 SCREENING DESIGN FOR LOWER VISIBLE LIGHT INITIATOR CONDITIONS.
FIGURE 3.3 SCAFFOLD PARAMETERS AND CYTOTOXICITY OF VISIBLE LIGHT INITIATION COMPARED TO UV LIGHT INITIATION
FIGURE 3.4 MSCs CHONDROGENESIS IN 10 % PEGDA SCAFFOLDS POLYMERIZED WITH VISIBLE VERSUS UV LIGHT
FIGURE 3.5 MSCs CHONDROGENESIS IN SIPN AND PEPTIDE CONTAINING PEGDA SCAFFOLDS

CHAPTER 4: A BIORESPONSIVE HYDROGEL TAILORED TO CHONDROGENESIS

- FIGURE 4.1 IDENTIFICATION OF MMP-7 AS CANDIDATE SUBSTRATE FOR BIORESPONSIVE HYDROGELS
FIGURE 4.2 DEGRADATION KINETICS OF BIORESPONSIVE HYDROGELS
FIGURE 4.3 COLLAGEN DEPOSITION IN BIORESPONSIVE HYDROGELS
FIGURE 4.4 PROTEOGLYCAN DEPOSITION IN BIORESPONSIVE HYDROGELS
FIGURE 4.5 GENE EXPRESSION IN BIORESPONSIVE HYDROGELS

CHAPTER 5: TEMPORAL REQUIREMENT FOR CHONDROGENIC FACTORS DURING NEOCARTILAGE FORMATION & DEVELOPMENT OF BIOACTIVE SCAFFOLD

- FIGURE 5.1 MSCs UNDERGO CHONDROGENESIS IN THE ABSENCE OF DEXAMETHASONE
FIGURE 5.2 WITHDRAWAL OF TGF- β 1 AFFECTS MATRIX DEPOSITION
FIGURE 5.3 TGF- β 1 WITHDRAWAL IMPACTS COLLAGEN BIOSYNTHESIS
FIGURE 5.5 PEGYLATED TGF β EFFECTIVE AS SOLUBLE MOLECULE BUT NOT WHEN IMMOBILIZED INTO SCAFFOLD

CHAPTER 6: MESENCHYMAL STEM CELLS AND ARTICULAR CHONDROCYTES INFLUENCE EACH OTHER DURING COCULTURE IN TISSUE ENGINEERING SCAFFOLDS

- FIGURE 6.1 IMMUNOHISTOCHEMICAL CHARACTERIZATION OF CHONDROGENESIS IN SIPN SCAFFOLDS
FIGURE 6.2 TEMPORAL UPREGULATION OF HYPERTROPHY MARKERS IN MSC BUT NOT AC SEEDED HYDROGELS
FIGURE 6.3 HUMAN ACs CANNOT INDUCE DIFFERENTIATION OF HUMAN MSCs IN COCULTURE IN THE ABSENCE OF CHONDROGENIC FACTORS
FIGURE 6.4 COCULTURE INHIBITS HYPERTROPHY IN HYDROGEL SCAFFOLDS
FIGURE 6.5 BIOCHEMICAL ANALYSIS OF MSC-AC COCULTURED HYDROGELS
FIGURE 6.6 TRANSWELL EXPERIMENTS DO NOT REPLICATE DIRECT COCULTURE IN HYDROGELS.
FIGURE 6.7 COCULTURE PHENOTYPE IS CONTRIBUTED LARGELY BY ACs
FIGURE S6.1 PTHrP INHIBITS CHONDROGENESIS

CHAPTER 7: CONCLUSIONS & FUTURE DIRECTIONS

- FIGURE 7.1 CASEIN ZYMOGRAPHY FOR MMP-7 ACTIVITY IN HYDROGELS
FIGURE 7.2 CHARACTERIZATION OF 'COLLAGENASE' SENSITIVE LGPA-PEGDA BIORESPONSIVE SCAFFOLD
FIGURE 7.3 DEGRADATION KINETICS FOR PDT-LAT
FIGURE 7.4 MMP-7 EXPRESSION FROM ARTICULAR CHONDROCYTE PHOTOENCAPSULATED IN PEGDA-BASED SIPN HYDROGELS
FIGURE 7.5 ESCs CELLS ARE ALSO CANDIDATES FOR MMP-7 BIORESPONSIVE SCAFFOLD
FIGURE 7.6 SCHEMATIC OF TGF- β 1 BIOACTIVE SCAFFOLD DESIGN POSSIBILITIES

APPENDIX A: MECHANICAL STIMULATION OF HYDROGELS IN MATE BIOREACTOR

- FIGURE A.1 THE MATE BIOREACTOR DESIGN
FIGURE A.2 MATERIAL TEST RESULTS OF THE MATE AND INSTRON
FIGURE A.3 IMPACT OF DYNAMIC COMPRESSION ON MSC CHONDROGENESIS IN HYDROGEL SCAFFOLDS OF DIFFERENT MODULUS
FIGURE A.4 TEMPORAL EFFECT OF DYNAMIC LOADING
FIGURE A.5 TIME DEPENDENT MATERIAL BEHAVIOR OF HYDROGELS DURING COLLAGENASE DIGESTION

LIST OF ABBREVIATIONS

ACs	Articular Chondrocytes
ACT	Autologous Chondrocyte Transplant
ADAMTS	A Disintegrin and Metalloproteinase with Thrombospondin Motif
ALP	Alkaline Phosphatase
ANOVA	Analysis of Variance
aPEG-SCM	Acrylate-PEG-Succinimidyl Carboxymethyl
aPEG-SVM	Acrylate-PEG-Succinimidyl Valerate
APMA	Aminophenylmercuric Acetate
BMP	Bone Morphogenetic Protein
BSA	Bovine Serum Albumin
CCM	Chondrocyte Conditioned Medium
cDNA	Copy Deoxyribonucleic acid
CFE	Colony Forming Efficiency
CFU-F	Colony-Forming Unit-Fibroblasts
CSF	Colony Stimulating Factors
DAB	3,3'-Diaminobenzidine
DMEM	Dulbecco's Modified Eagle's Medium
DMMB	1,9-Dimethylmethylene Blue
DNA	Deoxyribonucleic Acid
EBs	Embryoid Bodies
EGF	Epidermal Growth Factor
ELISA	Enzyme-Linked Immunosorbent Assay
ESCs	Embryonic Stem Cells
EthD-1	Ethidium Homodimer-1
EtOH	Ethanol
FBS	Fetal Bovine Serum
FGF	Fibroblast Growth Factor
FISH	Fluorescence <i>In Situ</i> Hybridization
FRET	Fluorescence Resonance Energy Transfer
GAG	Glycosaminoglycan
GDF	Growth and Differentiation Factor
HRP	Horse Radish Peroxidase

I2959	Irgacure TM 2959, 1-[4-(2-Hydroxyethoxy)-phenyl]-2-hydroxy-2-methyl-1-propane-1-one
IGF	Insulin-like Growth Factor
IGFBP	Insulin Growth Factor Binding Proteins
iPS	Induced Pluripotent Stem Cells
MHC	Major Histocompatibility Complex
MMP	Matrix Metalloproteinases
mRNA	Messenger Ribonucleic Acid
MSCs	Mesenchymal Stem Cells
NVP	1-Vinyl-2 Pyrrolidinone
OA	Osteoarthritis
PBS	Phosphate Buffered Saline
PEG	Poly (Ethylene Glycol)
PEGDA	Poly (Ethylene Glycol) Diacrylate
PHEMA	poly(hydroyl ethyl methacrylate)
PLA	poly(lactic acid)
PLE-PEGDA	MMP-7 Bioresponsive PEGDA Scaffolds PLELRA Peptide
PLGA	poly(lactic-co-glycolic acid)
PNIPAAm	poly(N-isopropylacrylamide)
PVA	poly(vinyl alcohol)
RGD	Peptide Sequence (Arginine-Glycine-Aspartic Acid) For Integrin Binding
RT-PCR	Reverse Transcriptase Polymerase Chain Reaction
SCF	Stem Cell Factor
SCNT	Somatic Cell Nuclear Transfer
sIPN	Semi-Interpenetrating Network
SSC	Saline Sodium Citrate
sc-PEGDA	Non-Degradable Bioresponsive Scaffold Containing MLLVSTPG Peptide
TEA	Triethanolamine
TGF- β	Transforming Growth Factor β
TIMPs	Tissue Inhibitors of Metalloproteinases
tRGD	Tethered RGD ligand
tTGF β	Tethered Transforming Growth Factor β
UV	Ultraviolet
VPLS-PEGDA	MMP-7 Bioresponsive PEGDA Scaffolds VPLSLTMG Peptide

ACKNOWLEDGMENTS

“THE OBSTACLE TO DISCOVERY IS THE ILLUSION OF KNOWLEDGE.”
– DANIEL BOORSTIN 1986

I spent many afternoons having lunch on the bench in the OHSU research park courtyard where this quote was engraved and feel as though it adequately summarizes my motivation to come to graduate school: to learn the fundamentals of biology and research so that I could develop an independent career in tissue engineering that pursues new knowledge with the potential to have an impact on human health. To this end I am greatly appreciative of my mentor Brian Johnstone and the Department of Orthopaedics & Rehabilitation for their support. The advice given to us as new graduate students was to pick a thesis lab by mentor not project. I was very fortunate to find both a wonderful advisor and project that I was passionate about in Brian’s lab. Brian’s style of mentorship provided guidance that was balanced by the freedom to grow and think independently. Most importantly however, Brian’s mentorship turned into a friendship that I will continue to value.

In addition to the mentorship that Brian provided, a number of OHSU faculty helped guide me through graduate school. Bill Horton, Hans Peter Bächinger, Jamie Fitzgerald, Owen McCarty, and Ronen Schwitzer generously formed my Thesis Advisors Committee. The discussion and ideas generated during this meeting challenged and inspired my work. Allison Fryer and David Jacoby both welcomed me into their lab for a rotation and supported my research career at OHSU. The faculty and staff of the CDB department accepted my non-traditional research project and helped to foster my education. To all these supporters, thank you.

My training as scientist at OHSU was beyond research in the laboratory. Course work, journal clubs and seminars were an essential part of acquiring the basic knowledge that allowed me to ask, answer and present scientific questions in a meaningful way. I thank the many teachers and course organizers who volunteered their time to teaching. An important lesson acquired from the culmination of these courses was that what we know about biology is not an assembly of facts, but rather an organization of knowledge attempting to get closer to the truth by asking the question in more appropriate ways.

The research projects presented in the following thesis were supported intellectually and through hands-on skills by a number of people to whom I greatly appreciate their collaboration. Both past and present members of the Orthopaedic Research group were patient teachers of research techniques and helped to maintain cell culture that supported my research. I would like to thank the following people not only for their assistance, but more importantly for their friendship: Cathleen Moscibrocki, Amanda Buxton, Sinan Ozgur, Jackson Jones, Ruth Gao, Daniel Walker and Linli Pao.

Collaborative research with Jennifer West's lab in the Department of Bioengineering at Rice University was essential to the success of my thesis research and provided a cross-disciplinary perspective essential to the field of tissue engineering. I sincerely appreciate Dr. West's support during my thesis, not only in technical expertise on material synthesis, but for embodying an attitude that 'anything can be done'. I also want to thank two members of her lab in particular, Logan Hsu and Melissa McHale, for their direct assistance in the bioresponsive and bioactive scaffold projects.

A number of other scientist supported individual aspects of my research projects and I would like to acknowledge each for their enthusiasm during the inevitable 'problem solving' phase of our work together. Trevor Lujan at the Legacy Biomechanics Lab worked together with me to acquire mechanical properties of hydrogels while developing a novel bioreactor that I hope will improve the tools we currently have as tissue engineers to investigate the role of mechanical stimulation in development. Amy Hanlon Newell in the OHSU Cytogenetics Lab who patiently helped me de-bug a technique to allow us to visualize both the extracellular matrix in neocartilage constructs by immunohistochemistry and the human chromosomes by FISH. Hans Peter Bächinger and his lab in the Shriners' Hospital for helping us synthesize and evaluate the peptides that formed the foundation of the biodegradable scaffold. Doug Keen, also in the Shriners' Hospital, for expertly assisted in visualizing the extracellular matrix of hydrogel constructs by electron microscopy, these images provided us with a new perspective on the structural concerns of cartilage engineering.

Last, but not least I would like to thank my husband and family for their encouragement and unrelentless support. To them I hope that I can inspire you in the same way that you have me.

ABSTRACT

Translating cartilage engineering from a research concept to a clinical therapy is presently hindered by an inability to create a neocartilaginous tissue that can functionally replicate native articular cartilage. The main challenges are promoting the formation of a tissue with the phenotypic and mechanical characteristics of articular cartilage in a clinically relevant format. Tissue engineering technology utilizes a three-dimensional scaffold for the delivery of cells and bioactive components in a coordinated fashion to promote tissue formation. The best combination and delivery mechanism for these three components has not yet been determined. The overall goal of my research was to incorporate the biological principles of cartilage development into novel systems that could improve the functional outcome of tissue engineered cartilage.

One objective was to address the biomechanical inferiority of neocartilage constructs relative to articular cartilage. The operating hypothesis for this work was that non-native assembly of the extracellular matrix in neocartilage constructs is a major factor contributing to their lack of mechanical integrity. I took two separate experimental approaches to promote an improved ultrastructural assembly of the cartilage matrix. The first was to develop a bioresponsive scaffold with degradation specifically tailored to chondrogenesis and matrix elaboration from the encapsulated cells. By characterizing chondrogenesis in poly(ethylene glycol) diacrylate scaffolds I identified matrix metalloproteinase-7 (MMP-7) as a candidate enzyme for modulating degradation. Mesenchymal stem cells (MSCs) encapsulated in scaffolds with MMP-7 degradable peptides produced a more extensive collagen II matrix that resulted in an increased dynamic compressive modulus. Furthermore, during the development of this bioresponsive scaffold, I validated a visible light photoinitiator system that facilitated faster and more complete formation of scaffolds using a technique that offers clinical advantages over ultraviolet photoinitiators. The second approach was to apply mechanical stimuli to the hydrogel

constructs during MSC chondrogenesis to drive an anisotropic assembly of the extracellular matrix. Preliminary evidence from this research indicated inhibition of MSC chondrogenesis with compressive stimuli during development and the project was not pursued in depth.

In parallel, I also tried to identify methods to promote a more hyaline cartilage phenotype from encapsulated mesenchymal stem cells following chondrogenic differentiation. This work involved evaluating the temporal significance of bioactive factors in maximizing production of the correct types of cartilage matrix molecules. I found that transforming growth factor- β (TGF- β) was essential to initiating MSC differentiation in scaffolds, and that its inclusion was required for at least three weeks to maximize collagen biosynthesis. However, dexamethasone, previously considered essential to MSC chondrogenesis, was dispensable in this culture format. Furthermore, excluding dexamethasone from the medium promoted a more hyaline cartilage phenotype in the neocartilage constructs. These data were used to design a bioactive scaffold with TGF- β tethered directly to the scaffold in a system that would be amenable to *in vivo* cartilage engineering. In a separate approach, I also developed a coculture system containing both MSCs and articular chondrocytes to investigate whether these cells would influence chondrogenesis. I found coculture promoted a synergistic relationship between the encapsulated cells and resulted in a neocartilage constructs with a hyaline cartilage phenotype.

Taken together the work presented in this thesis provides the foundation for novel approaches to improve cartilage engineered constructs. Bioresponsive and bioactive scaffolds, such as those detailed in this research, aim to incorporate aspects of developmental biology into system design to improve functional outcome of engineered cartilage. Furthermore, by modulating the culture conditions through coculture and temporal regulation of bioactive factors I have found ways to promote MSC-derived neocartilage constructs with a hyaline cartilage phenotype.

CHAPTER 1:
INTRODUCTION & BACKGROUND

1.1 TISSUE ENGINEERING FOR REPAIR OF ARTICULAR CARTILAGE DEFECTS

Knee osteoarthritis is the leading cause of disability in the United States. In a recent government study it was estimated that approximately one in two adults (46 %) will develop a symptomatic form of this disease¹. Osteoarthritis is characterized by degeneration of the cartilage that lines the articulating surfaces of diarthrodial joints. The etiology of this chronic condition is unknown, but in many cases is initiated acutely from a focal lesion to the articular cartilage. These partial thickness chondral defects have limited spontaneous repair due to the avascular nature of the tissue and subsequent lack of inflammatory response to injury²⁻⁴. Furthermore, this superficial damage to the articulating surface disrupts joint biomechanics and produces a metabolic change in the cells, such that cartilage degeneration is most often irreversible⁵⁻⁸. Presently there are very few therapeutic options available for the treatment of osteoarthritis. Given the high impact of this disease it is essential that more effective therapies be developed, especially those appropriate for early treatment and prevention of disease progression.

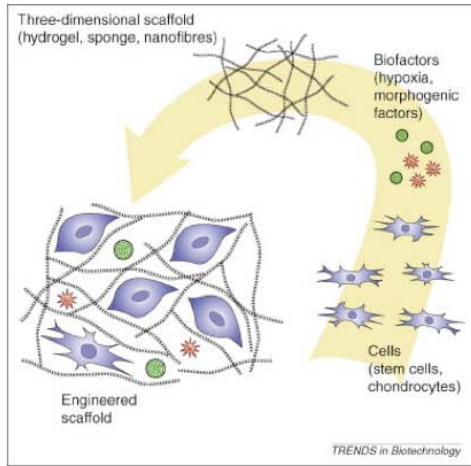
Tissue engineering is a form of regenerative medicine that may be appropriate for the early treatment of osteoarthritis through localized repair of focal lesions in articular cartilage. Cartilage engineering aims to provide a functional tissue regenerate to areas of damaged or diseased tissue that is capable of restoring joint biomechanics and preventing further tissue degeneration. The concept of tissue engineering arose in the early 1980s through a multidisciplinary effort to integrate the fields of engineering, biology and medicine. An application towards articular cartilage appeared in the literature approximately ten years later, motivated by the clinical significance of cartilage degeneration and the perceived simplicity of the tissue's composition. In recent years the challenges associated with reproducing a load-bearing tissue have been realized and engineering approaches are now trying to incorporate key

attributes of cartilage development to promote tissue formation with more native form and function.

The general approach for cartilage engineering is to use a three-dimensional scaffold to deliver cells and bioactive factors in a coordinated fashion to promote tissue regeneration (Figure 1.1). Cartilage is an avascular and aneural tissue containing only a single cell type, the chondrocyte, embedded within an extracellular matrix composed largely of collagen II and aggrecan. The complexity of engineering cartilage tissue lies in generating a neocartilaginous structure with biomechanical properties sufficient to withstand the high stresses associated with joint motion. The strength in native articular cartilage is derived from the composition and structural organization of this extracellular matrix. To date neocartilage has been unable to correctly reproduce the extracellular matrix of articular cartilage and constructs remain biomechanically inferior.

The inability of neocartilage constructs to functionally replicate articular cartilage is due largely to the challenge associated with regulating the metabolic activity of the encapsulated cell. More specifically, the engineered system needs to promote encapsulated cells to make ample quantities of the correct type of extracellular matrix. These matrical components then need to be assembled with the appropriate ultrastructural organization for biomechanical integrity. Designing a scaffold that both facilitates tissue formation, but does not interfere with matrix assembly, is a central problem in cartilage engineering. The shortcomings associated with cartilage engineered constructs developed to date have prompted a new level of sophistication in scaffold design: recent efforts are focused on incorporating bioactive and bioresponsive elements into the scaffold to promote and/or modify cellular behavior. *The overall goal of my research was to incorporate the biological principles of cartilage development to create novel strategies for improving tissue engineered cartilage.*

(A)



(B)

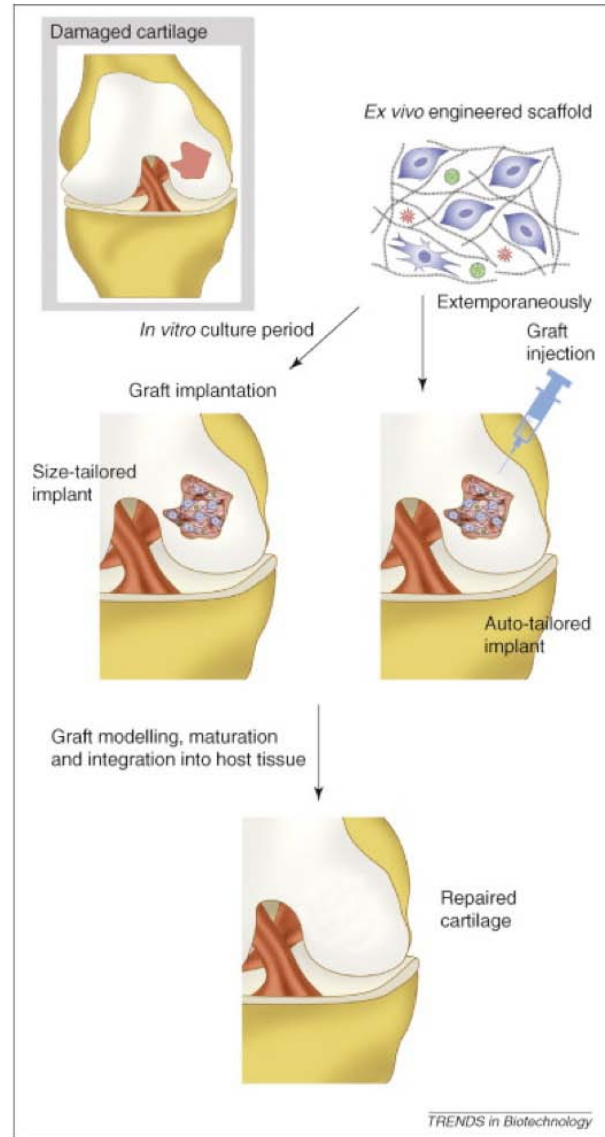


FIGURE 1.1 – SCHEMATIC REPRESENTATION OF CARTILAGE ENGINEERING⁹, reproduced with permission from Vinatier *et al* © 2009, Elsevier. (A) Interaction of cells, scaffold and bioactive factors. (B) Schematic representation of the implantation of engineered scaffolds. A focal cartilage lesion is depicted in the upper left insert, followed by two possible options for applying cartilage-engineered scaffolds. In the first option (shown on the right), injectable scaffolds are directly applied to the cartilage defect. In the second approach (shown on the left), engineered scaffolds are synthesized *ex vivo* and after a variety of specialized culture protocols, scaffolds are transplanted into the lesion.

1.2 SYNOVIAL JOINT FORMATION

Synovial, or diarthrodial joints, are the most common movable joint in the skeleton. Structurally this joint is composed of two opposing bones, lined by articular cartilage and enclosed in a synovial membrane. A variety of other tissue structures such as ligaments, tendons, and muscles help facilitate motion. Synovial joints arise through coordination of two distinct processes: (i) formation of long bones through endochondral ossification, and (ii) cavitation during which the joint space is formed by physical separation of the long bone elements. Surprisingly, to date, relatively little is known about the process of synovial joint formation during embryogenesis, or how the various elements of the joint capsule become established during fetal development.

1.2.1 Endochondral Ossification

The majority of details surrounding joint formation are understood in the context of long bone formation during endochondral ossification (Figure 1.2). In this process mesenchymal cells condense and undergo chondrogenic differentiation to form a cartilaginous outline of the future bone. Chondrocytes within this anlagen organize into morphologically and functionally distinct domains corresponding to their maturation state. Pools of proliferating chondrocytes are distinguished by their flattened morphology and are responsible for elongating the bone. In a complex regulatory process controlled in part by the feedback loop between Indian hedgehog (IHH) and parathyroid hormone related protein (PTHrP), chondrocytes exit the proliferating pool and transits towards a hypertrophic state (Figure 1.3). PTHrP expression from the perichondrium is believed to be directly responsible for inhibiting maturation of chondrocytes in the proliferating pool^{10,11}, while IHH expression in the prehypertrophic chondrocytes acts through molecular mediators Gli and Patch in a poorly understood manner to activate PTHrP in the perichondrial cells. Hypertrophic chondrocytes represent the terminal maturation state of these cells; they are

characterized by their enlarged round shape and expression of type X collagen. Hypertrophic chondrocytes undergo apoptosis and are replaced by bone and the marrow cavity.

The transient chondrocytes located in the epiphyseal cartilage of long bones are phenotypically distinct from articular chondrocytes lining the distal end of long bones. Articular chondrocytes are the single cellular component of articular cartilage and represent a stable phenotype characterized by the production of collagen II, but not collagens I or X. The origin of the articular chondrocyte and molecular mechanisms governing articular cartilage development are not well-understood¹²⁻¹⁵.

1.2.2 Joint Specification at the Interzone

The location of the presumptive joint is the interzone, a distinct population of compact cells that create a disruption in the mesenchymal condensate¹⁶ (Figure 1.4). The interzone is believed to generate all the various structures of the synovial joint, including articular cartilage^{13,17}. The functional role of the interzone was identified in early experiments demonstrating that microsurgical dissection of this region led to joint ablation *in ovo*¹⁸. It remains unclear which cells form the interzone region. One model suggests that all the cells in the mesenchymal condensate are competent to become interzone cells and that morphogenetic gradients are locally established to direct cells towards the interzone phenotype. Alternatively, some suggest that the interzone cells are a unique, pre-specified cell type. In support of this Holden *et al* showed that if you remove the developing radius and ulna, the interzone will still form¹⁸. More recently, Pacifici *et al* used DiI fate mapping in the embryonic chick to show that the interzone region includes a population of peri-joint cells that migrate into the incipient joint domain¹⁷. Together these data emphasize that the origin and phenotype of the interzone cells is complex.

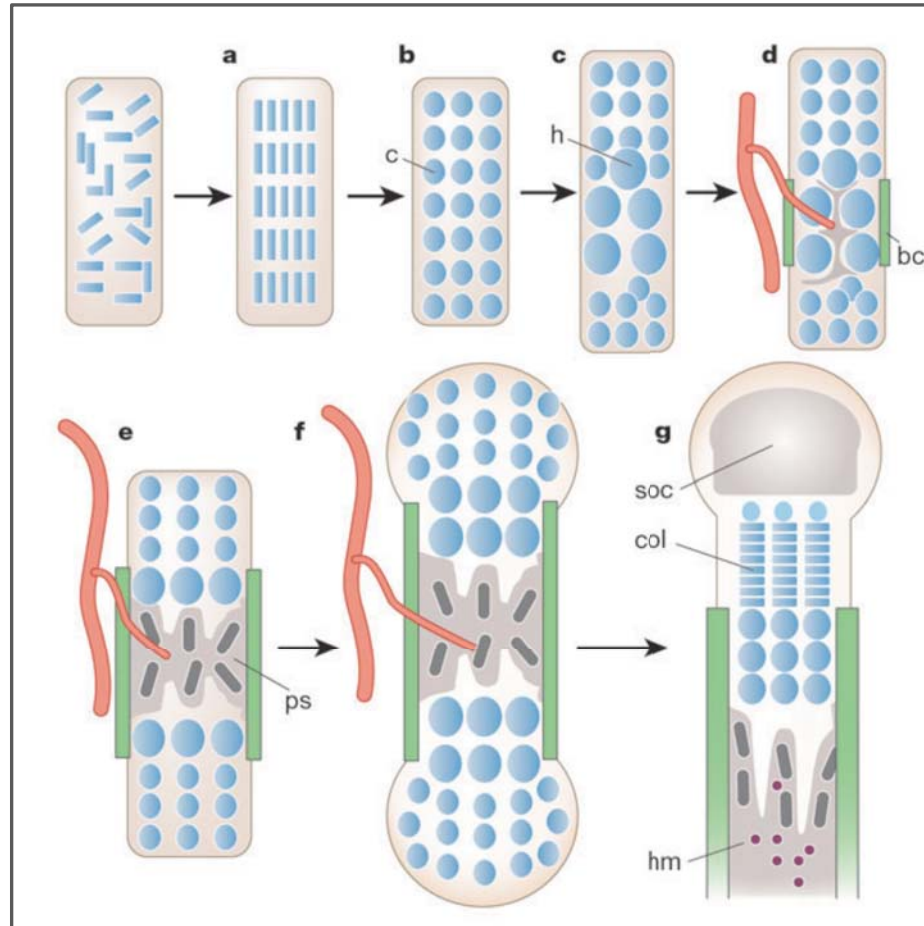


FIGURE 1.2 – ENDOCHONDRAL OSSIFICATION¹⁹, reproduced with permission from Kronenberg *et al* © Nature Publishing Group. (a) Mesenchymal cells condense. (b) Cells of condensations become chondrocytes (“c”). (c) Chondrocytes at the center of condensation become hypertrophic (“h”). (d) Perichondrial cells adjacent to hypertrophic chondrocytes become osteoblasts, forming bone collar (“bc”). Hypertrophic chondrocytes direct the formation of mineralized matrix, attract blood vessels, and undergo apoptosis. (e) Osteoblasts of primary spongiosa accompany vascular invasion, forming the primary spongiosa (“ps”). (f) Chondrocytes continue to proliferate, lengthening the bone. Osteoblasts of primary spongiosa are precursors of eventual trabecular bone; osteoblasts of bone collar become cortical bone. (g) At the end of the bone, the secondary ossification centre (“soc”) forms through cycles of chondrocyte hypertrophy, vascular invasion and osteoblast activity. The growth plate below the secondary centre of ossification forms orderly columns of proliferating chondrocytes (“col”). Hematopoietic marrow (“hm”) expands in marrow space along with stromal cells.

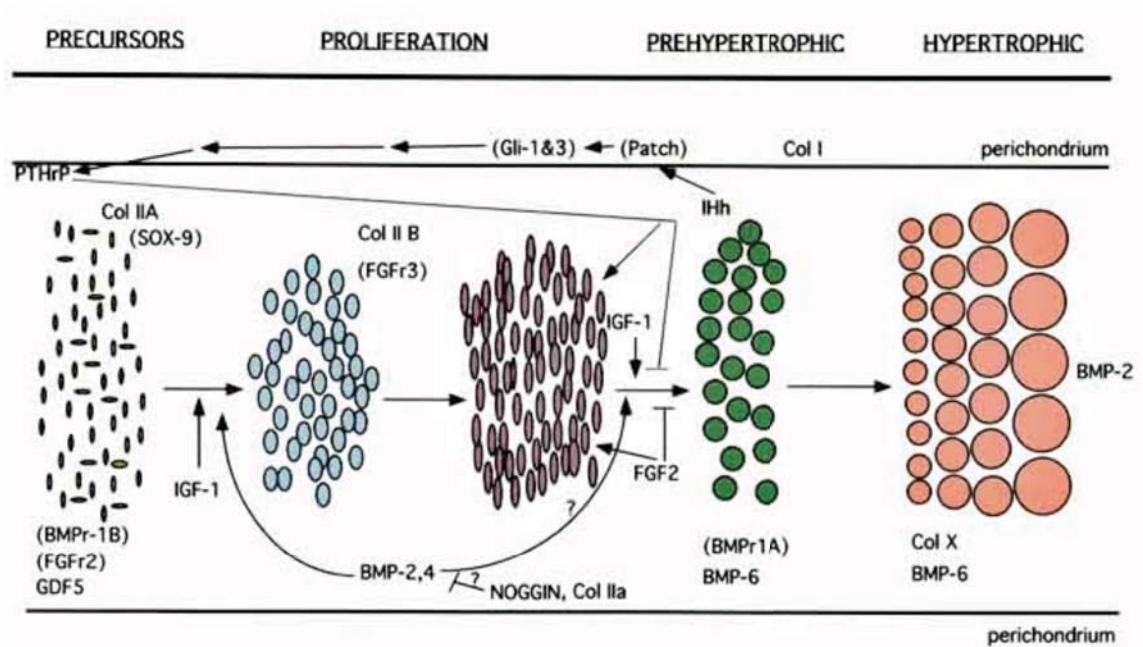


FIGURE 1.3 – REGULATION OF TRANSIENT CHONDROCYTE PHENOTYPE DURING EMBRYONIC BONE DEVELOPMENT, reproduced with permission from Sandell & Adler © 1999 Frontiers in Bioscience. IGF-1 = Insulin-like growth factor 1, PTHrP = Parathyroid Hormone related protein, Col IIA = Collagen IIA, Col IIB = Collagen IIB, BMPr = Bone Morphogenetic Protein receptor, FGFr = Fibroblast Growth Factor receptor, Ihh = Indian Hedgehog, BMP = Bone Morphogenetic Protein.

Although the origin of the interzone cells is not well understood a number of genetic and molecular markers have emerged to distinguish these cells from the surrounding transient chondrocyte population. As the interzone region becomes established within the mesenchymal condensate these cells lose expression of chondrogenic markers collagen II and SOX9, and begin to express a set of phenotypic markers now associated with the interzone: growth and differentiation factor-5 (GDF5)^{20,21}, Wnt9A (previously named Wnt14)²², chordin/noggin and CD44²³⁻²⁵. *In situ* hybridization localizing GDF5 mRNA transcripts is perhaps the most classic marker of the interzone, yet the role of GDF5 in joint formation is not clearly established. Interestingly, although GDF5 is expressed at all synovial joints, only a subset of joints (carpals, phalanges and tarsals) do not form in GDF5 knockout mice²⁰. Furthermore GDF5 protein is not localized specifically to the interzone, rather throughout the mesenchymal condensate suggesting that GDF5 is unlikely to contribute directly to joint formation but rather acts indirectly through paracrine signaling²⁶. Canonical Wnt signaling plays a role in both the early specification of the interzone²² and in maintaining joint cell fate^{13,27}. Chordin and noggin are both bone morphogenetic protein (BMP) antagonist required to suppress BMP activity in the interzone. Chordin expression appears restricted to the interzone²⁸ region in developing limbs, and joint development is not initiated in noggin null mice²⁹. Furthermore, overexpression of BMP using BMP2/4 soaked agarose beads, prevented joint formation³⁰. CD44 is the primary cell surface receptor for hyaluronan, which is expressed by cells at the interzone during joint formation and will be discussed further below.

Differential expression of matrix elements is also emerging as a technique for distinguishing the interzone cells from the cartilaginous anlagen and may help to map the cells that will continue to form articular cartilage. In the interzone, collagens type I, III and V are synthesized, while collagen II is found only in the epiphyseal cartilage during limb development or articular cartilage following joint formation³¹⁻³³. Matrilin-1 is expressed only in epiphyseal cartilage and not in either the interzone or articular cartilage³⁴. Conversely, versican is found in

the interzone and articular cartilage but never in the transient cartilage of the epiphyseal plate³⁵. Doublecortin, a microtubule-binding protein originally noticed for its role in migration and differentiation of neurons, has recently been described as a marker specific to articular chondrocytes³⁶.

1.2.3 Cavitation

Separation of the long bone rudiments and formation of the synovial capsule occurs at the interzone region through a process termed cavitation. A number of factors have been proposed to contribute to the process of cavitation including cell death, differential synthesis of matrix elements, and mechanical stimulation. Although frequently cited, evidence in support of apoptosis during joint formation is limited and based on early studies identifying dead cells in the joint space^{37,38}. More recent reports claim the extent of cell death is minimal or non-existent^{14,15}, finding no TUNEL-positive cells at the time of cavitation^{39,40}. Despite the scientific trend to disregard the role of apoptosis in joint formation, it may be that the process of cavitation is not conserved across all joints and/or all species (Johnstone Lab, unpublished data).

An alternative view of cavitation involves differential growth and remodeling of the extracellular matrix at the presumptive joint. This model encompasses data citing an increase in cell proliferation^{23,39}, matrix remodeling through selective expression of metalloproteinase enzymes³², and differential cartilage matrix synthesis to facilitate shaping the growing articular cartilage^{25,33}. Presently the strongest experimental data exists for that latter mechanism: multiple groups have demonstrated a selective increase in the local cellular capacity to synthesize hyaluronan^{23,25,41}. As discussed above, CD44, the principal cell surface receptor for hyaluronan, is preferentially localized to the interzone area. Expression of CD44 and hyaluronan is believed to influence cell adhesion and separation during cavitation. Increased hyaluronan synthesis prior to cavitation has been attributed to both selective activation of the MEK-ERK pathway⁴²⁻⁴⁴ and the application of mechanical stimulation⁴⁵⁻⁴⁷.

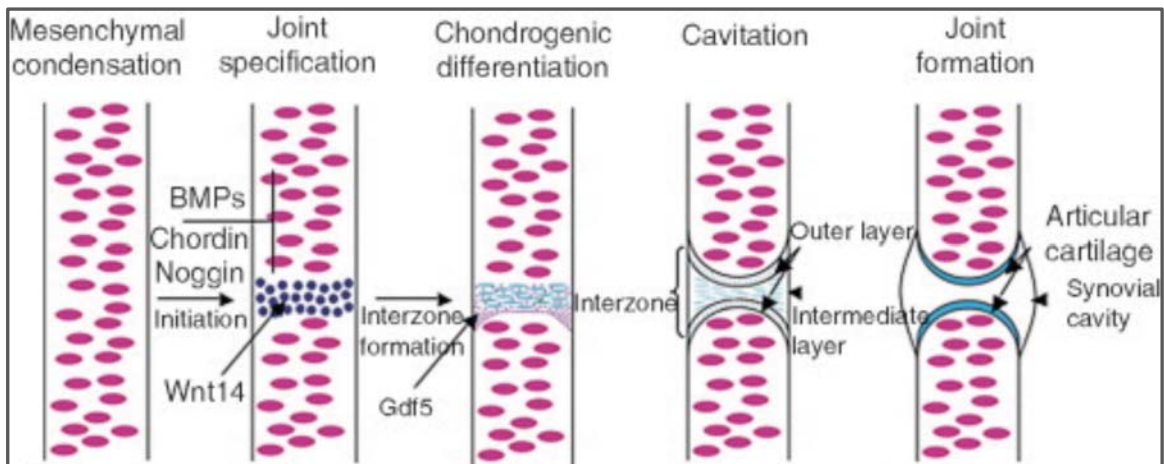


FIGURE 1.4 – CAVITATION DURING SYNOVIAL JOINT MORPHOGENESIS¹², reproduced with permission from Khan *et al* © 2007, Elsevier. Within an initial mesenchymal condensation, an unknown trigger stimulates wnt14 expression at the site of incipient joint formation. GDF5 is, thereafter, expressed and the cells take on an elongated morphology and significantly reduce sox9 and collagen type II expression. BMP antagonists chordin and noggin are expressed in the interzone cells and act to stabilize joint-inducing positional cues. The interzone adopts a three-layered structure (in the case of long bone elements) that undergoes separation or cavitation on mechanically induced synthesis of hyaluronan. The morphogenesis of the functional joint organ results in articular cartilage lining the ends of skeletal elements, which are bathed in synovial fluid, produced by a synovial membrane, and encased within a fibrous capsule.

The importance of embryonic motion to joint formation in the skeleton has been appreciated for a long time, primarily through paralysis experiments in the embryonic chick. Experiments using surgical techniques or neuromuscular inhibitors to immobilize the joint *in ovo* have demonstrated that blocking movement prior to, or during cavitation, prevents joint formation^{48,49}, while immobilization after cavitation causes paralysis due to cartilaginous fusion of the articulating surfaces^{50,51}. Similarly, *ex vivo* tests with 5-7 day old embryonic chick joint explants demonstrated fusion in the absence of simulated movement⁵². Although these experiments explore the temporal significance of motion during joint formation, details revealing the molecular mechanisms associated with transducing mechanical stimulation remain limited. As mentioned previously, data from Dowthwaite *et al*^{41,45,46} indicate that activation of hyaluronan synthesis is one mechanism through which mechanical stimulation may contribute to joint formation. More recently, Kahn *et al* have demonstrated that muscle contraction can regulate β -catenin activation (canonical Wnt) in the interzone during joint formation⁵³. Using three murine models that lack the ability to contract musculature, contrasted with a muscleless mouse, they show that Wnt signaling is needed to maintain the plasticity and proliferative abilities of the interzone cells prior to cavitations. Interestingly, loss of joint formation did not occur with 100 % penetrance in the absence of motion. In some joints, such as the knee and metacarpophalangeal (finger), β -catenin was elevated even without joint motion producing normally formed joints.

Together these data emphasize the complexity of joint formation and the difficulty in determining the developmental origin of cells contributing to articular cartilage. Presently it is unclear how the various signaling pathways and mechanical stimulation coordinate to contribute to the formation of articular cartilage. Advancing this basic science will be useful for improving cartilage engineering technology.

1.2.4 Metalloproteinases in Development

Remodeling of the cartilage matrix is an essential component for limb development and articular cartilage maturation. During endochondral ossification the cartilage anlagen is replaced by a vascular network and bony extracellular matrix following extensive remodeling. Similarly, during postnatal development articular cartilage matrix acquires a specific anisotropic architecture that confers biomechanical function (see section 1.3.2) and both new matrix synthesis and matrix degradation are parts of this process. Metalloproteinases represent of a large family of extracellular proteases capable of cleaving a number of the matrical components in cartilage. The metalloproteinase family includes both matrix metalloproteinase (MMP) and a disintegrin and metalloproteinase with thrombospondin motif (ADAMTS) enzymes. Metalloproteinase enzymes can broadly be classified according to their substrate specificity: the activity of a few of these enzymes with central roles in skeletogenesis will be highlighted below^{8,54}.

Collagenases are a category of metalloproteinase enzymes capable of cleaving the triple helical collagen fiber at a specific Gly-Leu/Gly-Ile bond. In human cartilage, this activity is principally mediated by MMPs-1,-8, and -13. MMP-13 is synthesized almost exclusively by the chondrocyte and is highly specific for type II collagen^{7,8}. Although classically associated with the hypertrophy of the chondrocyte, MMP-13 shows biphasic expression that is also observed during the proliferative phase⁵⁵. The critical nature of MMP-13 during skeletal development was demonstrated by expansion of the hypertrophic cartilage zone and increased trabecular mass in MMP-13 null mice⁵⁶.

After the collagen fibril has been initially cleaved by the collagenases, the gelatinases (MMP-2 &-9) are proteolytically active against denatured collagen. MMP-2 is perhaps the most widespread of all MMPs and made at relatively high and constant levels by the chondrocyte⁵⁷. MMP-2 null mice present with skeletal defects, perhaps due in part to the role of MMP-2 in activating proMMP-13⁵⁸. Both MMP-2 and -9 also have substrate activity towards aggrecan⁵⁹.

The ADAMTSs were first identified in 1997 (Kuno Nakashima Fujiki. 1997 JBC) for their ability to cleave aggrecan (ADAMTS-1, -4, -5, -8, -9, -15), but are now recognized to have a more broad activity^{7,60}. The role of ADAMTSs in development and disease is slowly being established, but progress has been made with respect to osteoarthritis pathogenesis. The cleavage products of ADAMTS-4 and -5 have consistently been identified in human osteoarthritis tissue samples⁶¹⁻⁶³ and are the most active aggrecanases⁶⁴. Significantly, mice with an inactive form of ADAMTS-5 show decreased cartilage loss from osteoarthritis⁶⁴. The spatiotemporal activity of ADAMTS-4 and -5 during osteoarthritis have not been clearly established; however, the presence of aggrecan protects collagen II from enzymatic cleavage *in vitro*⁶⁵ and therefore aggrecanases may have a critical role in early disease pathogenesis.

Another class of metalloproteinases involved in cartilage development are the N-terminal procollagen proteinases, which include ADAMTS-2,-3,-14 and MMP-3,-9,-7,-13. Removal of the both the N- and C-propeptides from fibrillar collagens (e.g. types I, II, and XI) is essential for efficient collagen assembly *in vivo*⁵⁹. Additionally, growth factors BMP-2 and transforming growth factor- β 1 (TGF- β 1) have been shown to bind to the extra-helical region of the collagen IIA propeptide, suggesting cleavage may also regulate availability of these bioactive factors in cartilage⁶⁶.

Metalloproteinase enzymes are tightly regulated at both the protein and gene level; misregulation of these enzymes is associated with cartilage degeneration observed in diseases such as osteoarthritis and rheumatoid arthritis^{8,54}. Enzymatic activity is controlled at the protein level by interfering with a conserved motif containing a catalytic zinc ion either through the presence of a prodomain or by the endogenous tissue inhibitors of metalloproteinases (TIMPs). Activation of the proenzyme for most of the cartilage related MMPs occurs in the extracellular space following cleavage of the prodomain either by serine proteinases or other activated MMPs. Proteolysis often occurs in the immediate vicinity of the cell to localize and concentrate the activated enzyme towards a specific substrate⁸. TIMPs non-covalently bind to the activated

metalloproteinases in a 1:1 ratio to inhibit their activity. Four different TIMPs have been identified and are spatiotemporally controlled during developments and disease to modulate cartilage homeostasis⁶⁷. MMPs are also tightly regulated at a transcriptional level to control gene activity in a tissue-specific manner.

1.3 STRUCTURE & FUNCTION OF ARTICULAR CARTILAGE

1.3.1 Types of Cartilage

There are three main types of cartilage – elastic, fibrous, and hyaline - that serve a variety of diverse structural roles throughout the body. The structural attributes of this tissue are the product of an extensive extracellular matrix: the content and assembly of this matrix distinguish the different cartilages from each other. Elastic cartilage is found in the outer ear, larynx and epiglottis. It is defined by the large amount of matrical elastin, which provides a flexible/bendable characteristic. Fibrocartilage resembles a mixture of fibrous, scar-like tissue and the classic cartilage matrix. It is the only cartilage that contains type I collagen and is found in the meniscus, annulus fibrosus of the intervertebral disc, temporomandibular joint, and pubic symphysis. Hyaline cartilage is composed predominately of type II collagen and sulfated proteoglycans. Articular cartilage is a hyaline-type cartilage located on the ends of bones in synovial joints. Hyaline cartilage is also found in the rib cage, nose, bronchial tubes, and trachea.

The hyaline matrix of articular cartilage assembles with a distinct, anisotropic ultrastructure to create a load-bearing surface capable of lubricating the articulating surfaces and absorbing stresses produced during joint movement (Figure 1.5A). Collagens, predominantly type II, provide a structural framework for articular cartilage and entrap both proteoglycans and chondrocytes within a fibril matrix. Collagen accounts for approximately 75 % of the dry weight of articular cartilage and 90 – 95 % of this collagen is type II⁶⁸. Smaller amounts of types IX and XI collagen are associated with the type II collagen fibrils and contribute to their assembly. Type

VI collagen is also present in the extracellular matrix of articular cartilage and is concentrated around the chondrocyte in a domain referred to as the chondron. The chondron is postulated to create a local microenvironment that protects the chondrocyte during load⁶⁹.

Proteoglycans, specifically aggrecan, account for the majority of the remaining dry weight in articular cartilage. Aggrecan, a large proteoglycan, is composed of a core protein that is heavily glycosylated by the covalent attachment of glycosaminoglycan (GAG) chains. Glycosaminoglycans are linear polysaccharides containing an amino and uronic acid or galactose; most common to cartilage are hyaluronan, chondroitin sulfate, and keratan sulfate. Aggrecan forms large aggregates with hyaluronan through non-covalent interactions that are stabilized by link protein. Smaller proteoglycans such as biglycan, decorin, cartilage oligomeric matrix protein, and versican are also present in articular cartilage with a much smaller frequency. Data suggest these proteoglycans may serve specific roles in collagen fibrillogenesis and ultrastructural organization of the cartilage matrix^{70,71}, the details of which are still being established.

1.3.2 Anisotropic Assembly and Biomechanical Properties of Articular Cartilage

The protein components of the solid matrix are assembled with an anisotropic ultrastructure that confers mechanically distinct properties onto the different domains of articular cartilage⁷² (Figure 1.5A). The most superficial layer of cartilage, the surface zone, occupies 10 - 20 % of the tissue's full thickness. The proteoglycan content of the superficial zone is relatively low and collagen fibrils comprise close to 85 % of the total dry weight. In this zone the collagen fibers are oriented parallel to the articulating surface to provide resistance to shear and tensile strains⁷³⁻⁷⁵. Cartilage is strongest in tension and the tensile modulus of healthy human articular cartilage has been measured between 5 - 40 MPa depending on the location of the tissue specimen⁷⁴⁻⁷⁶. Superficial chondrocyte morphology is also unique in that the cells possess a flat rather than rounded shape.

The middle, or transitional zone, of articular cartilage is characterized by a crosslinked network of collagen fibers, random distribution of round chondrocyte and high concentration of proteoglycans. Below the transitional zone, proximal to the subchondral bone, is the deep zone. The deep zone occupies approximately 20 - 30 % of the total thickness of articular cartilage. Here collagen fibrils are oriented perpendicular to the articulating surface and round-shaped chondrocytes align into columns alongside the collagen fibers. Together the deep and middle zones provide cartilage with its ability to resist compressive strains. Depending on joint architecture, the compressive modulus may be a full one to two orders of magnitude smaller than the tensile modulus⁷⁵.

The compressive resilience of cartilage is a complex, dynamic relationship between the assembly of the extracellular matrix and the fluid flow dynamics under load (Figure 1.5). The high concentration of proteoglycans in the middle and deep zone of cartilage impart a large net negative charge to the extracellular matrix due to the sulfate groups located in the GAG chains. This negative charge creates a swelling pressure that draws a saline rich (Na^+) interstitial fluid into the collagen matrix to create a charge-balanced, thermodynamically favorable environment. In an unstressed state, the equilibrium fluid content of cartilage is estimated at 65 - 85% of the wet weight of the tissue⁷⁶. Compressive loading pressurizes the interstitial fluid and causes flow out from and laterally within the surface zone matrix. The collagen fibril orientation and high proteoglycan concentration in the middle and deep zones make these regions impermeable to fluid flow and provide cartilage with its compressive resilience. The distinct stress relaxation behavior of cartilage is the result of this fluid redistribution and creates a non-linear viscoelastic response⁷⁷⁻⁸⁰. Following removal of a compressive load, cartilage recovers by imbibition of fluid to restore the equilibrium condition of the unstressed state. Full tissue recovery is a time dependent process (creep). The continual stress of daily activity in highly loaded joints can cause a volumetric change in the articular cartilage that can reduce thickness by up to 0.6 mm⁸¹.

The interstitial fluid component of articular cartilage not only facilitates shock absorbance under load but also provides excellent lubrication properties to the articulating joint. The interstitial fluid of the diarthroidal joint (synovial fluid) is a saline-based substance rich in hyaluronan, a glycosaminoglycan, and lubricin. Together they give synovial fluid a viscous consistency that significantly enhances lubrication. Synovial fluid components are made by surface zone chondrocytes and also by fibroblasts in the intimal lining of the synovial membrane that encases the joint. Production of synovial fluid by these fibroblast is essential to the maintenance of healthy joint mechanics and can be adversely effected by rheumatoid diseases that attack synoviocytes⁵.

During normal joint motion the interstitial synovial fluid flows out from the surface zone of cartilage: due to the orientation of collagen fibers in the middle and deep zone of cartilage, fluid dynamic models assume minimal flow laterally or deep within cartilage during compressive loading. Since fluid can not exit cartilage directly beneath the contact point of load the fluid “squeezes” out directly adjacent to the contact point and generates a thin film improving lubrication⁸² (Figure 1.5B). Cyclic dynamic loading is most effective at producing this thin film layer and therefore supports optimal joint lubrication. Under cyclic dynamic loading conditions with a normal stress of 500 kPa, the coefficient of friction for articular cartilage is 0.0026^{77,83}. This compares with 0.3 - 0.5 for oil lubricated metal, and 0.05 - 0.1 for Teflon.

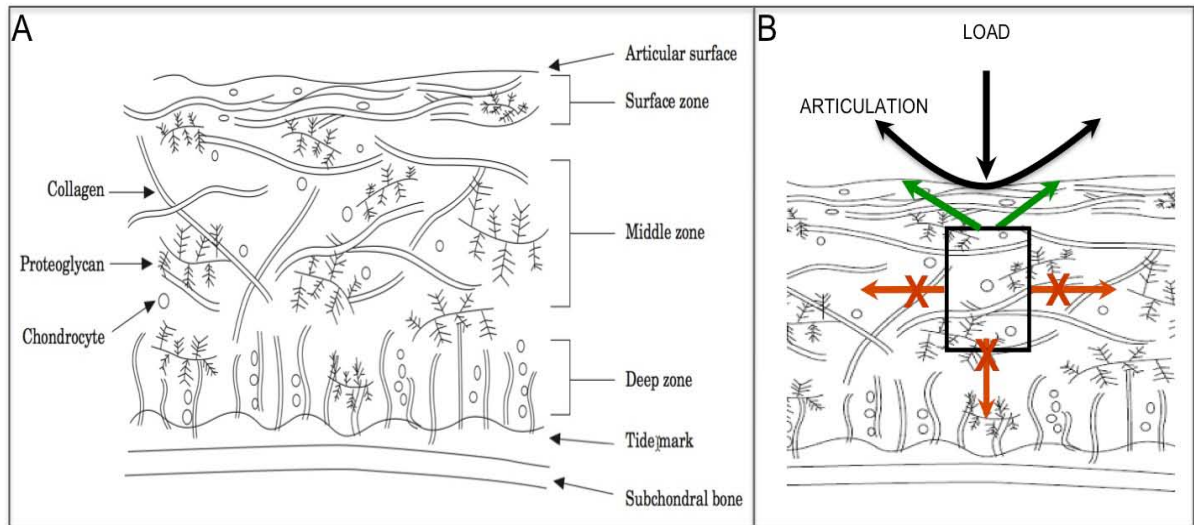


FIGURE 1.5 – ARTICULAR CARTILAGE FORM AND FUNCTION. (A) Schematic diagram of depth dependant anisotropy in articular cartilage. (B) Squeeze film theory of lubrication during articulation. Adapted with permission from ⁷⁶Setton *et al* © 1999, Elsevier.

1.4 CELL CHOICES IN CARTILAGE ENGINEERING

The goal of cartilage engineering is to functionally replicate articular cartilage by placing cells onto/in a scaffold to facilitate tissue growth. One strategy towards achieving this goal would be to mimic the developmental pathway of articular cartilage. However, as described above, neither the process of joint formation nor the precise origin of the articular chondrocyte are well understood. Consequently, one could envision using either articular chondrocytes or known chondrogenic progenitors such as the mesenchymal stem cell (MSC) in cartilage engineering applications. The clinical history and limitations of each of these cell types will be discussed further below. More recently embryonic stem cells (ESCs) and induced pluripotent stem cells (iPS) have also become available for research purposes.

1.4.1 Articular Chondrocytes

Based on the unique phenotype of articular chondrocytes, and the limited capacity of cartilage for repair, a surgical technique was developed in which autologous chondrocytes are transplanted into chondral defects to facilitate cartilage repair⁸⁴⁻⁸⁶. The technical basis of this procedure was first developed in a rabbit model of cartilage defects⁸⁷ and later translated into patients by Brittberg *et al* in 1994⁸⁸, where it has subsequently gone through three generations of improvements. The 1st generation of this technique involved harvesting cartilage tissue in a first operation, isolating resident chondrocytes (which represent only 2 – 5 % of the volume of cartilage) and then expanding the cells *in vitro* to obtain the large number of cells requisite to facilitating tissue repair. In a second operation the expanded chondrocytes are transplanted back into the chondral defect of a patient and secured into place by a periosteal flap sewn over the cartilage defect⁸⁸. Although autologous chondrocyte transplantation (ACT) procedures have reported to significantly reduce pain post-operatively^{89,90}, there are a number of significant drawbacks with both the procedure and the repair tissue^{91,92}. These problems include the requirement for two surgeries. In the first operation, chondrocytes are harvested for expansion

from a “non-weight” bearing location in the joint. Studies have subsequently shown that this harvest site can alter normal joint biomechanics⁹³, posing an increased risk of osteoarthritis⁹⁴. Additionally, in the majority of cases, the repair tissue that forms at the transplantation site resembles a fibrous scar tissue, fibrocartilage, rather than native hyaline cartilage⁹⁵⁻⁹⁷. The fibrocartilage repair tissue is estimated to be up to ten times weaker in compression than hyaline cartilage^{68,98}. Presently it is unclear what leads to the phenotypic change in the neotissue graft, but it has been proposed that type I collagen production is due to the dedifferentiation of chondrocytes that occurs during monolayer expansion *in vitro*⁹⁹⁻¹⁰².

A 2nd generation of autologous chondrocyte transplantation technology was developed to include scaffolds that replaced the need for the periosteal flap⁸⁵ and provided a structural framework for matrix elaboration. However, many of the initial limitations associated with cell sourcing and two surgical procedures remained. Third generation therapies are less easily summarized as they include the use of allogeneic chondrocytes, pre-culture and biomechanical stimulation of chondrocyte-containing scaffolds, and matrices that may have chondro-conductive and chondro-inductive properties⁸⁴. There is very limited clinical data on the use of the 3rd generation therapies. Cartilage repair with cell types other than chondrocytes, gene therapies, or more sophisticated scaffolds such as bioactive or bioresponsive scaffolds are considered 4th generation or ‘emerging’ therapies^{86,103}.

1.4.2 Mesenchymal Stem Cells

Mesenchymal stem cells (MSCs) are chondroprogenitors that offer a potential alternative to chondrocytes in cartilage engineering applications^{94,104-107}. These cells represent an adult derived multipotent cell population that can be isolated from multiple tissue sources including bone marrow^{108,109}, adipose tissue¹¹⁰, periosteum^{111,112}, and the synovial lining^{113,114}. The classic definition of an MSC includes the ability to differentiate towards adipose, cartilage, and bone tissues *in vitro*^{115,116}. Differentiation towards other cell types including tendon/ligament¹¹⁷,

muscle¹¹⁸, cardiac¹¹⁹, neuronal¹²⁰ and stromal¹²¹ have been reported, but it is unclear as to whether the MSCs engraft and differentiate directly into these cell types, or stimulate a repair response within these tissues¹²²⁻¹²⁴.

Part of this debate encompasses the controversy over the appropriate terminology to be used when describing these adult tissue-derived stem cells, with disagreement over the ‘stemness’ of the subpopulations¹²⁵⁻¹²⁷. The basis for most studies is to first plate mononuclear cells and look for colony formation, hence the original name of colony-forming unit-fibroblasts (CFU-F) given by Friedenstein *et al.* Non-adherent cells are removed with media changes. Colony forming efficiency (CFE) is one measure of the purity of this population. The population of MSCs in any tissue is small and decreases with age: for example, the adherent population of cells represents at most 1/1000 to 1/2000000 of the initial mononuclear cells of bone marrow¹²⁸ and this population is heterogeneous. With passage, a more homogenous population of cells is seen. This is the population used by many groups, including ours, for stem cell-related tissue engineering. Caplan *et al* popularized the term mesenchymal stem cell and this has become the most commonly used term for the adult cells with differentiation potential found in many postnatal tissues^{104,129,130}, despite the strong argument that they may not be the same cell type in each tissue¹³¹. Recently, there has been an international effort to define MSCs as plastic-adherent cells that express CD105, CD73 and CD90, and lack expression of CD45, CD34, CD14 or CD11b, CD79alpha or CD19 and HLA-DR surface molecules. This definition does not necessarily work for the cells *in vivo*, or across all species, but is accurate for monolayer-passaged non-rodent cells.

The use of MSCs for cartilage engineering applications has been possible since a method for *in vitro* chondrogenesis of bone marrow-derived MSCs was established by our group in 1998. Chondrogenesis was accomplished by utilizing scaffold-free pellet culture and a defined medium containing TGF- β 1 and dexamethasone^{108,109}. However, scaffold-free pellet culture has a size limitation that precludes this technology from translating directly to use in human articular cartilage defects. In 2003, Williams *et al* showed that goat MSCs could be photoencapsulated into

poly(ethylene glycol) scaffolds to facilitate chondrogenesis on a clinically relevant scale¹³². Interestingly, chondrogenesis occurred within these scaffolds despite the loss of direct cell-cell communication that was postulated to be very important to differentiation in the pellet culture system^{108,109}. However, the ability of a solitary, round progenitor cell to express cartilage matrix markers confirms that the cell-cell interactions are not required for chondrogenesis¹³³⁻¹³⁵. Presently it is unclear what developmental pathways are critical in enabling chondrogenesis given the fundamental differences between pellet and hydrogel cultures. Common to both is the spherical or rounded cellular conformation of MSCs critical for differentiation and supplementation with bioactive factors TGF- β and dexamethasone.

The relative accessibility of MSCs from multiple tissue sources, and the ability to readily expand these cell populations *in vitro*, offers a distinct advantage over autologous articular chondrocytes^{94,106}. Furthermore, MSCs themselves may be beneficial as transplant cells to the host tissue. MSCs do not display major histocompatibility complex (MHC) class II cell surface marker, rather only MHC class I without the co-stimulator molecules, indicating that they will not illicit an immune response during allogeneic use¹³⁶. Additionally, MSCs secrete immunosuppressive and anti-inflammatory cytokines such as interleukin-10¹³⁷, nitric oxide¹³⁸ and prostaglandins¹³⁹ that can prevent host versus graft rejection through modulation of T-cells^{140,141}. MSC regulation of T-cells appears to occur in an antigen-independent manner¹⁴² through the suppression of the primary and secondary T-cell response by inhibiting cell proliferation¹⁴³⁻¹⁴⁵.

Interestingly, this immunosuppressive behavior juxtaposes a ‘trophic’ effect of MSCs on host tissues¹²². It has long been appreciated that MSCs create a supportive microenvironment in the bone marrow stroma that facilitates survival and differentiation of hematopoietic stem cells¹⁴⁶. A limited amount of research has been done to identify the secretory molecules of MSCs that are responsible for their stimulatory effects. Measurable levels of bioactive factors such as TGF- β , stem cell factor (SCF), insulin-like growth factor (IGF), epidermal growth factor (EGF),

granulocyte and macrophage colony stimulating factors (G/M-CSF) have been identified in the medium and could contribute to their influence on other cells^{145,147}. More recent evidence suggests that these trophic effects of MSCs are responsible for tissue repair observed from MSC therapy in disease models such as stroke^{148,149} and myocardial infarct¹²⁴, rather than the mechanism where MSCs differentiate to replace these damaged tissues¹⁵⁰⁻¹⁵³.

1.4.3 Embryonic Stem Cells & Induced Pluripotent Stem Cells

Most recently the possible application of embryonic stem cells (ESCs) for cartilage tissue engineering have been considered and preliminary evidence suggests that they may be a viable source for generating cartilaginous tissues¹⁵⁴⁻¹⁵⁷. ESCs can be isolated from pluripotent cells of an early preimplantation embryo and propagated indefinitely *in vitro* in an undifferentiated state¹⁵⁸. Similar to genuine pluripotent cells, ESCs retain their ability to differentiate into cells representing the three major germ layers: endoderm, mesoderm or ectoderm or any of the 200+ cell types present in the adult body. Pluripotent cells resembling ESCs can also be derived experimentally by reprogramming of somatic cells by somatic cell nuclear transfer^{159,160} (SCNT) or direct reprogramming^{161,162} (iPS cells). Such pluripotent cells have an important role in cell replacement therapies since the patient's own somatic cells can be used for reprogramming thereby eliminating immune based rejection of transplanted cells.

Successful use of ESC cells for regenerative medicine applications requires the tight control of the differentiation process. The consequence of this has been demonstrated in experiments demonstrating the formation of teratomas following the injection of undifferentiated ESCs into the knee joint¹⁶³⁻¹⁶⁵. The use of growth factors may help consolidate resultant phenotypes; however, the application of chondrogenic factors TGF- β and BMP still produced heterotypic tissues following differentiation¹⁵⁵⁻¹⁵⁷. More recently the concept of generating cartilage tissue from ESCs by first inducing differentiation along the mesodermal lineage has been suggested¹⁶⁶⁻¹⁶⁸.

1.5 SCAFFOLD DESIGN

The scaffold is a critical component in a tissue engineering system as it creates a three-dimensional structure that physically supports encapsulated cells and provides a framework for tissue development. Scaffold design has a direct impact on cellular metabolism by providing both biophysical and biochemical cues that can trigger differentiation and/or matrix elaboration. Through polymer chemistry the mechanical properties and chemical composition of the scaffold can be tuned to the desired cellular system to improve tissue engineering outcomes. This section provides background on the photopolymerizable poly(ethylene glycol) diacrylate (PEGDA) based scaffolds that were the foundation for this work. Furthermore it will discuss critical aspects of scaffold design pertinent to building an improved system for cartilage engineering.

1.5.1 Hydrogels

Polymers are high molecular weight repeating subunits that represent a diverse class of synthetic and natural materials that can be formed into three-dimensional structures suitable for a variety of biomedical applications, including, scaffolds for tissue engineering, drug delivery vehicles, implantable medical devices and biosensors. As one of the basic tenets of tissue engineering, the scaffold plays a significant role in neotissue development. Technical advancements in material science were fundamental to the emergence of tissue engineering as a viable mechanism for regenerative medicine, but in recent years adding biological functionality has generated a new era of “smart” biomaterials¹⁶⁹⁻¹⁷¹. Adapting polymers towards biomedical applications requires careful consideration of how the material will interact with cells both during formation and afterwards during tissue development.

Hydrogels are a particular class of biocompatible, synthetic polymers that have become especially important in tissue engineering applications. These aptly named polymers are created by the covalent crosslinking of hydrophilic monomer subunits that can store a large amount of water, yielding biophysical properties similar to soft tissues. Suitable for tissue growth, hydrogels

are highly permeable to oxygen, nutrients and other water-soluble metabolites. Additionally, the physiochemical properties of hydrogels are readily tunable; making them amendable to modifications that can control cellular behavior and promote tissue development. For example, we and others have shown that the physical properties of the scaffold can have a significant effect on differentiation¹⁷² and matrix elaboration¹⁷³⁻¹⁷⁷ from encapsulated cells. More recently, chemical modifications and co-polymerization techniques have been developed to impart biological activity onto these otherwise inert biomaterials. This often involves incorporating extracellular matrix derivatives or synthetic peptides with defined functionality into the hydrogels through covalent or non-covalent additions. The design of such bioresponsive and bioactive scaffolds will be detailed further in sections 1.5.3 and 1.5.4 respectively.

A number of different synthetic monomers have been used to generate hydrogel scaffolds. The most commonly used materials include poly(ethylene glycol) (PEG), poly(vinyl alcohol) (PVA), poly(lactic acid) (PLA), poly(lactic-co-glycolic acid) (PLGA), poly(hydroxyethyl methacrylate) (PHEMA), poly(N-isopropylacrylamide) (PNIPAAm), and poly(anhydride). My work utilizes a acrylate-functionalized form of PEG, poly(ethylene glycol) diacrylate (PEGDA), with which I explored a number of chemical modifications aimed at improving neocartilage development.

1.5.2 Photopolymerization

The synthesis of crosslinked hydrogel structures requires a chemical reaction to induce gelation through reactive groups on monomer subunits. Generally speaking there are three main mechanisms of polymerization: physical, ionic, or covalent. Covalent polymerization offers the advantage of stably formed gels with readily controllable properties such as permeability, molecular diffusivity, equilibrium water content (swelling ratio), elasticity, modulus, and degradation characteristics¹⁷⁸. For covalent polymerization, gelation mechanisms are classified as either chain growth or step growth. Step growth occurs when two multifunctional monomer

subunits with mutually reactive chemical groups (ex: A and B) combine to form low molecular weight polymers (ex: A-B). These low molecular weight subunits continue to react with each other in “steps” to form fully crosslinked scaffolds ($-[A-B]_n-$). The Michael-type addition reaction between acrylated star PEG and dithiol, pioneered by the Hubbell group¹⁷⁹⁻¹⁸¹, and more recently the use of sequential “click” chemistry, adapted for biological applications by the Anseth group¹⁸², are two step-growth polymerization techniques that have been developed as cytocompatible methods for cellular encapsulation.

Chain growth polymerization requires the addition of an initiator molecule to activate functional groups on the monomer subunits, creating growth centers that will produce long kinetic chains. Photopolymerization has become a popular technique for chain growth polymerization in tissue engineering. In this technique, photoinitiator molecules form a radical when exposed to light at a specific wavelength. The rate of initiation depends on initiator efficiency, concentration and light intensity. Initiator radicals can then react with unsaturated bonds on the monomer subunits, typically a double or triple carbon bond such as the acrylate groups flanking the PEG monomer in PEGDA, to propagate polymerization. Polymerization is terminated by chain transfer or radical termination and is dependent upon the concentration of radicals in the system. Understanding reaction kinetics is critical towards designing an appropriate system for *in situ* photopolymerization: complete polymerization is almost never reached in these systems due to diffusion limitations, yet unreacted monomer can have significant effects on scaffold mechanics and immunoreactivity¹⁸³.

Advantages of photopolymerization include spatiotemporal control over gelation, and fast curing rates in a system that can be preformed at physiological conditions to enable non-toxic encapsulation of cells¹⁸⁴⁻¹⁸⁶. This technique has a long clinical history in dentistry to form sealants and dental restorations *in situ*^{187,188}; it is also amendable to minimally invasive surgical techniques appealing in cartilage engineering. Furthermore, Elisseff *et al* has demonstrated that photopolymerization can occur transdermally¹⁸⁹⁻¹⁹¹ offering unique clinical benefits in tissue

engineering and drug delivery applications. Interestingly, these experiments were all successful despite the use of a long-wave ultraviolet light initiating system, which is poorly transmitted through the skin. It would be expected that transdermal polymerization would be more effective with visible light or near infrared, which travels better through skin due to shorter wavelengths.

One concern with the use of photopolymerization is that free radicals created during this process can have the unintended side effect of damaging cell membranes, proteins and DNA. Considerable effort has been placed towards finding water soluble, cytocompatible photoinitiators that allow cells to be mixed with a macromer solution and encapsulated into hydrogels to produce constructs with a uniform distribution of cells. *Chapter three of this thesis specifically deals with validating a visible light initiator system for the non-toxic encapsulation of human MSCs in bioresponsive hydrogels.*

1.5.3 Bioresponsive Hydrogels

The concept of degradable polymers was suggested with the earliest material iterations introduced for tissue engineering applications. The need for this function was driven by the recognition that the artificial scaffold may interfere with the assembly of matrix components in the neotissue. This consideration is of particular importance in cartilage engineering as current scaffolds produce a mechanically inferior tissue regenerate. One factor contributing to the weakness observed in neocartilage is a pericellular restriction of extracellular matrix elements, presumably because the scaffold is preventing migration and assembly of the larger matrix components. In optimizing a scaffold for cartilage development two design considerations are at odds with one another. Initially there is need for a strong scaffold to support encapsulated cells and protect them from the loads native to the synovial joint. A high hydrogel modulus can be achieved with a tightly crosslinked scaffold, generated by either decreasing the molecular weight of monomer subunits or increasing the weight percentage of macromer. However, this increased strength is associated with decreased pore size and permeability in the scaffold, producing an

increased pericellular localization of cartilage matrix elements^{173,175}. Consequently, as the encapsulated cells begin to elaborate matrix it is necessary to have a looser scaffold to allow for interterritorial matrix distribution and assembly. Degradable scaffolds may offer the ideal solution for this problem, but there remains a significant challenge in engineering appropriate degradation kinetics. The ideal scaffold for cartilage engineering would degrade at a rate that corresponds to matrix production by the encapsulated cells (Figure 1.6).

A number of different strategies have been proposed to mediate hydrogel degradation including hydrolytic and/or enzymatically driven mechanisms^{192,193}. Hydrolytically degradable scaffolds most commonly break down through hydrolysis of ester linkages located at the crosslink or within the backbone. Examples of these degradable polymers include PVA, PLA, PGLA, polyfumarates, and phosphoesters. In these systems the scaffold begins to breakdown immediately when exposed to an aqueous environment. A significant effort has been made to design controlled degradation rates into these systems by co-polymerization with non-degradable subunits, for example PEG with PVA¹⁹⁴ or PLA¹⁹⁵. However, degradation rate remains an inherent property of the chemical composition of the scaffold: dependent entirely on the number and type of degradable linkages rather than developmental progression of the neotissue.

Enzymatic degradation is designed to be more specific and can be driven by either endogenous or exogenous mechanisms. The concept of utilizing endogenous cellular behavior to drive degradation was first introduced by our collaborator Jennifer West in 1999¹⁹⁶. Such scaffolds are now classified as “bioresponsive” hydrogels since the scaffold will change in response to cellular activity¹⁹⁷. Degradation in this scaffold was achieved by embedding collagenase and plasmin specific peptide substrates into the backbone a PEGDA-based hydrogel to facilitate cellular migration during wound healing. The peptide sequences and polymer chemistry have subsequently been re-engineered for faster degradation kinetics to increase the efficiency of fibroblast migration¹⁹⁸. Park *et al* explored the utility of a collagenase sensitive scaffold for cartilage engineering applications with encapsulated chondrocytes and suggested that

matrix was less constrained in the degradable hydrogel¹⁹⁹. However, the peptide sequence they incorporated into their hydrogels is reported to be cleaved by multiple matrix metalloproteinases (MMP-1,-2,-3,-7,-8,-9)^{198,200}, and therefore degradation was not optimized for cellular behavior. In an effort to determine an appropriate degradation rate for cartilage engineering applications, Rice and Anseth developed a lipase-sensitive PEGDA scaffold and demonstrated that degradation during the early phases of chondrogenesis produced structurally compromised neocartilage constructs²⁰¹. This technology provides a tool for exploring the temporal impact of degradation on the structural integrity of the system, but it is not practical for translational applications since scaffold degradation requires exogenous addition of lipase enzyme. Similarly, the Anseth group has also recently developed a novel photolytically degradable hydrogel chemistry that degrades locally with exposure to specific wavelengths of light²⁰². This technology is ideal for releasing bioactive factors tethered to the scaffold or generating local microenvironments by light-patterning the scaffold, but again is more of a tool for *in vitro* studies rather than clinically relevant cartilage therapies.

Taken together, these data emphasize the need to optimize scaffold degradation to the developmental processes specific to individual tissues. *One aim of my thesis work, detailed in Chapter Four, was to improve upon current biodegradable scaffolds used for cartilage engineering by developing a bioresponsive scaffold with degradation linked directly to chondrogenesis* (Figure 1.6).



FIGURE 1.6 – CELL-MEDIATED, BIORESPONSIVE DEGRADABLE HYDROGEL FOR TISSUE ENGINEERED CARTILAGE. Isolated cells are mixed with a PEGDA monomer containing a peptide sensitive to endogenous enzyme activity. This mixture can be polymerized using non-toxic photoinitiators and the application of light. Photoencapsulated cells differentiate into chondrocytes and make matrix proteins as well as enzymes that cleave the scaffold and enable interterritorial assembly of the matrix.

1.5.4 Bioactive Hydrogels

Providing instructive biological cues for tissue development is a facet of tissue engineering that is being included in modern biomaterials. During embryogenesis both the extracellular matrix and soluble signaling molecules are known to positively influence chondrogenesis, but it is only recently that the technology has existed to incorporate this bioactivity into synthetic biomaterials. Building bioactive features into scaffolds can be accomplished by either directly embedding functional peptides into the backbone, as described above, or by tethering them as pendant groups. Alternatively, substances can be non-covalently trapped into the scaffold. Spatiotemporal control of these bioactive factors can further optimize the scaffold towards development of a desired tissue. (Figure 1.7)

Growth factors play a significant role in regulating stem cell differentiation and matrix elaboration. For *in vitro* studies soluble signaling molecules can easily be included in the culture medium to determine their temporal requirement. However, translating tissue engineering into a clinically relevant technology requires alternative delivery techniques for *in vivo* application. There are a number of problems with systemic delivery of growth factors, or other bioactive molecules such as steroids, for cartilage engineering *in vivo*. These include inefficient delivery to cartilage tissue due to its avascular nature, short half-life, and the potential of serious systemic side effects. Local, controlled release of soluble substances can be achieved by encapsulating growth factors either into microporous nanoparticles or degradable microspheres²⁰³⁻²⁰⁵. Some success has been achieved by placing these particles within cell aggregates²⁰⁵ but it remains a significant challenge to design systems that can provide sustained delivery within a scaffold without disrupting its mechanical integrity²⁰⁴.

An alternative solution would be to covalently attach growth factors directly to the scaffold during the polymerization process. This technique has been used to deliver both TGF- β ²⁰⁶ and epidermal growth factor (EGF)²⁰⁷ to cells directly from the scaffold; demonstrating that biological activity can be maintained. The application of these bioactive scaffolds showed

improved matrix elaboration from vascular smooth muscle cells in the tethered TGF- β ²⁰⁶ scaffold, and an enhanced survival advantage of MSCs when EGF was immobilized to the scaffold²⁰⁷. Despite a well established role of chondrogenic factors such as TGF- β and dexamethasone for *in vitro* chondrogenesis, bioactive scaffolds containing immobilized growth factors have not been published for cartilage engineering applications. *Chapter Five explores the temporal requirement of both TGF- β and dexamethasone for chondrogenesis of human MSCs encapsulated in PEG-based hydrogels, and provides preliminary data for developing a bioactive scaffold for chondrogenesis of hMSCs.*

The significance of the extracellular matrix in influencing cell migration, morphology and differentiation has long been appreciated in biology and there is significantly more data in the literature regarding the incorporation of these matrical elements into scaffolds for cartilage engineering. Cellular recognition of the extracellular matrix occurs through integrins and this has been suggested as one mechanism for mechanotransduction in cartilage⁶. Integrins are heterodimeric cell-surface receptors composed of a variety of alpha and beta subunits that can bind to a diverse range of extracellular matrix components. The indispensable nature of integrin-matrix interactions has been demonstrated by the early embryonic lethality of integrin $\beta 1$ ²⁰⁸ and laminin²⁰⁹ genetic mouse knock-outs. One mechanism for providing these interactions to tissue engineered constructs is to incorporate purified matrix elements such as proteoglycans, collagens, laminin or hyaluronan. However, this technique is complicated by the risk of pathogen transmission and immunogenicity that has led to a desire for a fully synthetic bioactive system.

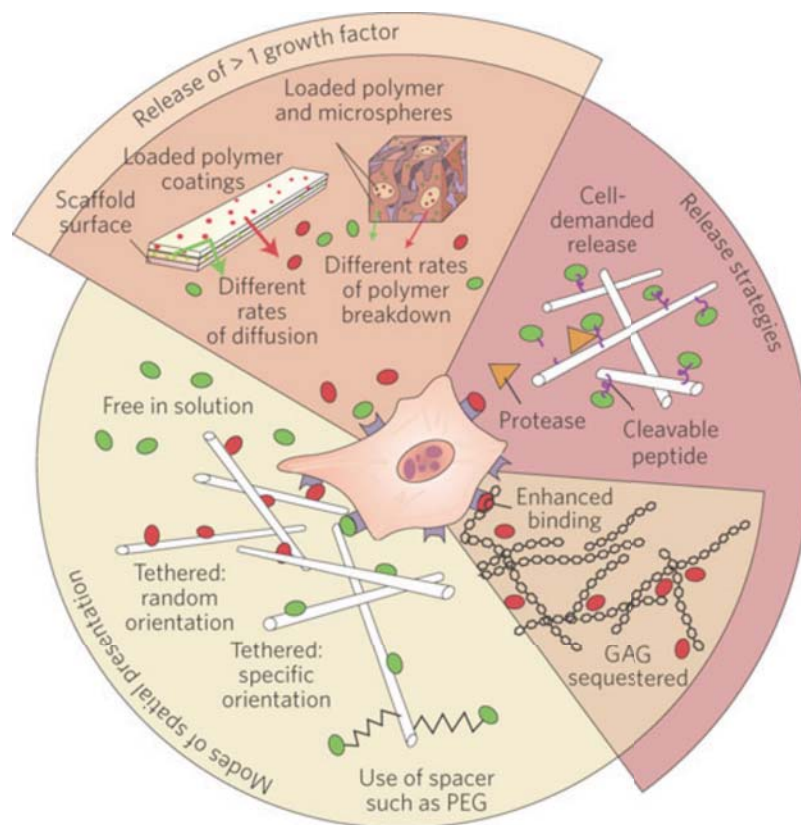


FIGURE 1.7 – BIOACTIVE SCAFFOLDS, reproduced with permission from Place *et al*²¹⁰. Clockwise, from top: growth factors can be loaded into polymers with release rates determined by degradation or diffusive properties of the polymer. Alternatively growth factors can be covalently attached to the scaffold and released by cell-mediated cleavage of a protease-sensitive peptide sequences within the tether. Bioactive components can also be non-covalently included in the scaffold; inclusion of extracellular matrix components such as glycosaminoglycans (GAGs) can not only have a bioactive function themselves but can also serve to adsorb growth factors and potentiate their activity. Bioactive factors can also be immobilized by embedding directly in the backbone of the scaffold or by attaching them using a non-releasable tether such as PEG.

The biological activity of the integrin-binding domain can be mimicked through small functional peptides that replace the full sequence protein, the best known is sequence arginine-glycine-aspartic acid (RGD) found on many extracellular matrix elements such as collagen, fibronectin, or laminin. Hern and Hubbell were the first to incorporate the RGD into PEGDA hydrogels and established that this addition could induce spreading of fibroblasts²¹¹. Work from the West laboratory enhanced this basic application by comparing the effectiveness of a variety of adhesion ligand mimics and demonstrated control of cellular migration in collagenase-degradable hydrogels^{212,213}.

The use of the RGD sequence to facilitate cartilage engineering has also been explored since it is known that cells express fibronectin during the initial mesenchymal condensation and it is therefore believed to facilitate chondrogenic differentiation²¹⁴⁻²¹⁶. By incorporating this sequence into PEGDA hydrogels, Anseth *et al* found that it promoted survival of MSC²¹⁷ and induced the early stages of chondrogenic differentiation²¹⁸. However, the sustained presentation of RGD inhibits chondrogenesis²¹⁹. Together these findings highlight the necessity for a temporal modulation of ligand presentation that recapitulates the endogenous system. Anseth *et al* have recently described two novel RGD-releasing mechanisms that provide the MSC with exposure to the RGD binding domain only during the early stages of chondrogenesis. One system conjugates RGD to a MMP-13 cleavable sequence found on aggrecan and tethers this moiety into a PEG hydrogel via a thiol-acrylate polymerization²²⁰. The RGD sequence can be released from the PEG backbone by the endogenous expression of MMP-13 and resulted in a ten-fold increase in proteoglycan production. Temporal expression of MMP-13 is upregulated within the first week of MSC chondrogenesis in micromass culture²²¹ and is also activated very early in hydrogels (Thesis Chapter Four). However it is important to note that this MMP-13 expression pattern is an undesirable component of *in vitro* chondrogenesis as MMP-13 is involved in terminal differentiation of chondrocytes during endochondral ossification⁵⁶. Ultimately it would be desirable to inhibit MMP-13 expression by MSCs since it is not expressed by healthy articular

chondrocytes, and appears to be highly activated only in patients suffering from osteoarthritis^{7,8}. In a second manuscript, the importance of temporal patterning for RGD was confirmed using photoreleasable RGD to get increased proteoglycan production from human MSC exposed to RGD only during early chondrogenesis²⁰². Less is known about the requirement for RGD interaction for other cells types undergoing chondrogenesis. Hwang *et al* have demonstrated improved chondrogenesis from human ESCs encapsulated in PEG hydrogels with RGD ligand¹⁵⁴; however, the temporal exposure to this ligand has not been explored for ESC. Likewise the interaction between RGD and chondrocytes is unclear in tissue engineered systems, but Bryant *et al* suggests that RGD acts as a mechanoreceptor in hydrogels subjected to dynamic load¹⁷⁷.

1.6 OSTEOARTHRITIS: THE CLINICAL SIGNIFICANCE OF CARTILAGE ENGINEERING

Osteoarthritis is a degenerative joint disease characterized by degradation of the extracellular matrix in articular cartilage. The lifetime risk of developing a symptomatic form of this disease is presently estimated at 1 in 2, with 85 % of the population over 65 presenting with physician-diagnosed osteoarthritis¹. Despite accounting for the largest cause of disability in the United States, there are very few therapeutic treatments available to address pain or prevent disease progression. The etiology of osteoarthritis remains unclear but risk factors include age, obesity, genetic predisposition and articular damage often by acute trauma²²². Misregulation of biomechanical stimuli appears to be a common factor underlying these various risk factors. Inappropriate stresses on chondrocytes leads to an irreversible metabolic change in chondrocyte biology such that degradation of the extracellular matrix proteins is not matched by matrix synthesis.

The biomechanical integrity of articular cartilage during motion is maintained by the gross morphological architecture of the synovial joint and the ultrastructural organization of the extracellular matrix within articular cartilage. Damage to supporting structures in the joint such as ligaments/tendons and the meniscus, can result in an imbalance of forces across the cartilage

surface during articulation. Acute trauma^{222,223} to these structures is a common source of disease initiation in young, otherwise healthy patients, but genetic alterations in these structures and obesity can also result in poor biomechanics. The importance of the composition and anisotropic ultrastructure of the cartilage matrix in conferring mechanical integrity was detailed previously (see section 1.3.2). Age related loss of collagen and proteoglycan from the extracellular matrix is a significant cause of the late onset of osteoarthritis. Acute chondral defects contribute to the early onset of the disease.

The articular chondrocyte is responsible for maintaining the production and assembly of the cartilage matrix, albeit at a relatively low turnover rate. The half-life of proteoglycans is 3 to 24 years, while collagens can sustain close to 100 years in healthy tissue⁵. Chondrocytes are mechanosensitive cells and motion is required both during early cartilage development^{48,50,51,53} (see section 1.2.3) and to maintain homeostasis of the extracellular matrix in the adult tissue^{5,6}. The molecular mechanisms underlying mechanotransduction in the chondrocyte are not well understood. A number of genes involved in the turnover of the extracellular matrix proteins have been shown to be mechanosensitive, including: collagen II, aggrecan, and matrix metalloproteinases (MMPs)^{72,224}. Growth factors (TGF β , BMP2, FGF2, FGF4), cell cycle proteins (cyclin, CDKs) and cytokines (IL-1,4,6) also respond to mechanical signals⁷². Misregulation of these signaling pathways, most significantly the MMPs, contributes to the elevated catabolism of cartilage matrix in osteoarthritis.

The mechanisms for sensing the mechanical signal and transducing it to the nucleus are not clearly defined. In other organ systems integrins, stretch activated ion channels and primary cilia are important mechanisms for mechanotransduction^{72,225-227}. Stretch activated calcium channels are capable of increasing intracellular calcium levels and initiating a well characterized secondary messenger cascade; these calcium channels can be opened by tension on the chondrocyte. Recently, the pathway for mechanotransduction through the primary cilium has been appreciated. The non-motile primary cilium is a single cytoplasmic organelle found

protruding 3-30 μ m from the cell surface into the extracellular environment of nearly all mammalian cells. The primary cilia of kidney epithelial cells are involved in flow sensation²²⁷. Chondrocyte primary cilium have an integrin receptor located at the distal end and defects in the cilium disrupts endochondral bone formation²²⁶. By analogy to the renal epithelial function, and evidence for a functional role in bone formation, it has been proposed that the chondrocyte primary cilium may also be central to mechanotransduction in articular cartilage²²⁵.

In designing a repair strategy for treating osteoarthritis early and preventing disease progression, re-establishing proper biomechanics as a mechanism to restore chondrocyte homeostasis is a governing concept behind cartilage engineering technology. Current technologies for creating a cartilage engineered regenerate tissue are primarily limited to the repair of focal lesions in articular cartilage rather than full tissue replacements or osteochondral defects. How close to the native tissue the regenerate needs to be to sufficiently effect repair remains to be defined, but generally neocartilage constructs aim to replicate the biomechanical function of articular cartilage as closely as possible.

1.7 THESIS AIMS & OUTLINE OF WORK

The long-term goal of cartilage engineering is to create a functional cartilage regenerate that can repair focal lesions in articular cartilage. This cell-based technology utilizes a scaffold and the delivery of bioactive factors to facilitate tissue development. A number of unresolved issues remain, including the type of cells and scaffold to use to best effect repair, and these factors serve as barriers to clinical translation. Failure of present therapies is in part rooted in the inability to replicate the metabolic and mechanical function of native cartilage. My thesis work focused on specific aspects of these issues, with the long-term goal of developing novel strategies that could improve neocartilage development and move closer to a clinically useful regenerate tissue.

SPECIFIC AIM 1: To improve the extracellular matrix ultrastructure in neocartilage constructs. Neocartilage constructs are mechanically inferior to native tissue. Pericellular restriction of the extracellular matrix proteins in neocartilage constructs prevents them from attaining biomechanical properties that approach those of native articular cartilage. Two separate hypotheses were tested as mechanisms to address this limitation in cartilage engineering.

HYPOTHESIS 1: *A bioresponsive scaffold with degradation kinetics tuned to chondrogenesis will promote interterritorial assembly of cartilage matrix proteins (Thesis Chapters 3 & 4).*

HYPOTHESIS 2: *Mechanical stimulation of neocartilage constructs will drive anisotropic assembly of matrix proteins (Appendix A).*

SPECIFIC AIM 2: To create a bioactive scaffold that stimulates stem cell chondrogenesis. Bioactive scaffolds are a strategy to deliver growth factors to encapsulated cells in a technology appropriate for *in vivo* implantation. The temporal requirement of chondrogenic factors that will promote chondrogenesis of MSCs in hydrogel scaffolds is not clear, but is required for the design of a bioactive scaffold that can facilitate appropriate differentiation and cartilage matrix elaboration.

Hypothesis: *Requisite chondrogenic factors can be immobilized into a synthetic PEGDA scaffold to promote chondrogenesis (Thesis Chapter 5).*

SPECIFIC AIM 3: To promote a permanent cartilage phenotype from encapsulated, differentiated MSCs. MSCs are considered a potential alternative to chondrocytes for cartilage engineering applications. However, phenotypic markers of both fibrocartilage (collagen I) and hypertrophic cartilage (collagen X & MMP-13) persist in MSC-derived neocartilage constructs cultured *in vitro*. This has led to the concern that the endochondral ossification will be the outcome of the *in vivo* application of cartilage engineered constructs with MSCs.

Hypothesis: *MSCs can be stimulated to differentiate into chondrocytes with a hyaline cartilage phenotype by manipulating the culture conditions (Thesis Chapters 5 & 6).*

CHAPTER 2: MATERIALS & METHODS

2.1 PREPARATION OF HYDROGEL SCAFFOLDS

2.1.1 Semi-Interpenetrating Networks

Poly(ethylene glycol) diacrylate (PEGDA, 6 kDa) was synthesized in the laboratory of Dr. Jennifer West (Department of Bioengineering, Rice University, Houston TX) as previously described²⁰⁶. PEGDA was prepared by combining 0.1 mM dry PEG with 0.4 mM acryloyl chloride and 0.2 mM triethylamine in anhydrous dichloromethane and stirred under argon overnight. The mixture was then precipitated in cold ethyl ether, vacuum dried overnight, lyophilized, and stored at 4 °C.

PEGDA-based semi-interpenetrating networks (sIPN) were made by mixing a non-crosslinking PEG-n-dimethyl ether (PEG, n=2000, MW 88kDa) with the crosslinking PEGDA such that the final concentration was 16 % (w/v) PEGDA and 32 % (w/v) PEG dissolved in PBS¹⁷³.

2.1.2 Peptide Synthesis

Peptides for bioresponsive hydrogels were synthesized in the laboratory of Dr. Hans Peter Bächinger on an ABI 433A peptide synthesizer (Applied Biosystems, Foster City, CA). Couplings were carried out on a H-L-*trans*-4-hydroxyproline-2-chlorotrityl resin (AnaSpec, San Jose, CA, USA). Fmoc-amino acids, (Fmoc-Gly-OH, Fmoc-Pro-OH (Applied Biosystems), Fmoc-4(R)Hyp(*t*Bu)-OH (Novabiochem, EMD Biosciences, Inc., San Diego, CA) were purchased, and used without further purification. HATU (O-(7-azabenzotriazol-1-yl)-1.1.3.3-tetramethyluronium hexafluorophosphate (Perseptive Biosystems)) and diisopropylethylamine were used as the coupling reagent. The peptide was cleaved from the resin with Reagent R (trifluoroacetic acid-thioanisole-1,2-ethanedithiol-anisole (90:5:3:2) at room temperature for 3

hours. Peptides were isolated by precipitation from the cleavage cocktail with diethyl ether at 4 °C, and diluted with 0.1 % TFA, and purified by preparative HPLC (Vydac® C18, 5 µm, 300 Å, 218TP101550 50 x 250 mm, and the guard column, 218TP15202503, W.R. Grace & Co., MD, USA) with a flow-rate of 36 ml/min and elution with 0 % to 50 % acetonitrile gradient in 0.1 % trifluoroacetic acid. The peptide was characterized by electrospray/quadrupole/time-of-flight mass spectrometry (Q-tof micro, Waters), and amino acid analysis. The peptides were stored at -20 °C before making stock solutions.

2.1.3 Bioresponsive Hydrogels

To generate bioresponsive hydrogels, peptides containing either a MMP-7 substrate (PLE-LRA²²⁸ and VPLS-LTMG²²⁹, dash indicating cleavage point), or a non-degradable scrambled peptide control (MLLVTPSG), were synthesized with short linker domains GGWGG and GGK at the N- and C- termini respectively to both facilitate enzyme accessibility to the substrate sequence and to enable degradation testing using the spectrophotometric release of tryptophan (W). Peptides were conjugated to acrylate-PEG-succinimidyl carboxymethyl (a-PEG-SCM, 3,400 Da; Laysan Bio Inc, Arab, AL) individually at a 1:2.1 (peptide/PEG) molar ratio in DMSO (Sigma-Aldrich, Milwaukee, WI) for 24 hours at room temperature to form an ABA block polymer (Figure 2.1). Diisopropylamine (DIPEA, Sigma-Aldrich, Milwaukee, WI) was added as a base catalyst at a 2:1 (DIPEA/PEG) molar ratio into the reaction. The resulting solution were then diluted in 10 ml of ultrapure water and purified by dialysis (MWCO 3500 Da; Fisher Scientific, Pittsburg, PA) against deionized water for 24 hours. The purified polymers were then lyophilized and stored under argon at -20°C. The conjugation products were analyzed by gel permeation chromatography (GPC, Polymer Laboratories, Amherst, MA) with UV-vis and evaporative light scattering detectors and the presence of the acrylate groups was verified using nuclear magnetic resonance (NMR).

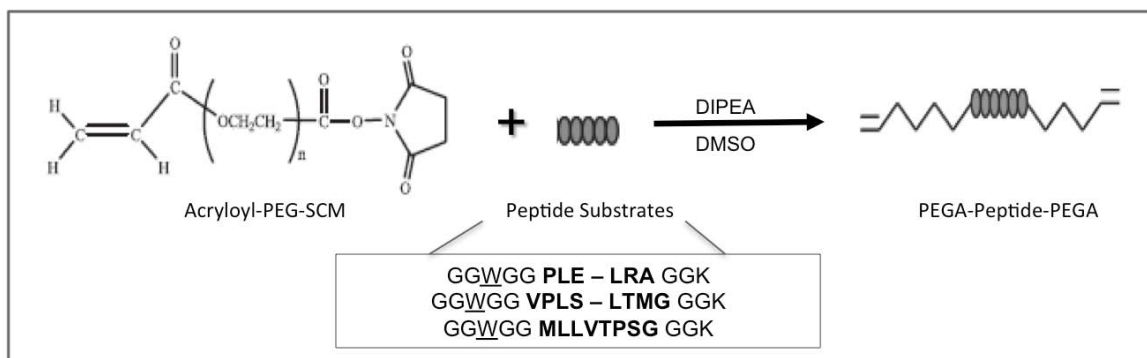


FIGURE 2.1 – SCHEMATIC DIAGRAM OF PEPTIDE-CONTAINING PEGDA. Peptides (boxed) are conjugated to acryloyl-PEG-SCM through the primary amine at the N-terminal and lysine (K) residue at the C-terminal. Bolded peptide sequences represent MMP-7 substrates (PLE-LRA and VPLS-LTMG), with the dash indicating the cleavage site, or the scrambled control MLLVTPSG. Tryptophan (W) residue in flanking sequence was inserted for use in the quantification of degradation by measuring its release spectrophotometrically.

2.1.4 Degradation Testing

3

Degradation of the bioresponsive scaffolds was detected by tryptophan release from cell-free scaffolds exposed to recombinant human MMPs. Macromer was dissolved at 10 % (w/v) in a sterile phosphate buffered saline (PBS) solution containing a photoinitiator system of 0.75 % triethanolamine (TEA), 0.1 mM eosin Y, and 37 mM 1-vinyl-2 pyrrolidinone (NVP). Droplets (10 ml) were photopolymerized and then swollen in PBS overnight at 37 °C. Hydrogels were then incubated in protease solution at 37 °C for up to 48 hrs and spectrophotometric measurement of tryptophan in the solution taken at intervals. Degradation by recombinant human MMP-1, -2, -7, and -13 (AnaSpec, Fremont CA) was tested against negative control (Tris Buffer), or positive control (0.2 mg/ml proteinase K). All MMP enzymes were activated by incubating with 1 mM 4-Aminophenylmercuric acetate (APMA) at 37 °C prior to testing with hydrogels. Percentage tryptophan release was normalized to complete dissolution (proteinase K digestion, 24 hrs). Values represent the mean \pm standard deviation.

2.1.5 Bioactive Scaffolds

3

Recombinant human TGF- β 1 (Peprotech, Rocky Hills NJ) was conjugated to PEG through a reaction with an excess of acryloyl-PEG-SMC (synthesized in the laboratory of Jennifer West, Rice University TX) in 50 mM sodium bicarbonate buffer (pH 8.5) at room temperature overnight. The resulting solution was then purified by dialysis (MWCO 3500 Da; Fisher Scientific, Pittsburg, PA) against deionized water for 24 hours to remove unreacted PEG-SMC. The purified monomer were then lyophilized and stored under argon at -20°C. Polymer solutions were sterilized via filtration (0.2 μ m filter; Gelman Sciences, Ann Arbor, MI) prior to use.

The integrin binding substrate RGDS (American Peptide, Sunnyvale CA) was conjugated to PEG through a reaction with acrylate-PEG-succinimidyl valerate (aPEG-SVM, Laysan Bio, Arab AL) at a molar ratio of 1.2:1 (peptide/PEG) diluted in PBS at pH 8.0. The reaction was

allowed to proceed for 12-16 hours, then the pH was restored to 7.0 and the resulting solution was purified by dialysis (MWCO 3500 Da; Fisher Scientific, Pittsburg, PA) against deionized water for 24 hours. The purified polymers were then lyophilized and stored under argon at -20°C. The conjugation product was analyzed by GPC with UV-vis and evaporative light scattering detectors and the presence of the acrylate groups was verified using NMR. Polymer solutions were sterilized via filtration (0.2 µm filter; Nalgene #180-1320) prior to use.

2.2 CELL CULTURE

2.2.1 Isolation and Expansion of Human Mesenchymal Stem Cells

Human mesenchymal stem cells (hMSCs) were isolated and expanded from iliac crest bone marrow aspirates as previously described^{108,109,173}. Briefly, human bone marrow was obtained from the iliac crests of consenting donors. Marrow aspirates were fractionated on a Percoll density gradient and plated in Dulbecco's Modified Eagle's Medium (DMEM) with 10 % fetal bovine serum (FBS, Invitrogen, lot selected for optimal cell growth and differentiation). Adherent cells were cultured at 37 °C, 5 % CO₂ with medium changes every four days. Once primary cells were confluent, serum-containing DMEM was supplemented with fibroblast growth factor (FGF-2, 10 ng/ml) to facilitate expansion with retention of chondrogenic potential. Expanded hMSCs at passages 1 to 3 were used for all experiments.

2.2.2 Isolation and Culture of Human Articular Chondrocytes

Human articular chondrocytes (ACs) were obtained from the discard tissue of fresh osteochondral allografts (donor tissue supplied by The Joint Restoration Foundation, Centennial, CO: age range 12-35). Chondrocytes were isolated by digesting finely minced cartilage tissue in 1 % pronase for 1 hour (37 °C, 5 % CO₂), followed by 1-3 hours in a 0.4 % collagenase II (Worthington Biochemical Corporation, Lakewood NJ) solution.

Isolated chondrocytes were either encapsulated directly into hydrogels or cultured as floating aggregate cultures²³⁰. To make aggregate cultures, 1×10^6 cells/per well were added to the Corning ultra-low attachment 24-well plates and cultured in Opti-MEM® I Reduced Serum Medium (Invitrogen). Chondrocyte conditioned medium (CCM) was harvested twice weekly and frozen at $-80\text{ }^{\circ}\text{C}$ until needed. Prior to using CCM all batches were combined and filter sterilized. Chondrocyte aggregate cultures were also used to condition the medium for co-culture experiments using transwell plates. In these experiments 5 mm diameter hydrogels were placed into the transwell insert (0.4 μm polyester membrane, Corning Catalog #3470) and chondrocytes were grown in floating aggregate culture in the Corning ultra-low attachment plates either with Opti-MEM® or defined chondrogenic medium.

2.2.3 Photoencapsulation using Ultraviolet (UV) Light

The water-soluble UV light photoinitiator IrgacureTM 2959 (1-[4-(2-Hydroxyethoxy)-phenyl]-2-hydroxy-2-methyl-1-propane-1-one, “I2959”, Ciba®, Tarrytown NY) was used to initiate photopolymerization for macromer solutions that did not contain peptides. I2959 has a peak absorbance of 280 nm (Figure 3.1A) but remains an effective photoinitiator for PEGDA at 365 nm^{231,232}. Disk-shaped hydrogels were formed by mixing filter-sterilized macromer (0.2 μm filter; Nalgene #180-1320) at twice the desired concentration with an equal volume of cells and 0.06 % I2959 dissolved in PBS. Macromer solutions were placed into a custom-built stainless steel mold and exposed to 6 min UV light (Spectroline UV lamp: 365 nm, 6 mW/cm²).

2.2.4 Photoencapsulation using Visible Light

The visible light initiating system included the photosensitizer eosin Y, initiator triethanolamine (TEA), and catalyst 1-vinyl-2 pyrrolidinone (NVP). Eosin Y has a peak absorbance at 510 nm (Figure 3.1B). To establish the effective limits of the visible light initiator

system, concentrations of both eosin Y and TEA were systematically adjusted and polymerization characterized (Figure 3.2). Macromer was dissolved in TEA to twice the final concentration and filter sterilized before being diluted with an equal volume solution containing either 25 or 50 x 10⁶ hMSCs/ml, eosin Y, and NVP. Disk-shaped hydrogels were fabricated following 2-minute exposure to visible light (Bartels & Stout V-LUX 1000). Following experiments to determine cytocompatible conditions for hMSCs (Thesis Chapter Three) 0.1 mM eosin Y and 0.75 % TEA was used for all subsequent experiments.

2.2.5 *In vitro* Hydrogel Culture

Hydrogels were cultured at 37°C, 5% CO₂ for up to 12 weeks in a defined chondrogenic medium^{108,109}. Complete (aka “control”) defined medium consisted of high-glucose DMEM with ITS⁺ Premix (Collaborative Biomedical Products), sodium pyruvate (1 mM), ascorbate-2-phosphate (37.5 µg/ml), dexamethasone (10⁻⁷ M), TGF-β1 (10 ng/ml, recombinant human, Peprotech, Rocky Hills NJ) and l-glutamine (4 mM). For some experiments, dexamethasone or TGF-β1 was excluded from the culture medium initially, or withdrawn after defined periods of culture (1, 2, 3, or 4 weeks). For comparison, control hydrogels were fabricated with the same human cell preparations and continuously exposed to the complete chondrogenic medium containing both TGF-β1 and dexamethasone.

2.3 LIVE-DEAD STAINING

Cellular toxicity of the photoinitiator system was visualized following 48 hours of *in vitro* culture using a Live-Dead Viability/Cytotoxicity Kit (Invitrogen, L-3224). This kit distinguishes live cells by the conversion of the non-fluorescent calcein AM to the green fluorescent calcein through intercellular esterase activity. Dead cells are stained with ethidium homodimer-1 (EthD-1), which is excluded by live cells, but fluoresces red upon uptake and binding to the intercellular nucleic acids in dead cells. Hydrogels were rinsed twice with PBS and then exposed to a mixture of 0.25 mM calcein AM and 0.5 mM EthD-1 in PBS for 40 minutes in

the incubator (37°C, 5% CO₂). Hydrogels were removed from the mixture, placed into PBS and fluorescence visualized immediately using confocal microscopy (Zeiss LSM-710, 20X objective, 0.80 apofart).

2.4 BIOCHEMICAL ANALYSIS

Hydrogels for biochemical analysis were removed from the culture media, washed twice with PBS and digested in 0.1 N sodium hydroxide overnight at 60 °C. Samples were neutralized with 0.1 N hydrochloric acid and then digested for an additional 18 hours at 60 °C with 125 µg/ml papain in 10 mM EDTA, 2 mM cysteine, pH 6.0 (Sigma, St. Louis, MO). Sulfated proteoglycan content of the digested cell-polymer construct was assessed spectrophotometrically using the 1,9-dimethylmethylene blue (DMMB) dye assay (Polysciences, Warrington PA, pH 3.0)²³³. Sample proteoglycan content was compared to shark cartilage chondroitin sulfate standards (Sigma-Aldrich, Oakville, Ontario, Canada). Proteoglycans released from the hydrogels into the medium were similarly quantified by comparing DMMB spectrophotometric shift from undiluted medium aspirates to the chondroitin sulfate standards diluted in DMEM medium containing phenol red.

DNA content was determined spectrofluorimetrically using the PicoGreen fluorescent DNA binding dye assay according to manufacturer's instructions (P11496, Invitrogen-Molecular Probes); sample fluorescence was compared to DNA standards included in the assay kit.

Hydroxyproline content was used as a measure of total collagen content²³⁴. This was determined by oxidation of hydroxyproline residues in collagen with chloramine T trihydrate (ICN Biomedicals, Aurora, OH), developed with p-dimethylaminobenzaldehyde (Ehrlich's reagent, ICN Biomedicals)²³⁴. Sample concentrations were compared to hydroxyproline standard solutions made from trans-4-hydroxy-L-proline (Fluka). All biochemical values represent mean ±

95 % confidence; statistical difference was tested using an ANOVA with significance set at a p-value of 0.05, followed by a pairwise comparison using Dunnett’s Test.

2.5 GENE EXPRESSION ASSAYS

Hydrogels were harvested into 1 ml TRIzol reagent (Invitrogen) and homogenized using the Ultra-Turrax® IKA-T10 basic homogenizer. Homogenates were left at room temperature for 5 minutes to facilitate mRNA extraction and then centrifuged at 12,000 x g for 15 minutes. The supernatant was removed and stored at -80 °C until all samples had been collected. mRNA was extracted per manufacturer’s instructions. cDNA was reverse transcribed using Quanta qScript™ cDNA SuperMix (Quanta Biosciences, 95048) with 1 mg mRNA per 20 µl reaction. Quantitative real time RT-PCR analysis was done on the BioRad MyiQ iCycler with cycle number set to 40.

Taqman Assay primer/probes designed to exclude genomic DNA by crossing the intron-exon border were used with TaqMan PCR master mix (ABI) (see TABLE 1 for summary of primer IDs). mRNA from cells harvested prior to encapsulation was used for comparison. Relative gene expression was calculated for each experiment by normalizing to the housekeeping gene (18S) and “day zero” gene expression of cells prior to encapsulation, ($\Delta\Delta C_T$). Graphs represent mean \pm 95 % confidence.

TABLE 2.1 – TAQMAN PRIMERS.

GENE NAME	TaqMan Assay ID
18S	hs9999999901_s1
COL1A1	hs00164004 ml
COL2A1	hs00264051 ml
COL10A1	hs00166657 ml
ACAN	hs00153936 ml
MMP1	hs00233958 ml
MMP2	hs00234422-ml
MMP7	hs00159163-ml
MMP13	hs00233958 ml
ADAMTS2	hs0102911 ml
ADAMTS3	hs00610744 ml
ADAMTS4	hs00192708 ml
ADAMTS5	hs00199841 ml
ADAMTS14	hs00365506 ml
SOX5	hs00374709 ml
SOX6	hs00264525 ml
SOX9	hs00165814 ml

2.6 HISTOLOGY AND IMMUNOHISTOCHEMISTRY

Hydrogels were fixed in 10 % neutral buffered formalin, embedded in paraffin and 5 µm sections cut onto silane coated slides. Representative slides were deparaffinized through a xylene

to PBS rehydration protocol: three washes in xylene (5 minutes), two washes in 100 % ethanol (EtOH, 10 minutes), two washes in 70 % EtOH (10 minutes), one wash in water (5 minutes), and a final wash in PBS (5 minutes).

2.6.1 Toluidine Blue Staining for Hydrogels

Toluidine blue staining (0.04 % toluidine blue in 0.1 M Sodium Acetate, pH 4) was used to visualize sulfated proteoglycans using 2 minute exposure to dye followed by four rinses in de-ionized water for 1 minute each. Sections were then re-dehydrated with sequential washes in 70 % ethanol (1 minute), 100 % ethanol (3 x 1 minute), xylene (4 x 1 minute). Coverslips were then mounted in xylene based Cytoseal™ XYL mounting medium (Richard-Allan Scientific, #8312-4, Kalamazoo, MI).

2.6.2 Collagen I Immunohistochemistry

For all immunohistochemical procedures slides were deparaffinized as described above and then blocked in 5 % bovine serum albumin (BSA) solution for 1 hour at room temperature. An antigen retrieval step was added prior to blocking with BSA to unmask collagen I epitopes. Slides were incubated in either sodium citrate buffer (10x stock: 2.94 g sodium citrate + 1L DDH₂O, pH 6.0) or a commercial antigen retrieval solution (Dako Target Retrieval Solution) for 1 hour in a 75°C water bath. Following the normal blocking protocol, sequential matrix digestion steps were taken: 15 minutes at 37°C in a 1 % hyaluronidase followed by 15 minutes at 37°C in pronase (1 mg/ml) solution. The primary collagen I antibody, a kind gift of Dr. Anthony Hollander (University of Bristol, UK), was diluted 1:400 in 1 % BSA and sections were incubated overnight at 4 °C. Detection was done using a goat-anti-rabbit AlexaFluor™ 594 linked secondary antibody. Coverslips were mounted using ProLong® Gold Antifade containing blue-fluorescent

nuclear counterstain DAPI (Invitrogen, P36934). Images were converted to grayscale in Photoshop.

2.6.3 Collagen II and X Immunohistochemistry

Following the blocking step described above, sections were washed with PBS and exposed to a pronase (1 mg/ml in PBS, 20 minutes at room temperature) digestion step. Sections were washed again with PBS and then incubated with the collagen II (II-II6B3, NIH Hybridoma Bank, University of Iowa) or collagen X, kindly provided by Dr. Gary Gibson (Henry Ford Institute, Detroit MI), mouse monoclonal antibodies diluted 1:200 in 1 % BSA and incubated overnight at 4 °C. Detection was done using the goat-anti-mouse AlexaFluor™ 594 linked secondary antibody. Coverslips were mounted using ProLong® Gold Antifade containing blue-fluorescent nuclear counterstain DAPI (Invitrogen, P36934). Images were converted to grayscale in Photoshop.

2.6.3 MMP-7 Immunohistochemistry

MMP-7 in hydrogels was detected with a pre-diluted mouse monoclonal MMP-7 antibody recognizing both the pro- and active form of human MMP-7 (GeneTex, GTX17B54). Detection was done using goat-anti-mouse AlexaFluor™ 594 linked secondary antibody. Images were converted to grayscale in Photoshop.

To detect MMP-7 in embryonic mouse limbs, frozen sections were briefly fixed in cold acetone, blocked with 5 % BSA for 1 hour, and then treated with 2 mg/ml type V hyaluronidase for 30 minutes at 37 °C. Sections were exposed to a 1:200 dilution of rat monoclonal anti-MMP7 antibody, kindly provided by Dr. Lynn Matrisian (Vanderbilt University, clone 338)^{235,236}. Detection was done using a 1:100 dilution of goat-anti-rat HRP and peroxidase substrate DAB plus nickel (Vector Laboratories, SK-100). Staining of a colon tumor metastasis in liver was used as a positive control and was consistent with the literature²³⁷⁻²³⁹.

2.6.4 Fluorescence *In Situ* Hybridization (FISH)

FISH staining was performed following immunohistochemistry to identify the cytogenetic source of extracellular matrix staining in hydrogels containing a coculture of human mesenchymal stem cells and human articular chondrocytes of opposite gender donors. Immunohistochemistry was done as described previously until after the secondary antibody step, where coverslips were non-permanently mounted with Vectashield® mounting medium containing DAPI (Vector Laboratories, #H-1200, Burlingame CA). Matrix staining was then photographed on a Nikon Eclipse E800 photomicroscope using CytoVision software from Applied Imaging at 600X. Coverslips were then removed by soaking in 2X saline sodium-citrate buffer (SSC) + 0.15 % Tergitol® NP-40 (Sigma, # MFCD00132411) and FISH staining for human chromosomes X and Y was performed. Slides were incubated in 2X SSC for 30 minutes at 37°C, followed by 0.005 % pepsin in 0.01N hydrochloric acid digestion for 13 minutes at 37 °C. Slides were rinsed in PBS for 5 minutes at room temperature and then further fixed in 1% formaldehyde/0.45% MgCl₂/PBS for 5 minutes at room temperature. Slides were again rinsed in PBS for 5 minutes at room temperature followed by sequential 2-minute washes in 70%, 80%, and 90% ethanol at room temperature to dehydrate the slide. Slides were allowed to air dry and the CEPX Spectrum Green/CEPY (Alpha) Spectrum Orange probe set was added to slide (Abbott). Coverslips were then applied and sealed by rubber cement. Slides were put on a HyBrite apparatus (Abbott) programmed for 80 °C for 5 minutes and 37 °C overnight. Following incubation, slides were post-washed in 2X SSC + 0.3 % NP-40 at 72 °C for 2 minutes, placed in 2X SSC + 0.15 % NP-40 for 30 seconds at room temperature, and coverslips were mounted with DAPI II (Abbott). Samples were analyzed for presence of X and Y chromosomes using DAPI, green and orange filters on a Nikon Eclipse E800 photomicroscope. Photographs were taken using CytoVision software from Applied Imaging. The cytogenetic score for co-culture slides was calculated by determining gender of 200 cells on three different sections, the presence of a single

Y chromosome was considered male, while visualization of only a single X chromosome was considered “unknown” gender.

2.7 ZYMOGRAPHY

Casein zymography was performed to semi-quantitatively access MMP-7 activity present in the hydrogel constructs and released to the media. Hydrogels and conditioned medium were harvested into sample buffer (2x sample buffer: 20 % glycerol, 2 % SDS, 0.02 % bromophenol blue, 20 mM Tris, 2 mM EDTA, pH 7) and stored at -80 °C until all time points had been collected. Conditioned medium was mixed equal volume with the sample buffer. Two large hydrogels per time point were harvested into a 1:2 dilution of sample buffer in water and then homogenized using the Ultra-Turrax® IKA-T10 homogenizer. Precast casein gels (BioRad, #8800718, Hercules CA) were pre-run for 4 hours to remove excess casein. Samples were loaded as well as a molecular weight protein ladder (BioRad Kaleidoscope Prestained Standards, Hercules CA), and recombinant human pro- and active-form MMP-7 (AnaSpec, Fremont CA). Electrophoresis of gels was performed in a Running Buffer (Biorad, Hercules CA) at 100 volts for approximately 2 hours, or until the bands reached the end of the gel. Gels were washed twice for 30 minutes in a Renaturation Buffer (2.5% Triton X-100) to remove SDS and then incubated 18 hours at 37 °C in Development Buffer. Gels were stained with 0.5 % coomassie brilliant blue in 40 % methanol and 10 % acetic acid for 1 hour, and then destained in 40 % methanol and 10 % acetic acid. Gels were preserved in cellophane and 1 % glycerol with 25 % ethanol.

2.8 MECHANICAL TESTING

Material properties of the hydrogels were measured with a custom apparatus designed and built by Drs. Trevor Lujan and Michael Bottlang and the Legacy Biomechanics Laboratory. The testing unit imposed unconfined compression to cell free scaffolds. Specimens were

compressed by a voice-coil force actuator (Model Cal36, SMAC, Carlsbad, CA) that was controlled using data acquisition software and hardware (National Instruments, LabVIEW 8.0, PCI 6221, Austin Texas). The actuator applied an upward force to a rigidly connected plunger to compress specimens into an impermeable aluminum platen (15 mm diameter). Compressive forces were measured by connecting the platen to a rigidly fixed load cell (Model 31, Sensotec, Morristown, NJ; resolution 0.005 N). Specimen displacement was measured with a glass-scale encoder integrated into the voice-coil actuator (resolution = 1 μm). The actuator was powered with a linear current amplifier (Model LCAM Quanser, Markham, Ontario) and the load cell was powered by a signal conditioner with a low-pass filter (PMD-465WB, Omega, Standord, CT). In the absence of a testing specimen, the test system yielded a dynamic stiffness of 1N/[m, which is over two orders of magnitude greater than the dynamic stiffness of standard hydrogels²⁴⁰. This force-controlled testing system was selected to ensure that the platen would not lift-off the specimen during testing²⁴¹.

For each material test, specimens were centered in a culture dish filled with 1 ml phosphate buffered saline (PBS), and loaded into the testing apparatus. To establish a consistent reference position for all samples, a 0.1 N preload was applied and specimen thickness was recorded (l_o). The samples were then loaded to 0.4 N and allowed 90 seconds to creep. Sinusoidal force waves were then applied for 30 cycles at 1 Hz to an amplitude of 0.5 N (peak-to-peak). These forces resulted in an average dynamic compression between 5% and 20% strain²⁴².

Dynamic modulus was calculated as the ratio of the first Piola-Kirchhoff stress (force in the present configuration to area in the reference configuration) and engineering strain ($(l-l_o) / l_o$, where l is the current thickness and l_o is the reference thickness). These values were extracted by fitting the final three cycles of stress and strain data to a four-parameter sine function in LabVIEWTM²⁴³. Data measurements represent means \pm standard deviation; data was analyzed using an ANOVA with significance set at 0.05, followed by a pairwise comparison to the control using Dunnett's test.

2.9 SWELLING RATIO CALCULATIONS (Q)

Cell-free scaffolds were fabricated as described above and swollen to equilibrium in PBS (minimum of 60 hours) at 37° C and 5% CO₂. After reaching equilibrium scaffolds were weighed (W_{eq}) and then dried in a vacuum chamber (Thermo Vacuum Oven Model #19: minimum of 48 hours at 37° C, 25 mmHg) to determine dry weight (W_{dry}). The volumetric swelling ratio (Q) was determined as the ratio of ($W_{eq} - W_{dry}$) over (W_{dry}). Data measurements represent mean \pm standard deviation; statistical significance was tested using t-test with significance set at 0.05.

CHAPTER 3:
**VISIBLE LIGHT PHOTOINITIATION OF MESENCHYMAL STEM
CELL-LADEN BIORESPONSIVE HYDROGELS**

AUTHORS

Bahney CS^{1,2}, Lujan TJ³, Hsu CW⁴, Bottlang M³, West JL⁴, Johnstone B^{1,2*}

¹Oregon Health & Science University, Department of Orthopaedics and Rehabilitation

²Oregon Health & Science University, Department of Cell and Developmental Biology

³Legacy Research & Technology Center, Biomechanics Laboratory

⁴Rice University, Department of Bioengineering

Submitted to eCM Journal, June 2010.

CSB participated in the planning and execution of all experiments; she was the primary author of the manuscript.

3.1 ABSTRACT

The ideal scaffold for tissue engineering should be uniquely tuned to self-sufficiently generate the physical and biological cues that facilitate development of a neotissue with properties as similar to the native tissue as possible. Recently, a wide variety of sophisticated biomaterials have advanced the field towards this goal by incorporating peptides that serve as enzyme-mediated degradation sites, cell adhesions sites that mimic the extracellular microenvironment or bioactive factors. One complication with the addition of these peptides is that aromatic amino acids absorb light at 285 nm and compete with the UV-sensitive photoinitiator IrgacureTM 2959 (I2959), which is the most commonly used initiator for photoencapsulation of cells into synthetic scaffolds. In this study we define non-toxic conditions for photoencapsulation of human mesenchymal stem cells using a visible light photoinitiator system composed of eosin Y, triethanolamine (TEA) and 1-vinyl-2 pyrrolidinone (NVP). Using dynamic modulus and swelling ratio to measure the physical properties of the scaffold, we establish very low concentrations of both eosin Y and TEA that can be used to avoid cytotoxicity while creating hydrogels that crosslink more quickly and completely than with the I2959 photoinitiator.

3.2 INTRODUCTION

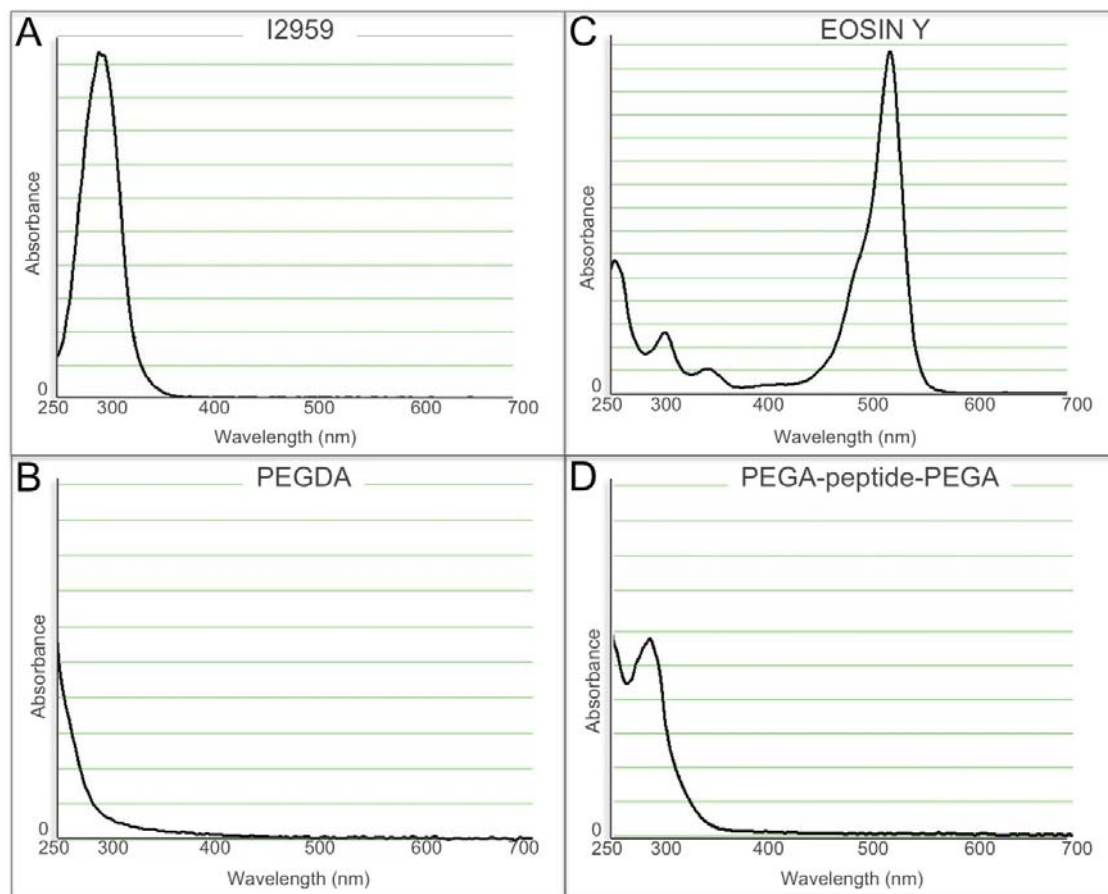
Tissue engineering is an experimental concept that has been in the literature for approximately 25 years, with an application to cartilage first introduced in the early 1990s²⁴⁴. A principle of cartilage engineering is to utilize three-dimensional scaffolds to support chondrogenic cells and facilitate the development of a neocartilaginous construct that can functionally replace damaged or diseased tissue *in vivo*. Since tissue engineering was first introduced, the role of the scaffold has evolved towards an instructive microenvironment that can facilitate cell migration, differentiation, adhesion, and cell-mediated degradation²⁴⁵⁻²⁴⁷. In many cases adding these biological activities to the scaffold requires the spatiotemporal incorporation

of peptides. As we advance our understanding of what biological functionality needs to be added to scaffolds for improved neotissue formation, it becomes essential to expand our range of techniques for scaffold development, specifically with respect to the impact of scaffold formation on the cells.

Synthetic scaffolds such as poly(ethylene glycol) diacrylate (PEGDA) are popular biomaterials for tissue engineering because their physical and chemical properties can be easily tailored to suit the individual needs of developing tissue. For example, we, and others, have previously demonstrated that physical modifications to the scaffold can result in significant changes to matrix production and distribution in cartilage engineering applications^{173,175,248,249}. Furthermore, the inclusion of cell adhesion ligands^{154,213,250}, growth factors²⁰⁶, and enzymatic cleavage sites¹⁹⁶ can chemically modify scaffolds to make them bioactive and bioresponsive.

Another specific advantage of PEGDA scaffolds is that they can be formed under physiological conditions through the process of photopolymerization,³ which allows for the uniform encapsulation of cells¹⁸⁴⁻¹⁸⁶. Photopolymerization uses light to dissociate initiator molecules into free radicals that can react with macromers functionalized with double or triple chemical bonds (i.e. the acrylate groups in PEGDA) to propagate radical chain polymerization. One problem with this system is that free radicals created during this process can have the unintended side effect of damaging cell membranes, proteins and DNA. Consequently, considerable effort has been made into finding cytocompatible photoinitiators. The most well established initiator for photoencapsulation is IrgacureTM 2959 (1-[4-(2-Hydroxyethoxy)-phenyl]-2-hydroxy-2-methyl-1-propane-1-one, "I2959"). I2959 is tolerated by many cell types at a concentration of 0.03 – 0.1 %²³¹; however, it has been shown that different cell types will display variable degrees of cytocompatibility²⁵¹. This photoinitiator reacts in the ultraviolet (UV) range with a peak absorbance of ~280 nm (Figure 3.1A), but remains effective at initiating polymerization at the longer wavelength 365 nm, which is better tolerated by cells²³².

Both the direct incorporation of peptide sequences into the monomer backbone and tethering of peptides is central to the design of the bioactive and bioresponsive scaffolds discussed above. However, aromatic amino acids absorb at 285 nm, thus competing with I2959 during photoinitiation (Figure 3.1D). High concentrations of I2959 can outcompete the effect of the peptide, however cellular toxicity is documented at concentrations above 0.1 %^{231,251,252}. One potential solution is to use a photoinitiator effective at a much different wavelength, such as those that operate in the visible light range. In this study, we explored the cytotoxicity of the photosensitizer eosin Y, which has peak absorbance at ~510 nm (Figure 3.1C), used with initiator TEA and accelerator 1-vinyl-2 pyrrolidinone (NVP) for use with human mesenchymal stem cells (hMSCs). This photoinitiator system has previously been studied in regards to islet cell viability and encapsulation efficiencies using an argon ion laser²⁵³ and visible light photoencapsulation of a fibroblast cell line MRC-5²⁵⁴. However, we found the photoinitiator concentrations used in those studies to be toxic for the photoencapsulation of hMSCs. Here we demonstrate significantly lower concentration of both eosin Y and TEA can be used to effectively facilitate polymerization while avoiding the cytotoxicity of these reagents.



3

FIGURE 3.1 – SPECTROPHOTOMETRIC ABSORBANCE OF PHOTOINITIATORS AND MACROMER FORMULATIONS. (A) Irgacure™ 2959 UV sensitive photoinitiator. (B) 10 % (w/v) PEGDA macromer. (C) Eosin Y photosensitizer. (D) 10 % (w/v) peptide containing PEGDA macromer.

3.3 RESULTS

IrgacureTM 2959 (I2959) is a commonly used photoinitiator for encapsulation of cells within hydrogels due to its well-established cytocompatibility below a concentration of 0.1 % (w/v). When we incorporated peptides into PEGDA scaffolds to impart biological activity we found that I2959 could not effectively initiate photopolymerization at concentrations below 0.3 %, well above the cytotoxicity point for hMSCs. A number of peptide sequences were tested, but common to them all was the presence of the aromatic amino acid tryptophan. Since aromatic amino acids absorb energy at 285 nm we hypothesized that their presence in the macromer was competing with I2959 during the polymerization reaction (Figure 3.1A, D) and were motivated to develop a photoinitiator effective in the visible light spectrum for encapsulation of hMSCs within peptide containing PEGDA hydrogels.

Eosin Y is a photosensitizer with peak absorbance of 510 nm (Figure 3.1C) and is used in conjunction with initiator TEA and catalyst NVP for photopolymerization under bright white light. In preliminary experiments we found the published concentrations of eosin Y (≥ 0.1 mM) and TEA (≥ 1.5 % w/v), but not NVP (37.5 mM), to be toxic to hMSCs. Cytotoxicity was tested by exposing confluent, monolayer-plated hMSCs to each initiator components for 5 minutes, both with and without exposure to visible light. Using fluorescently activated calcein, live cells were visualized both immediately following treatment and 24 hours later. Eosin Y, at a concentration of 0.1 mM, was toxic to hMSCs only when activated by white light, presumably due to the presence of free radicals that could not be adequately quenched by the polymerization reaction. In contrast, TEA was toxic to the hMSCs both with and without exposure to light at a concentration of 1.5 %.

To determine lower concentrations of eosin Y and TEA that were still effective in initiating photopolymerization of a 10 % (w/v) PEGDA, we created a fractional factorial test design that measured dynamic modulus and swelling ratio for hydrogels formed with 0.001 – 0.1 mM eosin Y and 0.01 – 1.5 % TEA (Figure 3.2A). We reasoned that by establishing this

relationship we could decrease the concentrations of both eosin Y and TEA without significantly impacting polymerization. Scaffold properties such as dynamic compressive modulus and swelling ratio after hydrogels have reached equilibrium conditions can be used as a functional output of crosslinking density. We found that dynamic modulus was not a linear function of either eosin Y or TEA (Figure 3.2B). Rather, any hydrogel that polymerized completely formed scaffolds with an equivalent dynamic compressive modulus (Figure 3.2C) or swelling ratio (Figure 3.2D). Polymerization was considered incomplete if greater than 25 % of the original macromer volume did not react (Figure 3.2A, groups G-I). Neither extending the time of light exposure from 2 to 10 minutes, nor doubling the concentration of the catalyst NVP, was sufficient to carry the polymerization reaction to completion at these initiator concentrations.

To test cytocompatibility during photoencapsulation of hMSCs in a 10 % PEGDA scaffold we chose both a “high” (0.1 mM eosin Y & 0.75 % TEA) and “low” (0.01 mM eosin Y & 0.1 % TEA) concentration of eosin Y and TEA from our previous screen to compare with I2959 as a control (Figure 3.3). Although there were lower concentrations of eosin Y and TEA that were effective in initiating polymerization (Figure 3.2A, groups D-F) we chose not to test boundary conditions (Figure 3.2A) since the high density of cells can interfere with the polymerization efficiency. Scaffolds formed by either visible light photopolymerization reaction had significantly higher crosslinking density than those formed with I2959 and UV-light as demonstrated by a stronger dynamic compressive modulus (Figure 3.3A) and smaller swelling ratio (Figure 3.3B). Cytotoxicity was assessed by quantifying DNA content in the hydrogels from day 1-14 (Figure 3.3C) and through live-dead staining of hMSCs 48 hours after polymerization (Figure 3.3D-F). Testing hMSCs toxicity after photoencapsulation is a more appropriate method than monolayer exposure since the reaction of the initiator components with the acrylate groups during photopolymerization will significantly affect the presence of free radicals. When cell content was normalized to the number of cells initially encapsulated into each of the hydrogels, I2959 polymerized hydrogels had a lower relative number of cells at all times than either of the

eosin-TEA polymerized hydrogels (Figure 3.3C). However, this is likely due more to cell loss from the scaffold as a consequence of lower crosslinking (Figure 3.3A,B) than increased toxicity (Figure 3.3D).

We next tested if hMSC chondrogenesis was differentially affected by the UV versus visible light polymerization process in 10 % PEGDA scaffolds. Following six weeks of *in vitro* culture we found that the lower concentration of eosin-TEA (0.01 mM eosin Y & 0.1 %) accumulated significantly more sulfated proteoglycans (GAG) than the I2959 hydrogels, and total collagen production, as measured by hydroxyproline content, was significantly decreased at high concentrations of eosin-TEA (Figure 3.4A). The impact of the higher concentration of eosin-TEA photoinitiators on chondrogenesis was amplified on a per cell basis considering DNA content was higher in these scaffolds throughout culture (Figure 3.3C, 3.4B). We also looked at GAG release to the media from each of the scaffolds: significantly more GAG was released from the I2959 scaffolds between weeks 1-4 (Figure 3.5C), again, presumably due to the lower crosslinking density (Figure 3.3B,C). GAG release from the lower concentration of eosin-TEA reached the same levels at the I2959 scaffold by weeks 5 and 6 (Figure 3.4C), consistent with the higher crosslinking density (Figure 3.3B,C) and higher GAG accumulation (Figure 3.5A), while GAG release from the higher eosin-TEA scaffold remained consistently lower.

This visible light photoinitiator was also effective in initiating polymerization of scaffolds containing peptides with aromatic amino acids (aPEG-peptide-PEGa); polymerization of this scaffold was not possible with I2959 at a concentration below 0.1 % (w/v). Live-dead staining of hMSCs encapsulated in the aPEG-peptide-PEGa hydrogel confirmed cytocompatibility with minimal cell death observed at 48 hours (Figure 3.5C). The dynamic compressive modulus of the aPEG-peptide-PEGa scaffold was significantly lower than that of the 10 % PEGDA due to the increased molecular weight of the monomer subunit as a result of the addition of the peptide (Figure 3.5A). We next evaluated chondrogenesis of hMSCs in the 10 % PEGDA, aPEG-peptide-PEGa and a PEGDA-based semi-interpenetrating network (sIPN) in

which we have previously shown improved matrix production and distribution during hMSC chondrogenesis due to the increased pore size in the sIPN scaffold¹⁷³. Chondrogenesis was improved in both of these scaffolds as measured by accumulation of extracellular matrix proteins (Figure 3.5B) and visualized with toluidine blue (Figure 3.5D-I) and type II collagen immunohistochemistry (Figure 3.5G-J).

3.4 DISCUSSION

Synthetic hydrogels, such as PEGDA, are useful biomaterials for tissue engineering applications because their physical^{173,175,249} and chemical^{154,220,255,256} properties can be optimized for the tissue of interest. Techniques now exist to impart biological activity to these scaffolds through the addition of peptides that can be tuned to facilitate a variety of cellular functions. However, we found that when peptides containing aromatic amino acids were incorporated into the macromer design they interfered with photopolymerization using the most commonly applied UV initiator, I2959. A specific advantage of hydrogels scaffolds is the uniform and non-toxic encapsulation of cells. In this study we established cytocompatible conditions for photoencapsulation of hMSCs using a visible light photoinitiator that would not compete in the UV spectrum at which both aromatic amino acids and I2959 absorb (Figure 3.1A,D).

2
A

Category	TEA (%)	Eosin Y (mM)	Complete Polymerization?
A	1.500	0.100	yes
B	0.750	0.100	yes
C	0.100	0.010	yes
D	0.100	0.005	yes
E	0.050	0.010	yes
F	0.050	0.005	yes
G	0.010	0.010	no
H	0.010	0.100	no
I	0.050	0.001	no

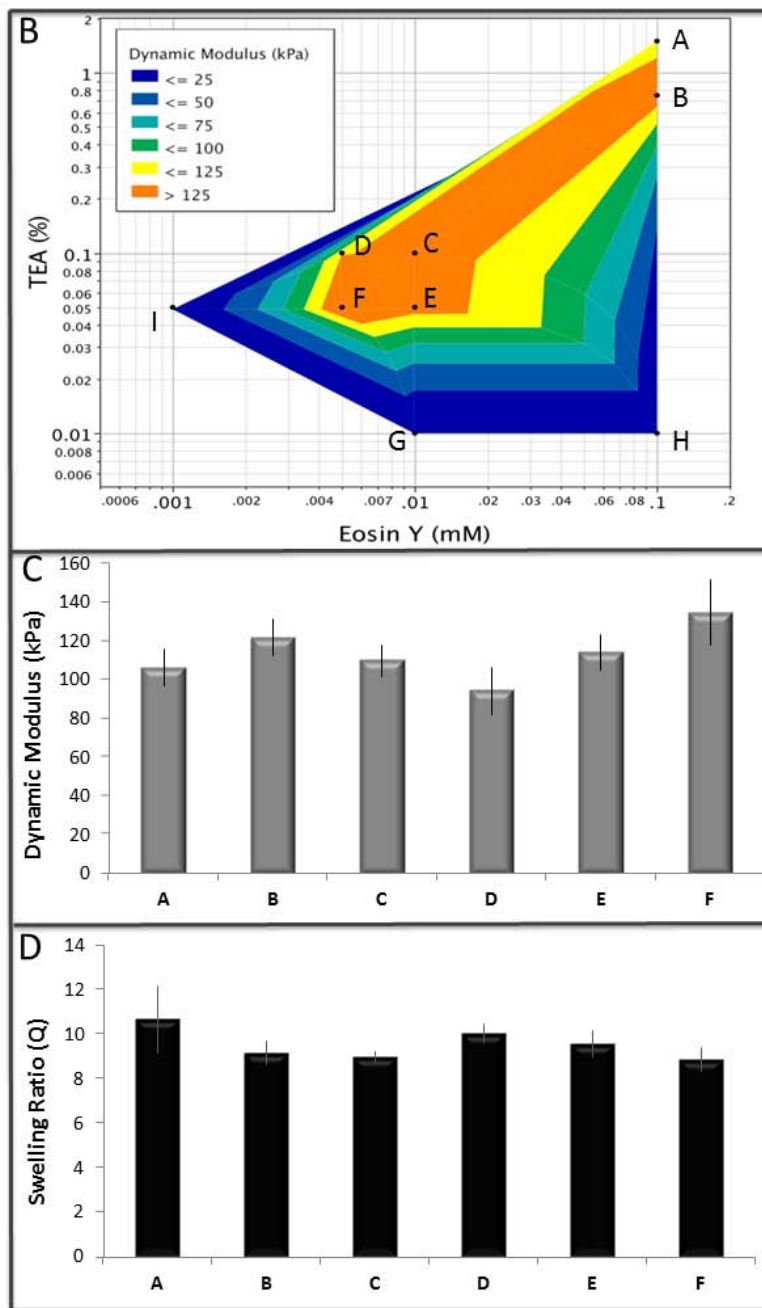


FIGURE 3.2 – SCREENING DESIGN FOR LOWER VISIBLE LIGHT INITIATOR CONDITIONS. (A) Table of input parameters. (B) Dynamic modulus response model. (C) Dynamic compressive modulus. (D) Swelling ratio.

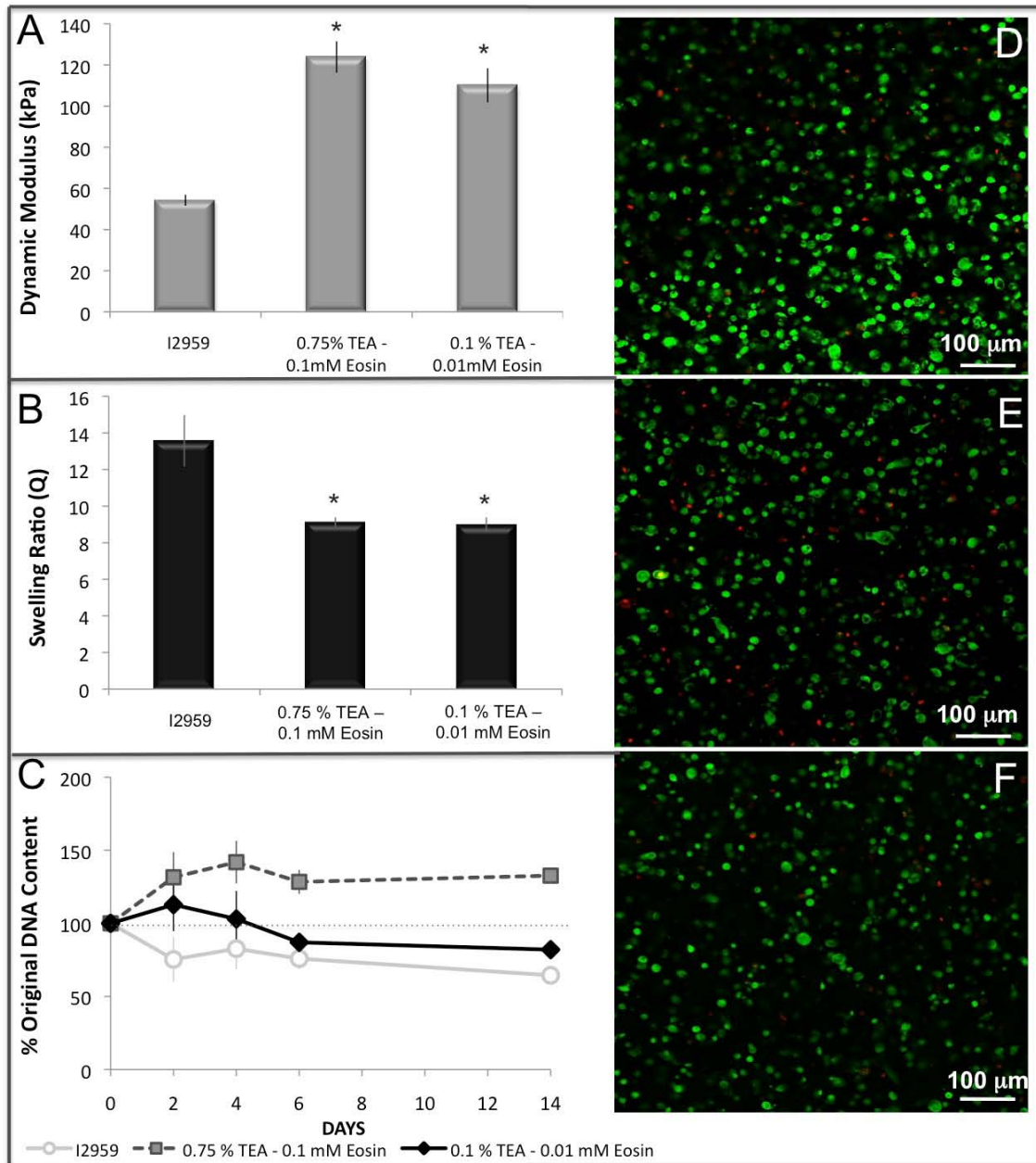


FIGURE 3.3 – SCAFFOLD PARAMETERS AND CYTOTOXICITY OF VISIBLE LIGHT INITIATION COMPARED TO UV LIGHT INITIATION. (A) Dynamic compressive modulus. (B) Swelling ratio. (C) DNA content normalized to initial seeding density. Live (green) – Dead (red) staining of hMSCs 48 hours after photoencapsulation in a 10 % PEGDA scaffold with (D) I2959, (E) 0.75 % TEA & 0.1 mM eosin Y, (F) 0.1 % TEA & 0.01 mM Eosin Y.

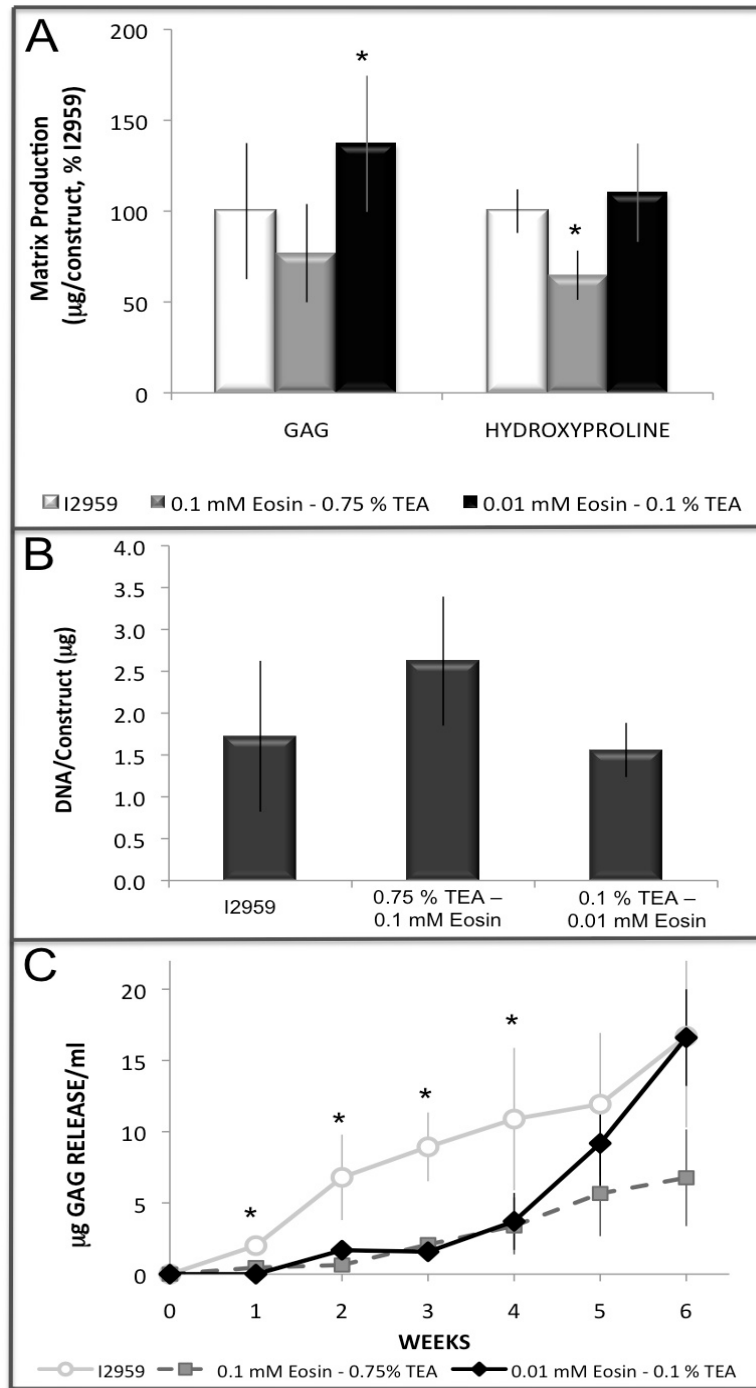


FIGURE 3.4: MSCs CHONDROGENESIS IN 10 % PEGDA SCAFFOLDS POLYMERIZED WITH VISIBLE VERSUS UV LIGHT. (A) GAG and total collagen accumulation of eosin-TEA polymerized hydrogels normalized to I2959-scaffolds. (B) DNA content measured after 6 weeks. (C) GAG release to the medium.

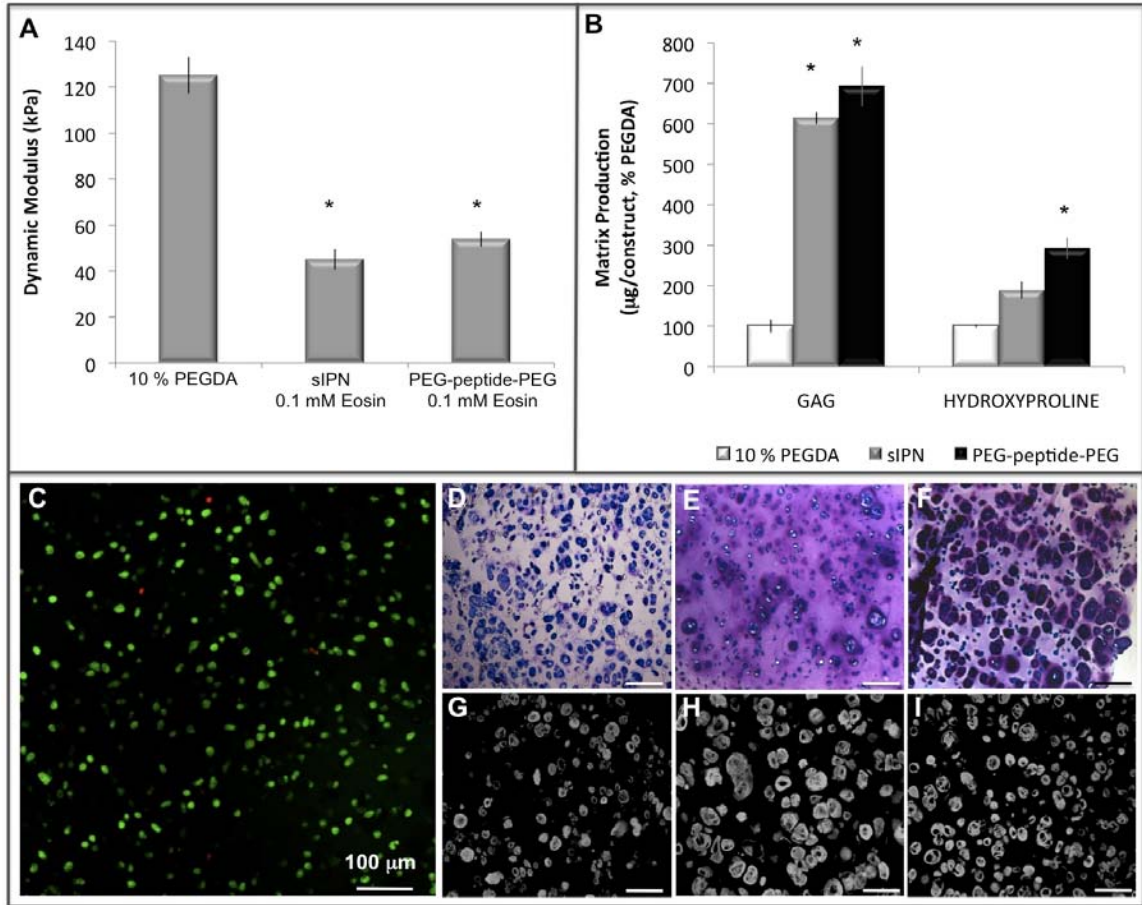


FIGURE 3.5 – MSCs CHONDROGENESIS IN sIPN AND PEPTIDE CONTAINING PEGDA SCAFFOLDS. (A) Dynamic compressive modulus. (B) GAG and total collagen accumulation normalized to 10 % PEGDA. (C) Live (green) – Dead (red) staining of hMSCs in peptide containing PEGDA scaffold. Toluidine blue staining for proteoglycans in (D) 10 % PEGDA, (E) sIPN, (F) peptide containing PEGDA. Collagen II immunohistochemistry in (G) 10 % PEGDA, (H) sIPN, (I) peptide containing PEGDA; scale bar = 100 μ m.

The use of cells, such as MSCs^{106,244} and embryonic stem cells^{247,257}, for tissue engineering applications is becoming increasingly popular as mechanisms to control differentiation towards a desired phenotype are being established. An important part of validating scaffold design for differentiation of stem cells is the consideration of photoinitiator toxicity. The most commonly used photoinitiator for hydrogel polymerization is I2959 and its cytocompatible range has been established as $\leq 0.1\%$ (w/v), with both a time and temperature dependency in the reaction^{231,251,252}. However, different cells exhibit variable degrees of cytocompatibility²⁵¹ and the impact on differentiation should be considered when working with progenitor cells²⁵². A number of visible light initiators have been described to have a cytotoxic effect, including 9-fluorenone and camphorquinone (CQ) used with either ethyl 4-N, N-dimethylaminobenzoate or triethanolamine (TEA) and the photosensitizer isopropyl thioxanthone^{231,258}.

We chose to test a system comprised of the photosensitizer eosin Y, initiator TEA, and accelerator NVP that has previously been described for encapsulation of pancreatic islet cells using an argon laser²⁵³ and visible light photoencapsulation of a fibroblast cell line MCR-5²⁵⁴. In preliminary experiments we found the concentration of eosin Y and TEA used for those cell types to be cytotoxic to hMSCs. To determine if lower concentrations of eosin Y and TEA could be used effectively for hMSC encapsulation we used dynamic modulus to efficiently screen for polymerization conditions that minimized photoinitiator concentration (Figure 3.2). Physical properties such as dynamic modulus and swelling ratio correspond to crosslinking density and can be used as a measurable output parameter to validate the polymerization reaction. In our screen we identified a number of groups in which greater than 25 % of the macromer solution did not polymerize (Figure 3.2A). Under these conditions we looked to see if a longer light exposure could complete the polymerization reaction, but found no change in the reaction even after 10 minutes, suggesting that the problem was insufficient concentrations of initiator components.

Based on a model generated from this screen (Figure 3.2B) we chose to evaluate cytotoxicity and chondrogenesis of hMSCs at both a high (0.1 mM eosin Y & 0.75 % TEA) and

low (0.01 mM eosin Y & 0.1 % TEA) concentration of initiator. Although there were lower concentrations of both eosin Y and TEA sufficient to complete polymerization of cell-free 10 % PEGDA scaffolds, we chose these concentrations to avoid the boundary conditions of the reaction because the high density of cells at encapsulation can interfere with polymerization efficiency. Cytotoxicity during polymerization reactions has previously been tested predominantly using exposure of monolayer-plated cells to initiator components and light^{231,251}. Using this technique to screen for toxicity of eosin Y and TEA in preliminary experiments we found that free radicals generated during light-activation of eosin Y were very toxic to cells at a concentration of 0.1 mM. TEA had a toxic effect both with and without light exposure at a concentration of 1.5 % (v/v). However, this method for establishing toxicity does not adequately account for quenching of radicals that occurs during the process of radical chain polymerization of functionalized macromers. Consequently, our toxicity experiments examined DNA content and cell viability following photoencapsulation of hMSCs within a 10 % PEGDA hydrogel (Figure 3.3). Confocal images of live-dead staining after 48 hours indicates hMSC viability in the visible-light formed hydrogels is no different than photoencapsulation with I2959 (Figure 3.3D-F). Interestingly, there was an initial increase in the DNA content following photoencapsulation in the visible light system indicating proliferation (Figure 3.3C). It is unclear if the decrease in cell number in I2959-formed hydrogels is due to a lack of proliferation or due to a loss of cells from the more loosely crosslinked system (Figure 3.3A,B). These results further suggest that the eosin-TEA visible light initiator system is significantly more efficient at photopolymerization than I2959 within cytocompatible ranges for each initiator. Improved efficiency of the photoinitiator translated into significantly faster photopolymerization with the visible light system: 2 minutes, as compared to 6 minutes with UV light and I2959 at concentrations at 0.06 %^{132,173}.

We next investigated whether the visible light initiator system affected differentiation and matrix elaboration during hMSCs chondrogenesis. Our results show that at the lower concentration of eosin Y (0.01 mM & 0.1 % TEA) GAG production was increased relative to

I2959, while the higher concentrations (0.1 mM eosin Y & 0.75 % TEA) lead to a significant decrease in collagen accumulation (Figure 3.4A). The reduced production of matrix molecules with the higher eosin Y concentration is more significant given the trend towards increased cell numbers (Figure 3.3C, 3.4B) and reduced GAG release (Figure 3.4C). I2959 formed scaffolds resulted in a significantly increased loss of GAG to the medium during weeks 1-4 of matrix elaboration (Figure 3.4C), presumably due to the increase in pore size (Figure 3.3A-B). However, GAG released from the scaffold polymerized with 0.01 mM eosin matched that of the I2959 by week 4, consistent with the higher total GAG accumulation at 6 weeks (Figure 3.4A).

Since the visible light initiator did not appear to have any immediate impact on cytotoxicity (Figure 3.3C-F) it is difficult from these data to distinguish whether the impact on chondrogenesis was due to the different chemistries of the photoinitiator (Figure 3.4) or the change to the scaffold properties (Figure 3.3A-B) as has been suggested previously^{173,175,249}. Consequently, we next chose to examine chondrogenesis of hMSCs in both a PEGDA-based sIPN and a aPEG-peptide-PEGa scaffold. The aPEG-peptide-PEGa scaffold was representative of bioresponsive hydrogels^{196,198,199,213}, but we chose a peptide with no known biological activity²⁰⁰. The PEGDA-based sIPN scaffold was included because we have previously published an improved extracellular matrix production and distribution during chondrogenesis of hMSCs due to the larger pores formed by the inclusion of a non-crosslinking PEG component¹⁷³. The larger pore size in the sIPN is illustrated by the significantly reduced dynamic compressive modulus as compared with 10 % PEGDA (Figure 3.5A). The 10 % (w/v) peptide-containing scaffold (aPEG-peptide-PEGa) showed a similar reduction in modulus (Figure 3.5A). By inserting the peptide into the PEGDA backbone the molecular weight of the aPEG-peptide-PEGa monomer subunit was 8.27 kDa. Molecular weight has previously been shown to have a significant impact on crosslinking density^{176,249,259,260}, explaining the reduction in modulus of aPEG-peptide-PEGa relative to the 10 % PEGDA scaffold made from a 6 kDa monomer. Chondrogenesis in these three scaffolds was compared following six weeks of *in vitro* culture and we found significantly

improved proteoglycan accumulation (Figure 3.5B) and distribution (Figure 3.5D-F) in both the sIPN and PEGA-peptide-PEGA scaffold as compared with 10 % PEGDA, all polymerized with the visible light initiator. Collagen accumulation was significantly higher in the aPEG-peptide-PEGa scaffold (Figure 3.5B) but distribution did not change (Figure 3.5G-I). Together these data suggest that pore size has a more significant impact on cartilage matrix deposition than initiator chemistry provided both are cytocompatible, but also highlights that efficiency of photoinitiators can produce significantly different mechanical microenvironments for the cells by changing scaffold modulus.

3.5 CONCLUSION

This study validates a visible light photoinitiator system comprised of eosin Y, TEA, and NVP for cytocompatible encapsulation of hMSCs. We found this photoinitiator system to be more suitable for creating scaffolds containing peptide elements as the absorbance of aromatic amino acids can interfere with polymerization reactions in the UV light range. The visible light system also proved to be a more efficient photoinitiator than I2959: increasing scaffold modulus by approximately 123 % over that of I2959 with a polymerization time of only 2 minutes as compared to 6 minutes for I2959. Using this visible light initiating system we then compared hMSC chondrogenesis in a 10 % PEGDA, PEGDA-based sIPN, and peptide containing scaffold (aPEG-peptide-PEGa) representative of bioresponsive scaffolds. We found that scaffold modulus had a significant impact on matrix elaboration, with looser networks increasing matrix deposition and improving distribution of proteoglycans.

CHAPTER 4:
A BIORESPONSIVE HYDROGEL TAILORED TO CHONDROGENESIS

AUTHORS

Chelsea S Bahney^{1,2}, Chih-Wei Hsu³, Jung U Yoo^{1,2}, Jennifer L West³, and Brian Johnstone^{1,2+}

¹ Oregon Health & Science University, Department of Orthopaedics & Rehabilitation

² Oregon Health & Science University, Department of Cell & Developmental Biology

³ Rice University, Department of Bioengineering

Manuscript was submitted to FASEB Journal, August 2010.

CSB participated in the design and execution of all experiment; she was the primary author of the manuscript.

4.1 ABSTRACT

Cartilage tissue engineering aims to replace damaged or diseased tissue with a functional regenerate that restores joint function. Scaffolds are used to deliver cells and facilitate cartilage matrix production, but they can also interfere with the structural assembly of this extracellular matrix. Biodegradable scaffolds have been proposed to improve matrix deposition and the biomechanical properties of neocartilage. The challenge is to design scaffolds with appropriate degradation rates, ideally such that scaffold degradation is proportional to matrix deposition. In this study we developed a cell-mediated bioresponsive hydrogel with degradation aligned to the chondrogenic differentiation of human mesenchymal stem cells (hMSCs). We identified matrix metalloproteinase 7 (MMP7) as an enzyme with a temporal expression pattern that corresponded with cartilage development. By embedding MMP7 peptide substrates, or a non-degradable scrambled peptide, within a poly(ethylene glycol) diacrylate backbone, we built MMP7-sensitive hydrogels with distinct degradation rates. When MMP7-sensitive scaffolds were compared with non-degradable scaffolds *in vitro*, photoencapsulated hMSCs produced neocartilage constructs with more extensive collagenous matrices, as demonstrated through immunohistochemistry and biochemical quantification of matrix molecules. Furthermore, these changes translated into an increased dynamic compressive modulus. This work presents a practical strategy for designing biomaterials uniquely tuned to individual biological processes.

4.2 INTRODUCTION

Biodegradable scaffolds for tissue engineering applications have been proposed to improve formation of developing tissues by removing the interference to extracellular matrix elaboration that is imposed by a non-degradable scaffold^{193,261}. Biodegradable scaffolds impart immediate functional support to encapsulated cells, but the scaffold is eliminated as the cells begin to produce and assemble matrix proteins. The rate of scaffold degradation is critically important to the success of this system, and the ideal rate would be intimately tied to matrix production and assembly by the cells. This concept is of particular importance for structural tissues such as hyaline cartilage in which biomechanical function is dependent upon the expression and assembly of extracellular matrix components, predominantly collagen II and aggrecan^{6,72}.

Recreating the native structure of the extracellular matrix within neocartilage remains a significant challenge in the field. Synthetic polymers such as poly(ethylene glycol) diacrylate (PEGDA) are promising scaffolds for cartilage engineering applications since they can be formed *in situ* under cytocompatible conditions to enable uniform encapsulation of cells^{184-186,231,251}. Furthermore, the physical^{173,249,259} and chemical properties of PEGDA can be engineered to enhance chondrogenesis by providing stimulatory cues from the extracellular matrix^{202,220,255,256,262}. PEGDA is not inherently degradable, and the artificial scaffolding can result in pericellular restriction of the matrix molecules such that the physical properties of the neocartilage construct are limited to those of the PEGDA scaffold itself.

A number of different approaches have been used to create degradable synthetic biomaterials. Most commonly either a hydrolytic or enzymatic segment is built into the polymer backbone to facilitate degradation. Hydrolytically degradable scaffolds have shown some promise for cartilage engineering applications and typically dissolve through hydrolysis of an ester linkage when exposed to an aqueous environment^{194,195,263,264}. A limitation with this system is that the degradation rate is tied to macromer composition rather than cellular behavior, thus not allowing

for variation in differentiation or matrix elaboration between different patients' cells. Alternatively, peptide substrates can be engineered into the polymer in a fashion that exploits cellular activity to locally degrade the scaffold. In this study our goal was to produce a PEGDA-based degradable scaffold for cartilage engineering that was specifically tuned to chondrogenesis of human mesenchymal stem cells (hMSCs). We hypothesized that degradation driven through a cellular response concomitant with cartilage matrix deposition would improve the intracellular distribution of proteins and produce a stronger, more biologically relevant, neocartilage construct.

The first requirement in the design process was to identify an enzyme with a temporal expression profile that corresponded with chondrogenesis of encapsulated hMSCs. We chose to focus the screen on MMP (matrix metalloproteinase) and ADAMTS (a disintegrin and metalloproteinase with thrombospondin motifs) enzymes that have previously been characterized in skeletal development to either support collagen biosynthesis (ADAMTS-2, -3, -14 & MMP-7)^{60,265,266} or cleave extracellular matrix components during remodeling (MMP-1, -2, -13 & ADAMTS-4, -5)^{54,59}. By evaluating mRNA and protein expression patterns in hMSC-laden hydrogels, we identified MMP-7 as a secreted enzyme with an expression pattern that corresponds to chondrocyte differentiation. MMP-7 substrates were embedded into a PEGDA backbone and the resulting enzymatically degradable hydrogels provided for an intercellular expansion of the extracellular matrix produced by photoencapsulated hMSC differentiating to chondrocytes. This improved the dynamic compressive modulus of neocartilage constructs. This study highlights a successful technique for tailoring scaffold degradation for a desired biological process.

4.3 RESULTS

4.3.1 Identification of MMP-7 as Candidate Enzyme for Bioresponsive Hydrogels

In order to develop a bioresponsive scaffold with degradation directly related to cartilage matrix deposition it was necessary to identify an enzyme, expressed by the encapsulated hMSCs, which had a temporal profile that corresponded to chondrogenesis. Critical towards preventing premature scaffold degradation, it was also desirable for this enzyme to have to very low expression in the hMSC (Figure 4.1A). In order to identify candidate enzymes we screened hMSCs for their temporal expression of MMP and ADAMTS enzymes previously characterized in skeletal development during chondrogenesis in semi-interpenetrating (sIPN) PEGDA-based hydrogel (Figure 4.1B). Using RT-PCR, MMP-7 was identified as the only enzyme to have both nominal expression in hMSCs (Figure 4.1A) and demonstrate a relative increase in expression during *in vitro culture* in chondrogenic medium (Figure 4.1B). This temporal increase in MMP-7 positively correlated with chondrogenic markers collagen II and aggrecan at the mRNA level (Figure 4.1C).

Gene expression data for MMP-7 was validated at the protein level with immunohistochemistry. Representative sections from hydrogels cultured for 1, 4 and 6 weeks indicated that increased MMP-7 protein expression corresponded with the production of proteoglycans and collagen II (Figure 4.1D). Expression of MMP-7 was also detected at the protein level in the developing cartilaginous anlagen of embryonic mouse limbs using immunohistochemistry, suggesting that its expression in hydrogels is consistent with chondrogenesis during limb development (Figure 4.1E).

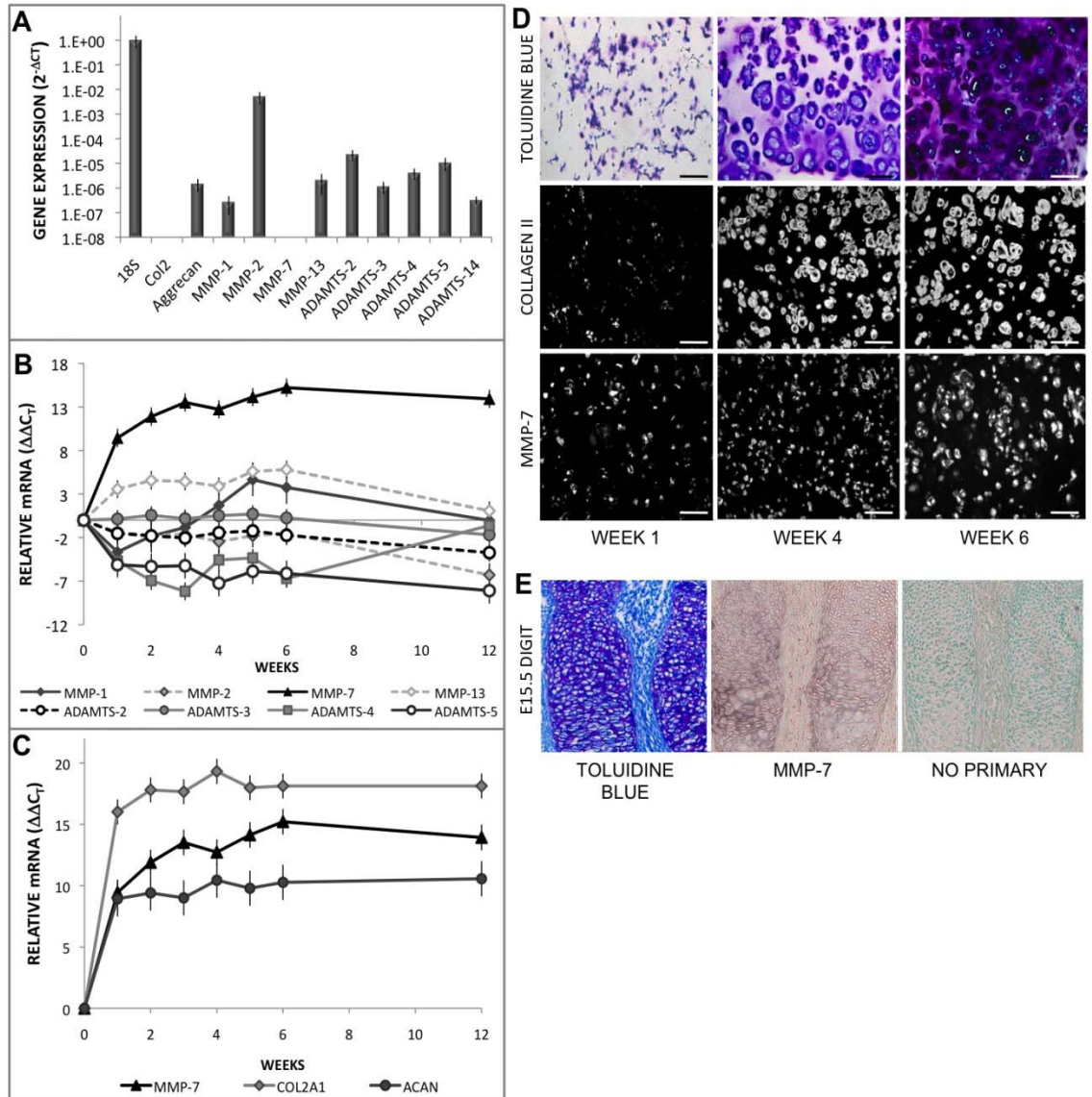


FIGURE 4.1 – IDENTIFICATION OF MMP-7 AS CANDIDATE SUBSTRATE FOR BIORESPONSIVE HYDROGELS. (A) Gene expression from expanded hMSCs prior to encapsulation as measured by quantitative real time RT-PCR. (B) Changes in metalloproteinase gene expression for hMSCs photoencapsulated in sIPN hydrogels over twelve weeks. (C) *MMP7* gene expression relative to chondrogenic markers, collagen II (*COL2A1*) and aggrecan (*ACAN*). (D) Toluidine blue staining for proteoglycans and immunohistochemistry for collagen II and MMP-7 at 1, 4 and 6 weeks. (E) Toluidine blue staining and MMP-7 immunohistochemistry on E15.5 mouse digits. Error bars (A-C) represent 95 % confidence intervals.

4.3.2 Design and Degradation Kinetics of Bioresponsive Hydrogels

Based on these data we chose to design a bioresponsive scaffold that would degrade by cell-secreted MMP-7. Two MMP-7 substrates, PLE—LRA and VPLS—LTMG, were synthesized with short linker domains included at the N- (GGWGG) and C- (GGK) termini. A scrambled version of VPLS-LTMG (MLLVTPSG) was used as a control. These peptide sequences were embedded within PEGDA by reacting the primary amines at both ends of the peptide with aPEG-SCM to generate the macromer foundation for three bioresponsive hydrogels: PLE-PEGDA, VPLS-PEGDA, and the MLLVTPSG scrambled control (“sc-PEGDA”) (Figure 2.1). Degradation for each of the peptide-containing PEGDA scaffolds was quantified by tryptophan (W) release from 10 % (w/v) cell-free hydrogels following treatment with human recombinant MMP-1, -2, -7, or -13 (Figure 4.2). Degradation from MMP exposure was compared to Proteinase K and Tris buffer as positive and negative controls, respectively. Both MMP-7 sensitive PEGDA scaffolds showed a dose-dependent response to the human recombinant MMP-7, but PLE-PEGDA was more rapidly degraded (Figure 4.2A, B). To test the specificity of the peptide sequences, cell-free scaffolds were exposed to 2 nM MMP-1, -2, -7, -13. MMP-13 was specifically chosen because it has a similar temporal pattern as MMP-7, while both MMP-1 and -2 have relatively constant expression during *in vitro* culture (Figure 4.1A, B) and represent a collagenase and gelatinase, respectively. Degradation of PLE-PEGDA was less specific than VPLS-PEGDA (Figure 4.2C, D). No degradation of sc-PEGDA was detected upon exposure to any of the MMPs, validating the MLLVTPSG sequence as a non-degradable control (Figure 4.2E).

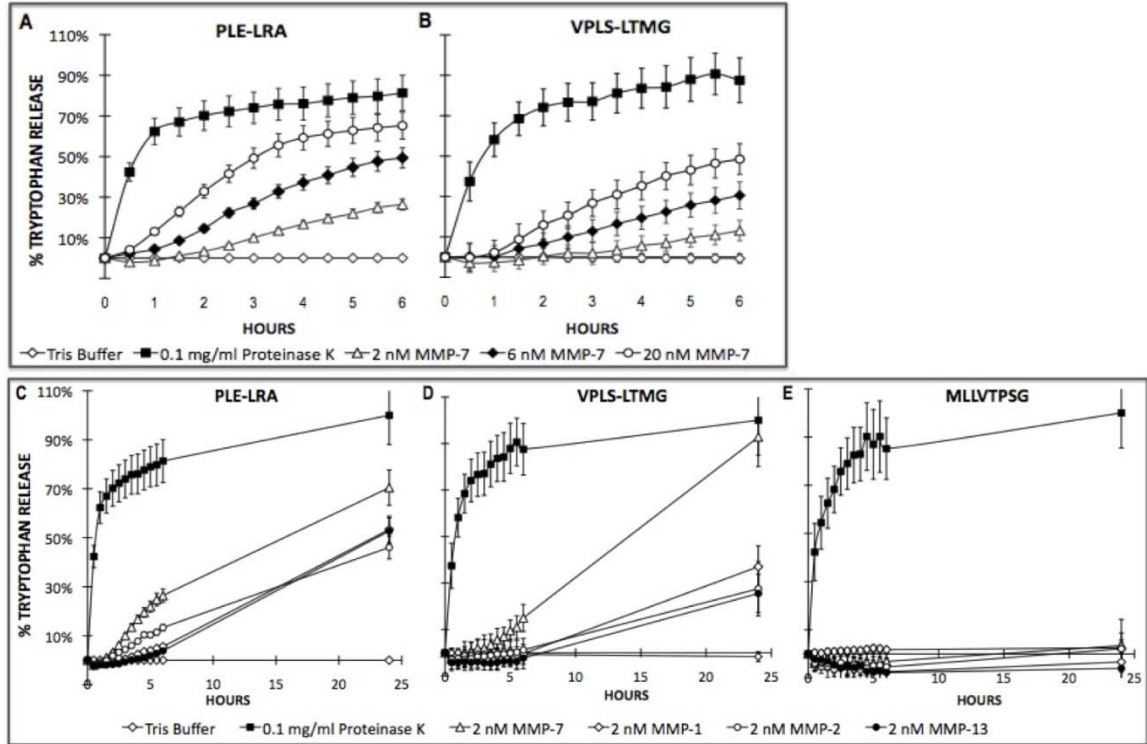


FIGURE 4.2 – DEGRADATION KINETICS OF BIORESPONSIVE HYDROGELS. Tryptophan release from (A) PLE- or (B) VPLS-PEGDA following exposure to 2, 6, or 20 nM recombinant MMP-7. Tryptophan release from (C) PLE-, (D) VPLS-, or (E) sc-PEGDA following exposure to 2 nM recombinant MMP-1, -2, -7, or -13. Degradation was normalized to Proteinase K at 24 hrs (100%), Tris buffer is negative control. Graph represents means \pm standard deviation.

4.3.3 *In Vitro* Chondrogenesis of hMSCs in MMP-7 Bioresponsive Hydrogels

hMSCs were photoencapsulated into the two MMP-7 bioresponsive hydrogels (PLE-PEGDA and VPLS-PEGDA) or one of three different non-degradable scaffolds (Table 4.1). Following *in vitro* culture of six and twelve weeks, immunohistochemical staining detected collagen II deposition restricted to the pericellular domain in all non-degradable scaffolds (Figure 4.3A, B). In contrast, interterritorial deposition was observed in both the VPLS-PEGDA and PLE-PEGDA MMP-7 sensitive scaffolds. Consistent with the faster and more permissive degradation of PLE-LRA (Figure 4.2), interterritorial deposition of collagen II was observed earlier in PLE-PEGDA than in VPLS-PEGDA hydrogels. Degradation of the PLE-PEGDA scaffold resulted in increased total collagen accumulation compared to the sc-PEGDA (Figure 4.3C). Together with the change in collagen distribution, this translated into a significantly increased dynamic compressive modulus after twelve weeks of culture (Figure 4.3D, $p < 0.05$).

Presumably due to the smaller size of proteoglycans, their deposition was observed throughout both the degradable and non-degradable scaffolds at both 6 and 12 weeks (Figure 4.4A-C). However, proteoglycan content was decreased in the MMP-7 sensitive hydrogels by 12 weeks (Figure 4.4D) and toluidine blue staining appeared less intense at the peripheral region of these hydrogels (Figure 4.4C). Changes in relative cell content were quantified by DNA measurements after 6 and 12 weeks of culture (Figure 4.4E). After 6 weeks of culture DNA content was lower in the sc-PEGDA than in either of the MMP-7 hydrogels, however this effect was reversed at 12 weeks such that DNA content was lowest in the MMP-7 hydrogels.

To determine if the presence of the peptide substrate changed anabolic or catabolic gene expression we analyzed cartilage matrix (Figure 4.5A) and metalloproteinase (Figure 4.5B) mRNA expression respectively. No significant differences were observed between the peptide-free 10 % PEGDA scaffold and the peptide-containing bioresponsive hydrogels.

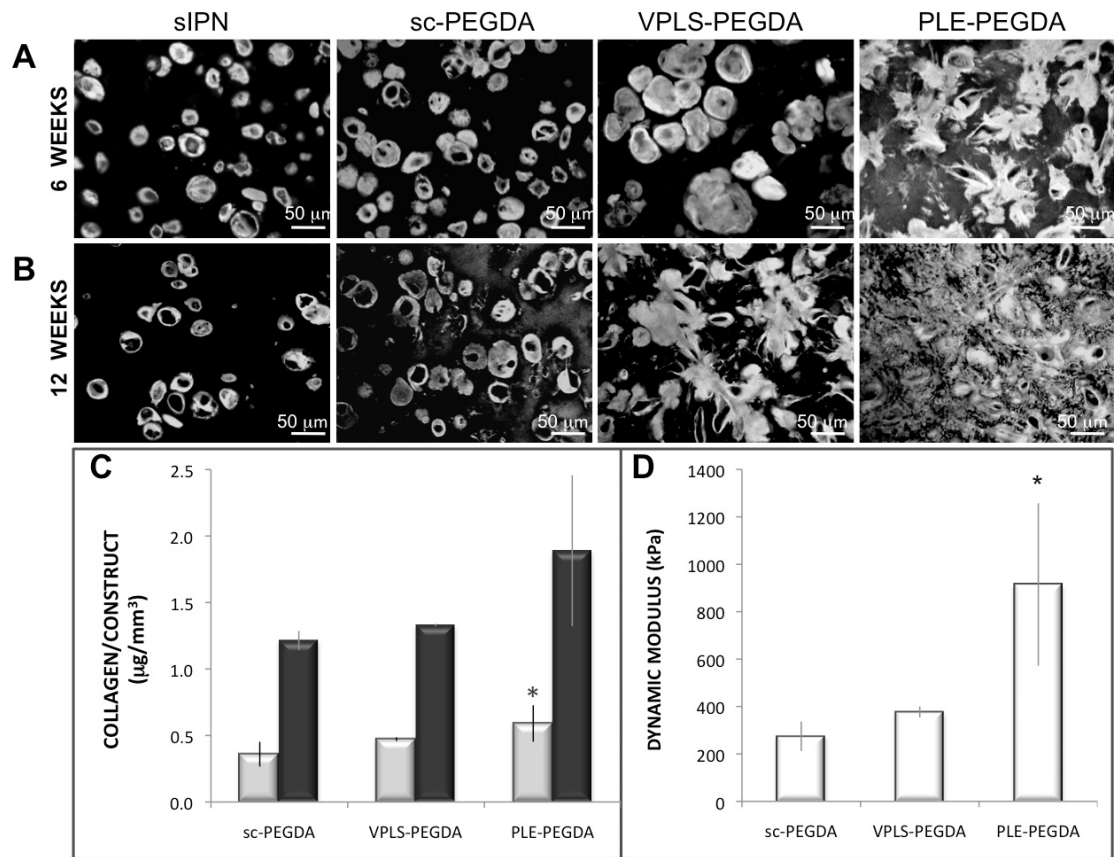


FIGURE 4.3 – COLLAGEN DEPOSITION IN BIORESPONSIVE HYDROGELS. Collagen II immunohistochemistry following (A) 6 or (B) 12 weeks of *in vitro* culture. (C) Total collagen content in hydrogels at 6 (grey) or 12 (black) weeks. (D) Dynamic compressive modulus of hydrogels following 12 weeks of *in vitro* culture. (* = $p < 0.05$)

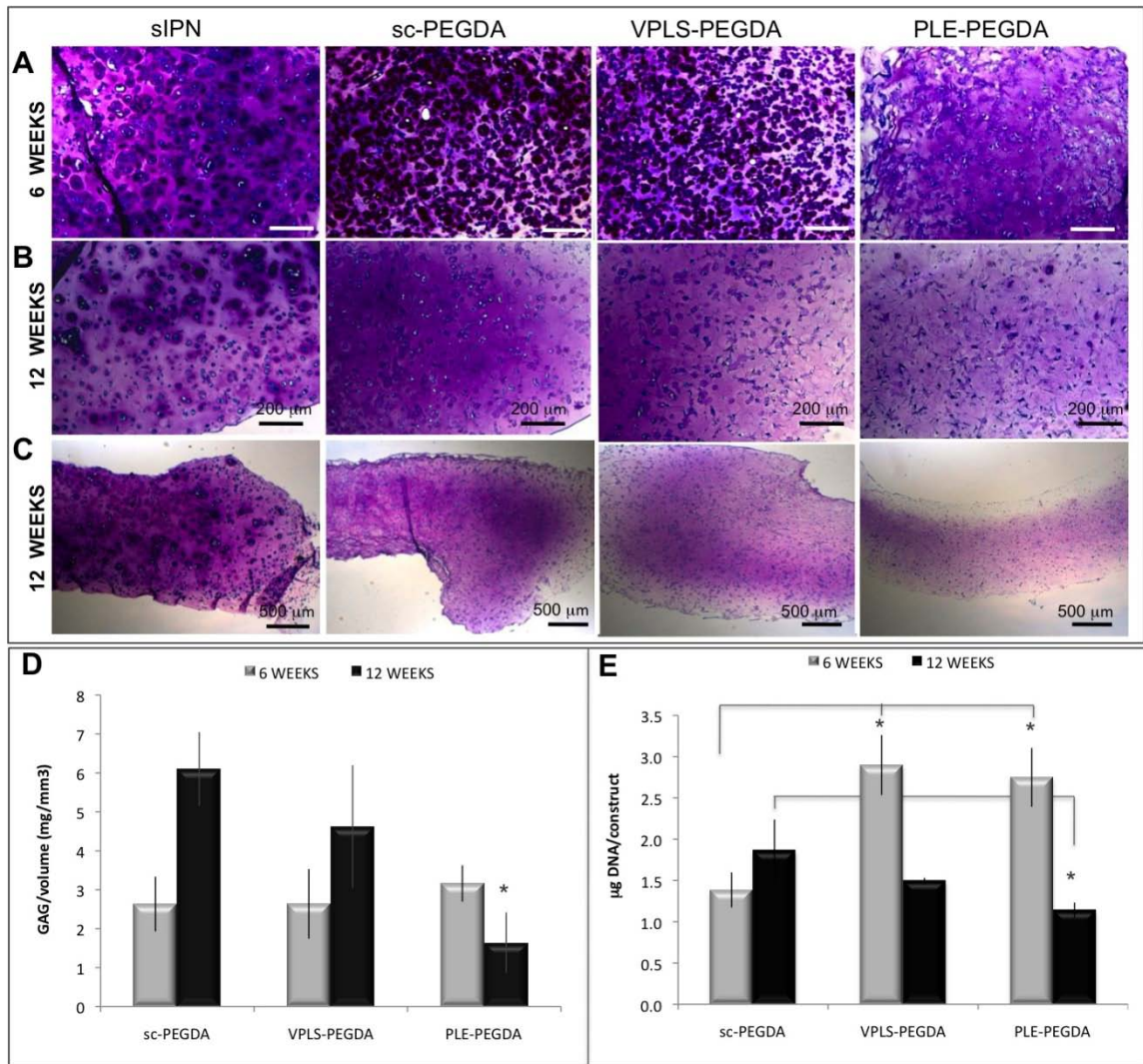


FIGURE 4.4 – PROTEOGLYCAN DEPOSITION IN BIORESPONSIVE HYDROGELS. Toluidine blue staining in hydrogels following (A) 6 and (B, C) 12 weeks of *in vitro* culture. (D) Proteoglycan deposition quantified after 6 (grey) or 12 (black) weeks of culture. (E) PicoGreen quantification of DNA in hydrogels after 6 (grey) or 12 (black) weeks of *in vitro* culture. (* = $p < 0.05$)

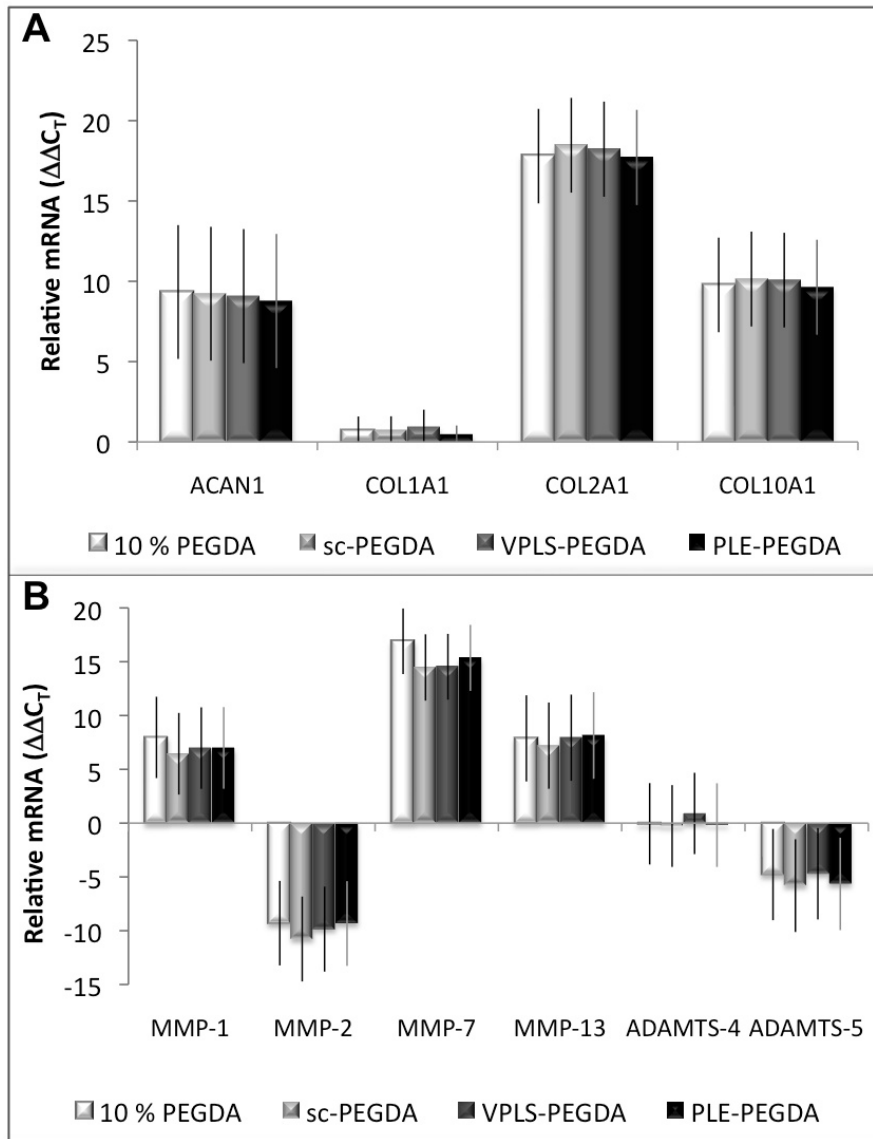


FIGURE 4.5 – GENE EXPRESSION IN BIORESPONSIVE HYDROGELS. Quantitative real time RT-PCR of changes in (A) matrix gene and (B) metalloproteinase gene expression from hMSCs cultured for 12 weeks in either 10 % PEGDA (no peptides), sc-PEGDA, VPLS-PEGDA or PLE-PEGDA.

4.4 DISCUSSION

Cartilage engineering is a therapeutic strategy that aims to produce a tissue regenerate competent to restore normal joint function, thereby reducing pain and preventing disease progression. The clinical success of a neocartilage construct depends on the ability to restore the metabolic and mechanical function of native tissue. In this study we present the design of a biodegradable scaffold for cartilage engineering that relies on intrinsic cellular mechanisms involved in hMSCs chondrogenesis to mediate degradation. We demonstrate that MMP-7 has a temporal expression pattern in hydrogels that corresponds to cartilage matrix elaboration, and that MMP-7 substrates can be effectively incorporated into a PEGDA backbone to facilitate cell-mediated degradation that enables expansion of the collagen II matrix and increases dynamic modulus in neocartilage constructs.

The best cell type for cartilage engineering applications has not yet been determined and will depend on the design of the supporting scaffold²⁶⁷. Chondrocytes, MSCs, and more recently embryonic stem cells^{154,166,257} have been incorporated into a variety of different scaffolds, and each cell-type has advantages and disadvantages^{106,247,268}. MSCs are well established as chondroprogenitors cells and offer the advantage that they are easily harvested and expanded. Cell choice was critically important to our design process since our study aimed to optimize scaffold degradation to chondrogenesis of the encapsulated cells. The importance of biological processes driving the evolution of biomaterials has recently been highlighted in the literature^{169,246,269,270}, but has never been specifically applied to tuning scaffold degradation for cartilage engineering.

Degradable scaffolds offer an advantage over permanent biomaterials in that the artificial scaffold can be completely replaced by an extracellular matrix made by the encapsulated cells. This is important since hydrogels formed *in situ* for cartilage repair require a high cross-linking density to impart mechanical functionality and restore the proper distribution of forces during joint movement. However, high cross-linking density corresponds to smaller pore size within the

scaffold, and these factors have previously been associated with reduced chondrogenesis and pericellular restriction of matrix proteins, specifically collagen^{173,175,176,249}. Tailoring the degradation rate such that it corresponds to the elaboration of cartilage matrix is one of the main challenges in designing a biodegradable scaffold: degradation that occurs too quickly could release cells and matrix components, whereas scaffolds that degrade too slowly inhibit matrix production and assembly. Hydrolytically degradable segments are one technique to incorporate degradation into a scaffold and recent design efforts show the rate of hydrolytic degradation may be better controlled by incorporating both fast and slow degrading elements^{263,271}. Enzymatically degradable scaffolds offer greater spatiotemporal control over hydrolytic degradation. Using exogenously triggered degradation of lipase-sensitive poly(ethylene glycol)-b-polycaprolactone dimethacrylate scaffolds, Rice and Anseth were able to explicitly control the timing of scaffold degradation²⁰¹. They found that adding lipase after allowing encapsulated chondrocytes to produce some matrix was preferred to stimulating early scaffold degradation, but in their system the exogenously driven degradation was not directly linked to cellular behavior.

Bioresponsive materials include those with cell-mediated degradation properties. The term 'bioresponsive' was adopted to convey a distinct physical or chemical response occurring within the biomaterial as a consequence of cellular behavior¹⁹⁷. The concept of engineering synthetic hydrogel scaffolds with cell-mediated degradation features was first introduced by West & Hubbell in 1999¹⁹⁶. Collagenase and plasmin specific peptide substrates were incorporated into a PEGDA-based hydrogel to facilitate cellular migration for wound healing. These peptide sequences and polymer chemistry were later modified for faster degradation kinetics to increase the efficiency of fibroblast migration¹⁹⁸. Park *et al* explored the utility of a collagenase sensitive scaffold for cartilage engineering with encapsulated chondrocytes and suggested that matrix was less constrained in the degradable hydrogel¹⁹⁹. However, the peptide sequence they incorporated into their hydrogels (GCRDGPQGIWGQDRCG) is cleaved by multiple matrix metalloproteinases (MMP-1, -2, -3, -7, -8, -9)^{198,200}, and therefore degradation was not optimized

for chondrogenesis. Our work represents a progression of this concept in that the bioresponsive scaffold is specifically linked to hMSCs chondrogenesis and cartilage matrix elaboration through MMP-7 expression and activity.

MMP-7 has a well-characterized role in tumor metastasis^{238,239}, yet recent data suggest that it may also play a role in chondrogenesis²⁷². Evidence suggests MMP-7 supports cartilage development by both facilitating collagen II maturation²⁶⁵ and modulating bioavailability of chondrogenic factors^{66,273,274}. During collagen maturation, MMP-7 can cleave the NH₂-propeptide from the native type IIA procollagen, the alternatively spliced form of collagen II synthesized by chondroprogenitors²⁶⁵. Both BMP-2 and TGF- β 1 can bind to the extra-helical region of the collagen IIA propeptide, supporting a role for MMP-7 in growth factor mobilization⁶⁶. MMP-7 can also cleave all six of the insulin growth factor binding proteins (IGFBP) responsible for mediating IGF activity²⁷³ and activate TGF- β indirectly through the activation of MMP-9²⁷⁴. The physiological activation of MMP-7, along with most MMPs, is not well understood, but activity can be regulated through gene expression, enzyme localization, and activation of the proenzyme. Recently it was suggested that highly sulfated glycosaminoglycans may regulate MMP-7 activity by promoting proenzyme activation through autolytic cleavage of the prodomain, or by providing an anchor to localize substrate activity²⁷⁵. Our data from both hydrogels (Figure 4.1A, C, D) and embryonic mouse limbs (Figure 4.1E) provides further evidence that MMP-7 is involved in chondrogenesis.

MMP-7 was chosen from a screen of MMP and ADAMTS enzymes reported to be involved in skeletal development⁵⁴. Using RT-PCR and IHC we found that only MMP-7 and MMP-13 demonstrated a temporal pattern that positively correlated with collagen II and aggrecan (Figure 4.1). MMP-13 was not chosen for further evaluation since its expression is associated with the final maturation state of chondrocytes during endochondral ossification. It is well established that MSCs express markers of the hypertrophic chondrocytes seen in endochondral ossification during *in vitro* culture^{94,109}, and this has led to the concern that bone could form

during *in vivo* implantation^{276,277}. Although beyond the scope of this work, we believe encapsulated MSCs can be driven to a permanent cartilage chondrocyte phenotype, which would therefore make MMP-13 an irrelevant choice²⁷⁹. Furthermore, MMP-13 was expressed by expanded hMSCs at the time of encapsulation (Figure 4.1B) and therefore creates the potential for premature degradation of the scaffold.

Validation of MMP-7 as a good candidate enzyme to mediate scaffold degradation during neocartilage formation was shown with long-term *in vitro* studies of photoencapsulated hMSCs (Figures 4.3-4.4). We found significantly improved distribution of the collagen II matrix (Figure 4.3A, B) and a higher dynamic compressive modulus (Figure 4.3D) in the MMP-7 sensitive hydrogels when compared to non-degradable controls. PLE-PEGDA had a more expansive collagen II matrix earlier than the VPLS-PEGDA scaffold (Figure 4.3A, B) presumably due to the faster degradation kinetics and lower specificity of the PLELRA substrate (Figure 4.2). The MLLVTPSG sequence has not been reported as degradable by any MMPs²⁰⁰, and was not degraded using recombinant MMPs-1, -2, -7, or -13 (Figure 4.2E).

However, although we have significantly improved collagen distribution within the bioresponsive hydrogels, we did get less retention of proteoglycan in these hydrogels than in controls. Proteoglycan accumulation in the bioresponsive hydrogels was equivalent to non-degradable controls following six weeks of culture, but was significantly decreased in the PLE-PEGDA by twelve weeks (Figure 4.4C). *ACAN* mRNA expression at twelve weeks was equivalent in both the degradable and non-degradable hydrogels (Figure 4.5A), suggesting aggrecan potential is similar per cell. Furthermore, there was no change to metalloproteinase expression in the bioresponsive scaffolds suggesting that the presence of a peptide substrate does not inherently increase enzyme production or matrix catabolism (Figure 4.5B). Together these data suggest that degradation of the bioresponsive scaffold results in decreased retention of proteoglycans and cells (Figure 4.4D). However, we postulate that this loss would decrease as the collagenous matrix is further elaborated and organized, but this remains to be tested. That the

elaborated extracellular matrix in the bioresponsive PLE-PEGDA hydrogel achieved greater biomechanical properties with a lower proteoglycan content indicates that removing the scaffold is allowing the assembly of a matrix with characteristics of cartilage; the collagenous framework is structured such that a swelling pressure is developed by the constrained proteoglycans.

4.5 CONCLUSIONS

The design process used to develop this MMP-7 sensitive scaffold represents a biology-focused approach for improving biomaterials for tissue engineering. In this study we demonstrate how the temporal characterization of hMSCs chondrogenesis within scaffolds can be effectively used to tune scaffold degradation to cellular mechanisms associated with chondrogenesis and matrix elaboration. This led to an improved intercellular distribution of the type II collagen matrix and increased the dynamic modulus in neocartilage constructs. Using a similar approach to tailoring degradation kinetics to chondrogenesis, we can similarly modify the PEGDA scaffold to contain biomimetic^{154,220,255,262} and bioactive²⁰⁶ features with temporally relevant presentations.

CHAPTER 5:
**TEMPORAL REQUIREMENT FOR CHONDROGENIC FACTORS DURING
NEOCARTILAGE FORMATION & DEVELOPMENT OF BIOACTIVE SCAFFOLD**

AUTHORS

Chelsea S Bahney^{1,2}, Amanda N Buxton³, Jung U Yoo^{1,2}, Jennifer L West⁴, and Brian Johnstone^{1,2+}

¹Oregon Health & Science University, Department of Orthopaedics and Rehabilitation

²Oregon Health & Science University, Department of Cell and Developmental Biology

³Case Western Reserve University, Department of Bioengineering

⁴Rice University, Department of Bioengineering

Data has been submitted/presented as:

Amanda N Buxton*, Chelsea S Bahney*, Jung U Yoo, and Brian Johnstone. (*co-first authors)
Influence of cell density and bioactive factors on the chondrogenesis of human mesenchymal stem cells in hydrogels. Tissue Engineering Part A, August 2010²⁷⁹

ORTHOPAEDIC RESEARCH SOCIETY 2010 New Orleans, LA. March 6-10. *Cell Chondrogenesis without Dexamethasone*. Bahney CS, Buxton AN, Ozgur S, Yoo J and Johnstone B. Poster Presentation

UNPUBLISHED DATA. *Design and development of a TGF β 1 bioactive scaffold to facilitate chondrogenesis of human mesenchymal stem cells*. Chelsea S. Bahney, Jennifer L West, and Brian Johnstone.

- ANB was the primary researcher on Figure 5.2
- CSB was the primary researcher for Figure 5.1, 5.3, 5.4
- CSB was the primary author of the manuscript and abstract

5.1 ABSTRACT

Translating cartilage engineering using mesenchymal stem cells (MSCs) from an *in vitro* to an *in vivo* setting requires a more detailed understanding of the temporal requirement for the bioactive factors that are responsible for inducing chondrogenesis and facilitating matrix deposition in scaffolds. Furthermore, a clinically applicable mechanism for delivering these factors is desired. The original experiments describing chondrogenesis in a scaffold-free pellet culture system established that both dexamethasone and TGF- β 1 were required for consistent chondrogenesis of human MSCs. In this study we show that dexamethasone is not required for MSCs chondrogenesis in a poly(ethylene glycol) diacrylate (PEGDA)-based scaffold: there was no difference in matrix deposition between hydrogels cultured with or without dexamethasone. Furthermore, without dexamethasone, *SOX9* gene expression was higher during early chondrogenesis and there was a significant reduction in collagen I deposition, suggesting a more hyaline cartilage phenotype. In contrast, differentiation of MSCs in hydrogels required initial exposure to TGF- β 1. To evaluate the sustained requirement for TGF- β 1, this growth factor was initially given in culture, but then removed in each subsequent week. TGF- β 1 withdrawal significantly impacted collagen production on a per cell basis, but also leads to an increase in cell number such that total collagen deposition was equivalent to controls when TGF- β 1 was included for at least 3 weeks. In an effort to develop a bioactive scaffold suitable for *in vivo* cartilage engineering we evaluated the activity of TGF- β 1 tethered to a PEGDA scaffold. The soluble form of PEGylated TGF- β 1 maintained activity as evident by deposition of extracellular matrix proteins, however when immobilized to the scaffold no chondrogenesis occurred. Further studies are required to determine whether scaffold modifications can be used to promote/maintain tethered TGF- β 1 activity.

5.2 INTRODUCTION

Using mesenchymal stem cells (MSCs) *in vivo* for the repair of cartilage defects requires both controlled differentiation of these progenitor cells towards the chondrogenic phenotype, and production of the appropriate extracellular matrix components, in the right ratios and conformations, essential to providing cartilage with its biomechanical functionality. *In vitro* chondrogenesis of bone marrow-derived MSCs was first accomplished by our group in 1998 utilizing scaffold-free pellet culture to approximate the mesenchymal condensation observed during limb development^{108,109}. The defined medium that facilitated differentiation included transforming growth factor- β 1 (TGF- β 1) and dexamethasone. More recently, tissue engineering strategies utilizing scaffolds have been used to translate this pellet culture method of *in vitro* chondrogenesis into a system capable of cartilage generation on a clinically relevant scale. The continued renewal of TGF- β 1 and dexamethasone within the medium is customary *in vitro* to facilitate chondrogenesis and matrix elaboration during long-term cultures. The *in vivo* application of cartilage engineering using undifferentiated MSCs requires a careful examination of which bioactive factors are required for this process, and for how long it is necessary to expose the cells to them.

Once the temporal requirement of chondrogenic factors is established, there is still the challenge of finding delivery mechanisms for *in vivo* application. Systemic delivery of growth factors for cartilage repair is typically not a viable option due to the avascular nature of cartilage, the short half-life of growth factors, and a number of serious side effects such as fibrosis in the kidney and liver when TGF- β is delivered in this manner^{280,281}. A more localized delivery of TGF- β by direct injection into the joint space has produced mixed results: it can lead to an increase in extracellular matrix production, but also inflammation, synovial hyperplasia and osteophyte formation²⁸². More sophisticated delivery systems have recently been developed in which bioactive factors are loaded into polymer microspheres. For example, degradable

microspheres made from either poly(L-lactic-*co*-glycolic acid) PLGA^{203,205} or gelatin²⁰⁴, provided sustained and local delivery of TGF- β to cells during chondrogenesis. Although these studies found improved matrix production in the presence of microspheres, controlled release requires careful engineering to ensure correct spatiotemporal delivery at the appropriate concentrations of the growth factor.

Bioactive materials in which the growth factor of interest is directly incorporated into the scaffold may be a more useful approach for *in vivo* tissue engineering applications. Recombinant growth factors can be tethered directly to the scaffold by attaching an acrylated PEG moiety to the growth factor and then including this PEGylated growth factor in the scaffold polymerization reaction²⁰⁶. Presently there are limited successful examples of this technique in the literature. A proof-of-concept study by Jennifer West's group²⁰⁶ demonstrated that tethering TGF- β 1 to a PEGDA scaffold induced greater matrix production by vascular smooth muscle cells than soluble TGF- β 1. Similarly, work from Linda Griffith's laboratory²⁰⁷ has shown that epidermal growth factor (EGF) remains active when tethered into scaffolds and can provide MSCs with a survival advantage. The goal of the experiments described in this chapter was to determine the temporal requirements for TGF- β 1 and dexamethasone of human MSCs (hMSCs) encapsulated within a PEGDA-based semi-interpenetrating network (sIPN), previously characterized by our group¹⁷³. These data will subsequently be used to design and test bioactive scaffolds for cartilage engineering applications.

5.3 RESULTS

5.3.1 Hydrogels Undergo Chondrogenesis in the Absence of Dexamethasone

The first experimental aim was to examine whether MSCs cultured in hydrogels have the same requirement for both dexamethasone and TGF- β 1 that has previously been established in pellet culture. Deposition of proteoglycans and hydroxyproline were not significantly different between hydrogels cultured without dexamethasone and control constructs receiving both dexamethasone and TGF- β 1 (Figure 5.1A). However, differences were observed in a more detailed study of the chondrogenic phenotype in the resultant neocartilage using immunohistochemistry (Figure 5.1 B-I) and gene expression analysis (Figure 5.1 J-K). Cartilage markers, aggrecan and collagen II, were similar at both the protein (Figure 5.1 B,F,D,H) and gene level (Figure 5.1 J-K) in constructs cultured with or without dexamethasone. In contrast, immunohistochemistry revealed a decrease in deposition of both collagen I (Figure 5.1 C,G) and X (Figure 5.1 E,I) in constructs cultured without dexamethasone (Figure 5.1 G,I). *COL1A* gene expression was also significantly decreased at both 1 and 6 weeks (Figure 5.1 J-K) in the absence of dexamethasone, but the decrease in the *COL10A1* gene expression was not statistically significant ($p = 0.06$, Figure 5.1 J-K). To investigate the differentiation potential of hMSCs cultured with and without dexamethasone we also determined the gene expression of *SOX9*, an early marker of chondrogenic potential. *SOX9* was significantly increased in hMSCs cultured without dexamethasone at 1 week (Figure 5.1J), but returned to control levels later in culture (Figure 5.1K).

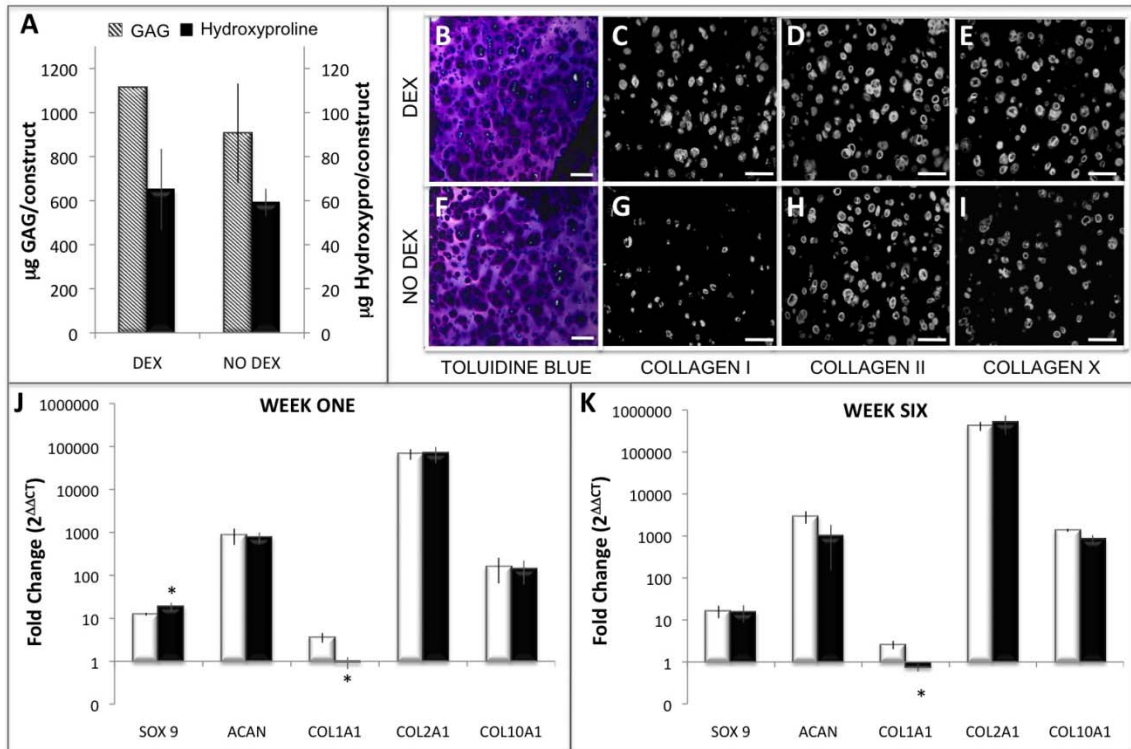


FIGURE 5.1 – MSCs UNDERGO CHONDROGENESIS IN THE ABSENCE OF DEXAMETHASONE. (A) Proteoglycan and hydroxyproline content per construct for hydrogels cultured with or without dexamethasone. (B,F) Toluidine blue, (C,G) collagen I, (D,H) collagen II, and (E,I) collagen X staining of hydrogels cultured (B-E) with or (F-I) without dexamethasone for six weeks, scale bars = 100 μm . Quantitative RT-PCR for *ACAN*, *COL1A1*, and *COL2A1* relative gene expression after (J) 1 or (K) 6 weeks of culture either (white) with or (black) without dexamethasone.

5.3.2 TGF- β 1 Withdrawal During Hydrogel Culture Affects Collagen Biosynthesis

In contrast to dexamethasone, TGF- β 1 was required for chondrogenesis of MSCs in hydrogel scaffolds (Figure 5.3 A-D). To study the temporal requirement for TGF- β 1, the growth factor was withdrawn from chondrogenic medium at day 7, 14, 21 or 28 (Figures 5.2). Constructs had higher total DNA and proteoglycan content at 6 weeks when TGF- β 1 was withdrawn at any time point when compared with controls that received continuous exposure to TGF- β 1 (Figure 5.2 A-B). Proteoglycan content normalized to DNA was unchanged by TGF- β 1 withdrawal (Figure 5.2B). However, hydroxyproline content, a quantification of total collagen, was significantly decreased after TGF- β 1 withdrawal at any time point when normalized to DNA content. Given the relative increase in cell number, collagen content per construct was comparable to control provided hydrogels received TGF- β 1 for at least 21 days (Figure 5.2C). Immunohistochemistry and quantitative real-time PCR of hydrogel constructs cultured for 6 weeks were used to analyze the individual contribution of collagens I, II and X in the neocartilage construct following TGF- β 1 withdrawal at 21 days (Figure 5.3 I-L). A clear reduction in both collagen I (Figure 5.3 F,J) and X (Figure 5.3 H,L) deposition is evident from immunohistochemistry, but RT-PCR showed a significant decrease in gene expression of all three collagens (Figure 5.3M).

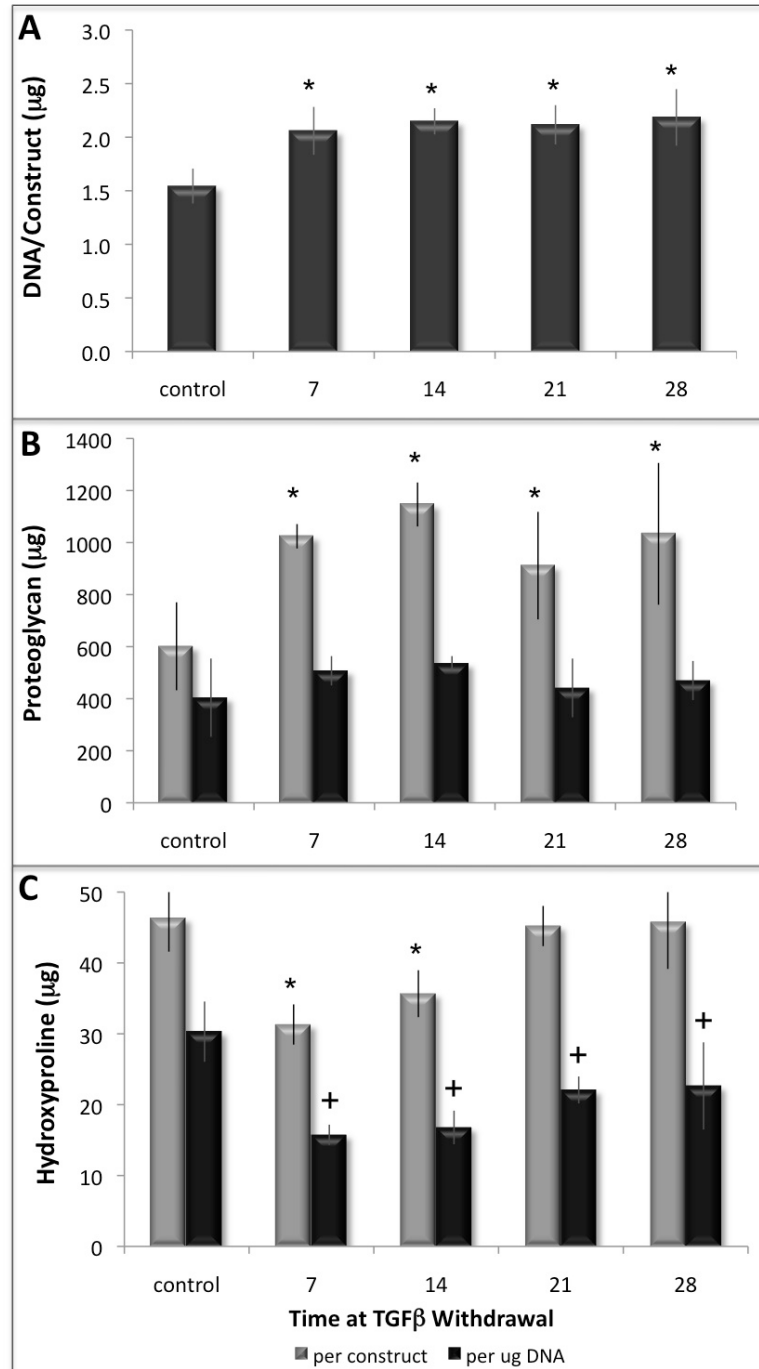


FIGURE 5.2 – WITHDRAWAL OF TGF- β 1 AFFECTS MATRIX DEPOSITION. Hydrogels were grown *in vitro* for 42 days in chondrogenic medium including TGF- β 1 (control) or TGF- β 1 was omitted after 7, 14, 21 or 28 days. Hydrogels were quantified for (A) DNA, (B) sulfated proteoglycans and (C) hydroxyproline; (gray) per construct or (black) normalized for DNA content.

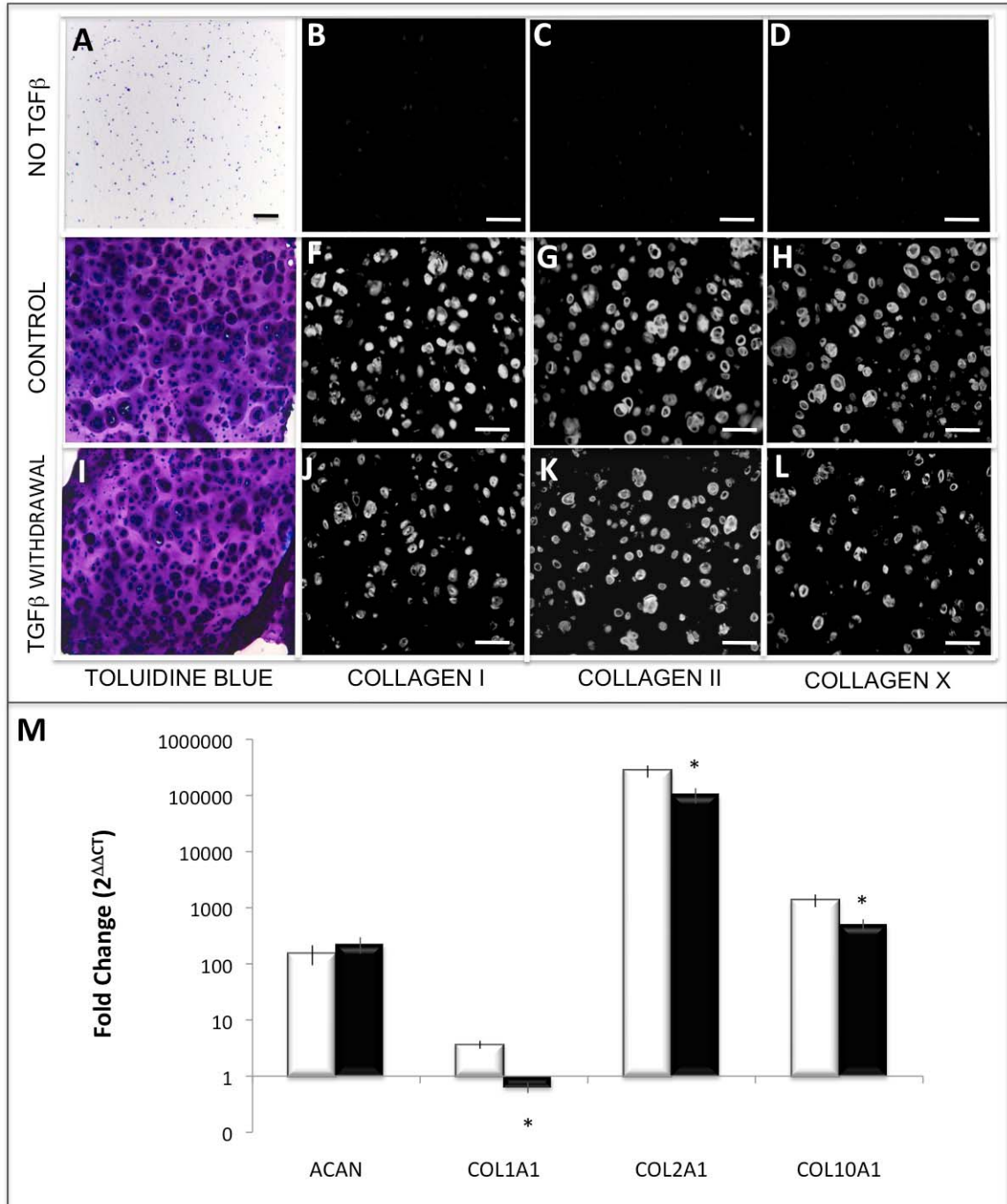


FIGURE 5.3 – TGF- β 1 WITHDRAWAL IMPACTS COLLAGEN BIOSYNTHESIS. Toluidine blue and collagens I, II and X immunohistochemistry of constructs cultured for 42 days either (A-D) without TGF- β 1, (E-H) with continuous TGF- β 1 and dexamethasone supplementation, control, or (I-L) TGF- β 1 withdrawal at 21 days; scale bars = 100 μ m. (M) Quantitative RT-PCR for fold change in gene expression of *ACAN*, *COL1A1*, *COL2A1*, *COL10A1* in control versus TGF- β 1 withdrawal at 21 days; * $p < 0.05$ compared with control per construct, + $p < 0.05$ compared with control per DNA.

5.3.2 Tethered TGF- β 1 is Insufficient for Maintaining Chondrogenesis

Given the requirement for TGF- β 1, but not dexamethasone, in MSCs chondrogenesis we next set out to develop a bioactive scaffold with a tethered form of recombinant human TGF- β 1 that would be suitable for *in vivo* cartilage engineering. To accomplish this, TGF- β 1 was conjugated to a 3.4 kDa PEG monomer through a reaction between available lysine residues and N-hydroxysuccinimide attached to the PEG precursor molecule. Additionally, the PEG monomer contained a single reactive acrylate group capable of covalently bonding to the scaffold through the unsaturated vinyl bonds in the PEGDA backbone. To test the basal activity of this tethered TGF- β 1 (tTGF- β 1) moiety it was delivered as a soluble molecule in chondrogenic medium and compared with recombinant non-tethered TGF- β 1. Following 6 weeks of *in vitro* culture, constructs receiving soluble tTGF- β 1 had an approximate 30 % reduction in both proteoglycan (70 ± 19 %, Figure 5.4B) and hydroxyproline (70 ± 7 %, Figure 5.4C) deposition. When matrix deposition was normalized to DNA content, proteoglycans and hydroxyproline production were only 6 % lower with soluble tTGF- β 1 than with TGF- β 1 due to a decreased cell content (Figure 5.4B,C). The PEGylated TGF- β 1 was then immobilized within the scaffold by adding it at a concentration of either 10 ng/ml or 100 ng/ml to the monomer reaction and then covalently attaching it to a 10 % w/v PEGDA scaffold during photoencapsulation of the hMSCs. Tethering TGF- β 1 at either 10 ng/ml or 100 ng/ml produced no matrix deposition following 6 weeks of *in vitro* culture (Figure 5.4). However, if 10 ng/ml of tTGF- β 1 was first polymerized into the scaffold and cultured in medium without TGF- β 1 for 10 days, but then soluble TGF- β 1 was added for the remaining culture period, proteoglycan (69 ± 7 %, Figure 5.4B) and hydroxyproline (72 ± 12 %, Figure 5.4C) deposition were restored once again to approximately 70 % of the control. Histology and immunohistochemistry confirm the matrix quantification data and indicate no change in matrix localization between TGF- β 1 and soluble tTGF- β 1 (Figure 5.5).

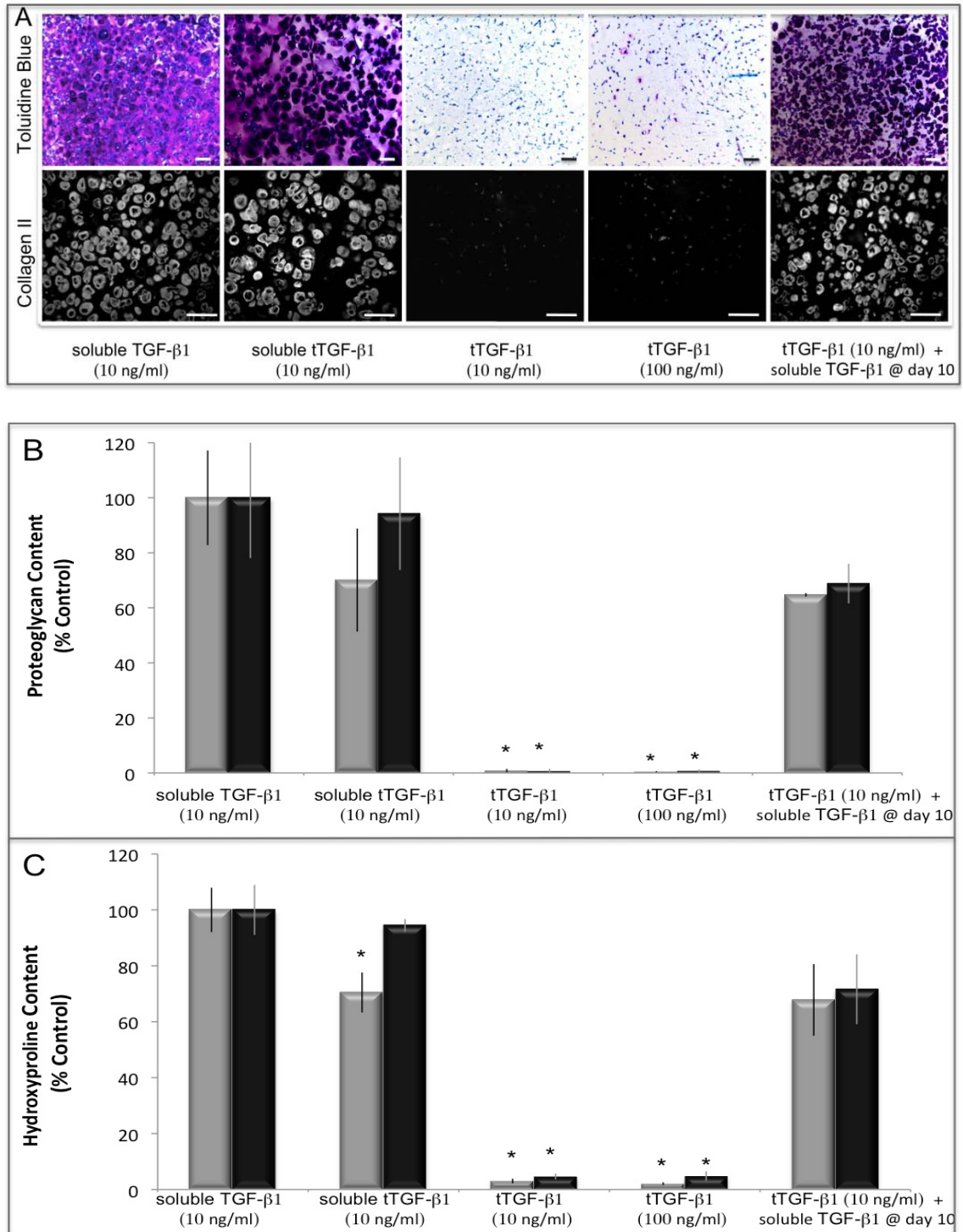


FIGURE 5.4 – PEGYLATED TGF β IS EFFECTIVE AS A SOLUBLE MOLECULE BUT NOT WHEN IMMOBILIZED. (A) Toluidine blue and collagen II immunohistochemistry of control and bioactive scaffolds, scale bars = 100 μ m. (B) Sulfated proteoglycan and (C) hydroxyproline content per construct (grey) or normalized to DNA content (black). * p <0.05 compared with soluble TGF- β 1.

5.4 DISCUSSION

Bioactive factors play a significant role in the differentiation and matrix production of MSCs during chondrogenesis. For MSCs to be considered as viable candidates for cartilage engineering therapies it is necessary to understand the temporal requirement for these bioactive factors. In this study we examined both dexamethasone and TGF- β 1 given their previously established role in chondrogenesis of hMSCs in pellet culture¹⁰⁹. In the hydrogel-based medium there was no significant difference in gene expression or matrix deposition of key markers of cartilage, aggrecan and collagen II, indicating that dexamethasone is not required for chondrogenesis within hydrogel scaffolds (Figure 5.1). This result provides a clear contrast to the pellet culture system where chondrogenesis was not observed in preparations lacking dexamethasone^{106,108,109}.

Dexamethasone is a synthetic glucocorticosteroid (GC) reported to promote differentiation in a number of systems, including the chondrogenic¹⁰⁸ and osteogenic²⁸³ differentiation of MSCs. The precise mechanism through which dexamethasone promotes chondrogenesis is unknown, but Derfoul *et al* have presented data showing dexamethasone acts indirectly through the major active form of the GC receptor, GC α , to induce cartilage matrix genes in pellet culture²⁸⁴. It is presently unclear what factors replace the need for dexamethasone in hydrogel-based culture of hMSCs. Fundamental differences clearly exist between scaffold-free pellets and hydrogels. Pellet culture was designed to approximate the mesenchymal condensation process and it was postulated that direct cell-cell communication was very important for differentiation^{108,109}. However, MSC chondrogenesis has now been established in a variety of scaffold-based systems that significantly limit direct cell-cell contact^{132,173,218,285}, implying that intercellular contact is not required for chondrogenesis. The common element to both *in vitro* culture systems is the spherical or rounded cellular conformation of hMSCs. This is achieved without cell-cell connections in the hydrogels compared with pellets. That such cell-cell

connections are of secondary importance to a chondrogenic progenitor cell is long-established; Solursh *et al* first noted that rounded solitary progenitor cells express cartilage matrix molecules¹³⁴, and they and others established that the induction of rounding of solitary progenitor cells induces chondrogenesis¹³³⁻¹³⁵. They further demonstrated that it is not simply round cell shape that promotes differentiation, but the disruption of mechanotransduction mechanisms²⁸⁶. This occurs in hydrogel encapsulation of hMSCs since the cells do not establish substratum connections with PEG. Thus, the rapid stabilization of the three-dimensional shape with disrupted mechanotransduction, and the increased access to TGF- β , which can readily diffuse throughout the hydrogel, may be important in facilitating chondrogenesis in the absence of dexamethasone in this system.

A secondary finding from culture without dexamethasone was an apparent change in the chondrogenic phenotype. *SOX9* gene expression, a marker of early chondrogenesis, was more highly activated after 1 week of culture without dexamethasone than in control cultures containing dexamethasone (Figure 5.1J). We also saw decreased deposition of both collagens I (Figure 5.1 C,G) and X (Figure 5.1 E,I) after 6 weeks of culture by immunohistochemistry. *COL1A* gene expression was also decreased throughout culture, while the decrease in *COL10A1* was not significant (Figure 5.1 J-K). It is well established that MSCs undergoing chondrogenesis have a propensity to express collagens I and X^{94,108}. The presence of these non-hyaline collagens during *in vitro* differentiation has led to the notion that use of MSCs *in vivo* for repair of full-thickness cartilage lesions will result in the formation of a fibrocartilaginous construct²⁸⁷ or endochondral ossification^{276,277}. These are important considerations since the biomechanical properties of articular cartilage are the product of the unique, anisotropic assembly of collagen II and proteoglycans in the extracellular matrix^{6,72}. Chondrogenesis *in vivo* is classically studied through the process of endochondral ossification that occurs during long bone formation, and relatively little is known about the developmental processes that produce either hyaline or

fibrocartilage¹²⁻¹⁴. These results suggest that *in vitro* a more hyaline chondrocyte phenotype is promoted by the exclusion of dexamethasone.

We also examined TGF- β , which has been documented to play an important role during both early^{288,289} and late phases²⁹⁰ of chondrogenesis by both initiating differentiation^{108,109,116,132} and increasing production of extracellular matrix proteins^{284,291}. As previously determined in pellet culture, we found that TGF- β 1 was required for initiating differentiation of hMSCs in the PEGDA-based sIPN. Constructs cultured without TGF- β 1 did not produce measurable quantities of either proteoglycan or collagen (Figure 5.3).

Despite the requirement for TGF- β 1 to initiate chondrogenesis, sustained exposure had a differential effect on proteoglycan and collagen production. Proteoglycan content of the constructs was increased after 6 weeks of culture when TGF- β 1 was withdrawn from the medium at any point after the first 7 days (Figure 5.2B). However, DNA content was also significantly higher with TGF- β 1 withdrawal, such that the proteoglycan production per cell was not significantly different between this and the control condition (Figure 5.2 A,B). Thus, one effect of TGF- β 1 withdrawal appears to be either greater cell proliferation and/or cell survival. Additionally, sustained TGF- β 1 supplementation does not appear to be essential for proteoglycan synthesis.

In contrast, collagen content per cell was significantly reduced by withdrawal of TGF- β 1 at any time-point compared with sustained exposure, suggesting TGF- β has a more direct role in collagen biosynthesis (Figure 5.2C). O'Driscoll and co-workers have also examined the effects of limiting chondrogenitor cell exposure to TGF- β 1^{112,292}. They reported that chondrogenesis of rabbit periosteal explants cultured in agarose was similar following either 2 or 14 days of TGF- β 1 treatment. However, matrix quantification was not normalized to DNA content. Since our data indicate a higher number of cells after TGF- β 1 withdrawal, this may explain the discrepancy between the studies.

When TGF- β 1 was tethered to a PEGDA scaffold to create a bioactive scaffold encapsulated hMSCs did not produce measurable quantities of matrix proteins (Figures 5.4). Although the reason for this is still unclear, it does not appear to be the result of lost growth factor activity: proteoglycan deposition from constructs supplemented with PEGylated TGF- β 1 in a soluble form was 70 % of constructs that received control recombinant TGF- β 1. One possible reason for failed chondrogenesis is that immobilized TGF- β 1 cannot be internalized by the encapsulated cells and that this processing is required for downstream TGF- β 1 activity. There is some evidence that, similar to BMP signaling, TGF- β 1 activity is conferred once the TGF- β 1 receptors are internalized and processed to the endosome²⁹³⁻²⁹⁵. However, Mann *et al* demonstrated that covalently tethered TGF- β 1 not only retained the ability to stimulate matrix production in vascular smooth muscle cells, but did so more than the soluble form of TGF- β 1²⁰⁶. Alternatively, extracellular proteases may be degrading the scaffold bound TGF- β 1 leading to a loss of activity. This mechanism is supported in part since rescuing a tethered TGF- β 1 construct with soluble TGF- β 1 after 10 days of culture provided matrix deposition once again at close to 70 % of the control level (Figures 5.4). However, we have also shown that removing soluble TGF- β 1 after two weeks of culture will decrease hydroxyproline content but lead to an increase in proteoglycans production (Figures 5.2), which was not observed with the immobilized TGF- β 1 (Figures 5.4), indicating the latter is not as active in the hydrogels.

5.5 CONCLUSIONS & FUTURE DIRECTIONS

The data shown in these studies suggest that bioactive scaffolds for cartilage engineering can be designed to include TGF- β 1 alone, and that dexamethasone is not required for hMSC chondrogenesis or matrix elaboration within PEGDA-based hydrogels. In contrast, TGF- β 1 was required to initiate chondrogenesis and collagen biosynthesis was decreased in constructs that did not receive TGF- β 1 for at least 3 weeks. Tethering TGF- β 1 to an acrylated-PEG monomer

provided up to 70 % of the activity of soluble TGF- β 1, but immobilizing this moiety within the scaffold led to no measurable accumulation of matrix molecules. Adding soluble TGF- β 1 to scaffold that contain 10 ng/ml tTGF- β 1 after 10 days restored matrix deposition to 70 % suggesting that tTGF- β 1 may have some initial activity. Future experiments will be aimed at clarifying the early activity of tTGF- β 1, testing higher concentrations of tTGF- β 1, and looking for mechanisms to adjunct the tTGF- β 1 activity.

CHAPTER 6:
MESENCHYMAL STEM CELLS AND ARTICULAR CHONDROCYTES
INFLUENCE EACH OTHER DURING COCULTURE IN TISSUE ENGINEERING SCAFFOLDS

AUTHORS

Chelsea S Bahney, Sinan E Ozgur, Dennis Crawford, and Brian Johnstone

Manuscript in preparation. Data has been submitted/presented as:

887e 8mAt DI s8t 7t A8se 878sIt 7A87777 8 e8 B orens,LA8Mnoe7878778 Influence of Chondrocytes on
 I esenchyc al Stec Cell Chondrogenesis in Hydrogels.88n7neA8s 7,88 nrAeo8D,8s on8 soo88D8nn88
 87nstone88 oster I resentation8

AI se t 8 88 78sIt 7A8 D888 818L8ms AL8 t 8m8tt 818m8 77778 8oston,8 MA8 MnA8 787778 Influence of
 Chondrocytes on I esenchyc al Stec Cell Chondrogenesis in Hydrogels.88n7neA8s 7,88 nrAeo8D8nn88
 87nstone88 oster I resentation8

8

887e 8mAt DI s8t 7t A8se 878sIt 7A87777 Lon88ene78 A88nmoA8787877778 I esenchyc al Stec
 Cells and orticular Chondrocytes Influence Each . ther during Coculture in Tissue Engineering
 Scaffolds.88n7neA8s 7,88nmm87t ,8 on8 soo88D8nn8887nstone88 nstract acceted8

6.1 ABSTRACT

Coculture is an experimental technique designed to mimic cellular interactions during embryonic development with the aim of stimulating tissue formation. In this study we explored the coculture of human mesenchymal stem cells (hMSCs) and human articular chondrocytes (hACs) in poly(ethylene glycol) diacrylate based scaffolds designed for cartilage engineering applications. Both cell types have previously been explored for cartilage repair, but their clinical application is limited by either the paucity of available chondrocytes from donor tissue or the non-hyaline differentiation of MSCs. This scaffold-based coculture technique was designed to test whether AC-MSc coculture could influence neocartilage development at a clinically relevant scale. We found that the presence of hACs could not induce chondrogenesis of hMSCs in the absence of TGF- β . However, coculture resulted in a significant reduction in collagen I and X expression, producing a more hyaline neocartilage phenotype than MSC monocultured constructs. Using FISH combined with immunohistochemistry we were able to examine the phenotype of the individual cells in mixed gender coculture experiments. Significantly, we found that approximately 85 % of the cells remaining in the coculture scaffold after 6 weeks of *in vitro* culture were hAC-derived. The remaining hMSCs did not stain positively for collagen I or X. DNA content of the cocultured constructs was also significantly higher than either monoculture scaffold. Taken together with the cytogenetic characterization, these data suggest that the hMSCs stimulated hAC proliferation. Coculture of hACs and hMSCs within our scaffold demonstrated that these cell types are mutually influential: ACs promoted a hyaline phenotype in differentiated MSCs, and MSCs enhanced proliferation and matrix production from ACs.

6.2 INTRODUCTION

Articular cartilage defects have a limited ability for spontaneous repair due to the avascular nature of the tissue and subsequent lack of inflammatory response to injury²⁻⁴. Chondral defects disrupt the normal distribution of forces across the joint during articulation⁶, leading to a

metabolic change in chondrocytes that can propagate cartilage loss^{5,8}. These chondral defects are a prominent risk factor contributing to chronic cartilage degradation in osteoarthritis. Joint dysfunction caused by cartilage degeneration is the leading cause of disability in the United States with 1 in 2 American's expected to present with a symptomatic form of this disease¹. Presently there are very few therapeutic treatments capable of preventing cartilage loss once initiated by acute damage or disease⁵. The standard treatment protocol is to address pain until severely impaired mobility necessitates a total joint replacement. Given the significant clinical impact of cartilage degeneration it is essential that more effective therapies be developed, especially those designed to prevent or abate tissue loss at an earlier stage.

Cartilage engineering is a cell-based therapy that could be used for the early treatment of chondral defects. The basis of tissue engineering is to utilize a three dimensional scaffold to deliver cells and bioactive factors in a coordinated fashion to facilitate tissue growth. Cartilage engineering aims to develop a functional tissue regenerate with the ability to restore joint biomechanics and prevent further tissue degradation. A number of unresolved issues remain regarding the clinical use of cartilage engineering, including the best type of cells and scaffold to use, and how close to the native tissue the regenerate needs to be to facilitate successful repair.

The two most well studied candidate cells for cartilage engineering are articular chondrocytes (AC) and mesenchymal stem cells (MSC). Chondrocytes are the only cell type in cartilage and are responsible for maintaining homeostasis of the extracellular matrix, albeit in a low-turnover state in adult tissue⁵. Chondrocytes were the first cell type explored for tissue engineering applications based on the precedence for their clinical use in autologous chondrocyte transplant^{87,88} (ACT) procedures. Since then, a number of disadvantages associated with the clinical use of ACs have been discussed, including damage to cartilage donor site during the biopsy harvesting procedure^{40,41}, the low cell yield from the biopsy site and dedifferentiation during *in vitro* expansion⁹⁹⁻¹⁰². Additionally, in the majority of cases, the repair tissue that forms at the transplantation site resembles a fibrous scar tissue, fibrocartilage, rather than native hyaline

cartilage⁹⁵⁻⁹⁷. The fibrocartilage repair tissue is estimated to be up to ten times weaker in compression than hyaline cartilage^{68,98}. Furthermore, due to their low metabolic state^{5,296}, it is questioned whether adult chondrocytes can produce sufficient quantities of matrix proteins to facilitate tissue repair.

Mesenchymal stem cells (MSCs) are chondroprogenitors that offer a potential alternative to ACs in cartilage engineering^{94,106,297}. These cells are easily isolated from a variety of tissue sources, including bone marrow, and can be readily expanded *in vitro*. However, the use of MSCs comes with the challenge of controlling the differentiation phenotype. In the original work from our laboratory, we designed a pellet culture system with a serum-free chondrogenic medium containing TGF- β 1 and dexamethasone that was sufficient to initiate chondrogenesis *in vitro*^{108,109}. It was established that this protocol for *in vitro* chondrogenesis of MSCs produces cartilage tissue with a ‘transient’ or endochondral phenotype. This characterization is based on the expression of markers classically associated with hypertrophic chondrocytes, leading to the concern that endochondral ossification will be the outcome of the *in vivo* application of MSCs^{276,277}. Furthermore collagen I, characteristic of fibrocartilage, also persists in MSC-derived neocartilage.

Coculturing of ACs and MSCs could provide an experimental method to overcome the limitations associated with monoculture of each of these cell types. This technique has previously been explored as a method to address the limited chondrocyte number in ACT procedures. For example, Gan and Kandel showed that the inclusion of 20 % primary ACs could significantly enhance the chondrogenic phenotype of passaged, cryopreserved ACs²⁹⁸. Similarly, Hildner *et al* proposed adipose-derived MSCs could replace a percentage of ACs in matrix assisted ACT procedures, but they saw persistence of the hypertrophic and fibrocartilaginous phenotype within their scaffolds²⁹⁹. More encouragingly, Fischer *et al* recently suggested PTHrP secreted from chondrocytes was a main factor contributing to inhibition of hypertrophic maturation of hMSCs in pellet coculture³⁰⁰. In this study we explore the effect of coculturing human bone-marrow

derived MSCs (hMSCs) and human ACs (hACs) from non-pathological donors to test the hypothesis that coculture will influence the amount and/or type of matrix synthesized by the cells when photoencapsulated in poly(ethylene glycol) diacrylate (PEGDA) based scaffolds designed for cartilage engineering applications.

6.3 RESULTS

6.3.1 Comparing chondrogenesis of human MSCs to ACs in hydrogel scaffolds

Human bone marrow derived MSCs, or healthy human ACs isolated from the femoral condyles of cadaveric donors, were photoencapsulated separately into a PEGDA-based semi-interpenetrating network (sIPN) at a concentration of 25×10^6 cells/ml¹⁷³. Toluidine blue staining for sulfated proteoglycans and type II collagen immunohistochemistry indicated that both hMSCs and hACs undergo chondrogenesis in these scaffolds following 6 weeks of *in vitro* culture in a serum-free defined medium containing TGF- β 1 and dexamethasone (Figure 6.1A,B).

However, hMSCs expressed collagens I and X, detectable at both the protein (Figure 6.1A) and gene level (Figure 6.2B). These extracellular matrix proteins are not part of the permanent hyaline cartilage phenotype observed in articular cartilage (Figure 6.1C), nor are they expressed by photoencapsulated hACs during hydrogel culture (Figure 6.1B, 6.2C). The robust increase in temporal expression of collagen X and MMP-13 from MSCs (Figure 6.2A,B) has led to the concern that the cells will undergo endochondral ossification *in vivo*.

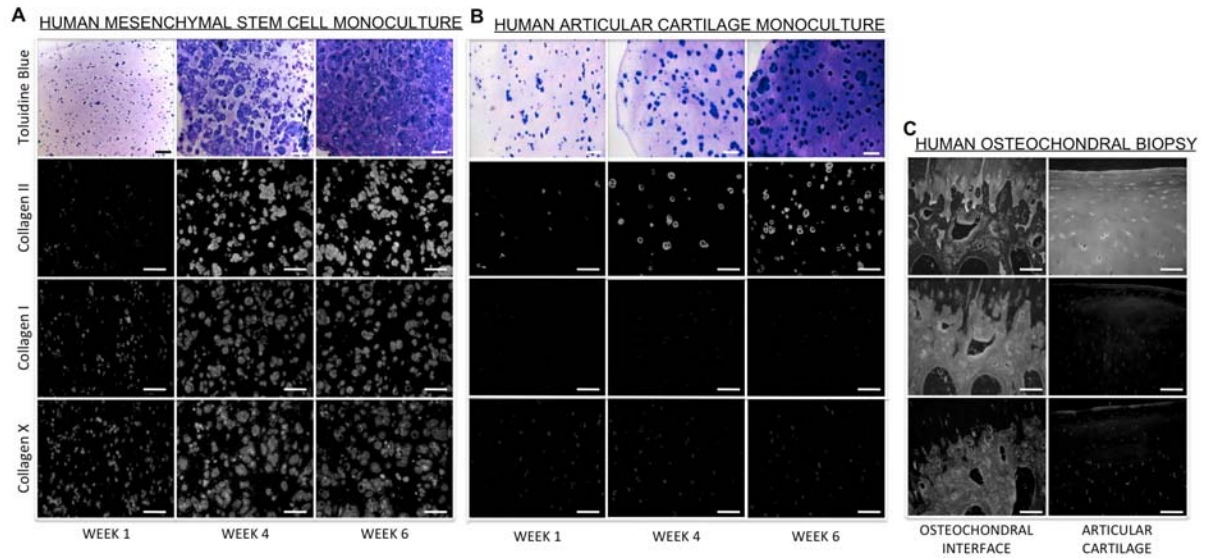


FIGURE 6.1 – IMMUNOHISTOCHEMICAL CHARACTERIZATION OF CHONDROGENESIS IN SIPN SCAFFOLDS. (A) hMSCs or (B) hACS in PEGDA-based sIPN hydrogels designed for cartilage engineering applications. (C) Human osteochondral sections from one of the cartilage tissue donors was used to validate the specificity of the antibodies used. Scale bar = 100 μ m.

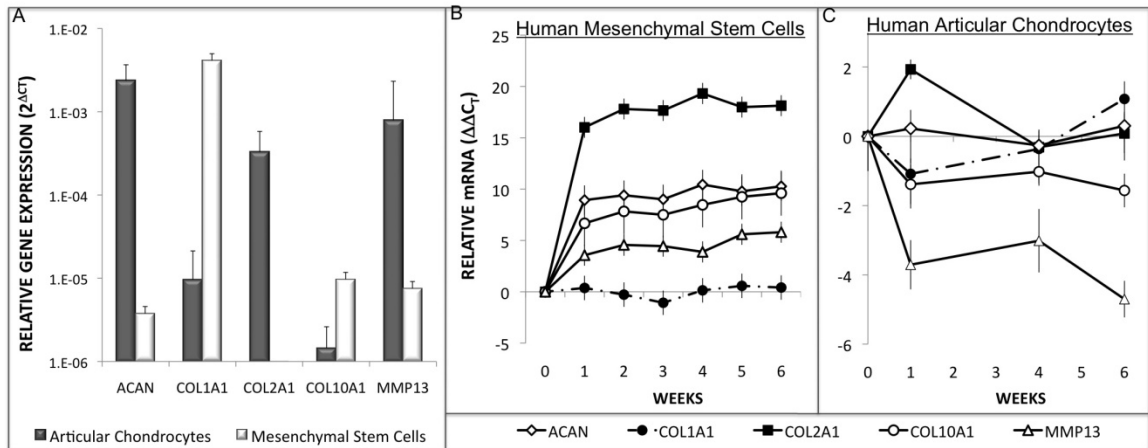


FIGURE 6.2 – TEMPORAL UPREGULATION OF HYPERTROPHY MARKERS IN MSC BUT NOT AC SEEDING HYDROGELS. (A) Gene expression of hACs (gray) and hMSCs (white) prior to encapsulation, normalized to 18S expression (ΔC_T). Relative mRNA expression of (B) hMSCs or (C) hACs during 6 weeks of *in vitro* culture in defined chondrogenic medium, expression normalized to gene expression prior to encapsulation ($\Delta\Delta C_T$).

6.3.2 Coculture of hMSCs and hACs

To examine whether hMSCs and hACs could influence each other during culture, the two cell types were photoencapsulated together in the PEGDA-based sIPN at a 1:1 ratio, keeping the final cell concentration constant at 25×10^6 cells/ml. This coculture experiment was designed to test two distinct hypotheses: (1) that hACs could induce chondrogenesis of hMSCs in the absence of chondrogenic factors TGF- β 1 and dexamethasone (Figure 6.3), and (2) that coculture of hACs and hMSCs could influence the chondrogenic phenotype of MSCs (Figure 6.4). To test whether hACs could induce chondrogenesis of hMSCs, baseline monoculture conditions were established for hACs in either 10 % FBS, 20 % FBS or serum-free chondrogenic medium containing TGF- β 1 and dexamethasone. hMSCs monoculture was conducted only in the chondrogenic medium since it has previously been established that differentiation will not proceed without TGF- β 1 (Figure 5.3A)^{278,279}. hACs produced significantly more extracellular matrix in medium containing TGF- β 1 than in DMEM supplemented with FBS. Similarly, coculture in 20 % FBS-containing medium resulted in very little proteoglycan or hydroxyproline deposition compared with monoculture of either cell type in chondrogenic medium. These data indicated that hACs were not able to induce chondrogenesis of hMSCs (Figure 6.3A,B).

Coculture of hACs and hMSCs in chondrogenic medium containing TGF- β 1 and dexamethasone tested whether this system could affect chondrogenesis by influencing the amount and/or type of matrix produced. Significantly, immunohistochemistry revealed limited deposition of non-hyaline markers, collagens I and X, in cocultured constructs following 6 weeks of *in vitro* culture (Figure 6.4A). At a gene level *COL10A1* expression was also significantly reduced from hMSCs alone, and not significantly different than hACs (Figure 6.4B, $p < 0.05$). Collagen II immunohistochemistry indicated more matrix deposition in the coculture than hACs alone, but less than hMSCs alone (Figure 6.4A). Gene expression for *COL2A1* was not statistically different

between any of the cell culture conditions despite a trend towards higher gene expression in the hMSC and coculture constructs (Figure 6.4B).

The influence of coculture on the quantity of matrix deposition was less straightforward due to significant variation in chondrogenesis between the 6 different hMSC donors. Matrix deposition was more consistent between hACs donors, perhaps due to a tighter demographic range and consistent healthy state of the donor tissue (12 – 25 years old, all male, Figure 6.5C). Consequently within each separate coculture experiment proteoglycan deposition was normalized to the amount of proteoglycan in the hAC-monocultured hydrogels. Proteoglycan deposition in hAC-hMSC cocultured constructs was always at least as good as that of hACs alone, and in 50 % of the experiments it was significantly higher (Figure 6.5A, $p < 0.05$). Coculture also corresponded with a significant increase in DNA content in 5 of the 6 experiments after 6 weeks relative to monoculture of either hACs or hMSCs (Figure 6.5B, $p < 0.05$).

6.3.3 Transwell culture of hMSCs and hACs

We next wanted to examine whether the effect of coculture could be replicated by paracrine signaling. For these experiments MSCs-monocultured hydrogels were placed in a transwell filters located above aggregate cultured hACs (Figure 6.6A). Aggregate culture was used to maintain the phenotypic state of *in vitro* cultured articular chondrocytes²³⁰ (data not shown) and initial cell ratios were kept at 1:1 for consistency with the direct coculture model discussed above. There was not a significant difference in proteoglycan deposition per construct between monocultured, cocultured, or transwell cultured MSCs (Figure 6.6B). Consistent with previous results, DNA content of cocultured gels was significantly higher than either monoculture condition, but was not significantly different for transwell cultured MSCs (Figure 6.6C, $p < 0.05$). Immunohistochemical staining for collagen X deposition was not decreased in transwell-cultured MSC constructs to the same extent as direct coculture (Figure 6.6D). Similarly, RT-PCR indicated a 5-fold reduction in *COL10A1* expression in transwell-cultured MSCs compared to

MSC monoculture constructs, significantly less than the 586-fold reduction in gene expression measured from direct coculture (Figure 6.6E, $p < 0.05$).

6.3.4 hMSCs influence hACs in coculture

These observations lead us to ask what the relative contribution of each cell type was to the phenotype observed in the direct cocultured constructs. To determine this we used FISH staining of the X and Y chromosome to distinguish mixed gender hACs (male) from hMSCs (female) following immunohistochemistry staining of the extracellular matrix (Figure 6.7A). Cytogenetic characterization of the coculture samples revealed that 82 ± 4 % of the cells were hACs, while only 12 ± 3 % of the cells could definitively be identified as hMSC-derived (Figure 6.7B). The identity of 6 ± 1 % of the cells could not be determined because only a single X-chromosome was visible in the section. Since the cells were initially mixed at 50 % hACs to 50 % hMSCs, this indicates a 1.7-fold relative increase in hACs and an approximate 5-fold decrease in of hMSCs. hMSC monoculture in this scaffold has previously been shown a 35 % decrease within the first two weeks of culture (Figure 3.3). Given this dramatic reduction of MSC-derived cells in the cocultured scaffolds, hMSCs appear to be stimulating both proteoglycan (Figure 6.5A) and collagen II deposition from the hACs (Figure 6.4A).

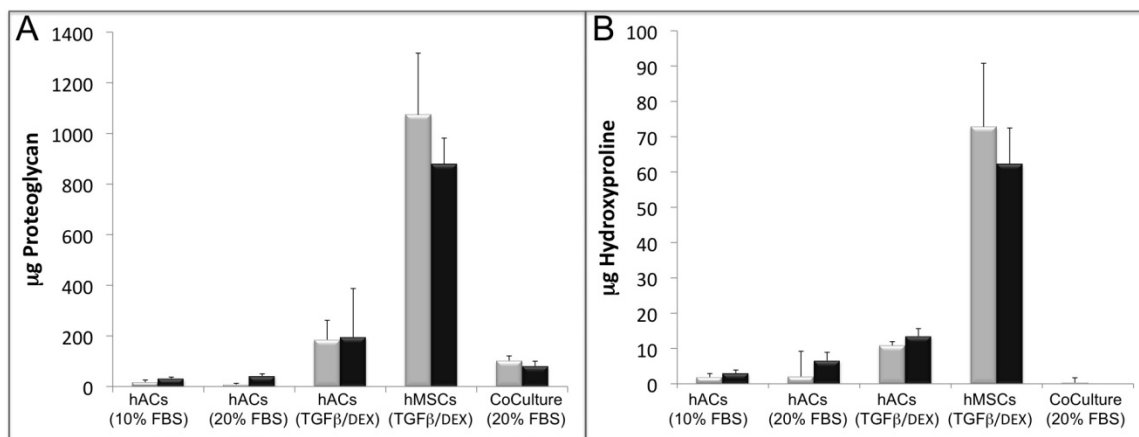


FIGURE 6.3 – HUMAN ACS CANNOT INDUCE DIFFERENTIATION OF HUMAN MSCS IN COCULTURE IN THE ABSENCE OF CHONDROGENIC FACTORS. (A) Proteoglycan and (B) hydroxyproline deposition per scaffold (gray) or normalized to DNA (black) from scaffolds cultured *in vitro* for 6 weeks.

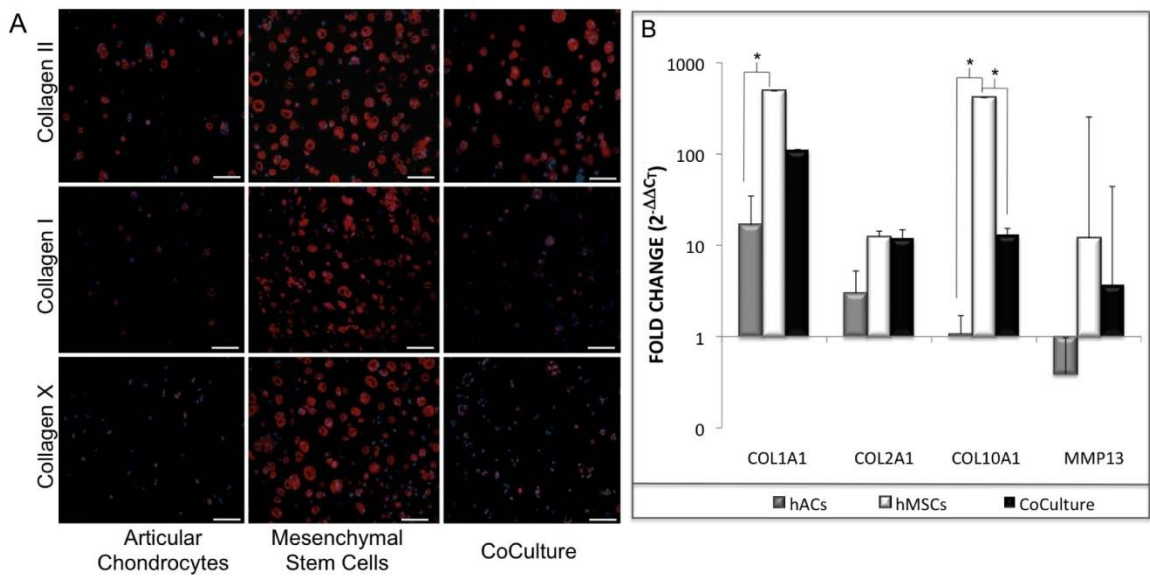
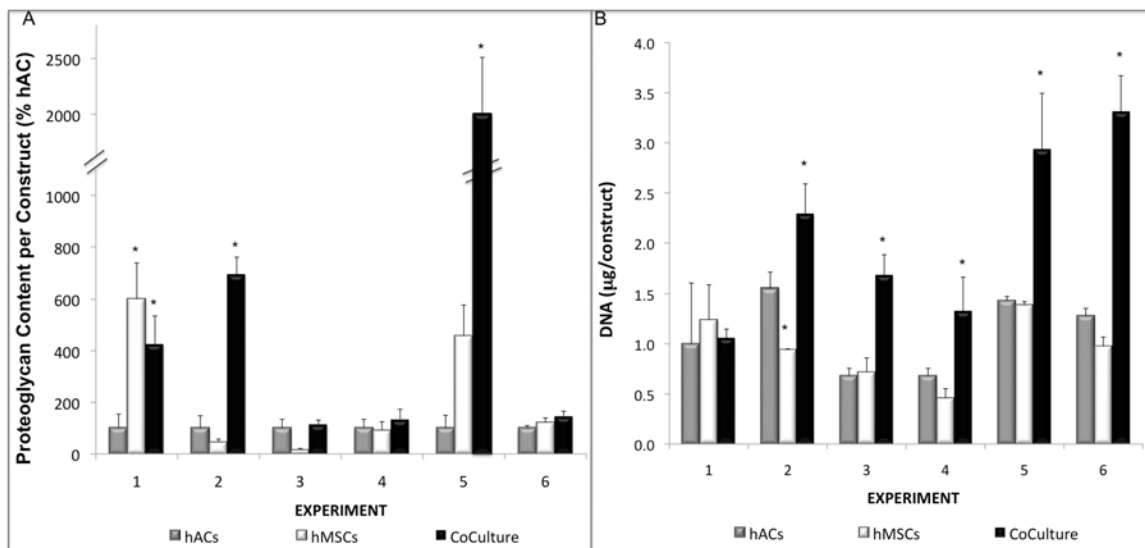


FIGURE 6.4 – COCULTURE INHIBITS HYPERTROPHY IN HYDROGEL SCAFFOLDS. (A) Immunohistochemistry for types II, I, and X collagen and (B) fold change in gene expression for either hACs, hMSCs or a 1:1 coculture of the two cell types in chondrogenic medium. Scale bar = 100 μ m. Gene expression represents mean \pm 95 % confidence, significance set at $p < 0.05$.



C

Experiment Number	Mesenchymal Stem Cell Donor Demographics		Articular Cartilage Donor Demographics	
	age	gender	age	gender
1	64	Female	25	Male
2	69	Female	17	Male
3	54	Female	24	Male
4	53	Male	24	Male
5	57	Female	23	Male
6	26	Male	12	Male

FIGURE 6.5 – BIOCHEMICAL ANALYSIS OF MSC-AC COCULTURED HYDROGELS. (A) Proteoglycan and (B) DNA content in scaffolds following 6 weeks of *in vitro* culture. Data represent mean \pm standard deviation; * = $p < 0.05$ compared to hAC. (C) Table with donor demographics for the 6 separate experiments.

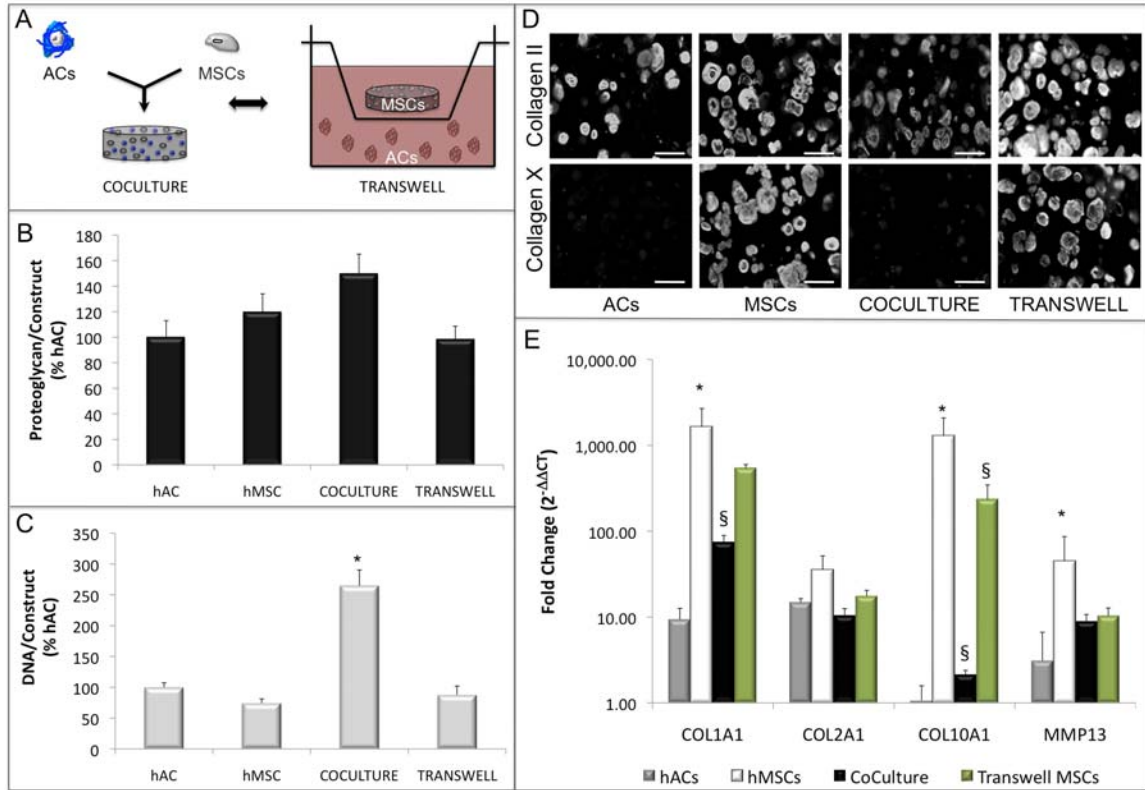


FIGURE 6.6 – TRANSWELL EXPERIMENTS DO NOT REPLICATE DIRECT COCULTURE IN HYDROGELS. (A) Schematic diagram of coculture versus transwell experimental design (B) Proteoglycan and (C) DNA content per construct in scaffolds following 6 weeks of *in vitro* culture; data represent mean \pm standard deviation; * = $p < 0.05$ compared to hACs. (D) Immunohistochemistry for types II and X collagen; scale bar = 100 μ m. (E) Fold change in gene expression; data represents mean \pm 95 % confidence, * = $p < 0.05$ from hACs and ξ = $p < 0.05$ from hMSCs.

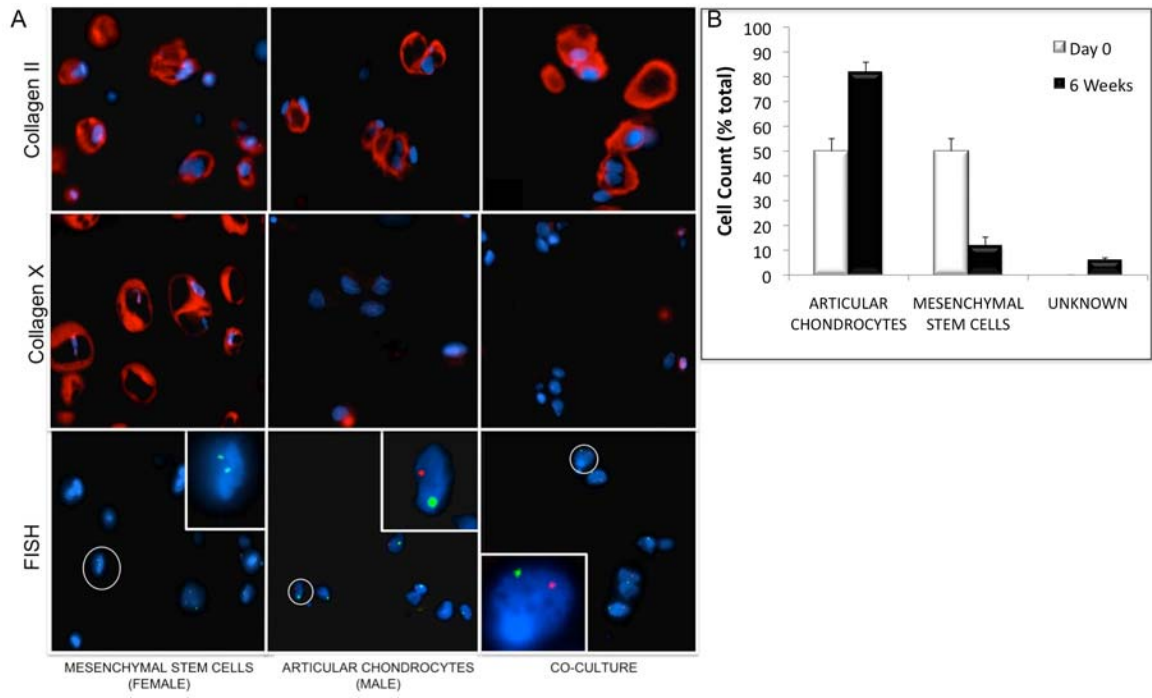


FIGURE 6.7 – COCULTURE PHENOTYPE IS CONTRIBUTED LARGELY BY ACS. Red-fluorescent IHC for (A) collagen II and collagen X with FISH counterstaining for male (orange+green) or female cells (2 x green). (B) Quantification of cell types by gender in cocultured hydrogels following 6 weeks of *in vitro* culture: 200 cells were counted from three different coculture experiments, data represent mean \pm standard deviation.

6.4 DISCUSSION

Coculture is an experimental technique employed for tissue engineering applications as a mechanism to either facilitate formation of complex tissues by supplying multiple cell types^{301,302}, or to enhance tissue formation. In this study we explored the direct coculture of human ACs and MSCs in hydrogel scaffolds to test the hypothesis that inclusion of both cell types could influence chondrogenesis and neocartilage formation at a clinically relevant scale. We found that a hyaline cartilage phenotype was promoted in coculture samples due to a synergistic relationship between ACs and MSCs.

The first question we addressed using our coculture system was whether hACs could induce *in vitro* chondrogenesis of hMSCs in the absence of chondrogenic factors TGF- β 1 and dexamethasone (Figure 6.3). There is evidence for the capacity of ACs to induce differentiation: osteogenesis of monolayer plated rat MSCs was stimulated through coculture with bovine ACs without sodium- β -glycerolphosphate and dexamethasone supplementation^{303,304}. However, the ACs could not sustain an osteogenic phenotype in the MSCs past 14 days of culture³⁰³. Chondrogenesis of MSCs requires a three-dimensional rather than monolayer culture system^{109,116}. Consequently, to test the ability of hACs to induce chondrogenesis we utilized a PEGDA-based sIPN scaffold that we previously described as promoting neocartilage formation²⁷⁸. In contrast to AC-induced osteogenesis, we saw very limited chondrogenic matrix deposition in cocultured scaffolds in the absence of TGF- β 1. Induction of MSC chondrogenesis may be possible with a higher concentration of ACs³⁰⁵, as we only tested a 1:1 ratio with 1×10^6 of each cell type within the scaffold. However, we found that ACs themselves produced low quantities of proteoglycans and hydroxyproline without TGF- β 1 (Figure 6.3); this finding is consistent with hAC chondrogenesis in pellet culture³⁰⁰.

We next examined whether coculture could influence the type or amount of cartilage matrix produced. Both immunohistochemistry and gene expression analysis indicated that ACs inhibited expression of fibrocartilage (collagen I) and hypertrophic cartilage (collagen X and

MMP-13) markers by encapsulated hMSC (Figures 6.4). The influence of ACs on chondrocyte maturation was first documented by Jikko *et al* in coculture experiments with growth plate chondrocytes and ACs³⁰⁶. ACs inhibited the terminal differentiation of growth plate chondrocytes either in direct coculture models or in transwell experiments with ACs grown on a collagen II substratum below growth plate chondrocytes cultured on a filter membrane. This inhibition could not be replicated with chondrocyte conditioned medium (CCM). Fischer *et al* also recently reported on the capacity for ACs to inhibit hypertrophy of MSCs in pellet culture³⁰⁰. In contrast to the work from Jikko *et al*, they found that the reduction in collagen X expression and alkaline phosphatase (ALP) activity was conserved with CCM. The methods for making CCM may contribute to the discrepancy between these results: Jikko *et al* used CCM from monolayer cultured ACs, whereas Fischer *et al* used CCM from AC pellet aggregates cultured in TGF- β containing chondrogenic medium. It is well known that ACs phenotypically de-differentiate when cultured in monolayer and therefore would release an altered set of morphogenetic factors and extracellular matrix molecules⁹⁹⁻¹⁰².

By analyzing their CCM Fischer *et al* concluded that PTHrP was the chondrocyte-derived molecule responsible for the main inhibitory effect on MSCs hypertrophy and could be reproduced with PTHrP supplementation³⁰⁰. Both PTHrP^{10,11} (Figure 1.3) and TGF- β ³⁰⁷ have been shown to inhibit hypertrophic maturation in the growth plate during endochondral ossification. TGF- β can also stimulate PTHrP production from chondrocytes³⁰⁸, potentially enhancing suppression of chondrocyte maturation. Since the CCM produced by Fischer *et al* was collected from pellet cultures supplemented with TGF- β , it is not clear how the addition of TGF- β affected PTHrP levels from ACs or the inhibition of hMSC hypertrophy from CCM. Furthermore, data published from the same laboratory³⁰⁹, and unpublished data from our laboratory (Supplemental Figure S6.1) indicate that PTHrP added to the medium also reduces collagen II and proteoglycan production. Taken together these data suggest that AC-secreted

PTHrP alone is not responsible for the change in the coculture phenotype since we observe a concomitant reduction in hypertrophy and increase in matrix deposition.

Despite discrepancy in the molecular source of hMSC phenotypic modulation during coculture, both our data (Figure 6.6) and others^{300,303,304,306} supports that the AC effects on MSCs are at least partially due to soluble factors. However, it should be emphasized that the soluble milieu of cocultured cells is complex and temporally influenced by the presence of both cells type. For example, ACs are known to produce TGF- β in several of isoforms, but the majority is secreted in the latent-form and associated with latent TGF- β binding proteins^{310,311}. Amongst other proteases, MMP-2, -9, and -13 can coordinate the activation of latent-form TGF- β in cartilage⁵⁷. MMP-2 is expressed at relatively high and constant levels by hMSCs during chondrogenesis in hydrogel scaffolds (Figure 4.1A,B). Thus, MSC mediated activation of AC-derived TGF- β via MMP-2 could cause ACs to stimulate PTHrP³⁰⁸ production and MSCs to increase collagen biosynthesis (Figure 5.2 & 5.3). Such coordination of signaling pathways relies on the influence of cells on each other and is typical during development (Figure 1.3); these complex paracrine interactions will likely not be simply simulated with conditioned medium.

In addition to the influence hACs had in promoting a hyaline phenotype from coculture differentiated hMSCs within our hydrogel scaffolds, the hMSCs themselves proved to have a significant effect on hACs (Figures 6.5 & 6.7). We found a significant increase in cell number within the cocultured-constructs compared to either monoculture system systems (Figure 6.5B). Cytogenetic analysis of cocultured constructs with mixed gender cell types strongly suggests this increase in DNA content is the result of MSC-stimulated AC proliferation. Matrix production may also be stimulated in ACs by MSCs as since we observed a 50 % incidence of increased proteoglycan deposition from cocultured constructs compared to hAC-monoculture (Figure 6.5A) and evidence of enhanced collagen II deposition by immunohistochemistry (Figure 6.4A).

This study did not directly investigate a mechanism for hMSCs induced proliferation of hACs, but two distinct, non-exclusive concepts have previously been proposed: secretion of bioactive factors^{122,147,312} and mitochondrial transfer from MSCs^{313,314}. The ability of MSCs to contribute to tissue regeneration through the secretion of bioactive factors was amongst their first appreciated functions, but more recently has been overshadowed by their ability to differentiate into a variety of different tissue types^{116,122,153}. MSCs were first identified as a subpopulation of stromal cells that are capable of supporting viability and differentiation of hematopoietic stem cells in the bone marrow cavity^{315,316}. Subsequent studies have identified a number of stimulatory cytokines secreted from MSCs including stem cell factor, TGF- β , IGF, and EGF^{147,312}. The bioactive factors from MSCs has been suggested to contribute to the increased viability and/or proliferation of nucleus pulposus³¹², cardiac³¹⁷ and neuronal^{148,149} cells in tissue repair models.

An alternative mechanism describing the ability of MSCs to induce proliferation is through transfer of mitochondria to donor cells in coculture systems. Mitochondria are essential organelles that contribute to a variety of cellular processes including oxidative phosphorylation and aerobic metabolism. When MSCs were cocultured with dermal fibroblast cells containing mutated mitochondrial DNA that caused growth inhibition, the proliferative capacity of the fibroblasts was restored through the transfer of mitochondria from MSCs³¹³. It is possible that the transfer of mitochondria to ACs could contribute to the increased proliferation. Mature ACs maintain a low metabolic state due in part to the hypoxic, avascular condition of the tissue⁵.

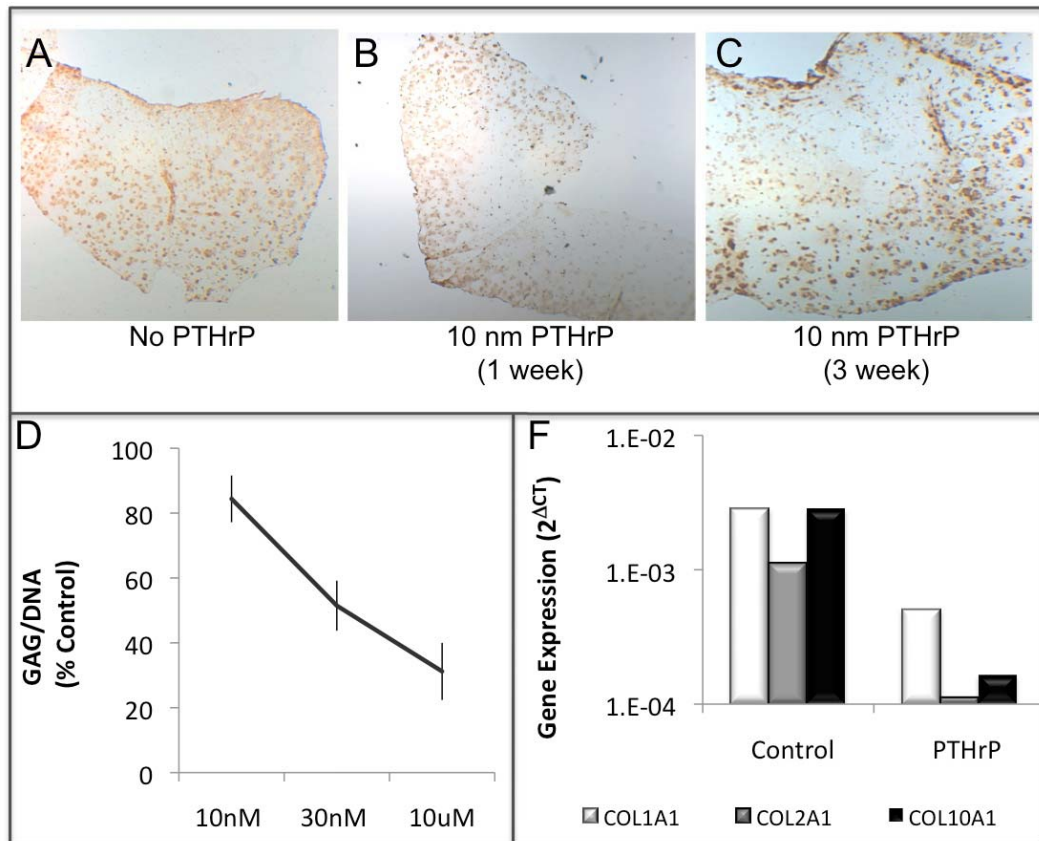
It is possible that some or all of the benefit observed during coculture is relayed through paracrine signaling, and is therefore replaceable by soluble factors. Data from both our transwell experiment (Figure 6.6) and others^{303,304,306} supports that the AC effects on MSCs are at least partially due to soluble factors. However the soluble milieu of cocultured cells is complex and temporally influenced by the presence of both cells type. For example, ACs are known to produce TGF- β in several of isoforms, but the majority is secreted in the latent-form and associated with latent TGF- β binding proteins^{310,311}. Amongst other proteases, MMP-2, -9, and -13 can coordinate

the activation of latent-form TGF- β in cartilage⁵⁷. In previous work we showed MMP-2 to be expressed at relatively high and constant levels by hMSCs during chondrogenesis in hydrogel scaffolds (Figure 4.1A,B). Thus, MSC mediated activation of AC-derived TGF- β via MMP-2 could cause ACs to stimulate PTHrP³⁰⁸ production and MSCs to increase collagen biosynthesis (Figure 5.2 & 5.3). Such coordination of signaling pathways relies on the influence of cells on each other and is typical during development (Figure 1.3); these complex paracrine interactions will likely not be simply simulated with conditioned medium.

In conclusion, our hydrogel coculture system demonstrated that MSCs and ACs worked synergistically to effect neocartilage formation in scaffolds. ACs inhibited the hypertrophic maturation of MSCs, while MSCs promoted AC proliferation and possibly matrix production. From a tissue engineering perspective, coculture within a three-dimensional scaffold may provide regulated presentation of chondrogenic factors that could replace the need for bioactive scaffolds.

Supplemental Data: PTHrP Inhibits Chondrogenesis

Soluble PTHrP added to PEGDA-based sIPN hydrogel constructs beginning at either 1 or 3 weeks was not sufficient to significantly inhibit collagen X deposition from MSCs following 6 weeks of chondrogenesis at a concentration of 10 nm (Figure S6.1A-C). Increasing PTHrP concentration to 10 μ m did result in a decreased gene expression of collagen X (Figure S6.1E, black bar), but lead to a significant decrease in proteoglycan deposition (Figure S6.1D) and collagen II gene expression (Figure S6.1E, grey bar).



SUPPLEMENTAL FIGURE S6.1 - PTHrP INHIBITS CHONDROGENESIS. (A-C) Collagen X immunohistochemistry of MSC containing hydrogels cultured for 6 weeks in complete chondrogenic medium containing either (A) no PTHrP, or 10 nm PTHrP added at either (B) 1 week or (C) 3 weeks. (D) Proteoglycan normalized to DNA content in hydrogels cultured for 6 weeks. (E) Gene expression for control constructs or those receiving continuous supplementation with 10 μ m PTHrP at 6 weeks.

CHAPTER 7: CONCLUSIONS & FUTURE DIRECTIONS

The thesis work detailed in chapters three through six represents novel scaffold and cell based techniques aimed at improving cartilage engineering. These were all tested independently and therefore the conclusions and future directions will be outlined in the same manner with respect to individual projects. The advantage of keeping these projects independent is that it allows them to proceed efficiently in parallel and isolate the variable being changed. However, ultimately the goal would be to develop a scaffold-based therapy suitable for clinical application and the “best” scaffold will require integration of these individual aspects.

7.1 BIORESPONSIVE HYDROGELS

The primary objective of the bioresponsive hydrogel project was to develop a scaffold with degradation kinetics that corresponded to chondrogenesis and matrix elaboration from MSCs (Figure 1.6). This aim was based on the hypothesis that the non-degradable scaffold interferes with extracellular matrix assembly and results in a mechanically inferior neocartilage construct. The shortcoming of degradable scaffolds tested to date for cartilage engineering applications is that degradation is not inherently tied to cellular activity. My project proposed to first identify an endogenous enzyme with the appropriate temporal activity, then to design and characterize a cell-mediated bioresponsive scaffold as a novel platform for cartilage engineering.

By characterizing the temporal expression of metalloproteinase enzymes known to be involved in cartilage development I identified MMP-7 as an endogenous enzyme with a pattern that correlated to collagen II and aggrecan expression from MSCs photoencapsulated in PEGDA based hydrogel scaffolds (Thesis Chapter Four). Based on these data two MMP-7 substrates were identified from the literature, 1241224²²⁴ and VPLS-LTMG²²⁹, and covalently embedded into a PEGDA backbone to create a MMP-7 sensitive scaffold (Figure 2.1). As a control, the second

sequence (VPLSLTMG) was scrambled to MLLVTPSG, which is not known to be degradable by any metalloproteinase and we show was not cleaved by MMP-1, -2, -7, -13²⁰⁰.

During the initial testing with these bioresponsive scaffolds I discovered they would not photopolymerize using the UV light initiation technique standard in the laboratory¹⁷³. Polymerization was achieved only by increasing the concentration of the photoinitiator I2959 from 0.06 % to 0.3 %, which is well above the 0.1 % cytocompatible limit for photoencapsulation of cells^{231,251}. These results led to the hypothesis that the aromatic tryptophan residue included in the scaffold to monitor degradation was competing with the I2959 photoinitiator whose peak absorbance is 285 nm. Consequently, prior to testing the MMP-7 scaffold for *in vitro* chondrogenesis it was necessary to find and validate an alternative photoinitiator system cytocompatible with human MSCs. Chapter three of this thesis describes the optimization of an visible light photoinitiator system composed of eosin Y, TEA and NVP.

In vitro testing of the two MMP-7 sensitive scaffolds with photoencapsulated human MSCs demonstrated improved intercellular distribution of the type II collagen matrix and increased the dynamic modulus in neocartilage constructs. Chapter four provides proof-of-concept data for this scaffold and forms the foundation for further optimization of a bioresponsive scaffold tuned to chondrogenesis. A number of possible opportunities for continued research on the MMP-7 bioresponsive scaffolds are discussed below.

7.1.1 Optimize Scaffold Degradation

The degradation rate for the MMP-7 sensitive scaffolds was experimentally quantified through tryptophan release from cell-free scaffolds exposed to recombinant MMP-7 (Figures 2.1, 4.2). Although these data demonstrated that the bioresponsive scaffolds were cleavable in a dose dependent manner, and provided a relative comparison of degradation kinetics between the two different MMP-7 substrates, the *in vitro* degradation rate by the photoencapsulated MSCs was not experimentally determined. Tryptophan release cannot be used to quantify degradation in the

same manner when cells are included in the scaffold because proteins synthesized by the cells will interfere with absorbance readings. To indirectly demonstrate cell-driven degradation I attempted to quantify MMP-7 activity in the scaffold. MMP-7 expression was semi-quantitatively assessed using RT-PCR and immunohistochemistry (Figure 4.1), but neither of these experimental techniques is capable of distinguishing the pro versus active form of the enzyme. To specifically look for MMP-7 activity I performed casein zymography on medium and homogenized hydrogel samples. The pro-form of MMP-7 could be detected in both, but not the active-form (Figure 7.1). The short half-life of active MMP-7 due to tight cellular regulation of MMPs may contribute to the inability to detect this enzyme in an active form. Neither concentrating the protein through columns nor running the zymogram for longer was sufficient to increase detection sensitivity for the active MMP7. Presently, antibodies specific to active MMP-7 do not exist. However, considering the emerging role of MMP-7 in cancer it is likely that these may tools be developed in the near future and could be used to detect the active enzyme histologically or by Western blot.

Presently, techniques to directly evaluate scaffold degradation kinetics by encapsulated cells are very limited. Laboratories have previously presented confocal images of cell morphology claiming that a spread out, rather than rounded, morphology is indicative of scaffold degradation³¹⁸. Immunohistochemical detection of the scaffold backbone itself, or of the cleaved peptide, are additional techniques that could provide indirect evidence of scaffold degradation. For example biotin could be incorporated into the PEGDA monomer and its presence detected by immunohistochemistry with an anti-biotin antibody. This technique would not distinguish between cleaved and intact polymer backbones, but could serve as a qualitative indicator of scaffold presence. To more specifically determine whether the peptide in the scaffold was being cleaved, neopeptide antibodies could be developed to the free ends of the broken PLE-LRA or VPLS-LTMG peptides to demonstrate that cells were degrading the embedded MMP-7 substrates. Alternatively, it is possible to adapt fluorescence resonance energy transfer (FRET)-

based systems such that the fluorescence between the two probes is quenched when the peptide substrate is whole, but active following cell-mediated cleavage. This technique was published by Lee *et al* from the West laboratory and could be developed for our system provided significant chemical modifications are made to our monomer chemistry. Developing an effective technique for characterizing cell-mediated degradation rate of scaffolds is one possible future direction of this work.

Regardless of the ability to directly quantify scaffold degradation by the cells, interterritorial expansion of the collagen matrix exclusively within the MMP-7 sensitive scaffolds is indirect evidence that these scaffolds are degrading (Figure 4.3). Additional modifications to the scaffold chemistry could be made to optimize the rate of degradation and/or initial strength of the scaffold. The initial modulus of the scaffold can easily be increased by changing the weight percentage of macromer in the polymerization reaction or the length of the PEGDA monomer. The concern with most modification that increase modulus through a decrease in pore size is that our models suggest this will lead to decreased matrix elaboration and increased pericellular localization of extracellular matrix proteins¹⁷³ (Figure A.2). Consequently in scaffolds with increased crosslinking density it could be advantageous to incorporate faster or earlier degrading sequences within the polymer backbone. For example MMP-2 is relatively highly expressed throughout chondrogenesis within PEGDA-based scaffolds (Figure 4.1) and therefore should produce early degradation. Co-polymerizing MMP-2 monomer with the MMP-7 monomer would generate bi-modal degradation of the scaffold. The ratio of the MMP-7 to MMP-2 could be tailored for desired outcomes.

Building a scaffold made completely from a MMP-2 sensitive macromer could also serve as a rigorous test of our MMP-7 bioresponsive hydrogel. The hypothesis would be that MMP-2 specific scaffolds would degrade too early causing loss of cells and extracellular matrix which would compromise the structural integrity of the developing neocartilage constructs. I attempted a conceptually similar experiment by building a scaffold from a LGPA peptide-containing

macromer provided by the West laboratory: the LGPA sequence is supposedly cleaved by a variety of collagenases. In comparison to the non-degradable sIPN and sc-PEGDA scaffolds, LGPA scaffolds did not produce a change in the distribution of collagen II matrix or accumulation of extracellular matrix proteins (Figure 7.2). The problem associated with these data is that the degradation behavior of this peptide sequence has not been well characterized. There is no published data concerning which enzymes cleave this substrate in the MEROPS database²⁰⁰ and because the LGPA peptide available did not have a tryptophan amino acid included in the linker domain (Figure 2.1) we could not verify degradation properties as done with the other peptide substrates (Figure 4.2). Furthermore, because the LGPA peptide was synthesized by the West laboratory based on the ‘general’ collagenase activity of this sequence, it may not be kinetically optimal. I have recently built a MMP-2 specific bioresponsive scaffold using the kinetically optimal sequence IPVS-LRSG²²⁹. This MMP-2 sensitive scaffold was designed with a tryptophan residue in the same fashion that the MMP-7 scaffolds were developed but have not yet been tested. The next steps with this scaffold will be to characterize degradation characteristics in a cell-free system as done previously (Figure 4.2). Both the dose dependent behavior with 2, 6 and 20 nM recombinant human MMP-2 and sequence specificity with 2 nM MMP-1, -2, -7, -13 should be established. Subsequently, *in vitro* chondrogenesis with the MMP-2 sensitive scaffold should be compared to MMP-7 sensitive and sc-PEGDA scaffolds with hMSCs encapsulated at a concentration of 20×10^6 and 40×10^6 cells/ml. Cell numbers permitting 10 % PEGDA and/or sIPN can be included as additional non-degradable controls.

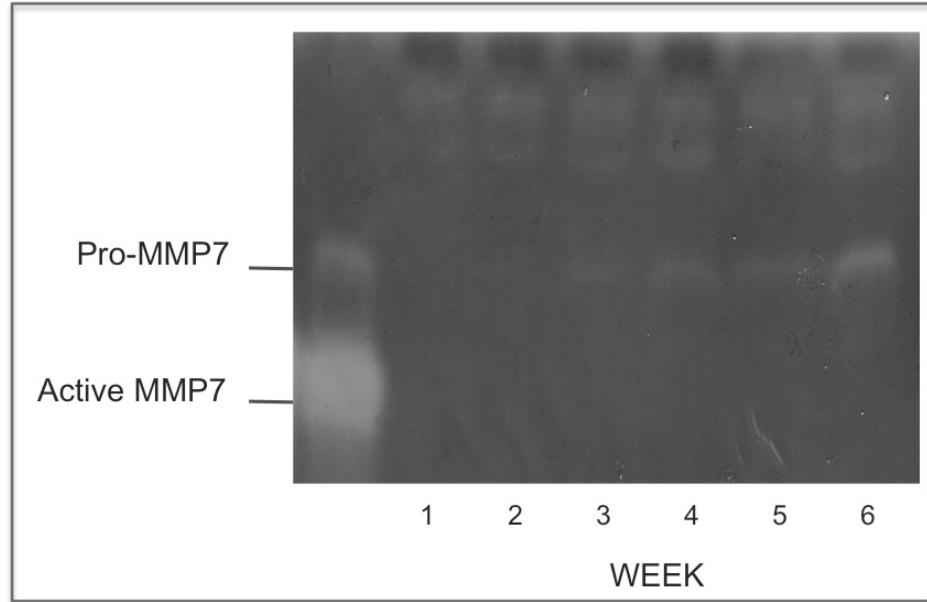


FIGURE 7.1 – CASEIN ZYMOGRAPHY FOR MMP-7 ACTIVITY IN HYDROGELS. Weekly medium aspirates collected from hydrogels with photoencapsulated hMSCs shows temporal accumulation of the pro-form of MMP-7, but does not detect the active-form. Samples were compared to recombinant human MMP-7 run on the same gel (left).

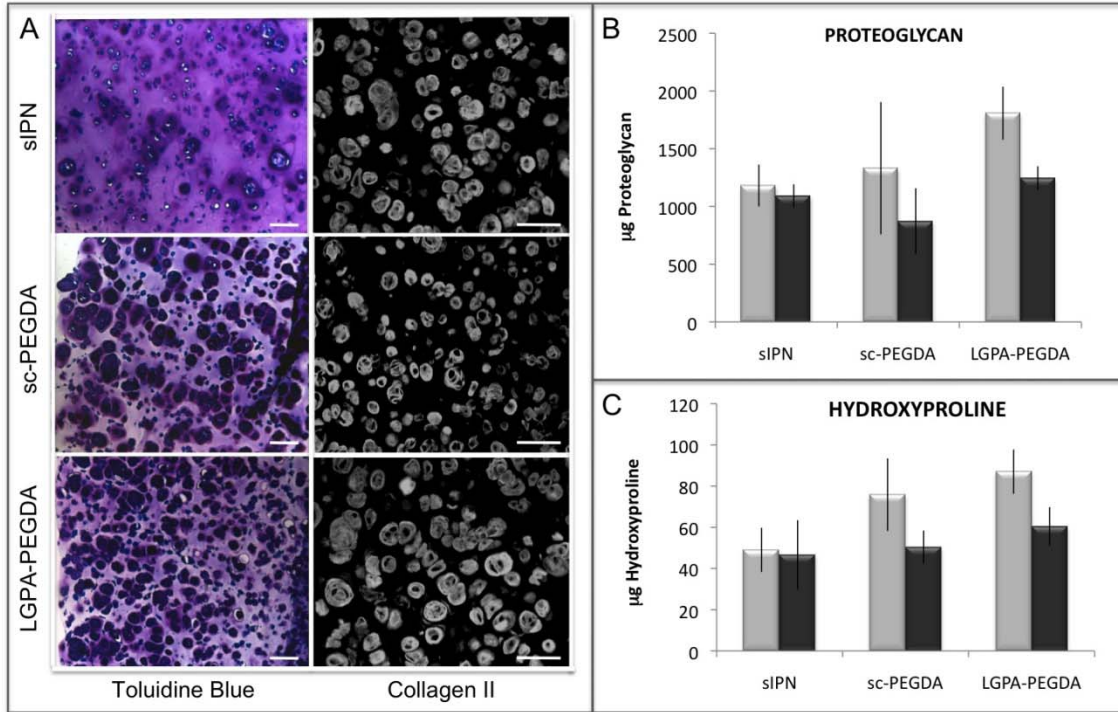


FIGURE 7.2 – CHARACTERIZATION OF ‘COLLAGENASE’ SENSITIVE LGPA-PEGDA BIORESPONSIVE SCAFFOLD. (A) Toluidine blue and collagen II staining comparing LGPA-PEGDA to non-degradable sIPN and sc-PEGDA scaffolds, scale bar = 100 μm . (B) Proteoglycan content per construct (grey) or per cell (black). (C) Hydroxyproline content per construct (grey) or per cell (black).

Another possible route for optimizing scaffold degradation for a bioresponsive scaffold tuned specifically to chondrogenesis would be to improve MMP-7 substrate specificity. The PLE-LRA²²⁸ and VPLS-LTMG²²⁹ substrates tested show some susceptibility to cleavage by other MMPs: PLELRA more so than VPLSLTMG (Figure 4.2). Fukui *et al* has identified ...ICPTD—LATAS... as an *in vivo* MMP-7 cleavage site in the second exon of collagen IIA that is not sensitive to cleavage by other MMPs²⁶⁵. To explore the possibility that this sequence would offer improved specificity, a peptide containing PTDLAT was synthesized with the GGWGG- and –GGK linker domains and conjugation to the PEGDA backbone, as described previously. No tryptophan release was observed from the polymer following treatment with 2 nM of MMP-7, which was sufficient for degradation of both PLE-LRA and VPLS-LTMG containing scaffolds (Figure 7.3). This specific 6 amino acid sequence (PDTLAT) has not previously been demonstrated as an effective sequence *in vitro*. Lack of activity could be because not enough of the peptide sequence was included for enzyme recognition or because a secondary structure is required. Continued optimization of this sequence is an additional opportunity for future experiments, but is perhaps not necessary given the relative success of the PLE- and VPLS-PEGDA scaffolds.

7.1.2 Explore Scaffold Utility using other Chondrogenic Cell Types

MMP-7 was identified as an enzyme that correlated to chondrogenesis of human MSCs in PEGDA-based hydrogels. Given its temporal association with collagen II and aggrecan we wondered if this relationship existed with other chondrogenic cell types such as articular chondrocytes and/or ESCs. The hypothesis was that MMP-7 activity corresponds to matrix production in multiple chondrogenic cell types, and that this scaffold will be universally applicable for cartilage engineering applications with different cell types because degradation will remain concomitant with cartilage matrix elaboration. Importantly, the MMP-7 degradable PEGDA also allows us to directly compare neocartilage production from different chondrogenic

cell types within a single scaffold. Studies directly comparing different chondrogenic cell types are limited and only compare either MSCs to ESCs³¹⁹ or articular chondrocytes^{174,285,320-322}.

Articular chondrocytes were evaluated for MMP-7 expression in the same manner described previously for MSCs (Figure 4.1A). Chondrocytes were harvested from the femoral condyles of non-pathological human donors and encapsulated into the PEGDA-based sIPN immediately after harvest. Quantitative real time RT-PCR confirmed that MMP-7 increased during *in vitro* culture in defined chondrogenic medium containing both TGF- β 1 and dexamethasone (Figure 7.4A). However, freshly isolated articular chondrocytes have a 100-fold relative increase in gene expression of MMP-7 compared to MSCs at the time of encapsulation (data not shown), indicating that scaffold degradation could initiate earlier with chondrocytes than MSCs. This low basal expression of MMP-7 from articular chondrocytes would be expected since they are isolated from mature cells presently making collagen II and aggrecan. Immunohistochemistry also revealed MMP-7 positive staining in the hydrogel matrix (Figure 7.4B).

Similarly in a collaborative project with Dr. Shoukhrat Mitalipov (Oregon National Primate Research Center, OHSU Portland OR) we looked for MMP-7 expression from embryoid body (EB) aggregates of rhesus SCNT-ESCs lines grown in chondrogenic medium containing 0.3 ng/ml TGF- β 1 and 500 ng/ml BMP for 37 days. EB aggregates stained positively for alcian blue, indicating that chondrogenic differentiation may have occurred (data not shown). Furthermore RT-PCR demonstrates a hyaline chondrogenic phenotype with an increase in collagen II and aggrecan expression, a decrease in collagen I expression, and no detection of type X collagen (Figure 7.5B). MMP-7 expression was increased with differentiation (Figure 7.5B), consistent with the data from human MSCs (Figure 4.1) and articular chondrocytes (Figure 7.4A).

Based on these data we encapsulated EBs into the PLE-M7 PEGDA hydrogel and cultured them for 6 weeks in defined chondrogenic medium containing 10 ng/ml TGF- β 1 and 10^{-7} M dexamethasone (Figure 7.5C-F). Toluidine blue staining of paraffin embedded hydrogel sections indicated production of a proteoglycan-rich matrix (Figure 7.5C) and immunostaining

showed type II collagen was abundant throughout the EBs (Figure 7.5D). However, unlike neocartilage matrix derived from MSCs, type X collagen was not detected in the EBs (Figure 7.5E).

While this provides good preliminary data that chondrogenesis is possible with rhesus ESCs encapsulated in hydrogels, the format for this experiment was not ideal because the cells were not distributed throughout the hydrogel and matrix formation was restricted to the EBs despite the use of a degradable scaffold. It is not entirely clear why the extracellular matrix did not expand beyond the EBs, however the current understanding is that the superficial layer of cells in the EB form a protective barrier that could be inhibiting expansion of the matrix into the hydrogel network. Consequently, it would be desirable to encapsulate ESCs from a single cell suspension into the hydrogel in the same manner that is currently done for MSCs. This proposal comes with significant technical barriers including how to grow sufficient numbers of viable ESCs without the use of EBs or feeder layers. A few mechanisms have now been proposed for differentiating ESCs to MSC-like populations^{155,166,257,323} that are more readily expandable in monolayer culture and could provide a cell population amenable to chondrogenesis within hydrogel scaffolds. The method published by the Elisseff laboratory in which single outgrowth ESCs are obtained from EBs grown on gelatin coated plates and then subsequently collected and expanded in monolayer on tissue culture plates chondrocyte conditioned medium could be reasonable technique to try in future directions^{154,166}.

The advantage of working with rhesus cells from the Oregon Primate Center is that they provide a platform for testing of all three chondrogenic cell types (ACs, MSCs, ESCs) from a single species that could subsequently be developed into an orthopaedically relevant *in vivo* animal model of chondral defects. The scope of this would be a 5 to 10 year, multi-institutional (OHSU, Rice, ONPRC), multi-departmental (Orthopaedic, Bioengineering, Stem Cell Center) collaborative project, but this aim is uniquely positioned to help translate this technology into an appropriate pre-clinical setting.

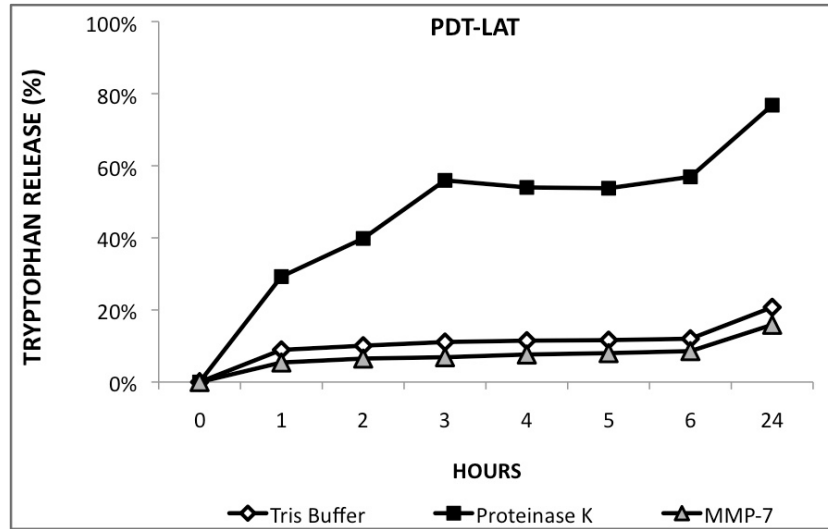


FIGURE 7.3 – DEGRADATION KINETICS FOR PDTLAT-PEGDA. Bioresponsive PEGDA containing the sequence PDTLAT identified from the *in vivo* sequence –IC- RA- RARARA -CiC-not-cleave-when-eRAoCeC-to-recoa vinant-hua an-MM- -A-

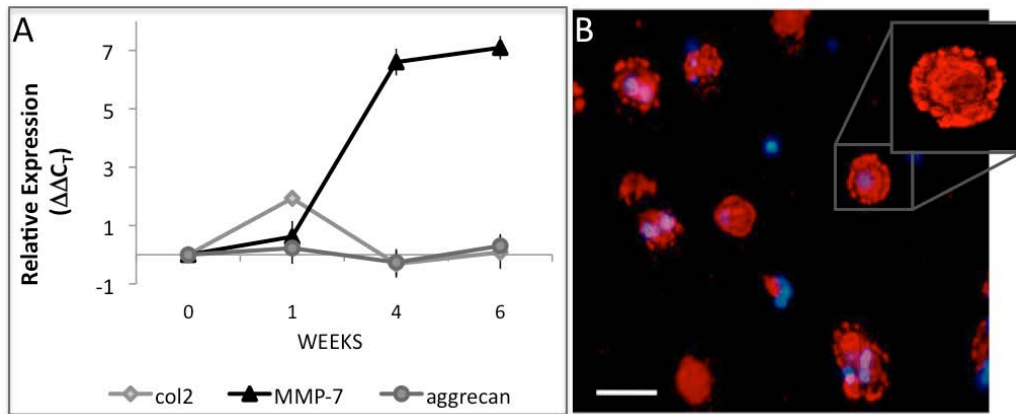


FIGURE 7.4 – MMP-7 EXPRESSION FROM ARTICULAR CHONDROCYTE PHOTOENCAPSULATED IN PEGDA-BASED SIPN HYDROGELS. (A) Change in gene expression of articular chondrocytes over six weeks (B) MMP-7 immunohistochemistry, scale bar = 100 μ m.

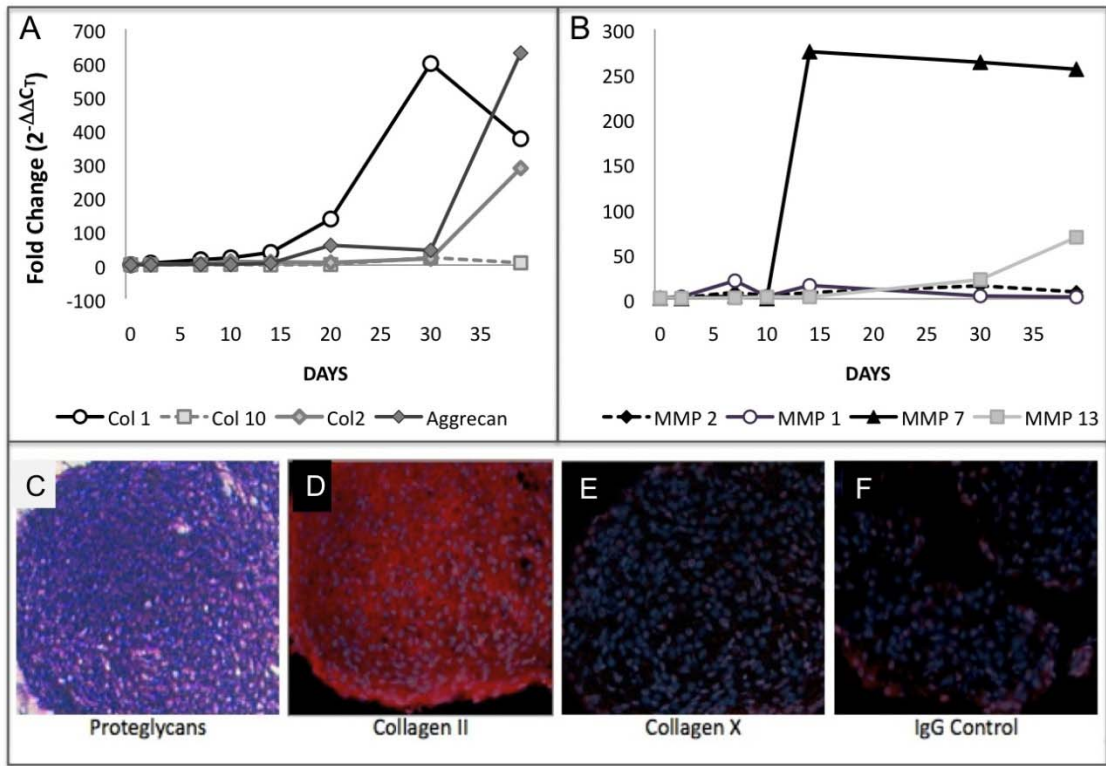


FIGURE 7.5 – ESCs ARE ALSO CANDIDATES FOR MMP-7 BIORESPONSIVE SCAFFOLD. Change in (A) chondrogenic or (B) MMP gene expression in embryoid bodies during 42 days of *in vitro* culture. Embryoid bodies photoencapsulated in the PLE-M7 PEGDA stain positively for (C) proteoglycans and (D) type II, but indicate no immunohistochemical staining for (E) type X collagen. (F) IgG control.

7.2 BIOACTIVE SCAFFOLDS

In order to design a bioactive scaffold appropriate for *in vivo* cartilage engineering, the temporal requirement for TGF- β 1 and dexamethasone within a PEGDA-based hydrogel scaffold needed to be determined (Thesis Chapter 5). Testing *in vitro* indicated that a minimum of three weeks of exposure to TGF- β 1 is required for chondrogenesis and matrix elaboration from MSCs (Figure 5.2-5.3), but that dexamethasone is dispensable in the hydrogel culture systems (Figure 5.1). Together these data suggest that a bioactive scaffold effective for *in vivo* implantation might only need a mechanism of sustained TGF- β 1 delivery for three weeks. I proposed to develop a bioactive scaffold in which TGF- β 1 was covalently attached to the backbone during photopolymerization. Tethering TGF- β (tTGF- β) to a PEGDA scaffold has previously been shown to stimulate *in vitro* matrix production from vascular smooth muscle cells more effectively than soluble TGF- β ²⁰⁶. This technique differs from other delivery systems in which growth factors are delivered through degradable microspheres²⁰³⁻²⁰⁵.

Attempts to generate a TGF β 1-bioactive scaffold capable of facilitating cartilage matrix deposition have thus far been unsuccessful (Figure 5.4), but data from these preliminary experiments has provided direction for future work. Importantly, I have shown that the PEGylated TGF- β 1 delivered as a soluble moiety can stimulate chondrogenesis with approximately 70 % of the efficiency of non-PEGylated TGF- β 1. This indicates that the chemical processing of the recombinant protein did not rendered it inactive. Furthermore, the immobilized tTGF- β 1 does appear to have some initial activity. This is based on an observed color change in the medium during the first 10 days of culture, and the partial rescue of matrix deposition when soluble TGF- β 1 was provided in the medium of scaffolds containing a 10 ng/ml tTGF- β 1 following 10 days without TGF- β 1.

To continue the development of a TGF β 1-bioactive scaffold the first step should be to determine if the PEGylated TGF- β 1 is effectively tethering to the scaffold during polymerization

and if so how long it remains active. The polymerization reaction with visible light and the eosin y photoinitiator system is very efficient (Thesis Chapter 3), however, it is a formal possibility that the PEGylated TGF- β 1 is not covalently bonding to the scaffold but rather aggregating with itself. A number of experiments could be performed to indirectly assess polymerization efficiency. One technique would be to quantify TGF- β 1 in the scaffold and the solution following polymerization into a cell-free, non-degradable scaffold such as 10 % PEGDA. After equilibrium swelling is reached (> 48 hours) untethered PEGylated TGF- β 1 will be released from the scaffold due to its small size relative to the pores of the hydrogel. A simple Bradford protein assay could be used to spectrophotometrically quantify TGF- β 1 in solution relative to the scaffold following dissolution of the hydrogel in 0.1 N sodium hydroxide (see Chapter 2: Material & Methods). Alternatively, with the appropriate spectrophotometer, absorbance reading of the intact scaffolds with or without tTGF- β 1 could be completed. If this were done following equilibrium swelling it would be reasonable to assume that relative increase in absorbance at 285 nm over the control PEGDA scaffold was due to tTGF- β 1. It might also be possible to use immunohistochemistry on paraffin embedded TGF β 1-bioactive scaffolds with an anti-human TGF- β 1 antibody to detect attachment.

If the techniques suggested above demonstrate that TGF- β 1 is being effectively tethered to the scaffold then future experiments should focus on optimizing activity. One possible explanation for the limited, or short-lived, tTGF- β 1 activity is that extracellular proteases could be degrading the enzyme. Characterizing degradation of the tTGF- β 1 when cells are also embedded in the scaffold using spectrophotometry would be confounded by protein synthesis during chondrogenesis, but temporal immunohistochemistry may be an option for this evaluation. Experimental approaches focused on augmenting tTGF- β 1 activity may be a more direct approach.

The first, most straightforward option is to do a more complete titration of tTGF- β 1 concentration. Based on the data from Mann *et al*, tTGF- β 1 was more effective than soluble TGF- β 1²⁰⁶ at stimulating matrix production, and they found 1 ng/ml tTGF- β 1 was sufficient to generate the desired biological response. However, this relationship may not hold in our system where MSCs have a high demand for TGF- β 1 during both chondrogenesis and collagen biosynthesis (Figure 5.2). There was some histological evidence of pericellular toluidine blue staining in scaffolds containing 100 ng/ml tTGF- β 1 suggesting that perhaps higher concentrations of growth factor could be beneficial (Figure 5.4A), but an increase in concentration needs to be balanced against potential negative side effect such as the risk of apoptosis. Experiments are currently being conducted with tTGF- β 1 at concentrations from 1 – 1000 ng/ml within the 10 % PEGDA scaffold.

Additionally, unpublished data from the West laboratory suggests that tTGF- β 1 hydrogels also need the integrin binding ligand RGD to be included in the scaffold to affect a cellular response. However, data in the literature has shown that 2 – 10 mM tethered RGD (tRGD) will inhibit chondrogenesis from MSCs^{218,250} unless it is removed from the scaffold following an initial role in promoting MSC survival^{202,220}. I am currently testing bioactive scaffolds containing 10ng/ml tTGF- β 1 and 1.4 μ M tRGD. The latter was the lowest concentration of tRGD documented in the West laboratory as effective in synergistically activating tTGF- β 1. Additional concentrations of tRGD/tTGF- β 1 should be tested.

If neither higher concentrations of TGF- β 1 nor inclusion of the RGD-ligand prove to be effective then more significant design changes may be necessary (Figure 7.6). One option would be to generate TGF- β 1 nanoparticles with a micelle configuration (Figure 7.6B). This design could be achieved by simply polymerizing the PEGylated TGF- β 1 alone in a solution containing the visible light photoinitiators described in Chapter 3. Models predict that an average of 15 covalent acrylate bonds will form at nucleation sites during polymerization. Additionally the

hydrophobicity of the acrylate groups will drive aggregation in the water-soluble polymerization reaction to theoretically produce micelle like nanoparticles. These TGF β 1-micelles could subsequently be non-covalently incorporated into the scaffold. This is a novel technique that to my knowledge, has not yet been explored and will therefore require significant characterization to develop an appropriate protocol.

Another possible design modification would be to build bioresponsive tTGF- β 1 moieties (Figure 7.6C). This design would incorporate MMP substrates into the acroylPEG-linker that covalently attaches the recombinant TGF- β 1 to the PEGDA backbone. In addition to providing a releasable TGF- β 1 molecule, this design would also inherently lengthen the PEG-linking domain, which in itself may facilitate tTGF- β 1 activity through improved accessibility. This design also affords a sophisticated way to control temporal delivery of TGF- β 1 and test the hypothesis that TGF- β receptor internalization is critical to activity²⁹³⁻²⁹⁵. By utilizing the MMP characterization completed earlier (Figure 4.1A,B) we can choose peptide substrates that will produce ‘fast’, ‘medium’ and ‘slow’ TGF- β 1 rates release. For example MMP-2 since expressed by both by the MSC and throughout chondrogenesis at relatively high and constant levels, the MMP-2 specific IPVS-LRSG²²⁹ substrate could provide ‘fast’ release. MMP-7 would be an ideal candidate for ‘medium’ kinetic release because its expression is concomitant with chondrogenesis and therefore would be released as the cellular demand for TGF- β 1 associated with collagen biosynthesis occurred. MMP-1 is expressed at relatively low levels by the MSC and is downregulated in weeks 1-4 of chondrogenesis; this expression pattern could provide ‘slow’ release of TGF- β 1.

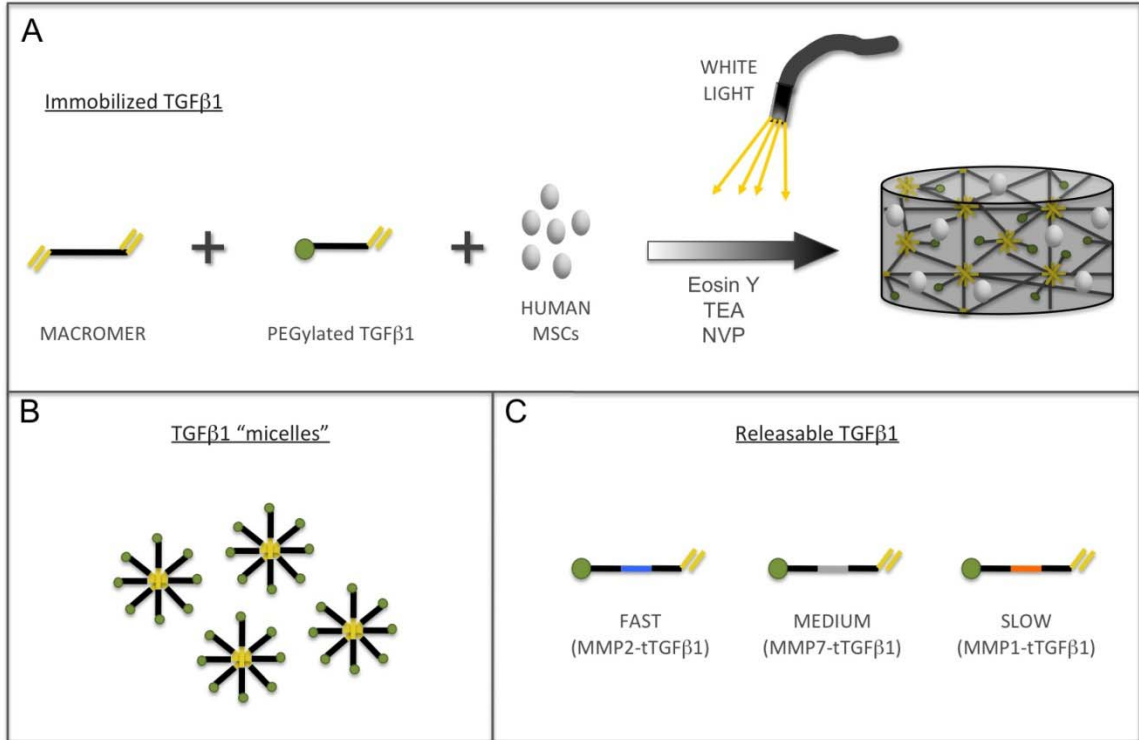


FIGURE 7.6 – SCHEMATIC OF TGF- β 1 BIOACTIVE SCAFFOLD DESIGN POSSIBILITIES. (A) PEGylated TGF β 1 immobilized to the scaffold during photopolymerization. (B) TGF β 1 micelle nanoparticles, non-covalently entrapped into scaffold. (C) TGF β 1 immobilized into scaffold on cell-mediated proteolytically sensitive PEG tethers, kinetically optimized for with appropriate release kinetics.

7.3 COCULTURE

A coculture system containing both hACs and hMSCs within PEGDA-based scaffolds was established to test whether these cells could influence each other on a scale that could affect repair of articular cartilage defects. This is important because both cell types have clinical limitations associated with their use. Chondrocytes are most often obtained from autologous donor tissue in very low numbers that need to be expanded *in vitro* to obtain a sufficient quantity of cells for transplant. However, it is well established that chondrocytes cultured in monolayer will lead to a phenotypic de-differentiation of ACs⁹⁹⁻¹⁰², which has been implicated in the formation of fibrocartilage tissue at the repair site. Furthermore, damage to the donor cartilage at the harvest site presents an increased risk for osteoarthritis^{6,93}. Allogenic ACs have been explored for their clinical utility, however the data are conflicting as to whether the cells themselves are immunoprivileged³²⁴⁻³²⁶ or require the associated extracellular matrix for immunoprotection³²⁷. MSCs are chondroprogenitors that have been proposed as an alternative source for cell-based therapies in cartilage repair^{94,106}. The concern with their use is that MSCs differentiate into chondrocytes with a non-hyaline phenotype: expressing markers of both fibrocartilage (collagen I) and hypertrophic chondrocytes (collagen X and MMP-13). I designed the coculture experiments to test two independent hypotheses: (1) that ACs could induce chondrogenesis of MSCs in the absence of TGF- β 1 and dexamethasone, and (2) that ACs could influence the differentiation of MSCs. My results indicated that ACs could not induce MSC chondrogenesis in the absence of chondrogenic factors at the coculture concentrations tested; perhaps due in part to a low cellular activity of ACs without TGF- β 1 (Figure 6.3). However, coculture did create a synergist relationship between the MSCs and ACs that produced neocartilage constructs with a more hyaline-like phenotype. ACs inhibited expression of collagens I and X (Figure 6.4 & 6.6), while MSCs stimulated proliferation of ACs (Figure 6.5 & 6.6). These preliminary results provide the basis for a number of future experiments that would evaluate the relationship between these

cells and optimize culture conditions to produce a hyaline-like neocartilage implant in a clinically useful format.

7.3.1 Identifying Soluble Mediators of Coculture Effect

One area for further experimentation is to examine whether the activity of either cell can be replaced by soluble factors in our hydrogel system. Both conditioned medium and transwell experiments should be utilized to test this hypothesis; many of the experiments proposed below have already been initiated. To make chondrocyte conditioned medium we chose to use floating chondrocyte aggregate cultures (section 2.2.2). Briefly, ACs were harvested from the femoral condyles of healthy human donors, isolated with a collagenase digestion and plated in Corning ultra-low cluster 24-well plates at a concentration of 1×10^6 cells/well. Aggregate cultures were maintained in Opti-MEM® I Reduced Serum Medium as previously described²³⁰. Chondrocyte conditioned medium (CCM) was harvested twice weekly and frozen at $-80\text{ }^{\circ}\text{C}$ until needed. Prior to using CCM, batches of different patients and harvest points were combined and filter sterilized. Preliminary data suggest that CCM cannot induce MSCs chondrogenesis in the absence of TGF- β 1 and dexamethasone, as would be expected based on the coculture data. Further testing needs to be completed to see if CCM with TGF- β 1 and dexamethasone can inhibit the hypertrophic phenotype of MSCs in hydrogels, but early evidence suggest that collagen X expression persists in CCM. Based on the recent data from Fischer *et al* changing the protocol for conditioning medium may impact this result: they cultured ACs with TGF- β 1 during pellet culture to generate CCM, which did effectively inhibit hypertrophic differentiation of MSCs.

We have also shown that MSCs stimulate AC proliferation. Consequently, the converse experiment should be carried out to evaluate the effect of MSC conditioned medium on ACs hydrogels. However, it is not clear what format the MSCs should be cultured in to effectively condition the medium since their monolayer behavior is significantly different from that in

hydrogels. One option is to create hMSC and hAC monoculture hydrogels and culture them together in medium containing TGF- β 1 and dexamethasone. This would exclude the opportunity of the cells to directly interact but most appropriately replicates previous experiments in which the effect of MSCs on ACs was determined. From our current data it is not clear whether the effect of MSCs on AC proliferation is from the undifferentiated MSC, the MSC-derived chondrocyte, or both. Medium could be collected from hMSCs monocultured hydrogels over 6 weeks of exposure to chondrogenic medium containing TGF- β 1 and dexamethasone and either batch-tested or pooled to examine the temporal effect of chondrogenesis on ACs. Alternatively, MSCs could be cultured in monolayer with different medium formulations, including FBS/FGF containing medium (standard monolayer culture protocol for maintaining and expanding MSCs, section 2.2.1), Opti-MEM, or chondrogenic medium containing TGF- β 1 and dexamethasone. Utilizing FBS in the culture medium of monolayer plated MSCs could be disadvantageous since we have previously shown that ACs do not synthesize an extensive extracellular matrix in hydrogels in the absence of TGF- β 1 and dexamethasone, and FBS can confound analysis of the media. However, this does not preclude the subsequent addition of TGF- β 1 and dexamethasone after conditioning, and may be the best option to test how MSCs in a progenitor state influence AC chondrogenesis. Opti-MEM is a reduced serum medium previously tested with ACs²³⁰, but it is unclear how monolayer cultured MSCs will do in this medium. Addition of TGF- β 1 and dexamethasone to the monolayer MSCs is also not ideal since MSCs cannot undergo chondrogenesis in monolayer and it is unclear how the phenotype of MSCs would be affected by these culture conditions.

Transwell culture provides an alternative method to conditioned medium that may help maintain the same concentration and temporal regulation of the soluble milieu during coculture. Transwell system inserts with a 0.4 μ m polyester membranes allow transfer of soluble molecules, but not cells, between the insert (top) and the tissue culture plate (bottom). Both MSC and AC

monoculture hydrogels can be cultured in the transwell insert (top) with the opposite cell below. I have initiated experiments with MSC-only hydrogels cultured above floating chondrocyte aggregates. The cell-to-cell ratio and medium volume were maintained to be consistent with the direct coculture experiments previously presented. AC-only hydrogels cultured above MSCs are complicated by the same challenge of modulating MSC phenotype discussed above. Both monolayer plated MSCs in FBS containing medium and MSCs pellet aggregates cultured in chondrogenic medium should be tested.

Identifying the soluble molecules that mediate the paracrine effect of coculture, and how they contribute to changes within the cells, offers an opportunity for more extensive future studies. A number of candidate molecules have been suggested in the literature as soluble factors that are released from ACs (PTHrP, TGF- β)^{300,308,310,311} or MSCs (TGF- β , IGF, EGF, SCF, ect)^{147,312} and may contribute to the coculture phenotype. Monitoring temporal expression of a of candidate bioactive molecules in media aspirates from both monoculture systems compared to the cocultured constructs would provide interesting data on how the protein expression changes between the different systems and throughout culture. Commercially available cytokine array kits or ELISAs could be used to complete this analysis on media aspirates for a finite number of candidate molecules. A more inclusive technique would be to do quantitative proteomics on fractionated samples of the media aspirates from each culture condition³²⁸. This analysis would enable an extensive analysis of which proteins are upregulated or downregulated in the coculture systems compared to the monoculture controls and could identify novel mechanisms that might otherwise be missed in the candidate screen approach.

Identifying temporal changes from monocultured constructs in either conditioned medium or with the other cell type separated by transwell filters could be performed and analyzed as previously described with quantitative RT-PCR and immunohistochemistry (ex: Figures 4.1 & 6.2). Deciphering temporal changes during direct coculture is more difficult. One option would be to use cells from different species with species-specific PCR primers/probes to separate

expression. For example, bovine ACs could be mixed with human MSCs and cocultured in hydrogels with samples harvested weekly to look for relative changes in each cell type compared with monoculture controls.

7.3.2 Optimizing the *In Vitro* Coculture System

In the experiments presented in Chapter 6 only a single coculture condition was tested with an equal number of MSCs and ACs (each at 25×10^6 cells/ml). In MSC monoculture hydrogels we have previously found that 25×10^6 cells/ml optimizes matrix production per cell and per construct²⁷⁸. However, this same concentration may not be optimal for ACs in our hydrogel culture system, and chondrocytes account for close to 85 % of the remaining cells after six weeks of *in vitro* culture. Consequently, experiments could be done that alter both the ratio and final number of cells.

Additionally, given that ACs would likely be the limiting cell type in a clinical setting, it would be interesting to determine the lowest number of ACs that will effectively reproduce the coculture results described in Chapter 6. In a study by Tsuchiya *et al*, coculture of ACs and MSCs in pellet aggregates was most effective with twice as many MSCs as ACs³²⁹. This result was particularly interesting because they got no chondrogenesis of MSCs monoculture pellets and very good matrix production from AC monoculture pellets. Clearly these results are confounded by the absence of MSC chondrogenesis in pellets, which is well established, but were useful in demonstrating MSC-driven stimulation of ACs in coculture. Furthermore, Gan and Kandel showed that coculturing as few as 20 % primary ACs with passaged, cryopreserved ACs was sufficient to increase GAG and collagen content²⁹⁸.

The coculture platform also provides a good setting to begin integrating the results from some of the individual studies. Specifically, chondrogenesis of MSCs without dexamethasone and the use of bioresponsive scaffolds. In Chapter 5 we demonstrated that chondrogenesis of MSCs in hydrogels does not require supplementation with dexamethasone (Figure 5.1). However, we do

not know how ACs will do if given TGF- β 1 without dexamethasone. It would also be interesting to see if coculture of ACs and MSCs in the absence of dexamethasone will augment the inhibition of collagen I and X expression seen individually in the two systems (Figures 5.1 & 6.4). Additionally, since ACs also express MMP-7 (Figure 7.4) the coculture system could be tested in MMP-7 bioresponsive gels (Chapter 4). ACs express low levels of MMP-7 at the start of culture, so including these cells will likely change the degradation rate. Furthermore, it is not known how the influence of MSCs and ACs on each other will effect MMP-7 expression. Temporal characterization of MMP expression in cocultured constructs using both RT-PCR and IHC should be replicated. These data will also be useful in validating that MMP-7 expression is associated with the hyaline cartilage phenotype rather than hypertrophic maturation. Increased gene expression of MMP-7 in the absence of MMP-13 and collagen X in both ESCs (Figure 7.5) and ACs (Figures 6.2 & 7.4) during chondrogenesis already suggests that MMP-7 expression is separate from hypertrophy, but coculture provides an additional opportunity to compare MMP-7 expression with and without hypertrophy.

7.3.3 Chondrogenesis and Hypertrophy of Cocultured Hydrogels *In Vivo*

The optimized coculture conditions determine in section 7.3.2 should be translated to an *in vivo* model to validate that these scaffolds maintain a hyaline cartilage phenotype and do not undergo endochondral ossification. Subcutaneous implantation on the dorsal side of a nude mouse is an established assay for this purpose and allows us to continue working with human cells³³⁰⁻³³². Briefly, athymic mice (~20 g, 6 weeks-old) would be anesthetized with 4 % isoflurane and kept under sedation with 2 % isoflurane streamed through a nose cone during the surgical procedure. Cranial to caudal incisions approximately 2 cm long can be made to create six subcutaneous pockets for the hydrogels on the dorsal side of the mice. Scaffolds containing each of the three cell types (MSC, AC, or coculture) could be placed into the subcutaneous pockets in replicate. The skin incisions can be closed with tissue adhesive and animals would be treated with

analgesia immediately post-op and for two further days. Mice would be allowed free cage activity until they euthanasia 12 weeks post-implantation. Following euthanasia hydrogels would be dissected free of surrounding soft tissues and subjected to high resolution X-ray (Faxitron) to determine whether mineralization had occurred. The qualitative and quantitative methods described for *in vitro* analysis could be used to evaluate chondrogenesis and hypertrophy in the harvested implants (Chapter 2: Material & Methods); modifications for mineralization will be made as necessary. Four hydrogels cut in half provide sufficient material for testing biochemistry and gene expression in triplicate, with two ½ hydrogels remaining for histology. Consequently, only two mice are needed to test for AC and MSC monoculture and a single coculture conditions in a pilot study. Results of the pilot study would guide additional testing, allow for increased power of analysis and permit the inclusion of additional coculture conditions. *In vivo* study design will always be limited by the number of available cells and mostly likely will need to be conducted as a series of batch experiments for logistical reasons. We have already received IACUC approval for this procedure.

APPENDIX A:
MECHANICAL STIMULATION OF HYDROGELS IN MATE BIOREACTOR

AUTHORS

Chelsea S Bahney^{1,2}, Trevor J Lujan³, Kyle M Wirtz³, M Bottlang³, Johnstone B^{1,2}—

¹Oregon Health & Science University, Department of Orthopaedics and Rehabilitation

²Oregon Health & Science University, Department of Cell and Developmental Biology

³Legacy Research & Technology Center, Biomechanics Laboratory

The MATE unit was designed and validated in the Legacy Biomechanics Laboratory. OHSU contributed design input and performance requirements for biological systems. Chelsea was specifically involved in the early optimization and debugging of the MATE unit, design and implementation of the collagenase sensitive hydrogel test (Figure A5), and preliminary experiments with mechanical loading of MSC-laden hydrogel constructs (Figures A3 & A4). Data from this chapter contributed to the following abstracts/publications.

- Lujan TJ,³ Wirtz KM,³ Bahney CS,^{1,2} Madey SM,³ Johnstone B,^{1,2} Bottlang M³. *A Novel Bioreactor for the Dynamic Stimulation and Mechanical Evaluation of Multiple Tissue Engineered Constructs*. Submitted to Tissue Engineering Part C June 2010.
- —x xp —pppl —x ppxsp —x —s lpxl —xp —xonl —BeJ ch—s p —H nuJ ry —p —p —xp —HighH Hhghughput Mechanical Evaluatihn hf Hissue Engineeed Chnstgucts Duging Incubatihn. xupj n—x—Jn—W—K—M—B—J—hney—s—x—M—J—sey—x—M—Johns—W—ne—B—B—W—J—nl—M—Hbstgact sube itted

A.1 ABSTRACT

Cartilage engineering is a cell-based therapy that aims to create mechanically viable replacement tissues capable of repairing damaged articular cartilage to restore joint biomechanics. To date there is not a clear definition of what is required of a neocartilaginous implant to induce sufficient repair of joint cartilage. However, improving neocartilage biomechanics through production and assembly of an extracellular matrix with ultrastructural similarity to native articular cartilage would be advantageous. An important step in this process is maximizing production of extracellular matrix proteins and facilitating interterritorial assembly within the implant. Mechanical stimulation is known to influence both joint development and the anisotropic assembly of the cartilage matrix. We hypothesized that *in vitro* mechanostimulation of human mesenchymal stem cells (MSCs) in a hydrogel scaffold designed for cartilage engineering would improve production and assembly of the neocartilage matrix. These experiments were dependent upon developing a reliable bioreactor that could provide long-term stimulation of hydrogel constructs during *in vitro* culture. We worked with the Legacy Biomechanics Laboratory to provide design input and validation testing of their mechano-active transduction and evaluation (MATE) bioreactor described below. Preliminary testing of MSC-encapsulated hydrogels indicated an inhibition of chondrogenesis with dynamic compressive loading. However, we were able to detect time dependent changes to degradable scaffolds indicating this tool will be useful in providing non-destructive mechanical feedback of the constructs during tissue development and/or scaffold degradation.

A.2 INTRODUCTION

A goal of tissue engineering is to create a functional tissue regenerate that can replace damaged or diseased tissue *in vivo*. Presently, the clinical application of tissue engineering technology in load-bearing tissue such as articular cartilage has been limited by the biomechanical inferiority of the engineered constructs.³³³⁻³³⁵ This lack of mechanical integrity is

caused in part by the improper production and assembly of matrical components during culture.^{336,337} A potential strategy to improve the composition and ultrastructural distribution of the extracellular matrix components in neocartilage constructs is to apply mechanical stimuli during culture with a bioreactor.^{333,334,338}

This concept is rooted in the requisite role of mechanostimulation during joint formation⁴⁸⁻⁵¹ and the histomorphological maturation observed in articular cartilage with weight bearing^{6,30,72}. Presently it is not entirely clear how mechanical stimulation regulates either joint formation or ultrastructural distribution of extracellular matrix molecules in articular cartilage.^{17,30} During embryonic development motion stimulates hyaluronan production^{41,45,46} and canonical Wnt signaling⁵³ at the presumptive joint site, factors suggested as critical for initiating cavitation and/or maintaining the developing joint. It is not until postnatal development that articular cartilage establishes its characteristic anisotropic ultrastructure (Figure 1.4A) and strain histories are highly associated with the different architectural morphologies across joints. Despite limited details regarding the molecular mechanisms controlling cartilage development it is reasonable to hypothesize that the addition of mechanical stimulation could improve the form and function of neocartilage constructs.

The ability to properly test the role of mechanostimulation in neocartilage development is limited by current bioreactor technology. An appropriate design would enable continuous, non-destructive stimulation of the tissue engineered constructs during long-term *in vitro* culture. Furthermore, it is essential that the bioreactor can deliver accurate and repeatable stimulation to the constructs in a manner that can be systematical programmed by the operator to tune for developmentally optimal loading protocols³³⁹. In addition to the ability to reliably stimulate the samples, functional outputs including material properties would provide real-time monitoring of changes to tissue properties during development. Depending on the sensitivity of the bioreactor, this feedback could be a useful mechanism for evaluating matrix elaboration or scaffold

degradation. Attaining accurate mechanical properties in most systems is a time consuming process designed to evaluate only a single specimen at a time.^{334,340-342}

These design requirements become a particular challenge in developing a bioreactor capable of providing accurate and reproducible stimulation to hydrogel constructs that have a low compressive modulus and viscoelastic behavior. Current designs most often use a single actuator to provide distance-controlled compression of multiple constructs.^{248,343-347} Although this protocol permits physiological loading²⁴¹ and high testing volume, it assumes that all specimens are being equally strained. However, construct thickness can vary by more than 10 %^{241,348} and consequently a group of uniformly displaced constructs will be non-uniformly strained. This resulting divergences in strain application impacts experimental repeatability and can affect construct development.³⁴⁹ Furthermore, few studies that compress constructs account for alterations in specimen thickness during culture.³⁵⁰

This appendix chapter discusses the validation of a mechano-active transduction and evaluation (MATE) bioreactor with a platform designed to efficiently and accurately apply mechanical stimulations and assess material properties. The technology utilizes six electromagnetic voice-coil actuators^{241,351,352} to simultaneously stimulate and/or evaluate individual constructs within the confines of a tissue culture incubator (Figure A.1). Validation of this unit demonstrated repeatability and reliability at the same level as an Instron. Furthermore we show that it is sensitive enough to detect changes in thickness and bulk modulus of collagenase sensitive hydrogel constructs during degradation. Preliminary studies using the MATE to apply dynamic compressive loading to hydrogel constructs containing MSCs began to explore the role of mechanostimulation in neocartilage development, but were not continued because we found significant inhibition with our system protocols.

A.3 RESULTS

A.3.1 Bioreactor Design and Validation

The MATE bioreactor (Figure A.1A) was designed to accommodate the requirements and constraints of a tissue-culture laboratory environment. The culture module that houses the constructs was built to intimate a six-well plate (Figure A.1B). This module facilitates the use of standard 35 x 10 mm cell culture dishes, provides for air-flow, and enables sterile transfer of constructs for medium exchange. A translucent polysulfone lid secures the culture module to the MATE frame (Figure A.1C). The lid includes 10 mm diameter impermeable loading posts that are centered 5 mm over each culture well. To minimize the potential for contamination, all instrumentation was housed beneath the culture wells in an enclosed environment (Figure A.1C). The overall dimensions of the bioreactor were kept sufficiently small (15 x 16 x 22 cm) for housing in a standard CO₂ incubator.

A.3.2 Mechanical Stimulation of Hydrogels with Encapsulated MSCs

Preliminary, unpublished experiments were performed to evaluate the developmental role of mechanostimulation in neocartilage formation. Specifically we hypothesized that dynamic compressive loading would stimulate matrix formation and assembly during chondrogenesis. MSCs were photoencapsulated into PEGDA-based sIPN scaffolds and cultured in the MATE bioreactor either with or without daily stimulation for 6 weeks. The mechanostimulation protocol was 30 minutes of 0.4 N applied force (corresponding to approximating 15 – 20 % compression) at 1 Hz, followed by 1 hour of rest: repeated 4 times daily. Under these conditions we found that daily loading inhibited matrix production by the MSCs (Figures A.2 & A.3).

It was not clear which factors lead to inhibition of chondrogenesis in these scaffolds but an increased number of dead cells were detected with live-dead staining after 2 weeks of loading as compared with unloaded samples (data not shown). Consequently, I hypothesized that

increasing the initial strength of the scaffold could provide increased protection to the encapsulated MSCs. By increasing the molecular weight of the crosslinking PEGDA component in the sIPN scaffold from 16 % (w/v) to 32 % (w/v) the cell-free modulus of the scaffold was approximately doubled (data not shown). However, this increased scaffold modulus inhibited matrix production from MSCs even in the absence of load (Figure A.2). Matrix production was also not improved, but rather worse in these higher modulus scaffolds under stimulation.

The next experiment was designed to test whether delayed loading of the MSC-encapsulated constructs would stimulate matrix production. This experiment tested the hypothesis that the loading protocol was too extensive for MSCs but could benefit the MSC-differentiated chondrocytes during matrix elaboration and assembly. Constructs that were loaded for 3 weeks, during chondrogenesis, produced no proteoglycan matrix (Figure A.3B). If MSCs were allowed to undergo chondrogenesis in free-swelling conditions for 3 weeks, then stimulated for the last three weeks proteoglycan deposition was observed (Figure A.3C), but not at the intensity of unloaded controls (Figure A.3D).

Further testing of different chondrogenic conditions under load was significantly limited by system-related problems in the MATE unit. Principally we could not reliably lower the force input to generate dynamic compressive strains under approximate 15 %, which was added to a 10 % preload strain. These high strains may have contributed to the inhibition of chondrogenesis. Furthermore there were a number of design flaws that lead to unrepeatable stimulation and inconsistencies between test platens. Testing in our lab identified voltage drops across the output cables and an inability of the actuators to perform to specification at the temperature and/or humidity of standard tissue culture incubators as significant sources of error. These findings prompted an extensive re-design of the MATE bioreactor (2008-2010).

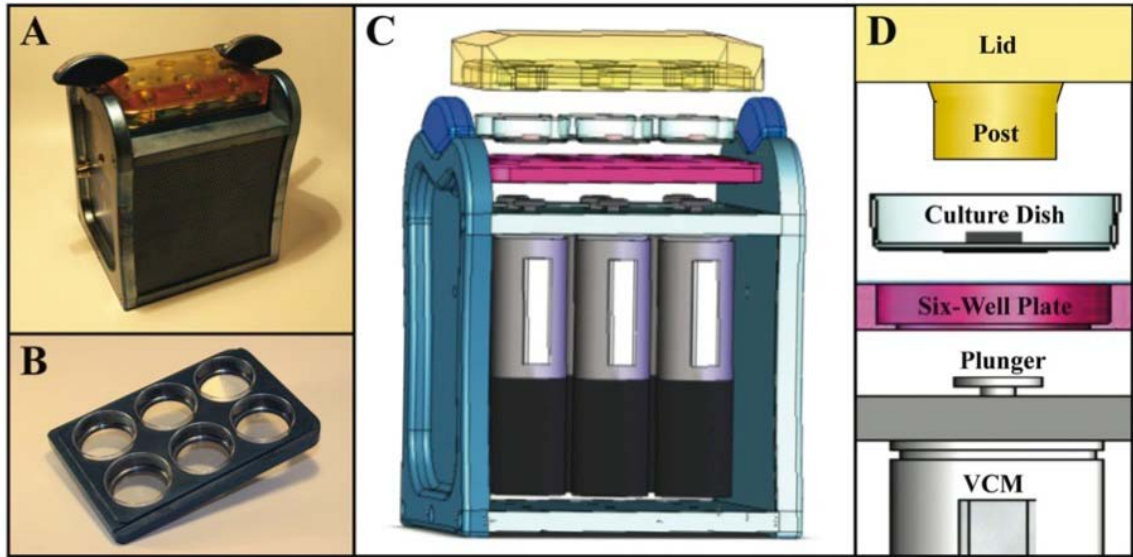


FIGURE A.1 - THE MATE BIOREACTOR DESIGN. (A) The MATE is compact and readily fits into standard incubators. All machined surfaces consist of non-corrosive anodized aluminum. (B) Specimens are loaded onto culture dishes that sit on a six-well plate. (C) The lid fastens the six-well plate onto the MATE frame. Electromagnetic voice coil motors are dedicated to each chamber and are housed beneath the specimens. (D) The voice coil motors (VCM) raise the plungers and culture dishes, thereby compressing specimens with impermeable posts.

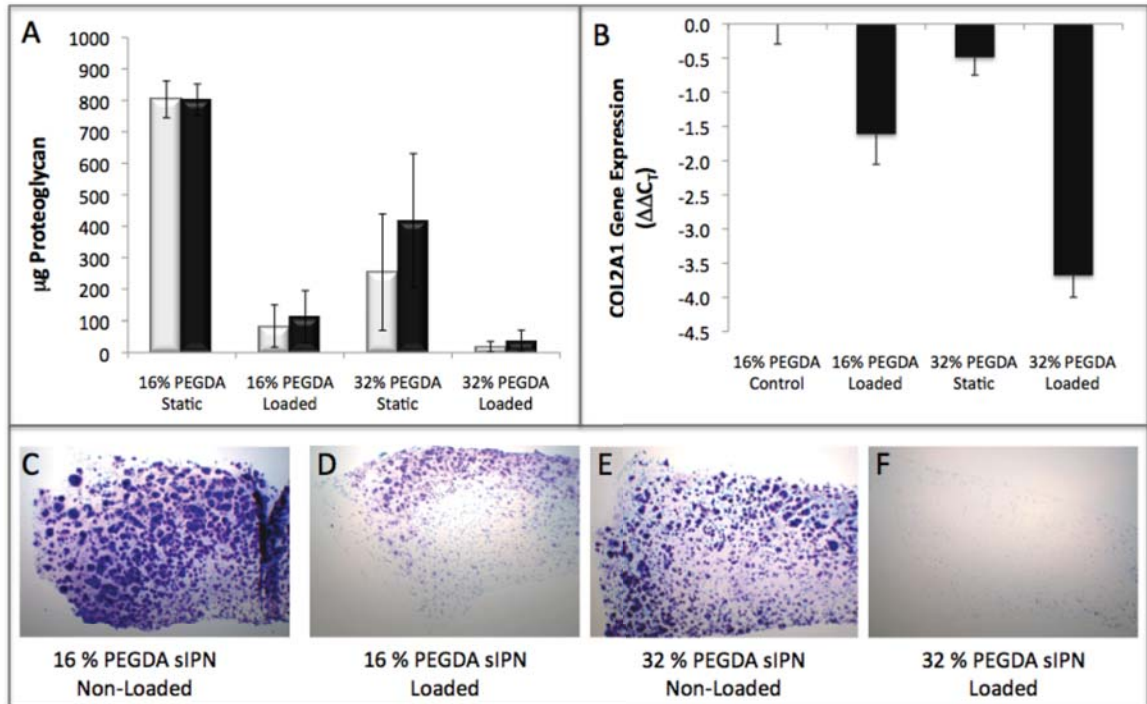


FIGURE A.2 – IMPACT OF DYNAMIC COMPRESSION ON MSC CHONDROGENESIS IN HYDROGEL SCAFFOLDS OF DIFFERENT MODULUS. (A) Proteoglycan deposition per construct (white) or normalized to DNA content (black). (B) Relative COL2A gene expression after 6 weeks of *in vitro* culture. Toluidine blue staining for proteoglycan deposition in 16 % PEGDA (C) non-loaded sIPN control and (D) loaded sIPN constructs, (E) non-loaded and (F) loaded sIPN constructs with 32 % PEGDA that corresponded to twice the initial compressive modulus of the 16 % controls.

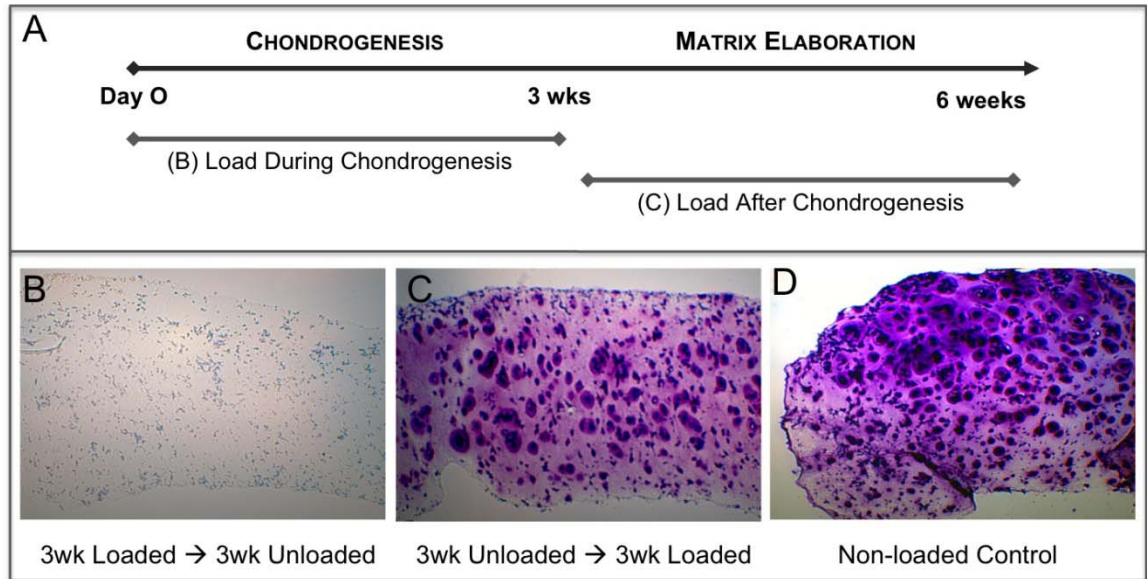


FIGURE A.3 – TEMPORAL EFFECT OF DYNAMIC LOADING. (A) Schematic diagram of loading durations. Toluidine blue staining for constructs (A) loaded during chondrogenesis, (B) loading after chondrogenesis, or (C) not loaded.

A.3.1 MATE Verification & Validation Testing

In the newly designed MATE unit average forces delivered strongly correlated with the target forces prescribed by the user during static and dynamic loading (data not shown). For static loading, there was small variability between the six MATE chambers when 0.1 N was prescribed (0.10 ± 0.01 N, error = 0 ± 10 %) and when 10 N was prescribed (10.01 ± 0.04 N, error = 0.1 ± 0.4 %). When loaded dynamically, the variability between the six MATE chambers increased when delivering a 0.1 N prescribed force (0.09 ± 0.02 N, error = 9 ± 18 %). However, each MATE chamber exhibited good accuracy under dynamic amplitudes of 0.2 N (0.20 ± 0.02 N, error = 0 ± 8 %) or greater. On average, the force output at 10 Hz was 2.1 % greater than the force output at 1 Hz ($p < 0.001$).

The material properties acquired from the MATE's force-displacement data were not significantly different than the material properties acquired by the Instron (Figure A.4). On average, the equilibrium and dynamic modulus determined from the MATE's six chambers were within 5 % of Instron results for soft hydrogels ($p=0.3$, $p=0.4$, respectively; Figure A.4A), and within 8 % for mature bovine articular cartilage ($p=0.2$, $p=0.3$, respectively; Figure A.4B). There was no difference in intra-specimen standard deviation between the test systems ($p=0.15$). The material testing protocols applied maximum strains under 20 % for all tested specimens,^{241,353} and no time dependence existed in the repeated testing of hydrogel and cartilage specimens ($p=0.42$, $p=0.13$, respectively).

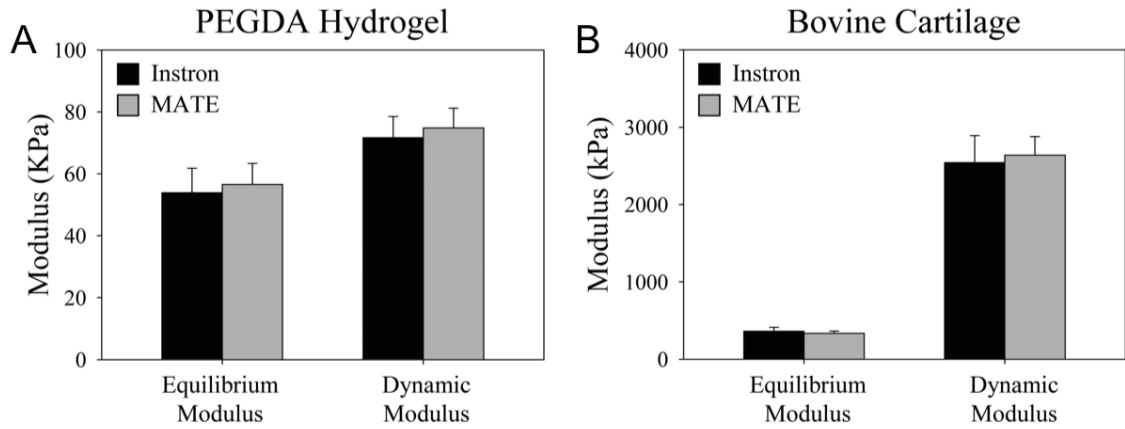


FIGURE A.4 - MATERIAL TEST RESULTS OF THE MATE AND INSTRON. (A) For PEGDA hydrogels (n=6), there was no difference between the systems in determining equilibrium modulus (p=0.3) and dynamic modulus (p=0.4). (B) For bovine patellar cartilage (n=6), there was no difference between the systems in determining equilibrium modulus (p=0.2) and dynamic modulus (p=0.3). Graph represents mean data \pm standard deviation.

A.3.3 Detecting Scaffold Degradation with MATE

The MATE system was able to detect minor changes in the material properties of degradable (collagenase sensitive LGPA-PEGDA) and non-degradable (10 % PEGDA) hydrogels over a 10 day time period (Figure A.5). Material characteristics of degradable hydrogels were altered during incubation with 0.005 % collagenase (41 % change in thickness, $p < 0.001$; 42 % change in equilibrium modulus, $p = 0.02$; 20 % change in dynamic modulus, $p = 0.005$), but were unaltered in the non-degradable group (1 % change in thickness, $p = 0.19$; 3 % change in equilibrium modulus, $p = 0.47$; 1 % change in dynamic modulus, $p = 0.27$). In the degradable group, a 24 hour reduction in thickness (15 %, $p < 0.001$) and equilibrium modulus (12%, $p = 0.03$) were evident. In the non-degradable group, any overall changes to thickness, equilibrium modulus, and dynamic modulus were less than 16 %, 16 %, and 19 %, respectively (95 % confidence interval). Maximum strains during mechanical testing were 17 ± 5 %.

A.4 DISCUSSION

Mechanostimulation plays an important role in the cavitation of synovial joints^{48-51,53} and the development of mature articular cartilage with an anisotropic assembly of extracellular matrix proteins that can resist the stresses associated with skeletal motion^{6,72}. Our lab at OHSU worked with the Legacy Biomechanics Laboratory to design the mechano-active transduction and evaluation (MATE) bioreactor described here. The unit was first built and minimally validated by Legacy before we received the unit for *in vitro* cell-based experiments in February 2007. We wanted to test the hypothesis that mechanostimulation of neocartilage constructs would improve extracellular matrix elaboration and assembly.

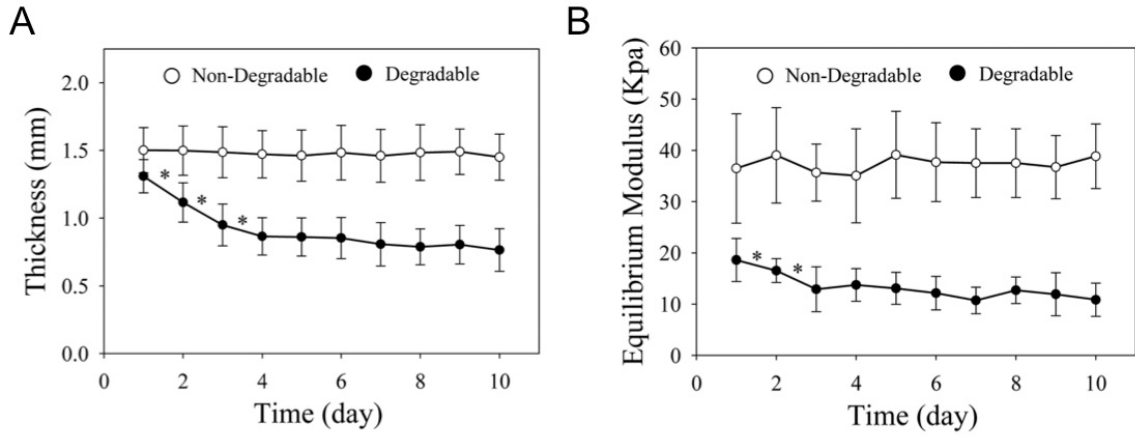


FIGURE A.5 - TIME DEPENDENT MATERIAL BEHAVIOR OF HYDROGELS DURING COLLAGENASE DIGESTION. (A) The thickness of the degradable group was reduced by 41 % during incubation ($p < 0.001$), while the non-degradable group was unaltered ($p = 0.2$). (B) The equilibrium modulus of the degradable group was reduced by 42 % during incubation ($p < 0.001$), while the non-degradable group was unaltered ($p = 0.5$). Most alterations in the degradable group occurred in the first two days of collagenase digestion. Graph represents mean data \pm standard deviation. * $p < 0.05$

In preliminary experiments we found inhibition of chondrogenesis with the application of load. This may have been because the loading regimen was too intense for the MSCs encapsulated within the hydrogel constructs. However, increasing the initial compressive modulus of the hydrogel by doubling the crosslinking PEGDA component in the sIPN scaffold produced further inhibition of proteoglycan deposition either with or without loading. This was presumably due to restriction of matrix elaboration by the small pore size of the scaffold.^{173,175,249}

Alternatively, it is possible that the application of compressive modulus was not at the appropriate time or level. Perhaps counterintuitive with the other data showing the requisite role of movement during cavitation, loading during joint specification has been shown to downregulate collagen II gene expression in the interzone region of the developing mouse limb⁵³. We looked at delaying the application of dynamic compression until 3 weeks after beginning static culture, during which time MSCs have significantly upregulated collagen II and aggrecan gene expression and begun to deposit extracellular matrix (Figure 4.1). Although we observed considerably more proteoglycan deposition in these constructs, it is less than the non-loaded control. It is not clear whether loading lead to a subsequent inhibition of matrix production or if it caused the already synthesized matrix to be degraded.

As mentioned above further cell-based experiments were suspended to address electromechanical problems in the MATE unit that prompted a complete system re-design. The function of the re-designed MATE was validated in a manuscript submitted to Tissue Engineering Part C, June 2010. Part of the validation testing including calibrating the system for the soft properties of hydrogels. This testing specifically highlights the mechanical disparity between a 10 % PEGDA scaffold (cell-free) and bovine articular cartilage: the starting modulus of a hydrogel scaffold is approximately 30-fold weaker than native tissue. One advantage of the newly built MATE unit was an increased sensitivity that was able to detect changes in modulus and thickness of scaffolds that could be used to identify biodegradation of scaffolds during *in vitro* culture.

REFERENCES

- 1 Murphy, L. *et al.* Lifetime risk of symptomatic knee osteoarthritis. *Arthritis Rheum* **59**, 1207-1213(2008).
- 2 Buckwalter, J. A. Articular Cartilage Injuries. *Clinical Orthopaedics and Related Research* **402**, 21-37 (2002).
- 3 Jackson, D. W., Lalor, P. A., Aberman, H. M. & Simon, T. M. Spontaneous repair of full-thickness defects of articular cartilage in a goat model. A preliminary study. *J Bone Joint Surg Am* **83-A**, 53-64 (2001).
- 4 Vrahas, M. S., Mithoefer, K. & Joseph, D. The long-term effects of articular impaction. *Clin Orthop Relat Res*, 40-43 (2004).
- 5 Goldring, M. B. & Marcu, K. B. Cartilage homeostasis in health and rheumatic diseases. *Arthritis Res Ther* **11**, 224 (2009).
- 6 Carter, D. R. *et al.* The mechanobiology of articular cartilage development and degeneration. *Clin Orthop Relat Res*, S69-77 (2004).
- 7 Burrage, P. S., Mix, K. S. & Brinckerhoff, C. E. Matrix metalloproteinases: role in arthritis. *Front Biosci* **11**, 529-543 (2006).
- 8 Cawston, T. E. & Wilson, A. J. Understanding the role of tissue degrading enzymes and their inhibitors in development and disease. *Best Pract Res Clin Rheumatol* **20**, 983-1002 (2006).
- 9 Vinatier, C., Mrugala, D., Jorgensen, C., Guicheux, J. & Noel, D. Cartilage engineering: a crucial combination of cells, biomaterials and biofactors. *Trends Biotechnol* **27**, 307-314 (2009).
- 10 Iwamoto, M., Shimazu, A. & Pacifici, M. Regulation of chondrocyte maturation by fibroblast growth factor-2 and parathyroid hormone. *J Orthop Res* **13**, 838-845 (1995).
- 11 O'Keefe, R. J. *et al.* Differential regulation of type-II and type-X collagen synthesis by parathyroid hormone-related protein in chick growth-plate chondrocytes. *J Orthop Res* **15**, (1997).
- 12 Khan, I. M. *et al.* The development of synovial joints. *Curr Top Dev Biol* **79**, 1-36 (2007).
- 13 Koyama, E. *et al.* A distinct cohort of progenitor cells participates in synovial joint and articular cartilage formation during mouse limb skeletogenesis. *Dev Biol* **316**, 62-73 (2008).
- 14 Ito, M. M. & Kida, M. Y. Morphological and biochemical re-evaluation of the process of cavitation in the rat knee joint: cellular and cell strata alterations in the interzone. *J Anat* **197 Pt 4**, 659-679 (2000).
- 15 Pacifici, M., Koyama, E. & Iwamoto, M. Mechanisms of synovial joint and articular cartilage formation: recent advances, but many lingering mysteries. *Birth Defects Res C Embryo Today* (2005).

- 16 Mitrovic, D. R. Development of the metatarsophalangeal joint of the chick embryo: morphological, ultrastructural and histochemical studies. *Am J Anat* **150**, 333-347, (1977).
- 17 Pacifici, M. *et al.* Cellular and molecular mechanisms of synovial joint and articular cartilage formation. *Ann N Y Acad Sci* **1068** (2006).
- 18 Holder, N. An experimental investigation into the early development of the chick elbow joint. *J Embryol Exp Morphol* **39**, 115-127 (1977).
- 19 Kronenberg, H. M. Developmental regulation of the growth plate. *Nature* **423**, 332-336 (2003).
- 20 Storm, E. E. & Kingsley, D. M. GDF5 coordinates bone and joint formation during digit development. *Dev Biol* **209**, 11-27 (1999).
- 21 Francis-West, P. H. *et al.* Mechanisms of GDF-5 action during skeletal development. *Development* **126**, 1305-1315 (1999).
- 22 Hartmann, C. & Tabin, C. J. Wnt-14 plays a pivotal role in inducing synovial joint formation in the developing appendicular skeleton. *Cell* **104**, 341-351 (2001).
- 23 Archer, C. W., Morrison, H. & Pitsillides, A. A. Cellular aspects of the development of diarthrodial joints and articular cartilage. *J Anat* **184 (Pt 3)**, 447-456 (1994).
- 24 Craig, F. M., Bayliss, M. T., Bentley, G. & Archer, C. W. A role for hyaluronan in joint development. *J Anat* **171**, 17-23 (1990).
- 25 Edwards, J. C. *et al.* The formation of human synovial joint cavities: a possible role for hyaluronan and CD44 in altered interzone cohesion. *J Anat* **185 (Pt 2)**, 355-367 (1994).
- 26 Kavanagh, E. *et al.* Differential regulation of GDF-5 and FGF-2/4 by immobilisation in ovo exposes distinct roles in joint formation. *Dev Dyn* **235**, 826-834 (2006).
- 27 Guo, X. *et al.* Wnt/beta-catenin signaling is sufficient and necessary for synovial joint formation. *Genes Dev* **18**, 2404-2417 (2004).
- 28 Francis-West, P. H., Parish, J., Lee, K. & Archer, C. W. BMP/GDF-signalling interactions during synovial joint development. *Cell Tissue Res* **296**, 111-119 (1999).
- 29 Brunet, L. J., McMahon, J. A., McMahon, A. P. & Harland, R. M. Noggin, cartilage morphogenesis, and joint formation in the mammalian skeleton. *Science* **280**, 1455-1457 (1998).
- 30 Archer, C. W., Dowthwaite, G. P. & Francis-West, P. Development of synovial joints. *Birth Defects Res C Embryo Today* **69**, 144-155 (2003).
- 31 von der Mark, K., von der Mark, H. & Gay, S. Study of differential collagen synthesis during development of the chick embryo by immunofluorescence. II. Localization of type I and type II collagen during long bone development. *Dev Biol* **53**, 153-170 (1976).

- 32 Craig, F. M., Bentley, G. & Archer, C. W. The spatial and temporal pattern of collagens I and II and keratan sulphate in the developing chick metatarsophalangeal joint. *Development* **99**, 383-391 (1987).
- 33 Bland, Y. S. & Ashhurst, D. E. Development and ageing of the articular cartilage of the rabbit knee joint: distribution of the fibrillar collagens. *Anat Embryol (Berl)* **194**, 607-619 (1996).
- 34 Hyde, G., Dover, S., Aszodi, A., Wallis, G. A. & Boot-Handford, R. P. Lineage tracing using matrilin-1 gene expression reveals that articular chondrocytes exist as the joint interzone forms. *Dev Biol* **304**, 825-833 (2007).
- 35 Snow, H. E., Riccio, L. M., Mjaatvedt, C. H., Hoffman, S. & Capehart, A. A. Versican expression during skeletal/joint morphogenesis and patterning of muscle and nerve in the embryonic mouse limb. *Anat Rec A Discov Mol Cell Evol Biol* **282**, 95-105 (2005).
- 36 Zhang, Y. *et al.* Doublecortin is expressed in articular chondrocytes. *Biochem Biophys Res Commun* **363**, 694-700 (2007).
- 37 Kimura, S. & Shiota, K. Sequential changes of programmed cell death in developing fetal mouse limbs and its possible roles in limb morphogenesis. *J Morphol* **229**, 337-346 (1996).
- 38 Mori, C. *et al.* Programmed cell death in the interdigital tissue of the fetal mouse limb is apoptosis with DNA fragmentation. *Anat Rec* **242**, 103-110 (1995).
- 39 Kavanagh, E., Abiri, M., Bland, Y. S. & Ashhurst, D. E. Division and death of cells in developing synovial joints and long bones. *Cell Biol Int* **26**, 679-688 (2002).
- 40 Fernandez-Teran, M. A., Hinchliffe, J. R. & Ros, M. A. Birth and death of cells in limb development: a mapping study. *Dev Dyn* **235**, 2521-2537 (2006).
- 41 Dowthwaite, G. P., Edwards, J. C. & Pitsillides, A. A. An essential role for the interaction between hyaluronan and hyaluronan binding proteins during joint development. *J Histochem Cytochem* **46**, 641-651 (1998).
- 42 Pitsillides, A. A. & Ashhurst, D. E. A critical evaluation of specific aspects of joint development. *Dev Dyn* **237**, 2284-2294 (2008).
- 43 Lamb, K. J., Lewthwaite, J. C., Bastow, E. R. & Pitsillides, A. A. Defining boundaries during joint cavity formation: going out on a limb. *Int J Exp Pathol* **84** (2003).
- 44 Ward, A. C., Dowthwaite, G. P. & Pitsillides, A. A. Hyaluronan in joint cavitation. *Biochem Soc Trans* **27**, 128-135 (1999).
- 45 Dowthwaite, G. P. *et al.* A mechanism underlying the movement requirement for synovial joint cavitation. *Matrix Biol* **22**, 311-322 (2003).
- 46 Dowthwaite, G. P. *et al.* The effect of mechanical strain on hyaluronan metabolism in embryonic fibrocartilage cells. *Matrix Biol* **18**, 523-532 (1999).

- 47 Bastow, E. R. *et al.* Selective activation of the MEK-ERK pathway is regulated by mechanical stimuli in forming joints and promotes pericellular matrix formation. *J Biol Chem* **280**, 11749-11758 (2005).
- 48 Mikic, B., Isenstein, A. L. & Chhabra, A. Mechanical modulation of cartilage structure and function during embryogenesis in the chick. *Ann Biomed Eng* **32**, 18-25 (2004).
- 49 Mikic, B. *et al.* Differential effects of embryonic immobilization on the development of fibrocartilaginous skeletal elements. *J Rehabil Res Dev* **37**, 127-133 (2000).
- 50 Nowlan, N. C., Murphy, P. & Prendergast, P. J. Mechanobiology of embryonic limb development. *Ann N Y Acad Sci* **1101**, 389-411 (2007).
- 51 Osborne, A. C., Lamb, K. J., Lewthwaite, J. C., Dowthwaite, G. P. & Pitsillides, A. A. Short-term rigid and flaccid paralyses diminish growth of embryonic chick limbs and abrogate joint cavity formation but differentially preserve pre-cavitated joints. *J Musculoskelet Neuronal Interact* **2**, 448-456 (2002).
- 52 Lelkes, G. Experiments in vitro on the role of movement in the development of joints. *J Embryol Exp Morphol* **6**, 183-186 (1958).
- 53 Kahn, J. *et al.* Muscle contraction is necessary to maintain joint progenitor cell fate. *Dev Cell* **16**, 734-743 (2009).
- 54 Malemud, C. Matrix metalloproteinases: role in skeletal development and growth plate disorders. *Frontiers in Bioscience* **11**, 13 (2006).
- 55 Alvarez, J. *et al.* Different bone growth rates are associated with changes in the expression pattern of types II and X collagens and collagenase 3 in proximal growth plates of the rat tibia. *J Bone Miner Res* **15**, 82-94 (2000).
- 56 Inada, M. *et al.* Critical roles for collagenase-3 (Mmp13) in development of growth plate cartilage and in endochondral ossification. *Proc Natl Acad Sci U S A* **101**, 17192-17197 (2004).
- 57 Dangelo, M., Sarment, D. P., Billings, P. C. & Pacifici, M. Activation of transforming growth factor beta in chondrocytes undergoing endochondral ossification. *J Bone Miner Res* **16**, 2339-2347 (2001).
- 58 Pendas, A. M., Balbin, M., Llano, E., Jimenez, M. G. & Lopez-Otin, C. Structural analysis and promoter characterization of the human collagenase-3 gene (MMP13). *Genomics* **40**, 222-233 (1997).
- 59 Flannery, C. R. MMPs and ADAMTSs: functional studies. *Front Biosci* **11**, 544-569 (2006).
- 60 Porter, S., Clark, I. M., Kevorkian, L. & Edwards, D. R. The ADAMTS metalloproteinases. *Biochem J* **386**, 15-27 (2005).
- 61 Struglics, A. *et al.* Human osteoarthritis synovial fluid and joint cartilage contain both aggrecanase- and matrix metalloproteinase-generated aggrecan fragments. *Osteoarthritis Cartilage* **14**, 101-113 (2006).

- 62 Tortorella, M. D., Malfait, A. M., Deccico, C. & Arner, E. The role of ADAM-TS4 (aggrecanase-1) and ADAM-TS5 (aggrecanase-2) in a model of cartilage degradation. *Osteoarthritis Cartilage* **9**, 539-552 (2001).
- 63 Plaas, A. *et al.* Aggrecanolysis in human osteoarthritis: confocal localization and biochemical characterization of ADAMTS5-hyaluronan complexes in articular cartilages. *Osteoarthritis Cartilage* **15**, 719-734 (2007).
- 64 Glasson, S. S. *et al.* Deletion of active ADAMTS5 prevents cartilage degradation in a murine model of osteoarthritis. *Nature* **434**, 644-648 (2005).
- 65 Pratta, M. A. *et al.* Aggrecan protects cartilage collagen from proteolytic cleavage. *J Biol Chem* **278**, 45539-45545 (2003).
- 66 Zhu, Y., Oganessian, A., Keene, D. R. & Sandell, L. J. Type IIA procollagen containing the cysteine-rich amino propeptide is deposited in the extracellular matrix of prechondrogenic tissue and binds to TGF-beta1 and BMP-2. *J Cell Biol* **144**, 1069-1080 (1999).
- 67 Baker, A. H., Edwards, D. R. & Murphy, G. Metalloproteinase inhibitors: biological actions and therapeutic opportunities. *J Cell Sci* **115**, 3719-3727 (2002).
- 68 Anderson, D., Adams, D. & Hale, J. in *Human Kinetics* eds BM Nigg, BR MacIntosh, & J Mester) 283-305 (2000).
- 69 Poole, C. A. Articular cartilage chondrons: form, function and failure. *J Anat* **191 (Pt 1)**, 1-13 (1997).
- 70 Wiberg, C. *et al.* Complexes of matrilin-1 and biglycan or decorin connect collagen VI microfibrils to both collagen II and aggrecan. *J Biol Chem* **278**, 37698-37704 (2003).
- 71 Halasz, K., Kassner, A., Morgelin, M. & Heinegard, D. COMP acts as a catalyst in collagen fibrillogenesis. *J Biol Chem* **282**, 31166-31173 (2007).
- 72 Wong, M. & Carter, D. R. Articular cartilage functional histomorphology and mechanobiology: a research perspective. *Bone* **33**, 1-13 (2003).
- 73 Almaraz, A. J. & Athanasiou, K. A. Design characteristics for the tissue engineering of cartilaginous tissues. *Ann Biomed Eng* **32**, 2-17 (2004).
- 74 Kempson, G. E., Muir, H., Pollard, C. & Tuke, M. The tensile properties of the cartilage of human femoral condyles related to the content of collagen and glycosaminoglycans. *Biochim Biophys Acta* **297**, 456-472 (1973).
- 75 Huang, C. Y., Stankiewicz, A., Ateshian, G. A. & Mow, V. C. Anisotropy, inhomogeneity, and tension-compression nonlinearity of human glenohumeral cartilage in finite deformation. *J Biomech* **38**, 799-809 (2005).
- 76 Setton, L. A., Elliott, D. M. & Mow, V. C. Altered mechanics of cartilage with osteoarthritis: human osteoarthritis and an experimental model of joint degeneration. *Osteoarthritis Cartilage* **7**, 2-14 (1999).

- 77 Fung, Y. *Biomechanics. Mechanical Properties of Living Tissues* Vol. Second Edition (Springer, 2004).
- 78 Garcia, J. J. & Cortes, D. H. A nonlinear biphasic viscohyperelastic model for articular cartilage. *J Biomech* **39**, 2991-2998 (2006).
- 79 Mow, V. C., Kuei, S. C., Lai, W. M. & Armstrong, C. G. Biphasic creep and stress relaxation of articular cartilage in compression? Theory and experiments. *J Biomech Eng* **102**, 73-84 (1980).
- 80 Taylor, Z. A. & Miller, K. Constitutive modeling of cartilaginous tissues: a review. *J Appl Biomech* **22**, 212-229 (2006).
- 81 Waterton, J. C. *et al.* Diurnal variation in the femoral articular cartilage of the knee in young adult humans. *Magn Reson Med* **43**, 126-132 (2000).
- 82 Hou, J. S., Mow, V. C., Lai, W. M. & Holmes, M. H. An analysis of the squeeze-film lubrication mechanism for articular cartilage. *J Biomech* **25**, 247-259 (1992).
- 83 Malcom, L. *Friction and deformation responses of articular cartilage interfaces to static and dynamic loading.*, University of California, (1976).
- 84 Hettrich, C. M., Crawford, D. & Rodeo, S. A. Cartilage repair: third-generation cell-based technologies--basic science, surgical techniques, clinical outcomes. *Sports Med Arthrosc* **16**, 230-235 (2008).
- 85 Kon, E., Delcogliano, M., Filardo, G., Montaperto, C. & Marcacci, M. Second generation issues in cartilage repair. *Sports Med Arthrosc* **16**, 221-229 (2008).
- 86 McNickle, A. G., Provencher, M. T. & Cole, B. J. Overview of existing cartilage repair technology. *Sports Med Arthrosc* **16**, 196-201, doi:10.1097/JSA.0b013e31818cdb8200132585-200812000-00002 [pii] (2008).
- 87 Grande, D. A., Pitman, M. I., Peterson, L., Menche, D. & Klein, M. The repair of experimentally produced defects in rabbit articular cartilage by autologous chondrocyte transplantation. *J Orthop Res* **7**, 208-218 (1989).
- 88 Brittberg, M. *et al.* Treatment of deep cartilage defects in the knee with autologous chondrocyte transplantation. *N Engl J Med* **331**, 889-895 (1994).
- 89 Bentley, G. *et al.* A prospective, randomised comparison of autologous chondrocyte implantation versus mosaicplasty for osteochondral defects in the knee. *J Bone Joint Surg Br* **85**, 223-230 (2003).
- 90 Peterson, L. *et al.* Two- to 9-year outcome after autologous chondrocyte transplantation of the knee. *Clin Orthop Relat Res*, 212-234 (2000).
- 91 Niemeyer, P. *et al.* Characteristic complications after autologous chondrocyte implantation for cartilage defects of the knee joint. *Am J Sports Med* **36**, 2091-2099 (2008).

- 92 Luyten, F. P., Dell'Accio, F. & De Bari, C. Skeletal tissue engineering: opportunities and challenges. *Best Pract Res Clin Rheumatol* **15**, 759-769 (2001).
- 93 Lee, C. R., Grodzinsky, A. J., Hsu, H. P., Martin, S. D. & Spector, M. Effects of harvest and selected cartilage repair procedures on the physical and biochemical properties of articular cartilage in the canine knee. *J Orthop Res* **18**, 790-799 (2000).
- 94 Peltari, K., Steck, E. & Richter, W. The use of mesenchymal stem cells for chondrogenesis. *Injury* **39 Suppl 1**, S58-65 (2008).
- 95 Roberts, S. *et al.* Autologous chondrocyte implantation for cartilage repair: monitoring its success by magnetic resonance imaging and histology. *Arthritis Res Ther* **5**, R60-73 (2003).
- 96 Tins, B. J. *et al.* Autologous chondrocyte implantation in knee joint: MR imaging and histologic features at 1-year follow-up. *Radiology* **234**, 501-508 (2005).
- 97 Roberts, S., Menage, J., Sandell, L. J., Evans, E. H. & Richardson, J. B. Immunohistochemical study of collagen types I and II and procollagen IIA in human cartilage repair tissue following autologous chondrocyte implantation. *Knee* **16**, 398-404 (2009).
- 98 Wilson, C. G., Nishimuta, J. F. & Levenston, M. E. Chondrocytes and meniscal fibrochondrocytes differentially process aggrecan during de novo extracellular matrix assembly. *Tissue Eng Part A* **15**, 1513-1522 (2009).
- 99 Dell'Accio, F., De Bari, C. & Luyten, F. P. Molecular markers predictive of the capacity of expanded human articular chondrocytes to form stable cartilage in vivo. *Arthritis Rheum* **44**, 1608-1619 (2001).
- 100 Barlic, A., Drobic, M., Malicev, E. & Kregar-Velikonja, N. Quantitative analysis of gene expression in human articular chondrocytes assigned for autologous implantation. *J Orthop Res* **26**, 847-853 (2008).
- 101 Darling, E. M. & Athanasiou, K. A. Rapid phenotypic changes in passaged articular chondrocyte subpopulations. *J Orthop Res* **23**, 425-432 (2005).
- 102 von der Mark, K., Gauss, V., von der Mark, H. & Muller, P. Relationship between cell shape and type of collagen synthesised as chondrocytes lose their cartilage phenotype in culture. *Nature* **267**, 531-532 (1977).
- 103 Kessler, M. W., Ackerman, G., Dines, J. S. & Grande, D. Emerging technologies and fourth generation issues in cartilage repair. *Sports Med Arthrosc* **16**, 246-254 (2008).
- 104 Caplan, A. I. Review: mesenchymal stem cells: cell-based reconstructive therapy in orthopedics. *Tissue Eng* **11**, 1198-1211 (2005).
- 105 Johnstone, B. & Yoo, J. Mesenchymal cell transfer for articular cartilage repair. *Expert Opin Biol Ther* **1**, 915-921 (2001).
- 106 Johnstone, B., Yoo, J. & Stewart, M. *Cell Sources for Cartilage Tissue Engineering*. 83 - 111 (Wiley, 2006).

- 107 Hwang, N. S. & Elisseeff, J. Application of stem cells for articular cartilage regeneration. *J Knee Surg* **22**, 60-71 (2009).
- 108 Johnstone, B., Hering, T. M., Caplan, A. I., Goldberg, V. M. & Yoo, J. U. In vitro chondrogenesis of bone marrow-derived mesenchymal progenitor cells. *Exp Cell Res* **238**, 265-272 (1998).
- 109 Yoo, J. U. *et al.* The chondrogenic potential of human bone-marrow-derived mesenchymal progenitor cells. *J Bone Joint Surg Am* **80**, 1745-1757 (1998).
- 110 Zuk, P. A. *et al.* Human adipose tissue is a source of multipotent stem cells. *Mol Biol Cell* **13**, 4279-4295 (2002).
- 111 De Bari, C. *et al.* Mesenchymal multipotency of adult human periosteal cells demonstrated by single-cell lineage analysis. *Arthritis Rheum* **54**, 1209-1221 (2006).
- 112 Miura, Y., Fitzsimmons, J. S., Commisso, C. N., Gallay, S. H. & O'Driscoll, S. W. Enhancement of periosteal chondrogenesis in vitro. Dose-response for transforming growth factor-beta 1 (TGF-beta 1). *Clin Orthop Relat Res*, 271-280 (1994).
- 113 De Bari, C., Dell'Accio, F., Tylzanowski, P. & Luyten, F. P. Multipotent mesenchymal stem cells from adult human synovial membrane. *Arthritis Rheum* **44**, 1928-1942 (2001).
- 114 Sakaguchi, Y., Sekiya, I., Yagishita, K. & Muneta, T. Comparison of human stem cells derived from various mesenchymal tissues: superiority of synovium as a cell source. *Arthritis Rheum* **52**, 2521-2529 (2005).
- 115 Dominici, M. *et al.* Minimal criteria for defining multipotent mesenchymal stromal cells. The International Society for Cellular Therapy position statement. *Cytotherapy* **8**, 315-317 (2006).
- 116 Pittenger, M. F. *et al.* Multilineage potential of adult human mesenchymal stem cells. *Science* **284**, 143-147 (1999).
- 117 Young, R. G. *et al.* Use of mesenchymal stem cells in a collagen matrix for Achilles tendon repair. *J Orthop Res* **16**, 406-413 (1998).
- 118 Dezawa, M. *et al.* Bone marrow stromal cells generate muscle cells and repair muscle degeneration. *Science* **309**, 314-317 (2005).
- 119 Orlic, D. *et al.* Bone marrow cells regenerate infarcted myocardium. *Nature* **410**, 701-705 (2001).
- 120 Woodbury, D., Schwarz, E. J., Prockop, D. J. & Black, I. B. Adult rat and human bone marrow stromal cells differentiate into neurons. *J Neurosci Res* **61**, 364-370 (2000).
- 121 Majumdar, M. K., Thiede, M. A., Mosca, J. D., Moorman, M. & Gerson, S. L. Phenotypic and functional comparison of cultures of marrow-derived mesenchymal stem cells (MSCs) and stromal cells. *J Cell Physiol* **176**, 57-66 (1998).
- 122 Caplan, A. I. & Dennis, J. E. Mesenchymal stem cells as trophic mediators. *J Cell Biochem* **98**, 1076-1084 (2006).

- 123 Grassel, S. & Ahmed, N. Influence of cellular microenvironment and paracrine signals on chondrogenic differentiation. *Front Biosci* **12**, 4946-4956 (2007).
- 124 Laflamme, M. A. & Murry, C. E. Regenerating the heart. *Nat Biotechnol* **23**, 845-856 (2005).
- 125 Bianco, P., Riminucci, M., Gronthos, S. & Robey, P. G. Bone marrow stromal stem cells: nature, biology, and potential applications. *Stem Cells* **19**, 180-192 (2001).
- 126 Morrison, S. J., Shah, N. M. & Anderson, D. J. Regulatory mechanisms in stem cell biology. *Cell* **88**, 287-298 (1997).
- 127 Watt, F. M. & Hogan, B. L. Out of Eden: stem cells and their niches. *Science* **287**, 1427-1430 (2000).
- 128 Haynesworth, S., Goldberg, V. & Caplan, A. in *Musculoskeletal Soft-tissue Aging: Impact on Mobility* eds JA Buckwalter, VM Goldber, & SL-Y Woo) 79-87 (American Academy of Orthopaedic Surgeons, 1994).
- 129 Caplan, A. I. Mesenchymal stem cells. *J Orthop Res* **9**, 641-650 (1991).
- 130 Caplan, A. I. The mesengenic process. *Clin Plast Surg* **21**, 429-435 (1994).
- 131 Bianco, P., Robey, P. G. & Simmons, P. J. Mesenchymal stem cells: revisiting history, concepts, and assays. *Cell Stem Cell* **2**, 313-319 (2008).
- 132 Williams, C. G. *et al.* In vitro chondrogenesis of bone marrow-derived mesenchymal stem cells in a photopolymerizing hydrogel. *Tissue Eng* **9**, 679-688 (2003).
- 133 Archer, C. W., Rooney, P. & Wolpert, L. Cell shape and cartilage differentiation of early chick limb bud cells in culture. *Cell Differ* **11**, 245-251 (1982).
- 134 Solursh, M., Linsenmayer, T. F. & Jensen, K. L. Chondrogenesis from single limb mesenchyme cells. *Dev Biol* **94**, 259-264 (1982).
- 135 Solursh, M. & Reiter, R. S. Determination of limb bud chondrocytes during a transient block of the cell cycle. *Cell Differ* **4**, 131-137 (1975).
- 136 Le Blanc, K., Tammik, C., Rosendahl, K., Zetterberg, E. & Ringden, O. HLA expression and immunologic properties of differentiated and undifferentiated mesenchymal stem cells. *Exp Hematol* **31**, 890-896 (2003).
- 137 Bartholomew, A. *et al.* Mesenchymal stem cells suppress lymphocyte proliferation in vitro and prolong skin graft survival in vivo. *Exp Hematol* **30**, 42-48 (2002).
- 138 Sato, K. *et al.* Nitric oxide plays a critical role in suppression of T-cell proliferation by mesenchymal stem cells. *Blood* **109**, 228-234 (2007).
- 139 Aggarwal, S. & Pittenger, M. F. Human mesenchymal stem cells modulate allogeneic immune cell responses. *Blood* **105**, 1815-1822 (2005).

- 140 Tse, W. T., Pendleton, J. D., Beyer, W. M., Egalka, M. C. & Guinan, E. C. Suppression of allogeneic T-cell proliferation by human marrow stromal cells: implications in transplantation. *Transplantation* **75**, 389-397 (2003).
- 141 Krampera, M. *et al.* Bone marrow mesenchymal stem cells inhibit the response of naive and memory antigen-specific T cells to their cognate peptide. *Blood* **101**, 3722-3729 (2003).
- 142 Beyth, S. *et al.* Human mesenchymal stem cells alter antigen-presenting cell maturation and induce T-cell unresponsiveness. *Blood* **105**, 2214-2219, doi:2004-07-2921 [pii] 10.1182/blood-2004-07-2921 (2005).
- 143 Glennie, S., Soeiro, I., Dyson, P. J., Lam, E. W. & Dazzi, F. Bone marrow mesenchymal stem cells induce division arrest anergy of activated T cells. *Blood* **105**, 2821-2827 (2005).
- 144 Ramasamy, R. *et al.* Mesenchymal stem cells inhibit dendritic cell differentiation and function by preventing entry into the cell cycle. *Transplantation* **83**, 71-76 (2007).
- 145 Di Nicola, M. *et al.* Human bone marrow stromal cells suppress T-lymphocyte proliferation induced by cellular or nonspecific mitogenic stimuli. *Blood* **99**, 3838-3843 (2002).
- 146 Haynesworth, S. E., Goshima, J., Goldberg, V. M. & Caplan, A. I. Characterization of cells with osteogenic potential from human marrow. *Bone* **13**, 81-88 (1992).
- 147 Haynesworth, S. E., Baber, M. A. & Caplan, A. I. Cytokine expression by human marrow-derived mesenchymal progenitor cells in vitro: effects of dexamethasone and IL-1 alpha. *J Cell Physiol* **166**, 585-592 (1996).
- 148 Li, Y. *et al.* Gliosis and brain remodeling after treatment of stroke in rats with marrow stromal cells. *Glia* **49**, 407-417 (2005).
- 149 Chen, J. *et al.* Intravenous bone marrow stromal cell therapy reduces apoptosis and promotes endogenous cell proliferation after stroke in female rat. *J Neurosci Res* **73**, 778-786 (2003).
- 150 Caplan, A. I. Why are MSCs therapeutic? New data: new insight. *J Pathol* **217**, 318-324 (2009).
- 151 Bianco, P., Gehron Robey, P., Saggio, I. & Riminucci, M. "Mesenchymal" stem cells in human bone marrow (skeletal stem cells) - a critical discussion of their nature, identity, and significance in incurable skeletal disease. *Hum Gene Ther*, doi:10.1089/hum.2010.136 (2010).
- 152 Prockop, D. J. "Stemness" does not explain the repair of many tissues by mesenchymal stem/multipotent stromal cells (MSCs). *Clin Pharmacol Ther* **82**, 241-243 (2007).
- 153 Prockop, D. J. Repair of tissues by adult stem/progenitor cells (MSCs): controversies, myths, and changing paradigms. *Mol Ther* **17**, 939-946 (2009).
- 154 Hwang, N. S., Varghese, S., Zhang, Z. & Elisseeff, J. Chondrogenic differentiation of human embryonic stem cell-derived cells in arginine-glycine-aspartate-modified hydrogels. *Tissue Eng* **12**, 2695-2706 (2006).

- 155 Koay, E. J., Hoben, G. M. & Athanasiou, K. A. Tissue engineering with chondrogenically differentiated human embryonic stem cells. *Stem Cells* **25**, 2183-2190 (2007).
- 156 Kramer, J. *et al.* Embryonic stem cell-derived chondrogenic differentiation in vitro: activation by BMP-2 and BMP-4. *Mech Dev* **92**, 193-205 (2000).
- 157 Nakayama, N., Duryea, D., Manoukian, R., Chow, G. & Han, C. Y. Macroscopic cartilage formation with embryonic stem-cell-derived mesodermal progenitor cells. *J Cell Sci* **116**, 2015-2028 (2003).
- 158 Thomson, J. A. *et al.* Embryonic stem cell lines derived from human blastocysts. *Science* **282**, 1145-1147 (1998).
- 159 Wilmut, I., Schnieke, A. E., McWhir, J., Kind, A. J. & Campbell, K. H. Viable offspring derived from fetal and adult mammalian cells. *Nature* **385**, 810-813 (1997).
- 160 Byrne, J. A. *et al.* Producing primate embryonic stem cells by somatic cell nuclear transfer. *Nature* **450**, 497-502 (2007).
- 161 Takahashi, K. & Yamanaka, S. Induction of pluripotent stem cells from mouse embryonic and adult fibroblast cultures by defined factors. *Cell* **126**, 663-676 (2006).
- 162 Yamanaka, S. A fresh look at iPS cells. *Cell* **137**, 13-17 (2009).
- 163 Wakitani, S. *et al.* Embryonic stem cells form articular cartilage, not teratomas, in osteochondral defects of rat joints. *Cell Transplant* **13**, 331-336 (2004).
- 164 Wakitani, S. *et al.* Embryonic stem cells injected into the mouse knee joint form teratomas and subsequently destroy the joint. *Rheumatology (Oxford)* **42**, 162-165 (2003).
- 165 Nakajima, M., Wakitani, S., Harada, Y., Tanigami, A. & Tomita, N. In vivo mechanical condition plays an important role for appearance of cartilage tissue in ES cell transplanted joint. *J Orthop Res* **26**, 10-17 (2008).
- 166 Hwang, N. S., Varghese, S. & Elisseeff, J. Derivation of chondrogenically-committed cells from human embryonic cells for cartilage tissue regeneration. *PLoS ONE* **3**, e2498 (2008).
- 167 Lian, Q. *et al.* Derivation of clinically compliant MSCs from CD105+, CD24-differentiated human ESCs. *Stem Cells* **25**, 425-436 (2007).
- 168 Yamashita, A., Nishikawa, S. & Rancourt, D. E. Identification of five developmental processes during chondrogenic differentiation of embryonic stem cells. *PLoS One* **5**, e10998 (2010).
- 169 Huebsch, N. & Mooney, D. J. Inspiration and application in the evolution of biomaterials. *Nature* **462**, 426-432 (2009).
- 170 Lutolf, M. P., Gilbert, P. M. & Blau, H. M. Designing materials to direct stem-cell fate. *Nature* **462**, 433-441 (2009).

- 171 Chan, G. & Mooney, D. J. New materials for tissue engineering: towards greater control over the biological response. *Trends Biotechnol* **26**, 382-392 (2008).
- 172 Engler, A. J., Sen, S., Sweeney, H. L. & Discher, D. E. Matrix elasticity directs stem cell lineage specification. *Cell* **126**, 677-689 (2006).
- 173 Buxton, A. N. *et al.* Design and characterization of poly(ethylene glycol) photopolymerizable semi-interpenetrating networks for chondrogenesis of human mesenchymal stem cells. *Tissue Eng* **13**, 2549-2560 (2007).
- 174 Erickson, I. E. *et al.* Differential maturation and structure-function relationships in mesenchymal stem cell- and chondrocyte-seeded hydrogels. *Tissue Eng Part A* **15**, 1041-1052 (2009).
- 175 Erickson, I. E. *et al.* Macromer density influences mesenchymal stem cell chondrogenesis and maturation in photocrosslinked hyaluronic acid hydrogels. *Osteoarthritis Cartilage* **17**, 1639-1648 (2009).
- 176 Bryant, S. J., Durand, K. L. & Anseth, K. S. Manipulations in hydrogel chemistry control photoencapsulated chondrocyte behavior and their extracellular matrix production. *J Biomed Mater Res A* **67**, 1430-1436 (2003).
- 177 Bryant, S. J., Nicodemus, G. D. & Villanueva, I. Designing 3D photopolymer hydrogels to regulate biomechanical cues and tissue growth for cartilage tissue engineering. *Pharm Res* **25**, 2379-2386 (2008).
- 178 Kumar, A. & Gupta, R. *Fundamental of Polymers*. (McGraw-Hill, 1998).
- 179 Rizzi, S. C. *et al.* Recombinant protein-co-PEG networks as cell-adhesive and proteolytically degradable hydrogel matrixes. Part II: biofunctional characteristics. *Biomacromolecules* **7**, 3019-3029 (2006).
- 180 Rizzi, S. C. & Hubbell, J. A. Recombinant protein-co-PEG networks as cell-adhesive and proteolytically degradable hydrogel matrixes. Part I: Development and physicochemical characteristics. *Biomacromolecules* **6**, 1226-1238 (2005).
- 181 van de Wetering, P., Metters, A. T., Schoenmakers, R. G. & Hubbell, J. A. Poly(ethylene glycol) hydrogels formed by conjugate addition with controllable swelling, degradation, and release of pharmaceutically active proteins. *J Control Release* **102**, 619-627 (2005).
- 182 DeForest, C. A., Polizzotti, B. D. & Anseth, K. S. Sequential click reactions for synthesizing and patterning three-dimensional cell microenvironments. *Nat Mater* **8**, 659-664 (2009).
- 183 Fournier, E., Passirani, C., Montero-Menei, C. N. & Benoit, J. P. Biocompatibility of implantable synthetic polymeric drug carriers: focus on brain biocompatibility. *Biomaterials* **24**, 3311-3331 (2003).
- 184 Nguyen, K. T. & West, J. L. Photopolymerizable hydrogels for tissue engineering applications. *Biomaterials* **23**, 4307-4314 (2002).

- 185 Graham, N. B. Hydrogels: their future, Part II. *Med Device Technol* **9**, 22-25 (1998).
- 186 Graham, N. B. Hydrogels: their future, Part I. *Med Device Technol* **9**, 18-22 (1998).
- 187 Maffezzoli, A., Della Pietra, A., Rengo, S., Nicolais, L. & Valletta, G. Photopolymerization of dental composite matrices. *Biomaterials* **15**, 1221-1228 (1994).
- 188 Fleming, M. G. & Maillet, W. A. Photopolymerization of composite resin using the argon laser. *J Can Dent Assoc* **65**, 447-450 (1999).
- 189 Elisseeff, J. *et al.* Transdermal photopolymerization of poly(ethylene oxide)-based injectable hydrogels for tissue-engineered cartilage. *Plast Reconstr Surg* **104**, 1014-1022 (1999).
- 190 Elisseeff, J. *et al.* Transdermal photopolymerization for minimally invasive implantation. *Proc Natl Acad Sci U S A* **96**, 3104-3107 (1999).
- 191 Elisseeff, J. *et al.* Photoencapsulation of chondrocytes in poly(ethylene oxide)-based semi-interpenetrating networks. *J Biomed Mater Res* **51**, 164-171 (2000).
- 192 Nicodemus, G. D. & Bryant, S. Cell encapsulation in biodegradable hydrogels for tissue engineering applications. *Tissue engineering Part B, Reviews* **14**, 149-165 (2008).
- 193 Ifkovits, J. L. & Burdick, J. A. Review: photopolymerizable and degradable biomaterials for tissue engineering applications. *Tissue Eng* **13**, 2369-2385 (2007).
- 194 Martens, P. J., Bryant, S. J. & Anseth, K. S. Tailoring the degradation of hydrogels formed from multivinyl poly(ethylene glycol) and poly(vinyl alcohol) macromers for cartilage tissue engineering. *Biomacromolecules* **4**, 283-292 (2003).
- 195 Bryant, S. J. & Anseth, K. S. Controlling the spatial distribution of ECM components in degradable PEG hydrogels for tissue engineering cartilage. *J Biomed Mater Res A* **64**, 70-79 (2003).
- 196 West, J. & Hubbell, J. Polymeric biomaterials with degradation sites for protease involved in cell migration. *Macromolecules* **32**, 241-244 (1999).
- 197 Ulijn, R. V. *et al.* Bioresponsive Hydrogels. *Materials Today* **10**, 40-48 (2007).
- 198 Lutolf, M. P. *et al.* Synthetic matrix metalloproteinase-sensitive hydrogels for the conduction of tissue regeneration: engineering cell-invasion characteristics. *Proc Natl Acad Sci U S A* **100**, 5413-5418 (2003).
- 199 Park, Y., Lutolf, M. P., Hubbell, J. A., Hunziker, E. B. & Wong, M. Bovine primary chondrocyte culture in synthetic matrix metalloproteinase-sensitive poly(ethylene glycol)-based hydrogels as a scaffold for cartilage repair. *Tissue Eng* **10**, 515-522 (2004).
- 200 Rawlings, N., Morton, R., Kok, C., Kong, J. & Barrett, A. *MEROPS: the peptide database*, 2008).

- 201 Rice, M. A. & Anseth, K. S. Controlling cartilaginous matrix evolution in hydrogels with degradation triggered by exogenous addition of an enzyme. *Tissue Eng* **13**, 683-691(2007).
- 202 Kloxin, A. M., Kasko, A. M., Salinas, C. N. & Anseth, K. S. Photodegradable hydrogels for dynamic tuning of physical and chemical properties. *Science* **324**, 59-63 (2009).
- 203 Elisseeff, J., McIntosh, W., Fu, K., Blunk, B. T. & Langer, R. Controlled-release of IGF-I and TGF-beta1 in a photopolymerizing hydrogel for cartilage tissue engineering. *J Orthop Res* **19**, 1098-1104 (2001).
- 204 Park, H., Temenoff, J. S., Holland, T. A., Tabata, Y. & Mikos, A. G. Delivery of TGF-beta1 and chondrocytes via injectable, biodegradable hydrogels for cartilage tissue engineering applications. *Biomaterials* **26**, 7095-7103 (2005).
- 205 Solorio, L. D., Fu, A. S., Hernandez-Irizarry, R. & Alsberg, E. Chondrogenic differentiation of human mesenchymal stem cell aggregates via controlled release of TGF-beta1 from incorporated polymer microspheres. *J Biomed Mater Res A* **92**, 1139-1144 (2010).
- 206 Mann, B. K., Schmedlen, R. H. & West, J. L. Tethered-TGF-beta increases extracellular matrix production of vascular smooth muscle cells. *Biomaterials* **22**, 439-444 (2001).
- 207 Fan, V. H. *et al.* Tethered epidermal growth factor provides a survival advantage to mesenchymal stem cells. *Stem Cells* **25**, 1241-1251 (2007).
- 208 Stephens, L. E. *et al.* Deletion of beta 1 integrins in mice results in inner cell mass failure and peri-implantation lethality. *Genes Dev* **9**, 1883-1895 (1995).
- 209 George, E. L., Georges-Labouesse, E. N., Patel-King, R. S., Rayburn, H. & Hynes, R. O. Defects in mesoderm, neural tube and vascular development in mouse embryos lacking fibronectin. *Development* **119**, 1079-1091 (1993).
- 210 Place, E. S., Evans, N. D. & Stevens, M. M. Complexity in biomaterials for tissue engineering. *Nat Mater* **8**, 457-470, doi:nmat2441 [pii] 10.1038/nmat2441 (2009).
- 211 Hern, D. L. & Hubbell, J. A. Incorporation of adhesion peptides into nonadhesive hydrogels useful for tissue resurfacing. *J Biomed Mater Res* **39**, 266-276 (1998).
- 212 Gobin, A. S. & West, J. L. Cell migration through defined, synthetic ECM analogs. *FASEB J* **16**, 751-753 (2002).
- 213 Mann, B. K., Gobin, A. S., Tsai, A. T., Schmedlen, R. H. & West, J. L. Smooth muscle cell growth in photopolymerized hydrogels with cell adhesive and proteolytically degradable domains: synthetic ECM analogs for tissue engineering. *Biomaterials* **22**, 3045-3051 (2001).
- 214 DeLise, A. M., Fischer, L. & Tuan, R. S. Cellular interactions and signaling in cartilage development. *Osteoarthritis Cartilage* **8**, 309-334 (2000).
- 215 Tavella, S. *et al.* Regulated expression of fibronectin, laminin and related integrin receptors during the early chondrocyte differentiation. *J Cell Sci* **110** (Pt 18), 2261-2270 (1997).

- 216 Yamada, K. M. Integrin signaling. *Matrix Biol* **16**, 137-141 (1997).
- 217 Nuttelman, C. R., Tripodi, M. C. & Anseth, K. S. In vitro osteogenic differentiation of human mesenchymal stem cells photoencapsulated in PEG hydrogels. *Journal of biomedical materials research Part A* **68**, 773-782 (2004).
- 218 Salinas, C. N., Cole, B. B., Kasko, A. M. & Anseth, K. S. Chondrogenic differentiation potential of human mesenchymal stem cells photoencapsulated within poly(ethylene glycol)-arginine-glycine-aspartic acid-serine thiol-methacrylate mixed-mode networks. *Tissue Eng* **13**, 1025-1034 (2007).
- 219 Connelly, J. T., Garcia, A. J. & Levenston, M. E. Inhibition of in vitro chondrogenesis in RGD-modified three-dimensional alginate gels. *Biomaterials* **28**, 1071-1083, doi:S0142-9612(06)00896-9 [pii]
10.1016/j.biomaterials.2006.10.006 (2007).
- 220 Salinas, C. N. & Anseth, K. S. The enhancement of chondrogenic differentiation of human mesenchymal stem cells by enzymatically regulated RGD functionalities. *Biomaterials* **29**, 2370-2377 (2008).
- 221 Sekiya, I., Vuoristo, J. T., Larson, B. L. & Prockop, D. J. In vitro cartilage formation by human adult stem cells from bone marrow stroma defines the sequence of cellular and molecular events during chondrogenesis. *Proc Natl Acad Sci U S A* **99**, 4397-4402 (2002).
- 222 Felson, D. T. *et al.* Osteoarthritis: new insights. Part 1: the disease and its risk factors. *Ann Intern Med* **133**, 635-646 (2000).
- 223 Kujala, U. M. *et al.* Knee osteoarthritis in former runners, soccer players, weight lifters, and shooters. *Arthritis Rheum* **38**, 539-546 (1995).
- 224 Huang, C. Y., Hagar, K. L., Frost, L. E., Sun, Y. & Cheung, H. S. Effects of cyclic compressive loading on chondrogenesis of rabbit bone-marrow derived mesenchymal stem cells. *Stem Cells* **22**, 313-323 (2004).
- 225 Davis, E. E., Brueckner, M. & Katsanis, N. The emerging complexity of the vertebrate cilium: new functional roles for an ancient organelle. *Dev Cell* **11**, 9-19 (2006).
- 226 Haycraft, C. J. *et al.* Intraflagellar transport is essential for endochondral bone formation. *Development* **134**, 307-316 (2007).
- 227 Praetorius, H. A. & Spring, K. R. A physiological view of the primary cilium. *Annu Rev Physiol* **67**, 515-529 (2005).
- 228 Smith, M. M., Shi, L. & Navre, M. Rapid identification of highly active and selective substrates for stromelysin and matrilysin using bacteriophage peptide display libraries. *J Biol Chem* **270**, 6440-6449 (1995).
- 229 Turk, B. E., Huang, L. L., Piro, E. T. & Cantley, L. C. Determination of protease cleavage site motifs using mixture-based oriented peptide libraries. *Nat Biotechnol* **19**, 661-667 (2001).

- 230 Stewart, M. C., Saunders, K. M., Burton-Wurster, N. & Macleod, J. N. Phenotypic stability of articular chondrocytes in vitro: the effects of culture models, bone morphogenetic protein 2, and serum supplementation. *J Bone Miner Res* **15**, 166-174 (2000).
- 231 Bryant, S. J., Nuttelman, C. R. & Anseth, K. S. Cytocompatibility of UV and visible light photoinitiating systems on cultured NIH/3T3 fibroblasts in vitro. *Journal of biomaterials science Polymer edition* **11**, 439-457 (2000).
- 232 Bryant SJ, M. P., Elisseeff JH, Randolph M, Langer R, Anseth KS. *in: Chemical and Physical Networks Formation and Control of Properties*. Vol. 2 395-403 (1999).
- 233 Farndale, R. W., Buttle, D. J. & Barrett, A. J. Improved quantitation and discrimination of sulphated glycosaminoglycans by use of dimethylmethylene blue. *Biochim Biophys Acta* **883**, 173-177 (1986).
- 234 Sanford, L. P. *et al.* TGFbeta2 knockout mice have multiple developmental defects that are non-overlapping with other TGFbeta knockout phenotypes. *Development* **124**, 2659-2670 (1997).
- 235 Fingleton, B., Powell, W. C., Crawford, H. C., Couchman, J. R. & Matrisian, L. M. A rat monoclonal antibody that recognizes pro- and active MMP-7 indicates polarized expression in vivo. *Hybridoma (Larchmt)* **26**, 22-27 (2007).
- 236 Scherer, R. L., VanSaun, M. N., McIntyre, J. O. & Matrisian, L. M. Optical imaging of matrix metalloproteinase-7 activity in vivo using a proteolytic nanobeacon. *Molecular imaging : official journal of the Society for Molecular Imaging* **7**, 118-131 (2008).
- 237 Fingleton, B. M., Heppner Goss, K. J., Crawford, H. C. & Matrisian, L. M. Matrilysin in early stage intestinal tumorigenesis. *APMIS* **107**, 102-110 (1999).
- 238 Ii, M., Yamamoto, H., Adachi, Y., Maruyama, Y. & Shinomura, Y. Role of matrix metalloproteinase-7 (matrilysin) in human cancer invasion, apoptosis, growth, and angiogenesis. *Exp Biol Med (Maywood)* **231**, 20-27 (2006).
- 239 Wang, W. S., Chen, P. M. & Su, Y. Colorectal carcinoma: from tumorigenesis to treatment. *Cell Mol Life Sci* **63**, 663-671 (2006).
- 240 Kisiday, J. D., Jin, M., DiMicco, M. A., Kurz, B. & Grodzinsky, A. J. Effects of dynamic compressive loading on chondrocyte biosynthesis in self-assembling peptide scaffolds. *J Biomech* **37**, 595-604 (2004).
- 241 Park, S., Hung, C. T. & Ateshian, G. A. Mechanical response of bovine articular cartilage under dynamic unconfined compression loading at physiological stress levels. *Osteoarthritis Cartilage* **12**, 65-73 (2004).
- 242 Woodfield, T. B. *et al.* Design of porous scaffolds for cartilage tissue engineering using a three-dimensional fiber-deposition technique. *Biomaterials* **25**, 4149-4161 (2004).
- 243 Lujan, T. J., Underwood, C. J., Jacobs, N. T. & Weiss, J. A. Contribution of glycosaminoglycans to viscoelastic tensile behavior of human ligament. *J Appl Physiol* **106**, 423-431 (2009).

- 244 Ringe, J. & Sittinger, M. Tissue engineering in the rheumatic diseases. *Arthritis Res Ther* **11**, 211 (2009).
- 245 Lutolf, M. P. Biomaterials: Spotlight on hydrogels. *Nat Mater* **8**, 451-453 (2009).
- 246 Lutolf, M. P. & Hubbell, J. A. Synthetic biomaterials as instructive extracellular microenvironments for morphogenesis in tissue engineering. *Nat Biotechnol* **23**, 47-55 (2005).
- 247 Hwang, N. S., Varghese, S. & Elisseeff, J. Controlled differentiation of stem cells. *Adv Drug Deliv Rev* **60**, 199-214 (2008).
- 248 Bryant, S. J., Chowdhury, T. T., Lee, D. A., Bader, D. L. & Anseth, K. S. Crosslinking density influences chondrocyte metabolism in dynamically loaded photocrosslinked poly(ethylene glycol) hydrogels. *Ann Biomed Eng* **32**, 407-417 (2004).
- 249 Bryant, S. J., Nuttelman, C. R. & Anseth, K. S. The effects of crosslinking density on cartilage formation in photocrosslinkable hydrogels. *Biomed Sci Instrum* **35**, 309-314 (1999).
- 250 Salinas, C. N. & Anseth, K. S. The influence of the RGD peptide motif and its contextual presentation in PEG gels on human mesenchymal stem cell viability. *Journal of tissue engineering and regenerative medicine* **2**, 296-304 (2008).
- 251 Williams, C. G., Malik, A. N., Kim, T. K., Manson, P. N. & Elisseeff, J. H. Variable cytocompatibility of six cell lines with photoinitiators used for polymerizing hydrogels and cell encapsulation. *Biomaterials* **26**, 1211-1218 (2005).
- 252 Fedorovich, N. E. *et al.* The effect of photopolymerization on stem cells embedded in hydrogels. *Biomaterials* **30**, 344-353 (2009).
- 253 Cruise, G. M., Hegre, O. D., Scharp, D. S. & Hubbell, J. A. A sensitivity study of the key parameters in the interfacial photopolymerization of poly(ethylene glycol) diacrylate upon porcine islets. *Biotechnol Bioeng* **57**, 655-665 (1998).
- 254 Bikram, M. *et al.* Endochondral bone formation from hydrogel carriers loaded with BMP2-transduced cells. *Ann Biomed Eng* **35**, 796-807 (2007).
- 255 Salinas, C. N. & Anseth, K. S. Decorin moieties tethered into PEG networks induce chondrogenesis of human mesenchymal stem cells. *Journal of biomedical materials research Part A* (2008).
- 256 Varghese, S. *et al.* Chondroitin sulfate based niches for chondrogenic differentiation of mesenchymal stem cells. *Matrix Biol* **27**, 12-21 (2008).
- 257 Hwang, N. S. *et al.* In vivo commitment and functional tissue regeneration using human embryonic stem cell-derived mesenchymal cells. *Proc Natl Acad Sci USA* **105**, 20641-20646 (2008).
- 258 Atsumi, T., Murata, J., Kamiyanagi, I., Fujisawa, S. & Ueha, T. Cytotoxicity of photosensitizers camphorquinone and 9-fluorenone with visible light irradiation on a human submandibular-duct cell line in vitro. *Arch Oral Biol* **43**, 73-81 (1998).

- 259 Bryant, S. J. & Anseth, K. S. Hydrogel properties influence ECM production by chondrocytes photoencapsulated in poly(ethylene glycol) hydrogels. *J Biomed Mater Res* **59**, 63-72 (2002).
- 260 Hahn, M. S., McHale, M. K., Wang, E., Schmedlen, R. H. & West, J. L. Physiologic pulsatile flow bioreactor conditioning of poly(ethylene glycol)-based tissue engineered vascular grafts. *Ann Biomed Eng* **35**, 190-200 (2007).
- 261 Nicodemus, G. D. & Bryant, S. J. Cell encapsulation in biodegradable hydrogels for tissue engineering applications. *Tissue Eng Part B Rev* **14**, 149-165 (2008).
- 262 Benoit, D. S., Schwartz, M. P., Durney, A. R. & Anseth, K. S. Small functional groups for controlled differentiation of hydrogel-encapsulated human mesenchymal stem cells. *Nature materials* **7**, 816-823 (2008).
- 263 Rice, M. A. & Anseth, K. S. Encapsulating chondrocytes in copolymer gels: bimodal degradation kinetics influence cell phenotype and extracellular matrix development. *J Biomed Mater Res A* **70**, 560-568 (2004).
- 264 Sahoo, S., Chung, C., Khetan, S. & Burdick, J. A. Hydrolytically degradable hyaluronic acid hydrogels with controlled temporal structures. *Biomacromolecules* **9**, 1088-1092 (2008).
- 265 Fukui, N. *et al.* Processing of type II procollagen amino propeptide by matrix metalloproteinases. *J Biol Chem* **277**, 2193-2201 (2002).
- 266 Colige, A. *et al.* Domains and maturation processes that regulate the activity of ADAMTS-2, a metalloproteinase cleaving the aminopropeptide of fibrillar procollagens types I-III and V. *J Biol Chem* **280**, 34397-34408 (2005).
- 267 Vinatier, C., Mrugala, D., Jorgensen, C., Guicheux, J. & Noël, D. Cartilage engineering: a crucial combination of cells, biomaterials and biofactors. *Trends Biotechnol* **27**, 307-314 (2009).
- 268 Temenoff, J. S. & Mikos, A. G. Review: tissue engineering for regeneration of articular cartilage. *Biomaterials* **21**, 431-440 (2000).
- 269 Williams, D. F. On the nature of biomaterials. *Biomaterials* **30**, 5897-5909 (2009).
- 270 Burns, J. W. Biology takes centre stage. *Nat Mater* **8**, 441-443 (2009).
- 271 Chung, C., Beecham, M., Mauck, R. L. & Burdick, J. A. The influence of degradation characteristics of hyaluronic acid hydrogels on in vitro neocartilage formation by mesenchymal stem cells. *Biomaterials* **30**, 4287-4296 (2009).
- 272 Djouad, F. *et al.* Microenvironmental changes during differentiation of mesenchymal stem cells towards chondrocytes. *Arthritis Res Ther* **9**, R33 (2007).
- 273 Nakamura, M. *et al.* Matrix metalloproteinase-7 degrades all insulin-like growth factor binding proteins and facilitates insulin-like growth factor bioavailability. *Biochem Biophys Res Commun* **333**, 1011-1016 (2005).

- 274 Wang, F. Q., So, J., Reierstad, S. & Fishman, D. A. Matrilysin (MMP-7) promotes invasion of ovarian cancer cells by activation of progelatinase. *Int J Cancer* **114**, 19-31 (2005).
- 275 Ra, H. J. *et al.* Control of promatrilysin (MMP7) activation and substrate-specific activity by sulfated glycosaminoglycans. *J Biol Chem* **284**, 27924-27932 (2009).
- 276 Pelttari, K. *et al.* Premature induction of hypertrophy during in vitro chondrogenesis of human mesenchymal stem cells correlates with calcification and vascular invasion after ectopic transplantation in SCID mice. *Arthritis Rheum* **54**, 3254-3266 (2006).
- 277 Dickhut, A. *et al.* Calcification or dedifferentiation: requirement to lock mesenchymal stem cells in a desired differentiation stage. *J Cell Physiol* **219**, 219-226 (2009).
- 279 Buxton, A. N., Bahney, C. S., Yoo, J. & Johnstone, B. Temporal Exposure to Chondrogenic Factors Modulates Human Mesenchymal Stem Cell Chondrogenesis in Hydrogels. *Tissue Eng Part A* (2010).
- 280 Terrell, T. G., Working, P. K., Chow, C. P. & Green, J. D. Pathology of recombinant human transforming growth factor-beta 1 in rats and rabbits. *Int Rev Exp Pathol* **34 Pt B**, 43-67 (1993).
- 281 Stoop, R. Smart biomaterials for tissue engineering of cartilage. *Injury* **39 Suppl 1**, S77-87 (2008).
- 282 van Beuningen, H. M., van der Kraan, P. M., Arntz, O. J. & van den Berg, W. B. Transforming growth factor-beta 1 stimulates articular chondrocyte proteoglycan synthesis and induces osteophyte formation in the murine knee joint. *Lab Invest* **71**, 279-290 (1994).
- 283 Cheng, S. L., Yang, J. W., Rifas, L., Zhang, S. F. & Avioli, L. V. Differentiation of human bone marrow osteogenic stromal cells in vitro: induction of the osteoblast phenotype by dexamethasone. *Endocrinology* **134**, 277-286 (1994).
- 284 Derfoul, A., Perkins, G. L., Hall, D. J. & Tuan, R. S. Glucocorticoids promote chondrogenic differentiation of adult human mesenchymal stem cells by enhancing expression of cartilage extracellular matrix genes. *Stem Cells* **24**, 1487-1495 (2006).
- 285 Mauck, R. L., Yuan, X. & Tuan, R. S. Chondrogenic differentiation and functional maturation of bovine mesenchymal stem cells in long-term agarose culture. *Osteoarthritis Cartilage* **14**, 179-189, doi:S1063-4584(05)00255-4 [pii] 10.1016/j.joca.2005.09.002 (2006).
- 286 Zanetti, N. C. & Solursh, M. Induction of chondrogenesis in limb mesenchymal cultures by disruption of the actin cytoskeleton. *J Cell Biol* **99**, 115-123 (1984).
- 287 Bedi, A., Feeley, B. T. & Williams, R. J., 3rd. Management of articular cartilage defects of the knee. *J Bone Joint Surg Am* **92**, 994-1009 (2010).
- 288 Chimal-Monroy, J. & Diaz de Leon, L. Expression of N-cadherin, N-CAM, fibronectin and tenascin is stimulated by TGF-beta1, beta2, beta3 and beta5 during the formation of precartilaginous condensations. *Int J Dev Biol* **43**, 59-67 (1999).

- 289 Tuli, R. *et al.* Transforming growth factor-beta-mediated chondrogenesis of human mesenchymal progenitor cells involves N-cadherin and mitogen-activated protein kinase and Wnt signaling cross-talk. *J Biol Chem* **278**, 41227-41236 (2003).
- 290 Serra, R. *et al.* Expression of a truncated, kinase-defective TGF-beta type II receptor in mouse skeletal tissue promotes terminal chondrocyte differentiation and osteoarthritis. *J Cell Biol* **139**, 541-552 (1997).
- 291 Watanabe, H. Transcriptional Cross-talk between Smad, ERK1/2, and p38 Mitogen-activated Protein Kinase Pathways Regulates Transforming Growth Factor- β -induced Aggrecan Gene Expression in Chondrogenic ATDC5 Cells. *J Biol Chem* **227**, 14466-14473 (2001).
- 292 Miura, Y., Parvizi, J., Fitzsimmons, J. S. & O'Driscoll, S. W. Brief exposure to high-dose transforming growth factor-beta1 enhances periosteal chondrogenesis in vitro: a preliminary report. *J Bone Joint Surg Am* **84-A**, 793-799 (2002).
- 293 ten Dijke, P. & Hill, C. S. New insights into TGF-beta-Smad signalling. *Trends Biochem Sci* **29**, 265-273 (2004).
- 294 Di Guglielmo, G. M., Le Roy, C., Goodfellow, A. F. & Wrana, J. L. Distinct endocytic pathways regulate TGF-beta receptor signalling and turnover. *Nat Cell Biol* **5**, 410-421 (2003).
- 295 Hartung, A. *et al.* Different routes of bone morphogenic protein (BMP) receptor endocytosis influence BMP signaling. *Mol Cell Biol* **26**, 7791-7805 (2006).
- 296 Barbero, A. *et al.* Age related changes in human articular chondrocyte yield, proliferation and post-expansion chondrogenic capacity. *Osteoarthritis Cartilage* **12**, 476-484 (2004).
- 297 Richardson, S. M. *et al.* Mesenchymal stem cells in regenerative medicine: Opportunities and challenges for articular cartilage and intervertebral disc tissue engineering. *J Cell Physiol* (2009).
- 298 Gan, L. & Kandel, R. A. In vitro cartilage tissue formation by Co-culture of primary and passaged chondrocytes. *Tissue Eng* **13**, 831-842, doi:10.1089/ten.2007.13.ft-358 (2007).
- 299 Hildner, F. *et al.* Human adipose-derived stem cells contribute to chondrogenesis in coculture with human articular chondrocytes. *Tissue Eng Part A* **15**, 3961-3969, doi:10.1089/ten.TEA.2009.0002 (2009).
- 300 Fischer, J., Dickhut, A., Richter, W. & Rickert, M. Articular chondrocytes secrete PTHrP and inhibit hypertrophy of mesenchymal stem cells in coculture during chondrogenesis. *Arthritis Rheum* (2010).
- 301 Alsberg, E., Anderson, K. W., Albeiruti, A., Rowley, J. A. & Mooney, D. J. Engineering growing tissues. *Proc Natl Acad Sci USA* **99**, 12025-12030 (2002).
- 302 Mikos, A. G. *et al.* Engineering complex tissues. *Tissue Eng* **12**, 3307-3339 (2006).

- 303 Thompson, A. D., Betz, M. W., Yoon, D. M. & Fisher, J. P. Osteogenic differentiation of bone marrow stromal cells induced by coculture with chondrocytes encapsulated in three-dimensional matrices. *Tissue Eng Part A* **15**, 1181-1190 (2009).
- 304 Gerstenfeld, L. C. *et al.* Chondrocytes provide morphogenic signals that selectively induce osteogenic differentiation of mesenchymal stem cells. *J Bone Miner Res* **17**, 221-230 (2002).
- 305 Richardson, S. M. *et al.* Intervertebral disc cell-mediated mesenchymal stem cell differentiation. *Stem Cells* **24**, 707-716 (2006).
- 306 Jikko, A., Kato, Y., Hiranuma, H. & Fuchihata, H. Inhibition of chondrocyte terminal differentiation and matrix calcification by soluble factors released by articular chondrocytes. *Calcif Tissue Int* **65**, 276-279 (1999).
- 307 Bohme, K., Winterhalter, K. H. & Bruckner, P. Terminal differentiation of chondrocytes in culture is a spontaneous process and is arrested by transforming growth factor-beta 2 and basic fibroblast growth factor in synergy. *Exp Cell Res* **216**, 191-198 (1995).
- 308 Pateder, D. B. *et al.* PTHrP expression in chondrocytes, regulation by TGF-beta, and interactions between epiphyseal and growth plate chondrocytes. *Exp Cell Res* **256**, 555-562 (2000).
- 309 Weiss, S., Hennig, T., Bock, R., Steck, E. & Richter, W. Impact of growth factors and PTHrP on early and late chondrogenic differentiation of human mesenchymal stem cells. *J Cell Physiol* **223**, 84-93 (2010).
- 310 Pedrozo, H. A. *et al.* Growth plate chondrocytes store latent transforming growth factor (TGF)-beta 1 in their matrix through latent TGF-beta 1 binding protein-1. *J Cell Physiol* **177**, 343-354 (1998).
- 311 Pedrozo, H. A. *et al.* Vitamin D3 metabolites regulate LTBP1 and latent TGF-beta1 expression and latent TGF-beta1 incorporation in the extracellular matrix of chondrocytes. *J Cell Biochem* **72**, 151-165 (1999).
- 312 Yamamoto, Y. *et al.* Upregulation of the viability of nucleus pulposus cells by bone marrow-derived stromal cells: significance of direct cell-to-cell contact in coculture system. *Spine (Phila Pa 1976)* **29**, 1508-1514 (2004).
- 313 Spees, J. L., Olson, S. D., Whitney, M. J. & Prockop, D. J. Mitochondrial transfer between cells can rescue aerobic respiration. *Proc Natl Acad Sci U S A* **103**, 1283-1288 (2006).
- 314 Rustom, A., Saffrich, R., Markovic, I., Walther, P. & Gerdes, H. H. Nanotubular highways for intercellular organelle transport. *Science* **303**, 1007-1010 (2004).
- 315 Friedenstein, A. J., Chailakhyan, R. K., Latsinik, N. V., Panasyuk, A. F. & Keiliss-Borok, I. V. Stromal cells responsible for transferring the microenvironment of the hemopoietic tissues. Cloning in vitro and retransplantation in vivo. *Transplantation* **17**, 331-340 (1974).

- 316 Dexter, T. M., Allen, T. D. & Lajtha, L. G. Conditions controlling the proliferation of haemopoietic stem cells in vitro. *J Cell Physiol* **91**, 335-344 (1977).
- 317 Iso, Y. *et al.* Multipotent human stromal cells improve cardiac function after myocardial infarction in mice without long-term engraftment. *Biochem Biophys Res Commun* **354**, 700-706 (2007).
- 318 Anderson, S. B., Kissler, M. J. & Anseth, A. S. in *Society for Biomaterials*.
- 319 Seda Tigli, R. *et al.* Comparative chondrogenesis of human cell sources in 3D scaffolds. *J Tissue Eng Regen Med* (2009).
- 320 Huang, A. H., Stein, A., Tuan, R. S. & Mauck, R. L. Transient exposure to TGF-beta3 improves the mechanical properties of MSC-laden cartilage constructs in a density dependent manner. *Tissue Eng Part A* (2009).
- 321 Huang, A. H., Yeger-McKeever, M., Stein, A. & Mauck, R. L. Tensile properties of engineered cartilage formed from chondrocyte- and MSC-laden hydrogels. *Osteoarthritis Cartilage* **16**, 1074-1082 (2008).
- 322 Mauck, R. L., Byers, B. A., Yuan, X. & Tuan, R. S. Regulation of cartilaginous ECM gene transcription by chondrocytes and MSCs in 3D culture in response to dynamic loading. *Biomech Model Mechanobiol* **6**, 113-125 (2007).
- 323 Bigdeli, N. *et al.* Coculture of human embryonic stem cells and human articular chondrocytes results in significantly altered phenotype and improved chondrogenic differentiation. *Stem Cells* **27**, 1812-1821 (2009).
- 324 Adkisson, H. D. *et al.* The potential of human allogeneic juvenile chondrocytes for restoration of articular cartilage. *Am J Sports Med* **38**, 1324-1333 (2010).
- 325 Adkisson, H. D. *et al.* Immune evasion by neocartilage-derived chondrocytes: Implications for biologic repair of joint articular cartilage. *Stem Cell Res* **4**, 57-68 (2010).
- 326 Jones, S., Horwood, N., Cope, A. & Dazzi, F. The antiproliferative effect of mesenchymal stem cells is a fundamental property shared by all stromal cells. *J Immunol* **179**, 2824-2831 (2007).
- 327 Revell, C. M. & Athanasiou, K. A. Success rates and immunologic responses of autogenic, allogenic, and xenogenic treatments to repair articular cartilage defects. *Tissue Eng Part B Rev* **15**, 1-15 (2009).
- 328 Wilson, R. *et al.* Comprehensive profiling of cartilage extracellular matrix formation and maturation using sequential extraction and label-free quantitative proteomics. *Mol Cell Proteomics* **9**, 1296-1313 (2010).
- 329 Tsuchiya, K., Chen, G., Ushida, T., Matsuno, T. & Tateishi, T. The effect of coculture of chondrocytes with mesenchymal stem cells on their cartilaginous phenotype. *Materials Scienc & Engineering, Part C* **24**, 391-396 (2004).

- 330 Dennis, J. E., Konstantakos, E. K., Arm, D. & Caplan, A. I. In vivo osteogenesis assay: a rapid method for quantitative analysis. *Biomaterials* **19**, 1323-1328 (1998).
- 331 Huibregtse, B. A., Johnstone, B., Goldberg, V. M. & Caplan, A. I. Effect of age and sampling site on the chondro-osteogenic potential of rabbit marrow-derived mesenchymal progenitor cells. *J Orthop Res* **18**, 18-24 (2000).
- 332 Lennon, D. P., Haynesworth, S. E., Young, R. G., Dennis, J. E. & Caplan, A. I. A chemically defined medium supports in vitro proliferation and maintains the osteochondral potential of rat marrow-derived mesenchymal stem cells. *Exp Cell Res* **219**, 211-222 (1995).
- 333 Hung, C. T., Mauck, R. L., Wang, C. C., Lima, E. G. & Ateshian, G. A. A paradigm for functional tissue engineering of articular cartilage via applied physiologic deformational loading. *Ann Biomed Eng* **32**, 35-49 (2004).
- 334 Mauck, R. L. *et al.* Functional tissue engineering of articular cartilage through dynamic loading of chondrocyte-seeded agarose gels. *J Biomech Eng* **122**, 252-260 (2000).
- 335 Butler, D. L., Goldstein, S. A. & Guilak, F. Functional tissue engineering: the role of biomechanics. *J Biomech Eng* **122**, 570-575 (2000).
- 336 Daamen, W. F., Veerkamp, J. H., van Hest, J. C. & van Kuppevelt, T. H. Elastin as a biomaterial for tissue engineering. *Biomaterials* **28**, 4378-4398 (2007).
- 337 van Osch, G. J. *et al.* Growth factors in cartilage tissue engineering. *Biorheology* **39**, 215-220 (2002).
- 338 Nugent, G. E. *et al.* Dynamic shear stimulation of bovine cartilage biosynthesis of proteoglycan 4. *Arthritis Rheum* **54**, 1888-1896 (2006).
- 339 Preiss-Bloom, O., Mizrahi, J., Elisseeff, J. & Seliktar, D. Real-time monitoring of force response measured in mechanically stimulated tissue-engineered cartilage. *Artif Organs* **33**, 318-327 (2009).
- 340 Aufderheide, A. C. & Athanasiou, K. A. A direct compression stimulator for articular cartilage and meniscal explants. *Ann Biomed Eng* **34**, 1463-1474 (2006).
- 341 Steinmeyer, J. A computer-controlled mechanical culture system for biological testing of articular cartilage explants. *J Biomech* **30**, 841-845 (1997).
- 342 Stolz, M. *et al.* Dynamic elastic modulus of porcine articular cartilage determined at two different levels of tissue organization by indentation-type atomic force microscopy. *Biophys J* **86**, 3269-3283 (2004).
- 343 Basalo, I. M. *et al.* Cartilage interstitial fluid load support in unconfined compression following enzymatic digestion. *J Biomech Eng* **126**, 779-786 (2004).
- 344 Cassino, T. R. *et al.* Design and application of an oscillatory compression device for cell constructs. *Biotechnol Bioeng* **98**, 211-220 (2007).

- 345 Chahine, N. O., Ateshian, G. A. & Hung, C. T. The effect of finite compressive strain on chondrocyte viability in statically loaded bovine articular cartilage. *Biomech Model Mechanobiol* **6**, 103-111 (2007).
- 346 Mauck, R. L., Nicoll, S. B., Seyhan, S. L., Ateshian, G. A. & Hung, C. T. Synergistic action of growth factors and dynamic loading for articular cartilage tissue engineering. *Tissue Eng* **9**, 597-611 (2003).
- 347 Lee, C. R. *et al.* Fibrin-polyurethane composites for articular cartilage tissue engineering: a preliminary analysis. *Tissue Eng* **11**, 1562-1573 (2005).
- 348 Davisson, T., Kunig, S., Chen, A., Sah, R. & Ratcliffe, A. Static and dynamic compression modulate matrix metabolism in tissue engineered cartilage. *J Orthop Res* **20**, 842-848 (2002).
- 349 Waldman, S. D., Spiteri, C. G., Gryn timer, M. D., Pilliar, R. M. & Kandel, R. A. Long-term intermittent compressive stimulation improves the composition and mechanical properties of tissue-engineered cartilage. *Tissue Eng* **10**, 1323-1331 (2004).
- 350 Butler, D. L. *et al.* Using functional tissue engineering and bioreactors to mechanically stimulate tissue-engineered constructs. *Tissue Eng Part A* **15**, 741-749 (2009).
- 351 Chokalingam, K. *et al.* 3D-In vitro Effects of Compression and Time in Culture on Aggregate Modulus and on Gene Expression and Protein content of Collagen Type II in Murine Chondrocytes. *Tissue Eng Part A* (2009).
- 352 Bottlang, M., Simnacher, M., Schmitt, H., Brand, R. A. & Claes, L. A cell strain system for small homogeneous strain applications. *Biomed Tech (Berl)* **42**, 305-309 (1997).
- 353 Eckstein, F., Lemberger, B., Stammberger, T., Englmeier, K. H. & Reiser, M. Patellar cartilage deformation in vivo after static versus dynamic loading. *J Biomech* **33**, 819-825 (2000).